frontiers | Research Topics

Clinical and basic research on endovascular repair and branch reconstruction for the treatment of lesions involving the aortic arch

Edited by
Hongkun Zhang, Wayne Zhang, Emiliano Chisci
and Nabil Chakfe

Published in
Frontiers in Cardiovascular Medicine
Frontiers in Surgery

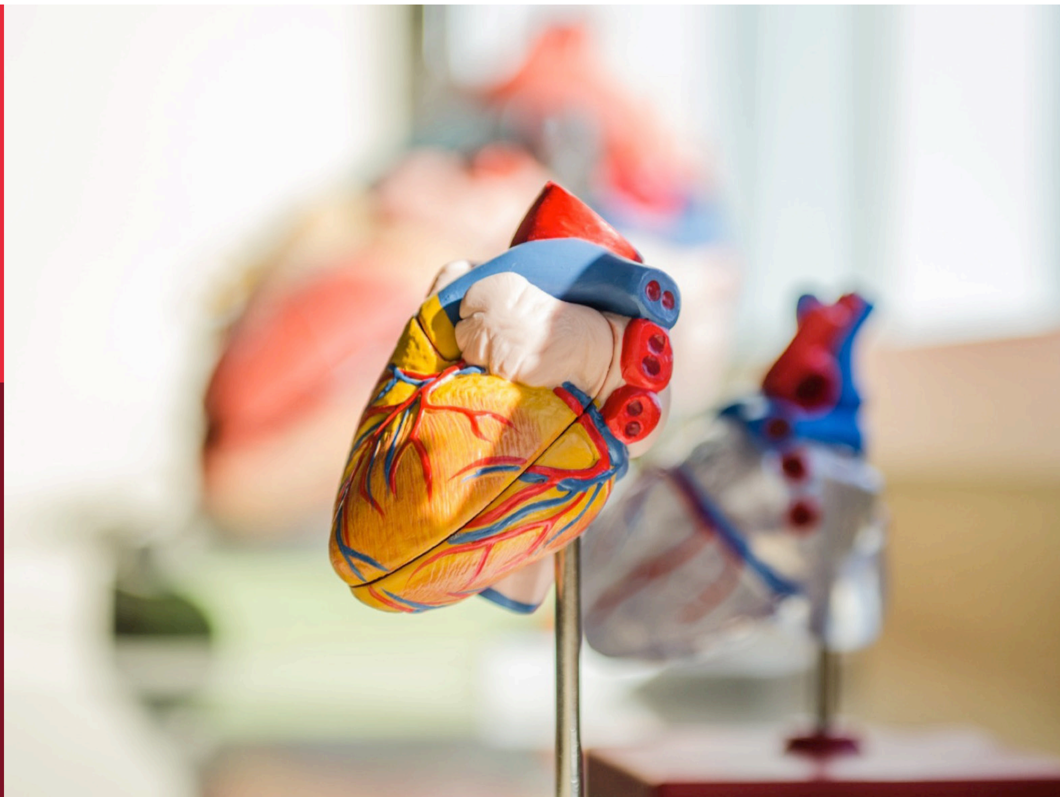

ISSN 1664-8714
ISBN 978-2-8325-3232-4
DOI 10.3389/978-2-8325-3232-4

About Frontiers

Frontiers is more than just an open access publisher of scholarly articles: it is a pioneering approach to the world of academia, radically improving the way scholarly research is managed. The grand vision of Frontiers is a world where all people have an equal opportunity to seek, share and generate knowledge. Frontiers provides immediate and permanent online open access to all its publications, but this alone is not enough to realize our grand goals.

Frontiers journal series

The Frontiers journal series is a multi-tier and interdisciplinary set of open-access, online journals, promising a paradigm shift from the current review, selection and dissemination processes in academic publishing. All Frontiers journals are driven by researchers for researchers; therefore, they constitute a service to the scholarly community. At the same time, the *Frontiers journal series* operates on a revolutionary invention, the tiered publishing system, initially addressing specific communities of scholars, and gradually climbing up to broader public understanding, thus serving the interests of the lay society, too.

Dedication to quality

Each Frontiers article is a landmark of the highest quality, thanks to genuinely collaborative interactions between authors and review editors, who include some of the world's best academicians. Research must be certified by peers before entering a stream of knowledge that may eventually reach the public - and shape society; therefore, Frontiers only applies the most rigorous and unbiased reviews. Frontiers revolutionizes research publishing by freely delivering the most outstanding research, evaluated with no bias from both the academic and social point of view. By applying the most advanced information technologies, Frontiers is catapulting scholarly publishing into a new generation.

What are Frontiers Research Topics?

Frontiers Research Topics are very popular trademarks of the *Frontiers journals series*: they are collections of at least ten articles, all centered on a particular subject. With their unique mix of varied contributions from Original Research to Review Articles, Frontiers Research Topics unify the most influential researchers, the latest key findings and historical advances in a hot research area.

Find out more on how to host your own Frontiers Research Topic or contribute to one as an author by contacting the Frontiers editorial office: frontiersin.org/about/contact

Clinical and basic research on endovascular repair and branch reconstruction for the treatment of lesions involving the aortic arch

Topic editors
Hongkun Zhang — Zhejiang University, China
Wayne Zhang — University of Washington, United States
Emiliano Chisci — Nuovo Ospedale San Giovanni di Dio, Italy
Nabil Chakfe — Université de Strasbourg, France

Citation
Zhang, H., Zhang, W., Chisci, E., Chakfe, N., eds. (2023). *Clinical and basic research on endovascular repair and branch reconstruction for the treatment of lesions involving the aortic arch*. Lausanne: Frontiers Media SA.
doi: 10.3389/978-2-8325-3232-4

Table of contents

frontiers | Frontiers in Surgery

TYPE Original Research
PUBLISHED 30 August 2022
DOI 10.3389/fsurg.2022.969995

Check for updates

OPEN ACCESS

EDITED BY
Emiliano Chisci,
Nuovo Ospedale San Giovanni di Dio, Italy

REVIEWED BY
Kexiang Liu,
Jilin University, China
Xiang Wei,
Tongji Medical College, Huazhong University of Science and Technology, China

*CORRESPONDENCE
Hailong Cao
caohailong@njglyy.com
Dongjin Wang
wangdongjin@njglyy.com

†These authors have contributed equally to this work.

SPECIALTY SECTION
This article was submitted to Heart Surgery, a section of the journal Frontiers in Surgery

RECEIVED 15 June 2022
ACCEPTED 11 August 2022
PUBLISHED 30 August 2022

CITATION
Qin X, Gao Y, Jiang Y, Zhu F, Xie W, Tang X, Xue Y, Wang D and Cao H (2022) The role of peripheral blood eosinophil counts in acute Stanford type A aortic dissection patients. Front. Surg. 9:969995. doi: 10.3389/fsurg.2022.969995

The role of peripheral blood eosinophil counts in acute Stanford type A aortic dissection patients

Xichun Qin[1,2†], Yaxuan Gao[1,2†], Yi Jiang[1,3], Feng Zhu[1,2], Wei Xie[1,2], Xinlong Tang[1,2], Yunxing Xue[1,2], Dongjin Wang[1,2*] and Hailong Cao[1,2*]

[1]Department of Cardio-Thoracic Surgery, Nanjing Drum Tower Hospital, The Affiliated Hospital of Nanjing University Medical School, Nanjing, China, [2]Institute of Cardiothoracic Vascular Disease, Nanjing University, Nanjing, China, [3]Department of Cardio-Thoracic Surgery, Nanjing Drum Tower Hospital Clinical College of Nanjing Medical University, Nanjing, China

Background: Acute Stanford-A aortic dissection (AAAD) is a devastating cardiovascular condition with high mortality, therefore identifying risk prognosis factors is vital for the risk stratification of patients with AAAD. Here, we investigated peripheral blood eosinophil (EOS) counts in patients with AAAD and their possible biological implications.

Methods: We performed a single center retrospective cohort study. From 2011 to 2021, a total of 1,190 patients underwent AAAD surgery. Patients were categorized first by death and then admission EOS counts (0.00×10^9/L or >0.00×10^9/L). Demographics, laboratory data, and outcomes were analyzed using standard statistical analyses. Ascending aorta specimens were used for western blotting and histological assessments.

Results: Death group patients had lower EOS counts than the non-death group ($P = 0.008$). When patients were stratified using mean blood EOS counts: 681 patients had low (0.00×10^9/L) and 499 had high (>0.00×10^9/L) counts. Patients with low EOS counts at admission were more likely to have a higher mortality risk ($P = 0.017$) and longer treatment in the intensive care unit (ICU) days ($P = 0.033$) than patients with normal EOS counts. Also, the five blood coagulation items between both groups showed significantly different ($P < 0.001$). Hematoxylin & eosin-stained cross-sections of the ascending aorta false lumen showed that EOSs were readily observed in thrombi in the false lumen of the aorta.

Conclusions: Peripheral blood EOS counts may be involved in thrombosis and could be an effective and efficient indicator for the diagnosis, evaluation, and prognosis monitoring of patients with AAAD.

KEYWORDS

acute Stanford-A aortic dissection, eosinophil, mortality risk, blood coagulation, thrombosis

Abbreviations
EOS, eosinophil; AAD, acute aortic dissection; ICU, intensive care unit; AAAD, acute Stanford-A aortic dissection; WBC, white blood cells; CVD, cardiovascular disease; CT, computed tomographic; BMI, body mass index; GAPDH, glyceraldehyde-3-phosphate dehydrogenase; IQR, inter quartile range; SD, standard deviation; SMC, smooth muscle cell; PLT, platelet; HTN, hypertension; DB, diabetes; COPD, chronic obstructive pulmonary disease; AF, atrial fibrillation; CABG, coronary artery bypass grafting; CTNT, troponin T; PT, prothrombin time; INR, international normalized ratio; PT, prothrombin time; INR, international normalized ratio; TT, thrombin time; APTT, activated partial thromboplastin time

Introduction

Acute aortic dissection (AAD) is a serious life-threatening disease, with a gradually increasing incidence rate in recent years (1). Depending on the rupture site, AAD is classified as Stanford-A when it involves the thoracic segment of the ascending aorta and/or the aortic arch, and Stanford-B when it involves the descending aorta and/or the thoracoabdominal aorta (2). Acute Stanford-A aortic dissection (AAAD) is the most common type, accounting for 75% of all cases. If treatment is not timely, many patients with AAAD will die suddenly due to aortic wall rupture. The mortality rate is as high as 90% (3). With the establishment of regional referral centers, more patients with AAAD can now receive timely surgical intervention, but all-cause mortality remains up to 10%–30% (4, 5).

Patients with AAAD usually undergo vital sign monitoring and blood tests upon admission in the emergency department, therefore, more clinicians are now heeding circulating biomarkers, such as routine bloods, in an attempt to analyze or predict the risk of death in these patients (6, 7). Laboratory test results are easily generated and do not impose additional risk and financial burden on patients. Many clinical and basic research studies have reported that inflammation has important roles in cardiovascular disease, with several inflammatory factors predicting cardiovascular disease (CVD) progression and prognosis (8, 9). These findings are also applicable to AAAD (10). White blood cells (WBC) are generally elevated in patients with AAAD and associated with a more severe prognosis and higher mortality (11). Eosinophils (EOS) are a type of WBC, and are implicated in several CVDs. For example, high blood EOS counts are positively associated with major cardiovascular risk factors and CVD prevalence (12), low EOS counts are negatively associated with peripheral arterial disease (13), and higher blood EOS counts are recorded in patients with abdominal aortic aneurysm when compared with normal controls, and can act as independent risk factors for the condition (14). However, we found that in the majority of patients with AAAD, EOS counts were $<0.02 \times 10^9$/L, and even dropped below the lower limit of detection (denoted as 0.00×10^9/L). Compared to the change in the WBC counts, the EOS counts which were "0.00" seemed to be more striking.

While research on the pathogenesis of AAAD has progressed, EOS alterations during the condition and their possible biological ramifications are rarely considered. In this study, we investigated this phenomenon, characterized EOS changes of AAAD patients, and examined their roles.

Methods

Materials and extension methods are described in **Supplementary Materials**.

Study design

The principal study was a single-center, retrospective study. That study was approved by the Ethics Committee of the Affiliated Drum Tower Hospital of Nanjing University Medical School.

Study patients

From January 2011 to December 2021, 1,190 AAAD surgeries were performed in Nanjing Drum Tower Hospital. An AAAD diagnosis was confirmed by aorta angiography using multi-detector computed tomographic scanning. Stanford type A (DeBakey I and II) dissection involved the ascending aorta and/or the aortic arch according to previously published criteria. All patients underwent serological testing in the emergency department preoperatively, and the results were considered as admission laboratory data. Patients were excluded if they died preoperatively or had no laboratory data (routine blood examinations including EOS counts) or had taken medications such as aspirin, antibiotics, and glucocorticoids affecting blood counts. The study was reviewed by the hospital Ethics Committee. Laboratory analytes measured at admission included routine blood examinations, biochemical analysis, D-dimer, cTNT, and five blood coagulation items.

Clinical character

Patient demographic data, including age, gender, body mass index (BMI), disease onset, and previous medical history, including hypertension, diabetes, atrial fibrillation, Marfan syndrome, chronic obstructive pulmonary disease, coronary artery bypass grafting history, and smoking and drinking status. Other clinical characteristics included symptoms and signs at admission. The rationale for surgery and the surgical strategy were both determined by attending surgeons.

Primary and secondary outcomes

The primary study outcome was inpatient mortality which was defined as all-cause death. Secondary outcomes included the time in the intensive care unit (ICU), post- tracheostomy, post-stroke, and post-intracranial hemorrhage after surgeries during the index hospitalization.

Statistical analysis

Continuous variables were expressed as the mean ± standard deviation and compared using t tests if they were normally distributed. Skewed continuous variables were analyzed as the median and inter quartile range (IQR), and comparisons were made using the Mann-Whitney U test, with significance accepted at $P < 0.05$. Binary and categorical variables were expressed as counts and percentages, and compared using the χ^2 or Fisher's exact test. A two-sided $\alpha < 0.05$ was considered statistically significant. Statistical analyses were performed in SPSS version 26.0 (SPSS, Inc., Chicago, IL, United States).

Results

In total, 1,190 patients with AAAD were investigated. We excluded patients with no laboratory data and who had taken medications affecting blood counts. Finally, 1,180 patients with AAAD were analyzed, of whom 1,009 survived and 171 died. Next, we divided AAAD patients into death and non-death groups. Demographics were similar between groups, except for age ($P < 0.001$) and hypertension history ($P = 0.005$). Moreover, patients in the death group were more likely to have hypotension (22 [12.2%] vs. 66 [6.5%], $P < 0.01$) and preoperative limb ischemia before surgery (44 [24.4%] vs. 135 [13.4%], $P = 0.001$) (Table 1).

In terms of laboratory data, normal EOS counts were between $0.02–0.52 \times 10^9$/L, however, over 80% of EOS counts below 0.02×10^9/L, and 57.7% of AAAD patients dropped below the lower limit of detection (0.00×10^9/L). Moreover, when EOS counts were considered as a continuous variable, we identified significant differences between death and non-death patients ($P = 0.008$), and EOS percentages lower in the death group ($P = 0.002$). When EOS counts were considered a categorical variable, we identified differences between groups ($P = 0.038/0.017$). Higher WBC and neutrophil counts were identified in the death group. In contrast, lymphocyte and monocyte counts in both groups were not significantly different (Table 2). These data suggested that reduced EOS counts were almost a universal feature in patients with AAAD.

We selected tissue from patients with AAAD (EOS count = 0.00×10^9/L) and normal human ascending aorta tissue (EOS count = $0.02–0.52 \times 10^9$/L), and investigated Siglec-8 expression (EOS marker protein). Interestingly, in ascending aortic tissue from patients with AAAD, we observed no abnormal Siglec-8 expression (Supplementary Figures S1A, B). Additionally, we observed no EOS infiltration or enrichment in AAAD patient's aorta tissue using H&E staining (Supplementary Figure S1C).

To further investigate the role of EOS counts in AAAD, we divided patients into two groups based on circulating EOS counts at admission; a lower EOS group (0.00×10^9/L) and a higher EOS group ($>0.00 \times 10^9$/L). No significant clinical differences were identified between groups. Similarly, no differences in age ($P = 0.628$), BMI ($P = 0.226$), and the median interval from onset to hospitalization ($P = 0.196$) were identified.

TABLE 1 Demographics and characteristics of non-death and death AAD patient.

Variables	Total (*n* = 1180)	Death (*n* = 171)	Non-death (*n* = 1009)	*P* value
Age, years	53 (44–63)	58 (49–68)	52 (44–62)	<0.001*
Gender (male/female)	883/297	124/47	759/250	0.505
BMI (kg/m^2)	25.3 (23.05–28.02)	25.39 (23.24–28.22)	25.40 (23.03–27.99)	0.811
Smoking history	293 (24.8%)	43 (25.1%)	250 (24.8%)	0.924
Drinking history	215 (18.2%)	36 (21.1%)	179 (17.7%)	0.335
Complications				
HTN	878 (74.4%)	138 (80.7%)	740 (73.3%)	0.046*
DB	41 (3.4%)	2 (1.2%)	39 (3.9%)	0.075
COPD	10 (0.8%)	2 (1.2%)	8 (0.8%)	0.645
AF	12 (1.0%)	3 (1.8%)	9 (0.9%)	0.398
Marfan	23 (1.9%)	1 (0.6%)	22 (2.2%)	0.234
CABG history	1 (0.1%)	1 (0.6%)	0 (0.0%)	0.145
Stroke history	35 (3.0%)	6 (3.5%)	29 (2.9%)	0.808
Symptoms				
Pain	1,101 (93.3%)	164 (95.9%)	937 (92.9%)	0.184
Chest pain	1,011 (85.7%)	147 (86.0%)	864 (85.6%)	1.000
Back pain	536 (45.4%)	77 (45.0%)	459 (45.5%)	0.934
Abdominal pain	79 (6.7%)	15 (8.8%)	64 (6.3%)	0.247
Nausea	175 (18.1%)	25 (18.4%)	150 (18.1%)	1.000
Vomiting	146 (15.1%)	20 (14.7%)	126 (15.1%)	0.200
Stroke hemiplegia	17 (1.4%)	6 (3.5%)	11 (1.1%)	0.026*
Sign				
Hypotension	88 (7.5%)	22 (12.9%)	66 (6.5%)	0.005*
Heart rate	80 (69–94)	84 (70–99)	80 (69–93)	0.127
Pericardial effusion	809 (68.6%)	116 (67.8%)	693 (68.7%)	0.859
Preoperative limb ischemia	174 (14.5%)	40 (23.4%)	134 (13.3%)	0.001*

BMI, body mass index; HTN, hypertension; DB, diabetes; COPD, chronic obstructive pulmonary disease; AF, atrial fibrillation; CABG, coronary artery bypass grafting.
*Statistically significant values.

The proportion of patients in the lower EOS group, who developed pericardial effusion (65.8% vs. 72.3%, $P = 0.017$) was significantly lower than the higher EOS group. Moreover, patients in the lower EOS group who developed cerebral ischemia attack (10.0% vs. 5.8%, $P = 0.010$) were higher than the higher EOS group (Table 3).

By examining primary and secondary outcomes in both EOS groups, patients with an admission EOS count of 0.00×10^9/L had higher mortality rates (113 [16.6%] vs. 58 [11.6%], $P = 0.017$) and increased ICU treatment days [5.0 days, (IQR 3.0–8.0) vs. 4.0 days, (IQR 3.0–7.0), $P = 0.033$]. No significant

TABLE 2 Laboratory test results of non-death and death AAD patients.

Variables	Total ($n = 1180$)	Death ($n = 171$)	Non-death ($n = 1009$)	*P* value
WBC (4.0–10.0 × 10^9/L)				
<4	14 (1.2%)	6 (3.5%)	8 (0.8%)	<0.001*
4–10	451 (38.2%)	48 (28.1%)	403 (39.9%)	
>10	715 (60.6%)	117 (68.4%)	598 (59.3%)	
Neutrophils (2.0–6.0 × 10^9/L)				
<2	4 (0.3%)	3 (1.8%)	1 (0.1%)	0.012*
2–6	175 (14.8%)	22 (12.9%)	153 (15.2%)	
>6	1,001 (84.8%)	146 (85.4%)	855 (84.7%)	
Lymphocytes (1.0–3.5 × 10^9/L)				
<1	735 (62.3%)	105 (61.4%)	630 (62.4%)	0.796
≥1	445 (37.7%)	66 (38.6%)	379 (37.6%)	
Monocytes (0.1–0.6 × 10^9/L)				
<0.6	500 (42.4%)	68 (39.8%)	432 (42.8%)	0.456
≥0.6	680 (57.6%)	103 (60.2%)	577 (57.2%)	
Eosinophils (0.02–0.52 × 10^9/L)				
0	681 (57.7%)	113 (66.1%)	568 (56.3%)	0.038*
0–0.02	276 (23.4%)	38 (22.2%)	238 (23.6.%)	
0.02–0.52	221 (18.7%)	20 (11.7%)	201 (19.9%)	
>0.52	2 (0.2%)	0 (0.0%)	2 (0.2%)	
Eosinophils (0.02–0.5 × 10^9/L)				
0	681 (57.7%)	113 (66.1%)	568 (56.3%)	0.017*
>0	499 (42.3%)	58 (33.9%)	441 (43.7%)	
Eosinophils (continuous)	0.00 (0.00–0.02)	0.00 (0.00–0.01)	0.00 (0.00–0.02)	0.008*
WBC (continuous)	11.2 (8.6–14.1)	12.4 (8.7–15.4)	11 (8.5–13.8)	0.002*
Neutrophils (continuous)	9.7 (7.13–12.4)	10.8 (7.2–13.9)	9.5 (7.1–12.2)	0.002*
Lymphocytes (continuous)	0.8 (0.5–1.1)	0.8 (0.5–1.1)	0.8 (0.5–1.1)	0.155
Monocytes (continuous)	0.6 (0.4–0.9)	0.4 (0.7–1.0)	0.6 (0.4–0.9)	0.741
Hemoglobin (115–150 g/L)	122 (101–139)	120 (93–139)	154 (101.5–139)	0.099
Platelet (100–400 × 10^9/L)	137 (98.25–177)	120 (72–172)	139 (102–180)	<0.001*
Neutrophils (40%–70%)	87.20 (81.83–90.30)	87.80 (83.30–89.90)	87.00 (81.70–90.40)	0.355
Lymphocytes (20%–50%)	6.95 (4.80–10.40)	6.50 (4.60–9.90)	7.00 (4.90–10.40)	0.241
Monocytes (3%–10%)	5.7 (4.1–7.6)	5.6 (4.3–7.2)	5.7 (4.1–7.8)	0.284
Eosinophils (0.4%–8%)	0.00 (0.00–0.10)	0.00 (0.00–0.10)	0.00 (0.00–0.20)	0.002*
C-reactive protein (0–10 mg/L)	45.55 (6.68–108.35)	53.75 (6.68–117.3)	45.15 (6.63–106.45)	0.619
Albumin (30–55 g/L)	37.00 (33.50–19.90)	34.95 (30.43–38.88)	37.30 (33.80–40.10)	<0.001*
D-dimer (0–0.5 mg/L)	5.19 (2.82–11.61)	8.26 (4.29–21.08)	4.80 (2.60–9.86)	<0.001*
CTNT (0.02–0.13 ug/L)	0.028 (0.01–0.16)	0.069 (0.019–0.35)	0.025 (0.01–0.131)	<0.001*
PT (10–15 s)	12.6 (11.7–14.2)	13.7 (12.5–16.6)	12.5 (11.6–14.0)	<0.001*
INR (0.8–1.3)	1.11 (1.02–1.24)	1.20 (1.09–1.46)	1.09 (1.01–1.22)	<0.001*

(*continued*)

TABLE 2 Continued

CTNT, troponin T; PT, prothrombin time; INR, international normalized ratio; WBC, white blood cell.
*Statistically significant values.

differences in tracheotomy (42 [6.3%] vs. 20 [4.1%], $P = 0.091$) and intracranial hemorrhage rates (8 [1.2%] vs. 5 [1.0%], $P = 1.000$) were identified (Table 3).

The results of univariate regression analysis of predictors of mortality were shown in Table 4. Admission EOS count was associated with mortality both as a continuous variable (OR = 0.004, 95% CI 0.000–0.241, $P = 0.006$) and as a cutoff value of >0.00 × 10^9/L (OR = 0.661, 95% CI 0.470–0.929, $P = 0.017$). Other risk factors associated with all-cause mortality included age, hypertension and WBC count. Add risk factors which $P < 0.05$ into multivariable logistic regression models. Multivariable-adjusted ORs for mortality according to per 1.0 × 10^9 cells/L increase, the cutoff value of 0.00 × 10^9/L, were presented in Table 5. Admission EOS count was an independent predictor of death when considered as a continuous variable (OR = 0.010, 95% CI 0.000–0.650, $P = 0.031$) or as a categorical variable (OR = 1.46, 95% CI 1.033–2.070, $P = 0.032$) using the cutoff value of 0.00 × 10^9/L after adjustment for age, hypertension and WBC count.

Aortic false lumen is a typical feature of AAAD (15). We noticed changes in coagulation function in AAAD patients, and some studies suggested that EOS might be involved in thrombosis (16, 17). Comparisons between EOS groups were significant for the five blood coagulation items. Patients with 0.00 × 10^9/L EOS counts had higher PT [(12.8 s, IQR 11.8–14.35 s) vs. (12.4 s, IQR 11.5–13.9 s), $P < 0.001$], APTT [(30.4 s, IQR 26.9–39.3 s) vs. (29.3 s, IQR 26.8–34.55 s), $P = 0.004$], INR [(1.12 s, IQR 1.03–1.25 s) vs. (1.09 s, IQR 1.00–1.22 s), $P < 0.001$], TT [(19.3 s, IQR 17.5–22.1 s) vs. (18.6 s, IQR 16.9–20.9 s), $P < 0.001$], and lower fibrinogen levels [(2.1 g/L, IQR 1.6–2.7 g/L) vs. (2.4 g/L, IQR 1.7–3.3 g/L), $P < 0.001$] (Table 6). Furthermore, EOSs were observed in thrombi in the false lumen of the aorta (Supplementary Figure S2). Therefore, decreased peripheral blood EOS counts may be due to the involvement of EOSs in aortic false lumen thrombosis.

TABLE 3 The effects of different eosinophil levels on the clinical characteristics, primary and secondary outcomes of patients with AAD.

Variables	Total ($n = 1180$)	EOS of 0.00 ($n = 681$)	EOS > 0.00 ($n = 499$)	*P* value
Age, years	53 (44–63)	53 (45–63)	53 (44–63)	0.628
Gender (male/female)	883/297	483/198	400/99	<0.001*
BMI (kg/m^2)	25.39 (23.05–28.02)	25.35 (22.99–27.91)	25.72 (23.18–28.34)	0.226
From onset to admission	10 (6–18)	10 (7–15)	9 (6–22)	0.196
Leg pain				
Left	42 (3.6%)	26 (3.8%)	16 (3.2%)	0.032*
Right	19 (1.6%)	6 (0.9%)	13 (2.6%)	0.010*
Both	10 (0.8%)	3 (0.4%)	7 (1.4%)	
Cerebral ischemia attack	97 (8.2%)	68 (10.0%)	29 (5.8%)	
Hypotension	88 (7.5%)	57 (8.4%)	31 (6.2%)	0.163
Pericardial effusion	809 (68.6%)	448 (65.8%)	361 (72.3%)	0.017*
Mortality	171 (14.5%)	113 (16.6%)	58 (11.6%)	0.017*
ICU admission	5 (3–8)	5 (3–8)	4 (3–7)	0.033*
Post tracheostomy	62 (5.4%)	42 (6.3%)	20 (4.1%)	0.091
Post stroke	79 (6.7%)	44 (6.5%)	35 (7.1%)	0.841
Post intracranial hemorrhage	13 (1.1%)	8 (1.2%)	5 (1.0%)	1.000

BMI, body mass index; ICU, intensive care unit.
*Statistically significant values.

TABLE 4 Predictors of mortality after AAAD surgery in univariate logistic regression.

Variables	Odds Ratio	95%CI	*P* value
Age, years	1.036	1.023–1.049	<0.001*
Gender, (male/female)	0.869	0.603–1.252	0.451
BMI (kg/m^2)	1.006	0.967–1.046	0.775
Hypertension	1.520	1.014–2.278	0.041*
WBC (continuous)	1.060	1.021–1.100	0.002*
Eosinophils (continuous)	0.004	0.000–0.241	0.006*
Eosinophils =0 cells/L	Reference		
Eosinophils >0 cells/L	0.661	0.470–0.929	0.017*
Neutrophils (continuous)	1.000	0.994–1.006	0.986

*Statistically significant values.

TABLE 5 Predictors of mortality after AAAD surgery in multivariable logistic regression.

Variables	Odds Ratio	95%CI	*P* value
Model 1			
Age	1.040	1.027–1.054	<0.001*
Hypertension	1.373	0.907–2.077	0.134
WBC (continuous)	1.075	1.033–1.119	<0.001*
Eosinophils (continuous)	0.010	0.000–0.650	0.031*
Model 2			
Age	1.04	1.027–1.055	<0.001*
Hypertension	1.37	0.906–2.075	0.135
WBC (continuous)	1.08	1.039–1.124	<0.001*
Eosinophils =0 cells/L	Reference		
Eosinophils >0 cells/L	1.46	1.033–2.070	0.032*

*Statistically significant values.

TABLE 6 Five blood coagulation items in both eosinophil groups.

Variables	Total ($n = 1180$)	EOS of 0.00 ($n = 681$)	EOS > 0.00 ($n = 499$)	*P* value
PT (10–15 s)	12.6 (11.7–14.2)	12.8 (11.8–14.35)	12.4 (11.5–13.9)	<0.001*
INR (0.8–1.3 s)	1.11 (1.02–1.24)	1.12 (1.03–1.25)	1.09 (1.00–1.22)	0.001*
TT (16–18 s)	18.9 (17.2–21.5)	19.3 (17.5–22.1)	18.6 (16.9–20.9)	0.001*
APTT (23–27 s)	29.9 (26.9–37)	30.4 (26.9–39.3)	29.3 (26.8–34.55)	0.004*
D-dimer (0–0.5 mg/L)	5.21 (2.83–11.74)	5.28 (3.04–11.44)	4.96 (2.43–12.07)	0.207
Platelet (100–400 × 10^9/L)	137 (98.25–177)	125 (86–163)	157 (123–201)	<0.001*
Fibrinogen (2–4 g/L)	2.2 (1.6–3.0)	2.1 (1.6–2.7)	2.4 (1.7–3.3)	<0.001*

PT, prothrombin time; INR, international normalized ratio; TT, thrombin time; APTT, activated partial thromboplastin time.
*Statistically significant values.

Discussion

Our study found that EOS counts in the peripheral blood of patients with AAAD were significantly lower; up to 81.1% patients EOS counts below 0.02×10^9/L and 57.7% of patients had undetectable EOS counts (0.00×10^9/L), concomitant with higher mortality and longer ICU treatment days. When we compared Siglec-8 expression in the control group with AAAD patients (preoperative EOS counts = "0.00"), and also histological examinations, we observed no evidence that EOSs accumulated in the aortic interstitial spaces of patients with AAAD. From statistical analyses of coagulation functions (APTT, TT, INR, PT, and Fibrinogen), D-dimer levels, and platelet counts in patients with AAAD, lower EOS counts tended to represent worse coagulation functions, higher D-dimer levels, and lower platelet counts. Furthermore, infiltrating EOSs were observed from the thrombus in the false lumen. Therefore, EOSs may be recruited from the peripheral blood into the false lumen and be associated with thrombus formation.

Aortic dissection is characterized by damage and remodeling of the aortic media leading to secondary thrombosis and inflammation, with systemic signs of inflammatory activation and local inflammatory cell infiltration (10, 18). Inflammatory cells, such as neutrophils (11), lymphocytes (19), and macrophages (20) have been investigated during AAAD pathogenesis, but EOS studies are lacking. EOSs are not only inflammatory effector cells, but they exert several immune regulatory functions. EOS counts in a large CVD patient cohort and experimental rat data on aortic aneurysms support the conclusion that EOS exert major protective roles in CVD (12). EOS deficiency increased abdominal aortic aneurysm growth, inflammatory cell lesion levels, angiogenesis, elastic rupture of the arterial wall, lesion cell apoptosis, SMC loss, and M1 macrophage marker expression (14). False lumen formation and subsequent thrombosis are important features in AAAD acute phases. Reports of thrombotic events in patients with EOS-related disease confirmed EOS involvement in thrombosis, i.e., promoting thrombosis through eosinophilic extracellular traps, thereby enhancing platelet activation, leading to atherosclerosis and stable thrombosis (16). Additionally, EOS may be involved in coronary thrombosis in acute myocardial infarction *via* inflammatory mechanisms (21). Activated PLT is associated with EOS pathology in several diseases, including asthma and hyper-eosinophilic syndrome (22). PLT is activated by EOS particles, major basic protein, and EOS peroxidase (23). Our data also suggested that EOS may be involved in false lumen thrombus formation in patients with AAAD.

Whether EOSs promote vascular injury, induce pro-inflammatory effects, or are simply recruited to tissue injury sites remain unclear. The main goal of AAAD surgery is to prevent fatal complications, and the more severe the preoperative vascular injury, the more likely it is to cause rupture, cardiac tamponade, and poor perfusion. Additionally, damaged vessels also make graft anastomosis more difficult during surgical treatment, resulting in postoperative complications such as bleeding and infection. Decreased EOS percentages may indicate severe vascular injury and more extensive thrombosis, therefore, EOS counts may be useful in assessing the extent of preoperative aortic injury in patients with AAAD.

Study limitations

Our research had some limitations. Most AAAD patients were first diagnosed in local hospitals, therefore it was difficult to obtain accurate information on false lumen thrombosis. Similarly, information on the effects of false lumen thrombosis on postoperative in-hospital survival rates are lacking. Partial thrombosis of the false cavity is an important independent predictor of mortality in patients with type B dissection, but it does not affect the long-term survival rate of AAAD survivors after discharge. Blood flow and thrombus may coexist, and most patients had EOS counts below the lower limit of detection, therefore it was difficult to quantify associations between false lumen thrombosis and the degree of EOS reduction through limited specimen. Additionally, in considering intraoperative bleeding, blood transfusion, and postoperative anti-infection treatment, we did not continuously monitor EOS counts during hospitalization. Therefore, when EOSs leave the peripheral blood system, are they deposited in a thrombus or elsewhere, or are they destroyed or degraded? Furthermore, peripheral blood eosinophil counts have a circadian rhythm (peaked during nighttime) (24), the time of drawing blood may affect results. These questions require further investigation.

Conclusions

Peripheral blood EOS counts may be valid indicators for preoperative risk assessment in patients with AAAD. Circulating EOS levels below detection limits may not only indicate thrombosis, but may be significant in predicting AAAD severity and prognosis in patients with AAAD. Therefore, a rapid, simple, and low-cost peripheral blood EOS count test can be used to effectively assess preoperative risk in patients with AAAD.

Data availability statement

The original contributions presented in the study are included in the article/Supplementary Material, further inquiries can be directed to the corresponding author/s.

Ethics statement

Written informed consent was obtained from the individual(s) for the publication of any potentially identifiable images or data included in this article.

Author contributions

HLC and DJW designed the project. YJ, FZ, WX, XLT, YXX participated in the collection of data. XCQ and YXG performed the experiments, analyzed data and wrote the manuscript. All authors participated in writing and provided feedback. All authors contributed to the article and approved the submitted version.

Funding

This study was supported by funds from Nanjing Medical Science and Technology Development Key Project (ZKX20026), the National Natural Science Foundation of China (81970401).

Conflict of interest

The authors declare that the research was conducted in the absence of any commercial or financial relationships that could be construed as a potential conflict of interest.

Publisher's note

All claims expressed in this article are solely those of the authors and do not necessarily represent those of their affiliated organizations, or those of the publisher, the editors and the reviewers. Any product that may be evaluated in this article, or claim that may be made by its manufacturer, is not guaranteed or endorsed by the publisher.

Supplementary material

The Supplementary Material for this article can be found online at: https://www.frontiersin.org/articles/10.3389/fsurg.2022.969995/full#supplementary-material.

References

1. Bossone E, Eagle KA. Epidemiology and management of aortic disease: aortic aneurysms and acute aortic syndromes. *Nat Rev Cardiol*. (2021) 18(5):331–48. doi: 10.1038/s41569-020-00472-6

2. Malaisrie SC, Szeto WY, Halas M, Girardi LN, Coselli JS, Sundt 3rd TM, et al., The American association for thoracic surgery expert consensus document: surgical treatment of acute type A aortic dissection. *J Thorac Cardiovasc Surg*. (2021) 162(3):735–58.e2. doi: 10.1016/j.jtcvs.2021.04.053

3. Cifani N, Proietta M, Tritapepe L, Di Gioia C, Ferri L, Taurino M, et al. Stanford-A acute aortic dissection, inflammation, and metalloproteinases: a review. *Ann Med*. (2015) 47(6):441–6. doi: 10.3109/07853890.2015.1073346

4. Evangelista A, Isselbacher EM, Bossone E, Gleason TG, Eusanio MD, Sechtem U, et al. Insights from the international registry of acute aortic dissection: a 20-year experience of collaborative clinical research. *Circulation*. (2018) 137(17):1846–60. doi: 10.1161/CIRCULATIONAHA.117.031264

5. Clough RE, Nienaber CA. Management of acute aortic syndrome. *Nat Rev Cardiol*. (2015) 12(2):103–14. doi: 10.1038/nrcardio.2014.203

6. Morello F, Piler P, Novak M, Kruzliak P. Biomarkers for diagnosis and prognostic stratification of aortic dissection: challenges and perspectives. *Biomark Med*. (2014) 8(7):931–41. doi: 10.2217/bmm.14.38

7. Zeng T, Shi L, Ji Q, Shi Y, Huang Y, Liu Y, et al. Cytokines in aortic dissection. *Clin Chim Acta*. (2018) 486:177–82. doi: 10.1016/j.cca.2018.08.005

8. Haybar H, Shokuhian M, Bagheri M, Davari N, Saki N. Involvement of circulating inflammatory factors in prognosis and risk of cardiovascular disease. *J Mol Cell Cardiol*. (2019) 132:110–9. doi: 10.1016/j.yjmcc.2019.05.010

9. Ajala ON, Everett BM. Targeting inflammation to reduce residual cardiovascular risk. *Curr Atheroscler Rep*. (2020) 22(11):66. doi: 10.1007/s11883-020-00883-3

10. Luo F, Zhou XL, Li JJ, Hui RT. Inflammatory response is associated with aortic dissection. *Ageing Res Rev*. (2009) 8(1):31–5. doi: 10.1016/j.arr.2008.08.001

11. Wen D, Wu HY, Jiang XJ, Zhang HM, Zhou XL, Li JJ, et al. Role of plasma C-reactive protein and white blood cell count in predicting in-hospital clinical events of acute type A aortic dissection. *Chin Med J*. (2011) 124(17):2678–82. doi: 10.3760/cma.j.issn.0366-6999.2011.17.020

12. Verdoia M, Schaffer A, Cassetti E, Di Giovine G, Marino P, Suryapranata H, et al. Absolute eosinophils count and the extent of coronary artery disease: a single centre cohort study. *J Thromb Thrombolysis*. (2015) 39(4):459–66. doi: 10.1007/s11239-014-1120-3

13. Shah AD, Denaxas S, Nicholas O, Hingorani AD, Hemingway H. Low eosinophil and low lymphocyte counts and the incidence of 12 cardiovascular diseases: a CALIBER cohort study. *Open Heart*. (2016) 3(2):e000477. doi: 10.1136/openhrt-2016-000477

14. Liu CL, Liu X, Zhang Y, Liu J, Yang C, Luo S, et al. Eosinophils protect mice from angiotensin-II perfusion-induced abdominal aortic aneurysm. *Circ Res*. (2021) 128(2):188–202. doi: 10.1161/CIRCRESAHA.120.318182

15. Yuan X, Mitsis A, Semple T, Castro Verdes M, Cambronero-Cortinas E, Tang Y, et al. False lumen intervention to promote remodelling and thrombosis-the FLIRT concept in aortic dissection. *Catheter Cardiovasc Interv*. (2018) 92(4):732–40. doi: 10.1002/ccd.27599

16. Marx C, Novotny J, Salbeck D, Zellner KR, Nicolai L, Pekayvaz K, et al. Eosinophil-platelet interactions promote atherosclerosis and stabilize thrombosis with eosinophil extracellular traps. *Blood*. (2019) 134(21):1859–72. doi: 10.1182/blood.2019000518

17. Mansiroglu AK, Sincer I, Cosgun M, Gunes Y. Dating thrombus organization with eosinophil counts in deep venous thrombosis. *J Vasc Surg Venous Lymphat Disord*. (2021) 9(4):874–80. doi: 10.1016/j.jvsv.2020.10.012

18. Zhang R, Zhou J, Feng J, Zhao Z, Liu J, Li Z, et al. Inducing false lumen thrombosis for retrograde type A aortic dissection. *J Thorac Cardiovasc Surg*. (2017) 153(1):57–65. doi: 10.1016/j.jtcvs.2016.09.022

19. Erdolu B, As AK. C-Reactive protein and neutrophil to lymphocyte ratio values in predicting inhospital death in patients with Stanford type A acute aortic dissection. *Heart Surg Forum*. (2020) 23(4):E488–E92. doi: 10.1532/hsf.3055

20. Wang X, Zhang H, Cao L, He Y, Ma A, Guo W. The role of macrophages in aortic dissection. *Front Physiol*. (2020) 11:54. doi: 10.3389/fphys.2020.00054

21. Jiang P, Wang DZ, Ren YL, Cai JP, Chen BX. Significance of eosinophil accumulation in the thrombus and decrease in peripheral blood in patients with acute coronary syndrome. *Coron Artery Dis*. (2015) 26(2):101–6. doi: 10.1097/MCA.0000000000000186

22. Ames PR, Aloj G, Gentile F. Eosinophilia and thrombosis in parasitic diseases: an overview. *Clin Appl Thromb Hemost*. (2011) 17(1):33–8. doi: 10.1177/1076029609348314

23. Ulfman LH, Joosten DP, van Aalst CW, Lammers JW, van de Graaf EA, Koenderman L, et al. Platelets promote eosinophil adhesion of patients with asthma to endothelium under flow conditions. *Am J Respir Cell Mol Biol*. (2003) 28(4):512–9. doi: 10.1165/rcmb.4806

24. Engert LC, Weiler U, Pfaffinger B, Stefanski V, Schmucker SS. Diurnal rhythms in peripheral blood immune cell numbers of domestic pigs. *Dev Comp Immunol*. (2018) 79:11–20. doi: 10.1016/j.dci.2017.10.003

frontiers | Frontiers in Cardiovascular Medicine

TYPE Original Research
PUBLISHED 30 August 2022
DOI 10.3389/fcvm.2022.981546

Check for updates

Hemodynamic numerical simulation of aortic arch modular inner branched stent-graft in eight early patients from the first-in-human case series

Yating Zhu[1†], Fen Li[2†], Hongpeng Zhang[1*], Hui Song[2], Xiaodan Ma[3], Long Cao[4], Wenjun Zhang[5] and Wei Guo[1*]

[1]Department of Vascular Surgery, First Medical Center of Chinese People's Liberation Army General Hospital, Beijing, China, [2]College of Mechanical and Vehicle Engineering, Taiyuan University of Technology, Taiyuan, China, [3]Equipment Department, The Fourth People's Hospital of Taiyuan, Taiyuan, China, [4]Department of General Surgery, People's Liberation Army No. 983 Hospital, Tianjin, China, [5]Department of Ultrasonic Diagnosis, People's Liberation Army No. 980 Hospital, Shijiazhuang, China

Background: The modular inner branched stent-graft (MIBSG) (WeFlow-Arch^{TM}) is an emerging device for challenging aortic arch pathologies. Hemodynamic numerical simulation is conducive to predicting long-term outcomes as well as optimizing the stent-graft design.

Objective: This study aims to analyze the hemodynamic characteristics of the MIBSG devices based on numerical simulation analyses.

Methods: From June 2019 to June 2021, MIBSGs were utilized in eight cases. Numerical simulation analyses of branch perfusion and indicators including the time-averaged wall shear stress, oscillatory shear index, and relative residence time were performed.

Results: Lesions involved Zone 1 ($n = 2$), Zone 2 ($n = 4$), and Zone 3 ($n = 2$). Branched stent-grafts were deployed in the innominate artery and left common carotid artery ($n = 5$) or in the innominate artery and left subclavian artery ($n = 3$). The hemodynamic change in common was increased perfusion in the descending aorta and left common carotid artery. Half of the patients had increased cerebral perfusion of 8.7% at most, and the other half of the patients showed a reduction of 5.3% or less. Case 3 was considered to have acquired the greatest improvement in hemodynamic features.

Conclusion: The MIBSG showed improved hemodynamic features in most cases. The design of the MIBSG could be partly modified to acquire better hemodynamic performance.

KEYWORDS

aortic arch, thoracic endovascular aortic repair (TEVAR), thoracic stent-graft, inner branched stent-graft, hemodynamics, numerical simulation

OPEN ACCESS

EDITED BY
Hongkun Zhang,
Zhejiang University, China

REVIEWED BY
Jian Zhou,
Second Military Medical University, China
Ziheng Wu,
The First Affiliated Hospital of Zhejiang University, China

*CORRESPONDENCE
Hongpeng Zhang
zhanghongpeng@vip.sina.com
Wei Guo
guoweiplagh@sina.com

†These authors have contributed equally to this work and share first authorship

SPECIALTY SECTION
This article was submitted to Heart Surgery, a section of the journal Frontiers in Cardiovascular Medicine

RECEIVED 29 June 2022
ACCEPTED 04 August 2022
PUBLISHED 30 August 2022

CITATION
Zhu Y, Li F, Zhang H, Song H, Ma X, Cao L, Zhang W and Guo W (2022) Hemodynamic numerical simulation of aortic arch modular inner branched stent-graft in eight early patients from the first-in-human case series. *Front. Cardiovasc. Med.* 9:981546. doi: 10.3389/fcvm.2022.981546

What this paper adds

A multicenter clinical trial (GIANT Study) of an emerging modular inner branched stent-graft (WeFlow-Arch™) for challenging aortic arch lesions is in progress in China. This study presents the results of the numerical simulation analyses that verified significant hemodynamic improvement in most of the first-in-human cases and may allow identification of high-risk patients with potential long-term complications who require close follow-up. Hemodynamic numerical simulation should be performed to guide preoperative planning and optimize device designs for complicated endovascular aortic arch reconstructions.

Introduction

Thoracic endovascular aortic repair (TEVAR) for the treatment of aortic arch pathologies (AAPs) involves the creation of a sufficient landing zone with simultaneous branch vessel preservation, making the procedure very challenging. Morphological and physiological factors such as a curved aortic arch, anatomical variations and angles among the branch vessels, and high-speed and high-pressure pulsatile blood flow have significant impacts on the safety and efficacy of endovascular aortic arch reconstruction (1). During the last decade, significant progress has been made in TEVAR for AAPs. The use of stent-grafts (SGs) designed with single or double inner branches has been reported with encouraging early results (2–12). The modular inner branched SG (MIBSG) (WeFlow-Arch™; Weiqiang Medical Technology Co., Ltd., Hangzhou, China) is a contemporary option for the endovascular repair of AAPs. It was first proposed and designed by our center for aortic arch reconstruction in 2005, and the technical feasibility has been verified through animal experiments (13). Based on the promising early postoperative results from the first-in-human cases, a multicenter clinical trial (GIANT Study, NCT04765592, ChiCTR2100044591) is currently in progress in China. In contrast to conventional fenestrated or parallel SGs, the complicated geometry of the MIBSG is characterized by the ascending aorta landing (Zone 0) (14) combined with more metal scaffolding overlaps; these features are considered to have a significant impact on the physiological curvature, elastic deformation, wall stress, and blood flow streamline around the aortic arch (Figure 1). Therefore, a thorough evaluation of the postoperative hemodynamic characteristics and potential risk of late surgery-related complications is necessary.

The current procedural planning and efficacy assessment of TEVAR mainly rely on anatomic criteria of morphological improvement obtained by computed tomography angiography (CTA) with multiplanar reconstruction instead of an in-depth quantitative analysis of hemodynamic characteristics. Patients with good postoperative imaging morphology may still have long-term risks of complications such as endoleaks, stroke, stent collapse or occlusion, or SG-induced new entry (11), indicating that the current treatment strategies and device design should be optimized. In recent years, numerical simulations have been utilized to investigate peri-TEVAR hemodynamic characteristics such as the stress distribution, changes in the flow velocity and flow field, and the friction stability of SGs. Hence, we performed the present fluid dynamics numerical simulation in the early eight patients of the first-in-human MIBSG case series to evaluate the hemodynamic outcomes and accordingly predict the prognosis and optimize the design of the MIBSG device. We obtained written informed consent from every reported patient. The study was approved by the Ethics Committee of the Chinese People's Liberation Army General Hospital (S2018-230-01) and adhered to the principles of the Declaration of Helsinki.

Abbreviations: AAPs, aortic arch pathologies; CTA, computed tomography angiography; DA, descending aorta; IA, innominate artery; LCCA, left common carotid artery; RCCA, right common carotid artery; LSA, left subclavian artery; RSA, right subclavian artery; MIBSG, modular inner branched stent-graft; OSI, oscillatory shear index; RRT, relative residence time; SGs, stent-grafts; TAWSS, time-averaged wall shear stress; TEVAR, thoracic endovascular aortic repair; WSS, wall shear stress.

Materials and methods

Patients and devices

From June 2019 to June 2021, eight patients with aortic arch aneurysms who underwent interventions with MIBSGs were included in this study. None of the patients had typical chest or back pain, and all had been diagnosed *via* CTA before hospitalization. CTA of the entire aorta was performed at 1 week, 6 months, and 12 months after the intervention and yearly thereafter. The flow velocity of the supra-arch branches was acquired *via* Doppler ultrasound (LOGIQ 9; GE Healthcare, Chicago, IL, USA).

The MIBSG device (WeFlow-Arch™) was manufactured by Weiqiang Medical Technology Co., Ltd. (Hangzhou, China) according to each patient's need. This modular SG consists of three modules (Figure 1). The first module is a cylindrical ascending aortic SG coupled with double embedded tunnels that provide access to the innominate artery (IA) and the left common carotid artery (LCCA) or left subclavian artery (LSA). The second module refers to the branched SGs. The third module is the extension SG in the distal arch and descending aorta (DA). The procedure was performed as described in our previous report (15). Concomitant LCCA–LSA bypass or coil embolization of the LSA was performed if necessary.

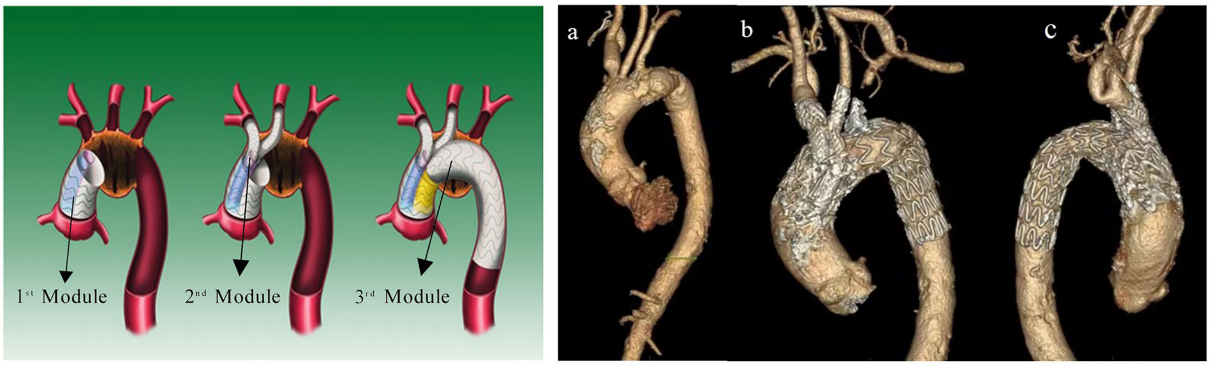

FIGURE 1
(Left) Diagram and **(right)** *in vivo* morphology of MIBSG. First module: main body stent-graft with double embedded tunnels landing in ascending aorta. Second module: two inner bridging stent-grafts to the supra-arch vessels. Third module: distal extending stent-graft in the descending aorta. **(a)** Preoperative morphology of aneurysm. **(b,c)** Postoperative morphology of MIBSG. MIBSG = modular inner branched stent-graft.

Geometrical reconstructions

Thin-slice CTA images of all the pathologies were acquired using a 256-row CT scanner (Revolution CT; GE Healthcare) with the following parameters: 512 × 512 × 700; pixel spacing, 0.785/0.785; resolution, 1.274 pixels/mm; and slice thickness, 1 mm. Three-dimensional geometric reconstruction with DICOM-format CTA images was then performed using commercial software (Mimics version 19.0; Materialise NV, Leuven, Belgium). Threshold segmentation and dynamic region growth commands were used to obtain the aortic contour model. The branches and the aortic arch were then separated and offset in 3-matic software (Materialise NV) to obtain the vascular wall with a vessel branch wall thickness of 1.0 mm and aortic wall thickness of 2.0 mm. The final model began above the level of the aortic sinus and ended at the level of the proximal renal artery. Commercial finite element method software (COMSOL 5; COMSOL, Inc., Burlington, MA, USA) was used for the computation of the fluid–structure interaction problem to analyze the coupling effects between blood flow and vessels. In default mode, COMSOL solvers dynamically adjust the time step, and the maximum time step was limited to 0.05 s to ensure that it was fine enough for the achievement of a time step-independent solution (Figure 2).

Computations framework

The blood flow and corresponding pulsatile vessel deformation substantially involve the fluid–structure interaction issue in computation. Blood is considered a homogeneous and incompressible Newtonian fluid in the aorta. In this study, we describe the blood flow behavior using the incompressible Navier–Stokes equation with the density and viscosity set at 1,060 kg/m^3 and 0.0035 Pa·s, respectively. An isotropic linear elastic material with Poisson's ratio of 0.49, Young's modulus of 7.5×10^5 Pa, and a density of 1,150 kg/m^3 was used as the vessel wall. The interaction between the blood and vessel wall was simulated using the arbitrary Lagrangian–Eulerian formulation.

Boundary condition

The pulsating blood flow within a cardiac cycle was simulated with the velocity boundary condition of the inlet measured with Doppler ultrasound and the pressure boundary condition of the outlet based on clinical monitoring (16, 17) (Figure 3). The formulas for velocity and pressure are as follows:

$$v(t) = \begin{cases} -0.3825cos\,(6.6667\pi\, t) + 0.6775, \\ 0 < t \leq 0.3\ s \\ -0.1405cos\,(3.3333\pi\ (t-0.3)) + 0.4355, \\ 0.3 < t \leq 0.6\ s \\ -0.1405cos\,(2.5\pi\ (t-1)) + 0.4355, \\ 0.6 < t \leq 1\ s \end{cases}$$

$$p(t) = \begin{cases} -25cos\,(4\pi t) + 115, \\ 0 < t \leq 0.35\ s \\ \left(p(0.35) - 90\right) \cos\,(0.7692\pi\ (t-0.35) + \pi - 1.5) \\ +p(0.35),\ 0.35 < t \leq 1\ s \end{cases}$$

Analysis of hemodynamic indicators

Three hemodynamic indicators based on wall shear stress (WSS) were quantified and calculated, namely, the time-averaged WSS (TAWSS), oscillatory shear index (OSI), and relative residence time (RRT). TAWSS is a scalar defined as

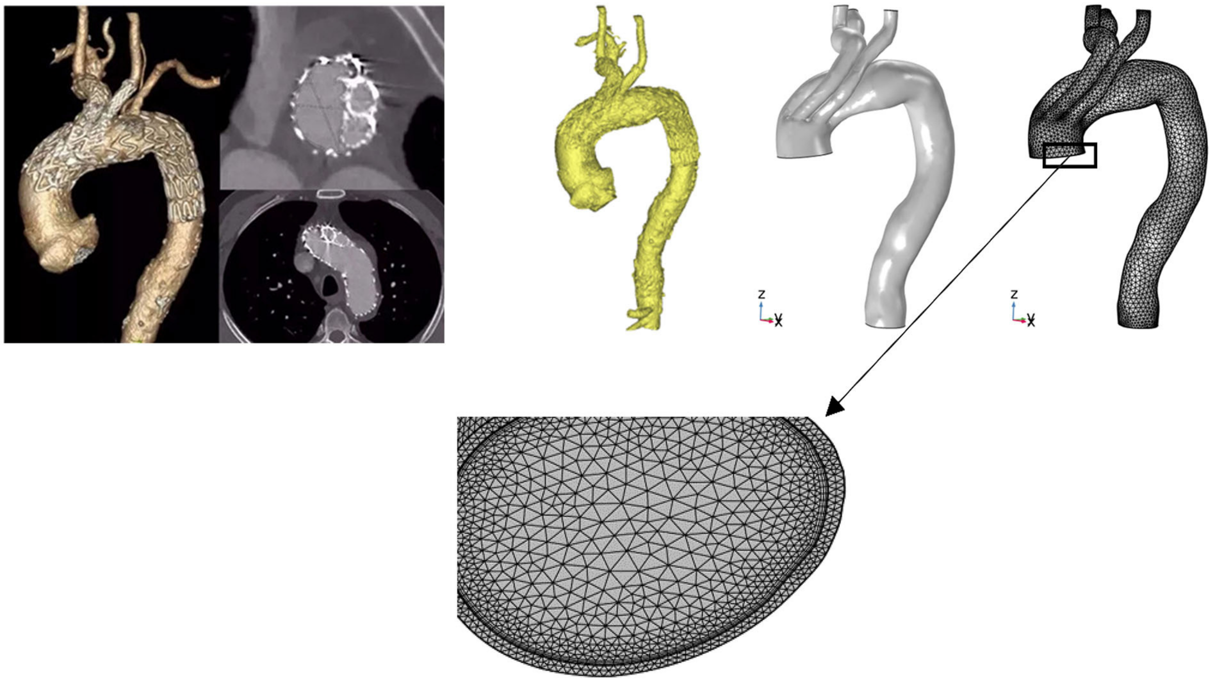

FIGURE 2
Three-dimensional reconstruction and mesh generation of MIBSG in Case 4. The three-dimensional geometry was reconstructed from computed tomography angiography images using Mimics 19.0. The branches and aortic arch were separated and offset in 3-matic software to obtain the vascular wall. Commercial finite element method software (COMSOL 5) was used for the computation of the hemodynamic flow. To obtain mesh-independent solutions, 2,927,088 elements were used for Case 4. Although the laminar model used in all instances was reportedly able to capture the characteristic flow patterns in the aortic arch, six layers of boundary layer mesh were used to resolve the near-wall flow accurately. MIBSG, modular inner branched stent-graft.

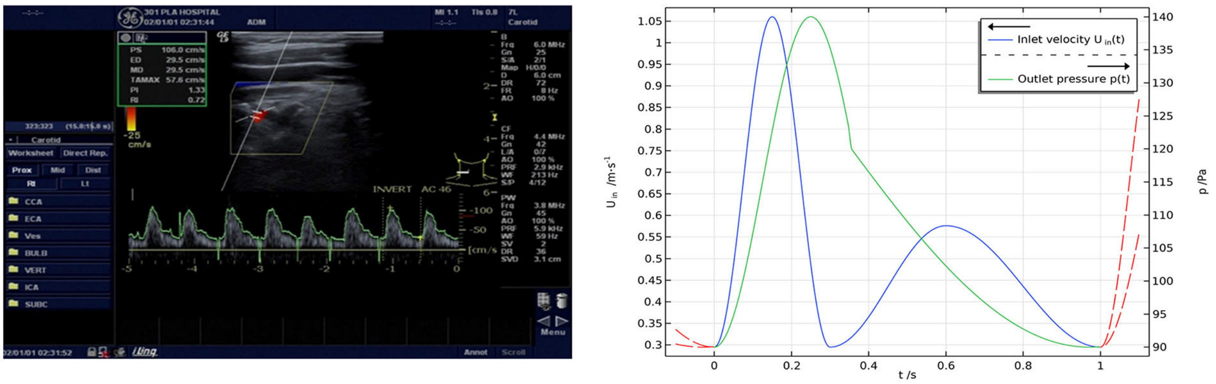

FIGURE 3
(Left) Results of Doppler ultrasonic velocimetry and **(right)** boundary conditions. The inlet boundary condition was set to a velocity condition measured with Doppler ultrasound, and the outlet boundary condition was set to a pressure condition according to clinical monitoring.

the time-averaged absolute magnitude of the surface traction vector. OSI refers to the wall shear stress oscillations within a cardiac cycle, and RRT represents the residence time of particles in a certain position. Regions with a TAWSS of <0.4 Pa, OSI of >0.25, and RRT of >5/Pa indicate a more remarkable tendency toward atherosclerosis (18). Areas with high-risk regions characterized by abnormal values of these indicators were distinguished to visualize this tendency. According to the mean shear stress defined by Taylor et al. (19) the formulas are expressed as follows:

$$TAWSS = \tau_{abs} = \frac{1}{T}\int_0^T \left|\overrightarrow{\tau_w}\right| dt$$

TABLE 1 Details of the eight interventions.

Cases	Lesions	Locations	Branch SGs	Assistant procedurals	Temporary pacemaker utilization	Complications
Case 1	Aneurysm	Zone 3	IA & LCCA	LCCA-LSA bypass, LSA embolization with coils	+	None
Case 2	Aneurysm	Zone 1	IA & LSA	LCCA-LSA bypass, proximal LCCA ligation	+	None
Case 3	Aneurysm	Zone 3	IA & LCCA	None	+	None
Case 4	Aneurysm	Zone 2	IA & LCCA	None	+	None
Case 5	Dissection aneurysm	Zone 1	IA & LSA	LCCA-LSA bypass, proximal LCCA ligation	+	Proximal endoleak (diminished in 6-months CTA)
Case 6	Aneurysm	Zone 2	IA & LCCA	LCCA-LSA bypass, LSA embolization with coils	+	None
Case 7	Aneurysm	Zone 2	IA & LCCA	None	+	None
Case 8	Aneurysm	Zone 2	IA & LSA	None	+	None

+, yes; CTA, computed tomography angiography; IA, innominate artery; LCCA, left common carotid artery; LSA, left subclavian artery; SGs, stent-grafts.

$$\tau_{mean} = \left| \frac{1}{T} \int_0^T \vec{\tau_w} dt \right|$$

$$OSI = \frac{1}{2}\left(1 - \frac{\tau_{mean}}{\tau_{abs}}\right)$$

$$RRT = \frac{1}{TAWSS\,(1 - 2\,OSI)}$$

Results

Interventions and morphological features

Details of the eight interventions and morphological features are presented in Table 1 and Figure 4. The diagnoses were saccular aneurysm ($n = 7$) and dissection aneurysm ($n = 1$). The lesions were located in the inner curvature ($n = 3$), anterior wall of the aorta ($n = 3$), or aortic full-cycle ($n = 2$); and involved Zone 1 ($n = 2$), Zone 2 ($n = 4$), or Zone 3 ($n = 2$). The branched SGs were deployed in the IA and LCCA ($n = 5$) or in the IA and LSA ($n = 3$). Concomitant LCCA–LSA bypass was performed in four cases. The original LSA was simultaneously occluded with several detachable fibered coils (Interlock-35; Boston Scientific, Natick, MA, USA). One immediate type I endoleak was observed in Case 5, and the leak had disappeared by the 6-month follow-up CTA.

Numerical simulations

Blood perfusion redistribution

The postoperative geometric morphologies of the SGs were good with fluent blood flows. The flow rate of each inlet and outlet was calculated *via* surface integration. Generally, the postoperative perfusions of branches differ from the preoperative baseline situation because of the influence of the MIBSG as well as the embolized LSA. Some changes in common included generally increased perfusions of the DA and LCCA, whereas the perfusion of the IA, right subclavian artery (RSA), and right common carotid artery (RCCA) decreased with some exceptions. The LSA perfusion was not calculated because most of the patients underwent intraoperative LSA coverage or embolization. Half of the patients had increased cerebral perfusion (sum of RCCA and LCCA, or sum of RCCA and LSA in patients with an occluded LCCA and in patients with auxiliary LCCA–LSA bypass) of 8.7% at most, and the other four patients showed slightly decreased perfusion at 5.3% or less. The detailed data are listed in Table 2.

Cases 2 and 7 represented opposite trends of perfusion changes. In Case 2, the perfusion increased in all branches except the RCCA, and the cerebral perfusion (sum of RCCA and LCCA) exhibited improvement. Within the whole cardiac cycle, backflow was observed in all branches except the RCCA (Figure 5). In contrast, the branch perfusions in Case 7 generally decreased (Figure 6). The perfusion in the DA within the whole cardiac cycle obviously increased; the perfusion in the LCCA stayed roughly the same; and the perfusion in the RSA, RCCA, and cerebral perfusion (sum of RCCA and LCCA) decreased compared with the preoperative baseline. Additionally, backflow was observed in all branches before and after TEVAR.

Case 3 is the unique patient with the unintended branch courses that the third module of the MIBSG coursed through the intersection angle between the two bridging SGs of the second module, leading to the separation of the bridging SGs on both sides of the third module instead of the desired morphology in the other seven cases. Despite this, the perfusions in Case 3 unexpectedly improved to a substantial degree. The perfusion

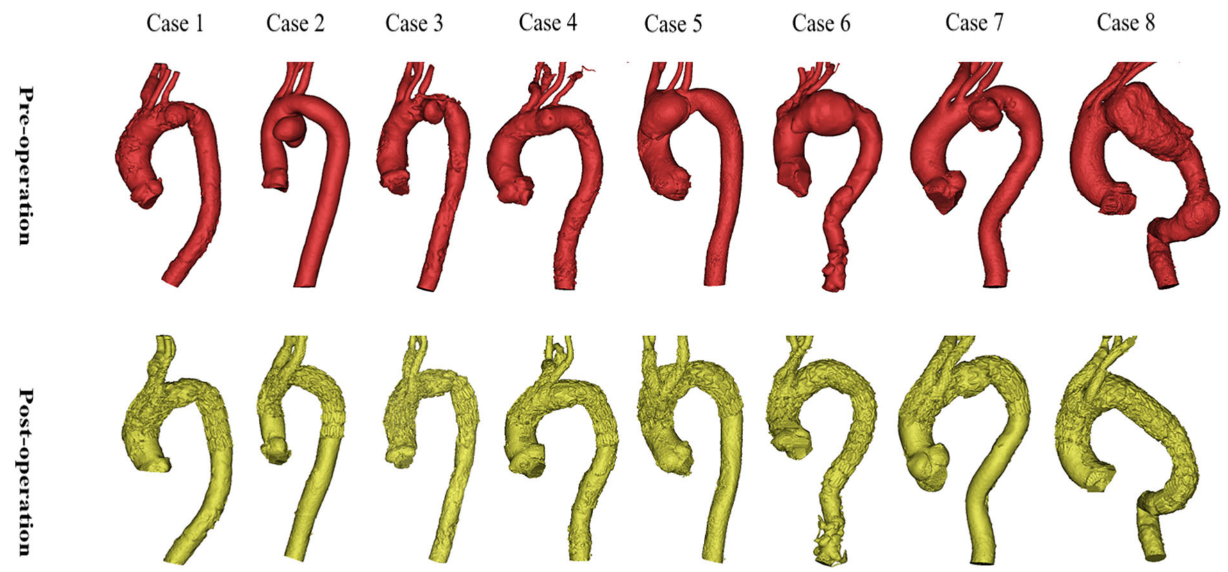

FIGURE 4
Preoperative and postoperative morphologies of the eight interventions. The morphologies and locations of the eight lesions are shown in the above images. The reconstructions of the arch and branch vessels are shown in the below images.

TABLE 2 Perfusion ratio changes of descending aorta and branches.

Cases	Branches with SGs	DA	IA	RSA	RCCA	LCCA/(LSA-LCCA)#	RCCA+LCCA/(RCCA +LSA)*
Case 1	IA & LCCA	↑ (83.3~86.4%)	↓ (9.9~8.9%)	↑	↓	↑	↓ (11.6~9.0%)
Case 2	IA & LSA	↓ (75.5~70.6%)	↑ (15.7~19.5%)	↑	↓	↑#	↑ (5.5~6.8%)*
Case 3	IA & LCCA	– (69.6~70.0%)	↓ (17.9~16.8%)	↓	–	↑	↑ (13.4~22.1%)
Case 4	IA & LCCA	↑ (83.8~85.4%)	↑ (8.2~9.8%)	↓	↑	↑	↑ (5.8~9.9%)
Case 5	IA & LSA	↑ (77.2~85.6%)	↓ (12.8~9.2%)	↓	↓	↑#	↑ (8.2~8.9%)*
Case 6	IA & LCCA	↑ (70.7~84.7%)	↓ (15.9~9.7%)	↓	↓	↓	↓ (13.9~9.4%)
Case 7	IA & LCCA	↑ (77.0~86.2%)	↓ (11.4~7.6%)	↓	↓	–	↓ (14.0~11.2%)
Case 8	IA & LSA	↑ (62.2~79.5%)	↓ (19.8~9.4%)	↓	↓	NA	↓ (21.9~16.6%)*

#, cases with LSA–LCCA bypass; *, perfusion of RCCA + LSA; ↑, increased; ↓, decreased; –, unchanged; NA, not available (occluded left internal carotid artery preoperatively); DA, descending aorta; IA, innominate artery; LCCA, left common carotid artery; RCCA, right common carotid artery; LSA, left subclavian artery; RSA, right subclavian artery; SGs, stent-grafts.

of the DA changed slightly, whereas the cerebral perfusion increased. Furthermore, during a single cardiac cycle, the amplitude between the maximum and minimum flow volume decreased compared with the preoperative baseline, and no backflow was observed (Figure 7).

Hemodynamic indicators

The postoperative WSS increased in two cases (Cases 4 and 7). They shared the same geometric features of the existing residual profile of the aneurysm postoperatively, and their areas containing a TAWSS of <0.4 Pa increased while the

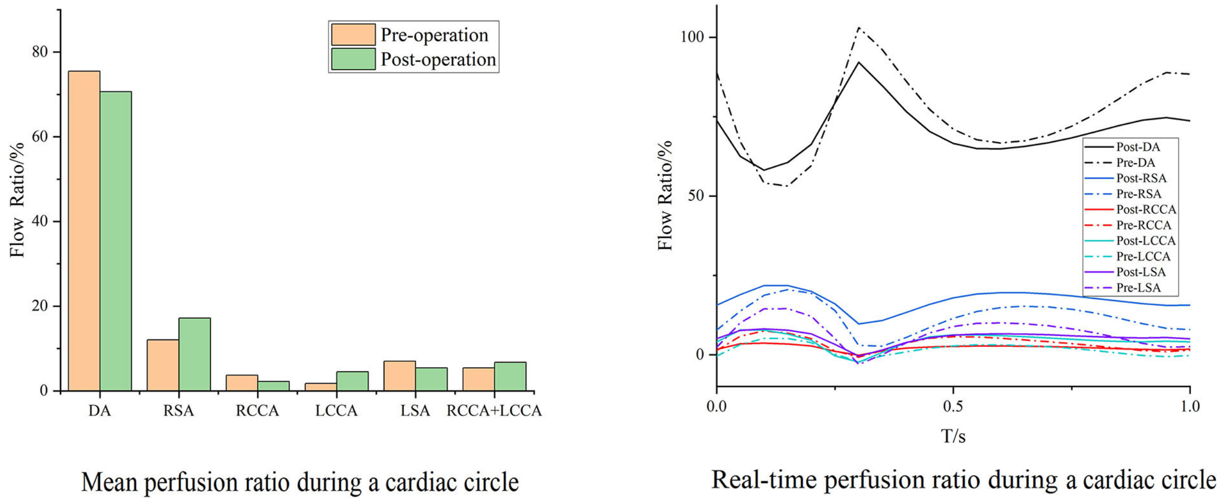

FIGURE 5
Blood flow perfusion ratios of branches in Case 2. The bar graph illustrates the changes in the flow perfusion ratios in different branches. The curve figure illustrates the real-time perfusion within a cardiac cycle. Curves below the 0 level indicate backflow. DA, descending aorta; LCCA, left common carotid artery; RCCA, right common carotid artery; LSA, left subclavian artery; RSA, right subclavian artery.

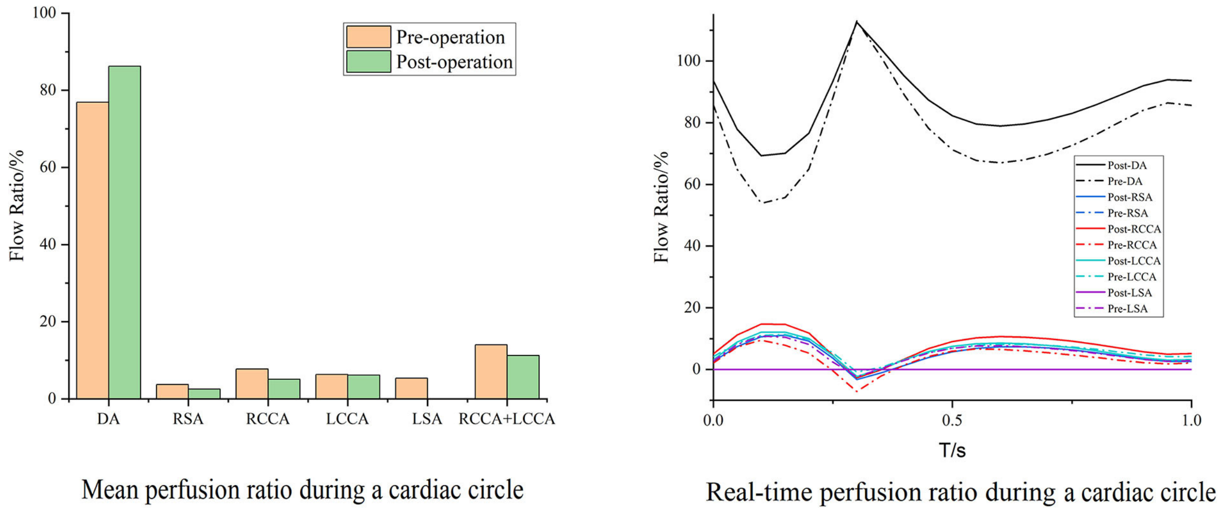

FIGURE 6
Blood flow perfusion ratios of branches in Case 7. The bar graph illustrates the changes in the flow perfusion ratios in different branches. The curve figure illustrates the real-time perfusion within a cardiac cycle. Curves below the 0 level indicate backflow. DA, descending aorta; LCCA, left common carotid artery; RCCA, right common carotid artery; LSA, left subclavian artery; RSA, right subclavian artery.

values decreased in the other six cases. Areas with an OSI of >0.25, indicating greater fluctuation of blood flow, increased postoperatively for all cases except Case 6. The areas with an RRT of >5/Pa increased in three cases, with larger values inferring a higher risk of atherosclerosis or stenosis (Table 3).

With the same consideration as in the aforementioned blood perfusion analyses, the hemodynamic features of Cases 2 and 7 were also analyzed in detail. The distributions of the TAWSS, OSI, and RRT in Case 2 are depicted in Figure 8. Preoperative characteristic TAWSS regions were mainly located at the aneurysm, the ostia of branches, and the DA. The total areas of a low postoperative TAWSS (<0.4 Pa) decreased significantly, while characteristic regions increased locally in the bridging SG in the LCCA. Areas with a higher OSI (>0.25) slightly increased in the LCCA and DA. The changes in the RRT were similar to the changes in the TAWSS. The preoperative flow patterns were complicated because of the aneurysm location and size. The aneurysm was sealed, after which the blood

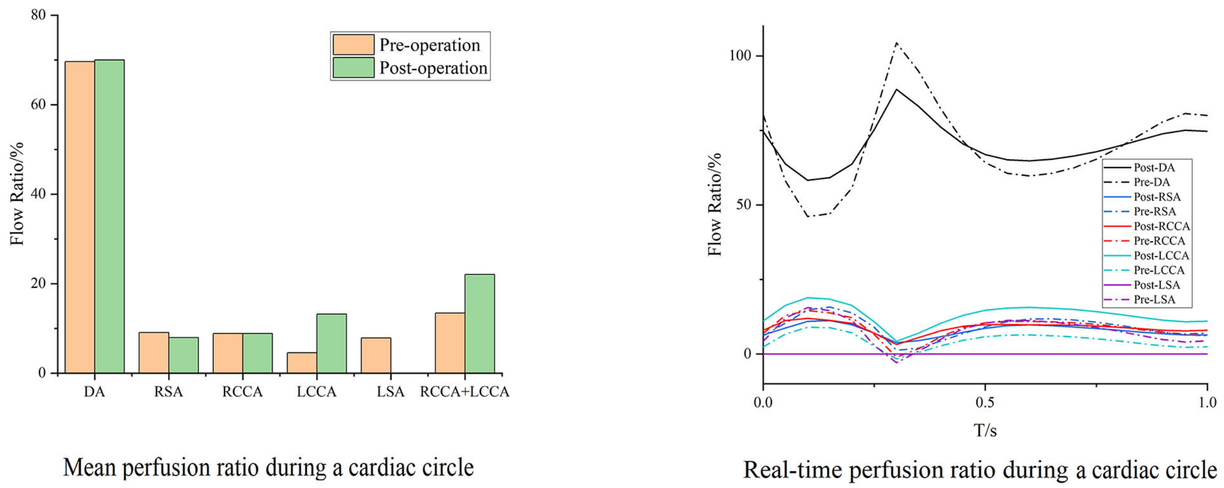

FIGURE 7
Blood flow perfusion ratios of branches in Case 3. The bar graph illustrates the changes in the flow perfusion ratios in different branches. The curve figure illustrates the real-time perfusion within a cardiac cycle. Curves below the 0 level indicate backflow. DA, descending aorta; LCCA, left common carotid artery; RCCA, right common carotid artery; LSA, left subclavian artery; RSA, right subclavian artery.

TABLE 3 Area changes of hemodynamic indicators.

Cases	TAWSS<0.4Pa	OSI>0.25	RRT>5(1/pa)	Areas increased in IA SGs	Areas increased in LCCA/LSA SGs
Case 1	↓	↑	↑	OSI, RRT	OSI, RRT
Case 2#	↓	↑	↓	None	TAWSS, OSI, RRT
Case 3	↓	↑	↓	None	None
Case 4	↑	↑	↑	TAWSS, OSI, RRT	TAWSS, OSI, RRT
Case 5#	↓	↑	↓	TAWSS, OSI, RRT	None
Case 6	↓	↓	↓	TAWSS, OSI, RRT	None
Case 7	↑	↑	↑	TAWSS, OSI, RRT	TAWSS, OSI, RRT
Case 8#	↓	↑	↓	TAWSS, OSI, RRT	None

#, cases with LSA SGs; ↑, increased; ↓, decreased; IA, innominate artery; LCCA, left common carotid artery; LSA, left subclavian artery; OSI, oscillatory shear index; RRT, relative residence time; SGs, stent-grafts; TAWSS, time-averaged wall shear stress.

flow streamlines became smoother. The distributions of the postoperative TAWSS and RRT then significantly improved.

The postoperative characteristic regions of Case 7 increased (Figure 9). Regions with a lower TAWSS (<0.4 Pa) appeared mainly at the former aneurysm site and in the lumens of SGs in the IA and LCCA. The regions with a larger OSI (>0.25) and RRT (>5/Pa) showed similar distributions. The characteristic regions appeared in the branched SGs, indicating fluctuation of blood flow to some extent. The postoperative residual profile of the aneurysm may have been the geometric morphological cause of these flow patterns.

Case 3 has obtained the greatest improvement in hemodynamic features according to the postoperative distributions of high-risk regions (Figure 10). The preoperative high-risk regions were located mainly around the ascending aorta, the aneurysmal sac, and the inner curve of the DA. There was less distribution of characteristic regions in the branch vessels, and it remained tiny postoperatively. This feature is very different from that of other cases. The postoperative areas with a TAWSS of <0.4 Pa decreased significantly. The distribution of these regions appeared mostly around the intersection point between the second and third modules. The postoperative distribution of an RRT of >5/Pa was highly consistent with that of a TAWSS of <0.4 Pa. Regions with an OSI of >0.25 increased slightly around the overlap zone of the inner branched SGs. In general, the above-mentioned special postoperative morphology of the bridging SGs did not complicate the blood flow pattern, and ideal hemodynamic features were observed in Case 3.

Discussion

The hemodynamic characteristics of the aortic arch are complex because of its special anatomical morphology. On

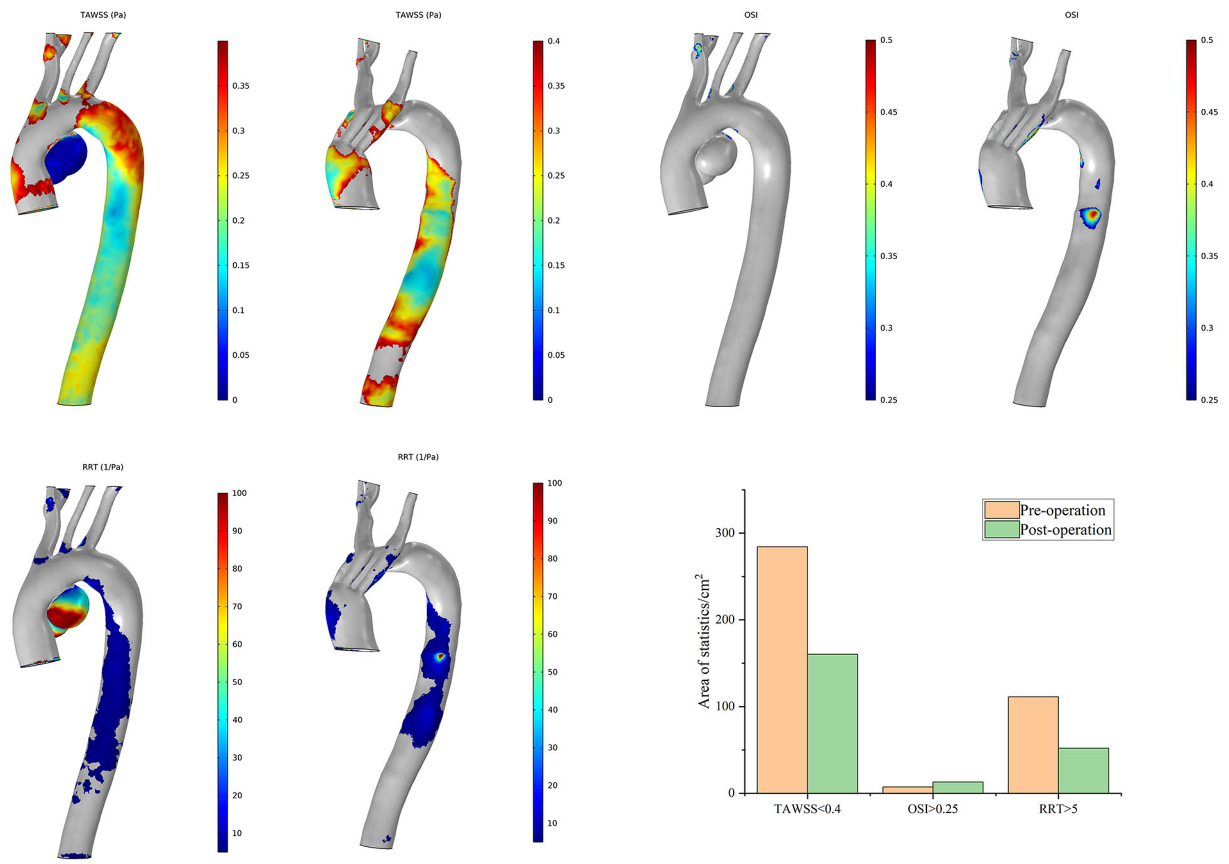

FIGURE 8
Distributions of changes in TAWSS, OSI, and RRT in Case 2. The hemodynamic characteristic regions are visually illustrated as a color distribution nephogram with each indicator in a group (left, preoperative; right, postoperative). Areas were calculated and illustrated in the bar graph. OSI, oscillatory shear index; RRT, relative residence time; TAWSS, time-averaged wall shear stress.

this basis, it is superimposed on the influences from either the lesions or the SGs, giving local individualized fluid and solid mechanical properties. These features are different from normal physiological conditions and are closely related to the long-term outcomes of TEVAR. In recent years, scholars have attempted to analyze the hemodynamic characteristics of AAPs through numerical simulation to better understand the pathophysiological influences of intervention (20, 21). Some studies have confirmed that the pulsating blood flow is subjected to the dual effects of the radial pressure gradient and centrifugal force when it flows through a twisted arch at high speed, and secondary flow thus forms perpendicular to the main flow direction (22, 23). Furthermore, the streamlines in the supra-arch branches are twisted to the distal end of the vessels, and a reflux phenomenon occurs at the proximal end of the branches (24, 25). These characteristics were verified in our simulation under steady-state conditions. Backflows were also observed preoperatively in most branches under normal physiological conditions. This is not the unique phenomenon caused by MIBSG implantation. In this respect, there is no significant change in the postoperative flow pattern.

Minimization of neurological complications remains a major concern of all procedures addressing AAPs, irrespective of whether open surgery or TEVAR is performed. The intra- and post-operation strokes are generally due to the embolism during manipulation. While the influence of that if the long-term flow perfusion changes after MIBSG intervention increases, the risk of late neurological adverse events should be considered. Perfusion of the supra-arch branches can be evaluated *via* numerical simulation analyses. Our results showed that the perfusion increased in the DA in most cases and accordingly decreased in the brachiocephalic vessels. Interestingly, however, elevated LCCA perfusion was observed in most cases, although the RCCA perfusion showed a general reduction. As a result of this, the cerebral perfusion increased in four cases but decreased in the other four cases with acceptable variations. In this sense, the redistribution of blood flow after MIBSG deployment does not necessarily increase the risk of neurological complications. The numerical simulation showed that both

10.3389/fcvm.2022.981546

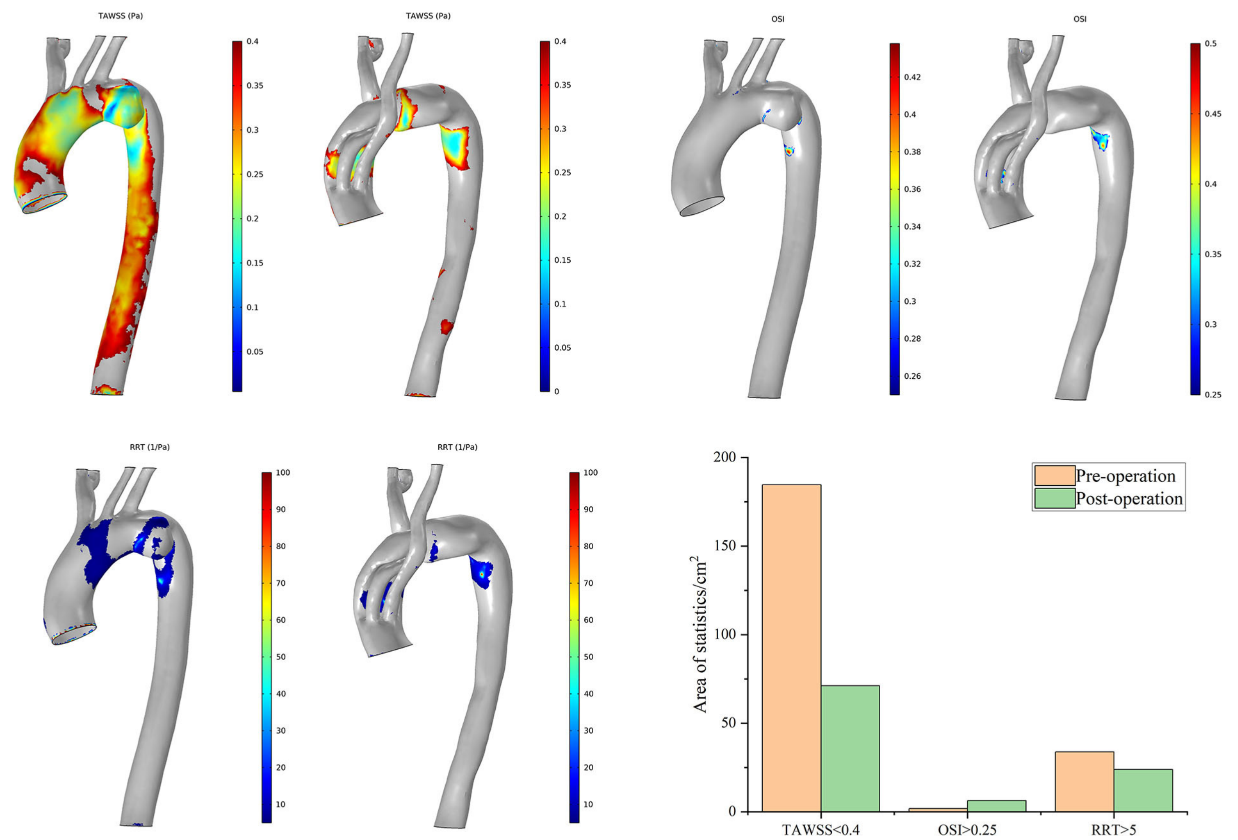

FIGURE 9
Distributions of changes in TAWSS, OSI, and RRT in Case 7. The hemodynamic characteristic regions are visually illustrated as a color distribution nephogram with each indicator in a group (left, preoperative; right, postoperative). Areas were calculated and illustrated in the bar graph. OSI, oscillatory shear index; RRT, relative residence time; TAWSS, time-averaged wall shear stress.

the flow rate and flow resistance were associated with the vessel diameters and the winding courses of the branches. Perfusion in the RCCA could be improved by enlarging the inner-branch diameters and adjusting the direction of the inner-branch tunnels. The parameters of the MIBSG could be accordingly modified to lower the flow resistance and reduce the tortuosity of the bridging SGs, eventually obtaining optimized hemodynamic properties.

From a hemodynamic viewpoint, regions with a TAWSS of <0.4 Pa, OSI of >0.25, and RRT of >5/Pa indicate a higher risk of atherosclerosis. In six cases, the improvements in low blood flow mechanical parameters were identified for that the areas with a TAWSS of <0.4 Pa decreased. A higher RRT indicates a longer time during which tangible substances stay in the vessels. Thus, the distribution of high-RRT regions is helpful to locate high-risk sites in which deposits are likely to form, eventually leading to atherosclerosis or restenosis. High-RRT areas increased in three cases in this study, and further follow-up will be required in these cases. A higher OSI represents a greater oscillation intensity in the shear stress direction and more frequent changes in the flow direction. In this study, areas with an OSI of >0.25 increased in most cases. This indicates that the disorder of blood flow characteristics increased throughout the whole cardiac cycle, resulting in the oscillation of the flow direction in the SGs. We inferred that this was related to the fact that the bridging SGs lengthened the distance of the supra-arch trunks from the top of the aortic arch into the proximal ascending aorta. Changes in the diameters and directions along this route can lead to streamline disorder. This is thought to be a systematic risk that originates from the unique structure of the devices used and cannot be completely avoided. To some extent, it is a limitation of all TEVAR procedures.

In general, the postoperative hemodynamic properties remarkably improved in most cases as indicated by the fact that the preoperative characteristic regions (which were mainly located around the aneurysm sac, the ostia or bifurcations of branches, and the DA) significantly decreased after coverage with the MIBSGs. However, the postoperative characteristic regions appeared in the lumens of the branched SGs in some cases (e.g., Case 7). Although the impact on the vessel intima may be relatively low because of the protection provided by the SG membrane, there are still long-term risks of atherosclerosis

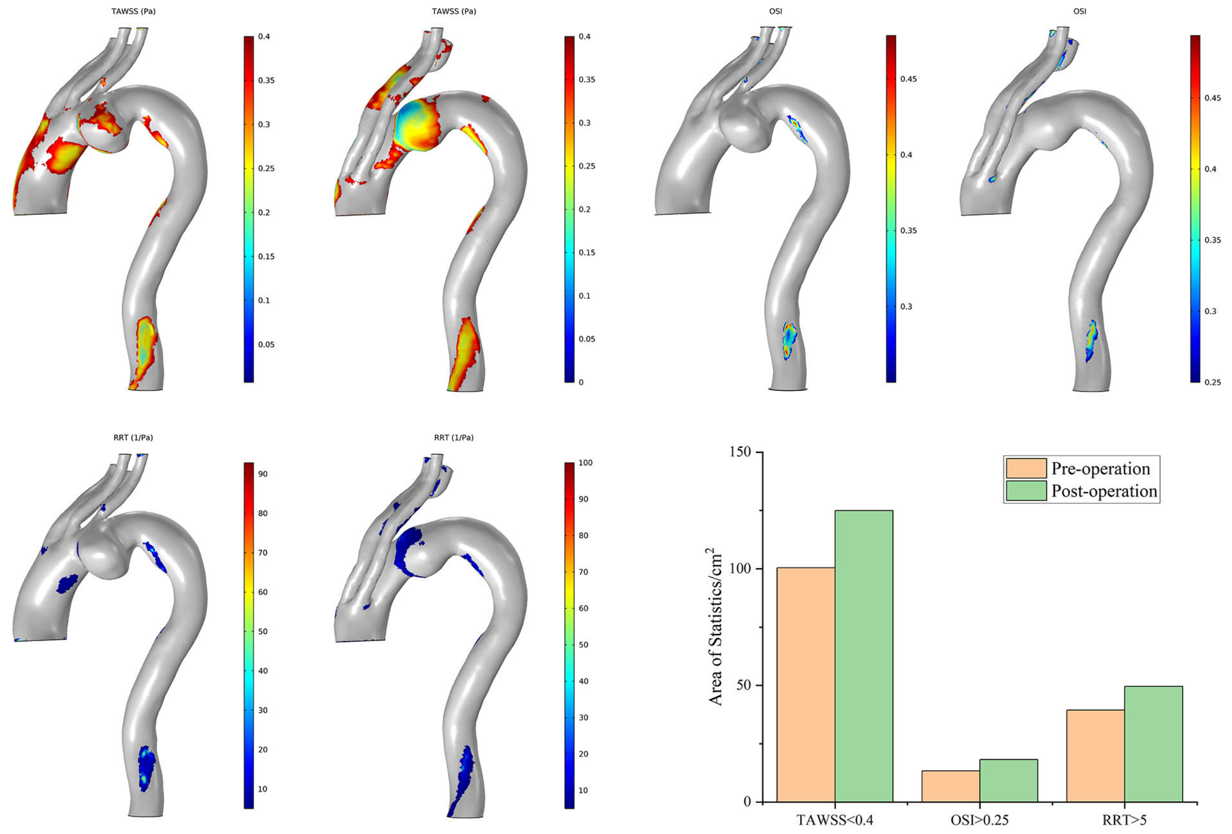

FIGURE 10
Distributions of changes in TAWSS, OSI, and RRT in Case 3. The hemodynamic characteristic regions are visually illustrated as a color distribution nephogram with each indicator in a group (left, preoperative; right, postoperative). Areas were calculated and illustrated in the bar graph. OSI, oscillatory shear index; RRT, relative residence time; TAWSS, time-averaged wall shear stress.

and subsequent restenosis in patients with postoperative residual characteristic regions around either the interface between the SGs and vessels or the IA bifurcation. Therefore, close follow-up is needed. Notably, the greatest hemodynamic improvement was observed in Case 3, which involved the unexpected deployment of the third module crossing the intersection angle between the two inner-branch SGs. This is inconsistent with the existing understanding based on CTA morphology. The presumed reason may be that the axes of both the first and second modules were almost parallel with the axis of the ascending aorta. Thus, there was minimal impact on the streamlines in this region.

These hemodynamic analysis results are helpful for predicting the risks of an adverse prognosis in individual patients. They can also be utilized in preoperative planning. For a patient who is presumed to have poor postoperative hemodynamic characteristics, the clinician may re-examine the rationality of the operative plan or individualize the devices to improve their hemodynamic performance. We recommend this hemodynamic evaluation as an important criterion for preoperative planning and postoperative follow-up in patients undergoing TEVAR involving the aortic arch.

Limitations

This study had two main limitations. First, to simplify the complex calculations, the rigidity of the implants was not considered. Second, the number of cases was small and the follow-up time was relatively short. The long-term result is needed to prove the effect of hemodynamic numerical simulation.

Conclusion

The MIBSG device provided promising early-term results in these eight first-in-human cases. The numerical analysis showed improved hemodynamic features of the aorta and supra-arch branches in most cases. Some patients required close follow-up because of the increased hemodynamic risks of late complications. The design of the MIBSG could be partly modified to acquire better hemodynamic performance and thus improve the long-term outcomes. Hemodynamic numerical simulation is a clinically valuable way to guide TEVAR management. Additional evidence is needed in patients with aortic arch involvement.

Data availability statement

The raw data supporting the conclusions of this article will be made available by the authors, without undue reservation.

Ethics statement

The studies involving human participants were reviewed and approved by Ethics Committee of the Chinese People's Liberation Army General Hospital (S2018-230-01). The patients/participants provided their written informed consent to participate in this study. Written informed consent was obtained from the individual(s) for the publication of any potentially identifiable images or data included in this article.

Author contributions

WG, YZ, FL, and HZ designed the study. YZ, FL, HS, XM, and WZ analyzed and interpreted the data. HZ and LC collected the data. YZ and FL drafted the article. All authors listed have made a substantial, direct, and intellectual contribution to the work and approved it for publication.

Funding

This research was supported by the Beijing Municipal Natural Science Foundation (Grant Number 7212095) and Capital's Funds for Health Improvement and Research (Grant Number 2020-2Z-5014).

Acknowledgments

We thank Angela Morben, DVM, ELS, from Liwen Bianji (Edanz) (www.liwenbianji.cn), for editing the English text of a draft of this manuscript.

Conflict of interest

WG is the designer of the modular inner branched stent-graft and the principal investigator of the GIANT clinical trials.

The remaining authors declare that the research was conducted in the absence of any commercial or financial relationships that could be construed as a potential conflict of interest.

Publisher's note

All claims expressed in this article are solely those of the authors and do not necessarily represent those of their affiliated organizations, or those of the publisher, the editors and the reviewers. Any product that may be evaluated in this article, or claim that may be made by its manufacturer, is not guaranteed or endorsed by the publisher.

References

1. Lioupis C, Abraham CZ. Results and challenges for the endovascular repair of aortic arch aneurysms. *Perspect Vasc Surg Endovasc Ther.* (2011) 23:202–13. doi: 10.1177/1531003511413608

2. Clough RE, Spear R, Van Calster K, Hertault A, Azzaoui R, Sobocinski J, et al. Case series of aortic arch disease treated with branched stent-grafts. *Br J Surg.* (2018) 105:358–65. doi: 10.1002/bjs.10681

3. Haulon S, Greenberg RK, Spear R, Eagleton M, Abraham C, Lioupis C, et al. Global experience with an inner branched arch endograft. *J Thorac Cardiovasc Surg.* (2014) 148:1709–16. doi: 10.1016/j.jtcvs.2014.02.072

4. Tsilimparis N, Detter C, Law Y, Rohlffs F, Heidemann F, Brickwedel J, et al. Single-center experience with an inner branched arch endograft. *J Vasc Surg.* (2019) 69:977–85e1. doi: 10.1016/j.jvs.2018.07.076

5. Czerny M, Rylski B, Morlock J, Schröfel H, Beyersdorf F, Saint Lebes B, et al. Orthotopic branched endovascular aortic arch repair in patients who cannot undergo classical surgery. *Eur J Cardiothorac Surg.* (2018) 53:1007–12. doi: 10.1093/ejcts/ezx493

6. Tazaki J, Inoue K, Higami H, Higashitani N, Toma M, Saito N, et al. Thoracic endovascular aortic repair with branched inoue stent graft for arch aortic aneurysms. *J Vasc Surg.* (2017) 66:1340–8e5. doi: 10.1016/j.jvs.2017.03.432

7. Patel HJ, Dake MD, Bavaria JE, Singh MJ, Filinger M, Fischbein MP, et al. Branched endovascular therapy of the distal aortic arch: preliminary results of the feasibility multicenter trial of the gore thoracic branch endoprosthesis. *Ann Thorac Surg.* (2016) 102:1190–8. doi: 10.1016/j.athoracsur.2016.03.091

8. Ferrer C, Cao P, Coscarella C, Ferri M, Lovato L, Camparini S, et al. iTalian RegIstry of doUble inner branch stent graft for arch PatHology (the TRIUmPH Registry). *J Vasc Surg.* (2019) 70:672–82.e1. doi: 10.1016/j.jvs.2018.11.046

9. Lioupis C, Corriveau MM, MacKenzie KS, Obrand DI, Steinmetz OK, Abraham CZ. Treatment of aortic arch aneurysms with a modular transfemoral multibranched stent graft: initial experience. *Eur J Vasc Endovasc Surg.* (2012) 43:525–32. doi: 10.1016/j.ejvs.2012.01.031

10. Ferrer C, Coscarella C, Cao P. Endovascular repair of aortic arch disease with double inner branched thoracic stent graft: the Bolton perspective. *J Cardiovasc Surg.* (2018) 59:547–53. doi: 10.23736/S0021-9509.18.10410-1

11. Spear R, Haulon S, Ohki T, Tsilimparis N, Kanaoka Y, Milne CP, et al. Editor's Choice- Subsequent results for arch aneurysm repair with inner branched endografts. *Eur J Vasc Endovasc Surg.* (2016) 51:380–5. doi: 10.1016/j.ejvs.2015.12.002

12. Anwar MA, Hamady M. Various endoluminal approaches available for treating pathologies of the aortic arch. *Cardiovasc Intervent Radiol.* (2020) 43:1756–69. doi: 10.1007/s00270-020-02561-y

13. Yang DH, Guo W, Liu XP, Yin T, Jia X, Zhang HP, et al. The feasibility study of endovascular reconstruction of aortic arch with modular branched stent-graft system in canine. *Zhonghua Wai Ke Za Zhi.* (2007) 45:1346–9. Chinese. doi: 10.3760/j.issn:0529-5815.2007.19.016

14. Fillinger MF, Greenberg RK, McKinsey JF, Chaikof EL, Society for Vascular Surgery Ad Hoc Committee on TEVAR Reporting Standards. Reporting standards for thoracic endovascular aortic repair (TEVAR). *J Vasc Surg.* (2010) 52:1022–33. doi: 10.1016/j.jvs.2010.07.008

15. Guo W, Zhang H, Liu X, Ren W, Wang Y. Endovascular repair of aortic arch aneurysm with a new modular double inner branch stent graft. *Ann Vasc Surg.* (2021) 77:347.e1–5. doi: 10.1016/j.avsg.2020.05.053

16. Grinberg L, Karniadakis GE. Outflow boundary conditions for arterial networks with multiple outlets. *Ann Biomed Eng.* (2008) 36:1496–514. doi: 10.1007/s10439-008-9527-7

17. Qiu Y, Yuan D, Wang Y, Wen J, Zheng T. Hemodynamic investigation of a patient-specific abdominal aortic aneurysm with iliac artery tortuosity. *Comput Methods Biomech Biomed Engin.* (2018) 21:824–33. doi: 10.1080/10255842.2018.1522531

18. Malek AM, Alper SL, Izumo S. Hemodynamic shear stress and its role in atherosclerosis. *JAMA.* (1999) 282:2035–42. doi: 10.1001/jama.282.21.2035

19. Taylor CA, Hughes TJ, Zarins CK. Effect of exercise on hemodynamic conditions in the abdominal aorta. *J Vasc Surg.* (1999) 29:1077–89. doi: 10.1016/S0741-5214(99)70249-1

20. Ong C, Xiong F, Kabinejadian F, Praveen Kumar G, Cui F, Chen G, et al. Hemodynamic analysis of a novel stent graft design with slit perforations in thoracic aortic aneurysm. *J Biomech.* (2019) 85:210–7. doi: 10.1016/j.jbiomech.2019.01.019

21. Tse KM, Chang R, Lee HP, Lim SP, Venkatesh SK, Ho P. A computational fluid dynamics study on geometrical influence of the aorta on haemodynamics. *Eur J Cardiothorac Surg.* (2013) 43:829–38. doi: 10.1093/ejcts/ezs388

22. Hashemi A, Fischer PF, Loth F. Direct numerical simulation of transitional flow in a finite length curved pipe. *J Turbul.* (2018) 19:664–82. doi: 10.1080/14685248.2018.1497293

23. Gao F, Watanabe M, Matsuzawa T. Stress analysis in a layered aortic arch model under pulsatile blood flow. *Biomed Eng Online.* (2006) 5:25. doi: 10.1186/1475-925X-5-25

24. Shahcheraghi N, Dwyer HA, Cheer AY, Barakat AI, Rutaganira T. Unsteady and three-dimensional simulation of blood flow in the human aortic arch. *J Biomech Eng.* (2002) 124:378–87. doi: 10.1115/1.1487357

25. Morris L, Delassus P, Callanan A, Walsh M, Wallis F, Grace P, et al. 3-D numerical simulation of blood flow through models of the human aorta. *J Biomech Eng.* (2005) 127:767–75. doi: 10.1115/1.1992521

frontiers | Frontiers in Cardiovascular Medicine

TYPE Original Research
PUBLISHED 13 September 2022
DOI 10.3389/fcvm.2022.979431

Check for updates

OPEN ACCESS

EDITED BY
Emiliano Chisci,
Nuovo Ospedale San Giovanni di Dio, Italy

REVIEWED BY
Laura DiChiacchio,
The University of Utah, United States
Sandeep Sainathan,
University of Miami Health System, United States

*CORRESPONDENCE
Tucheng Sun
suntucheng@126.com
Jinlin Wu
wujinlin@gdph.org.cn

†These authors have contributed equally to this work

SPECIALTY SECTION
This article was submitted to Heart Surgery, a section of the journal Frontiers in Cardiovascular Medicine

RECEIVED 27 June 2022
ACCEPTED 18 August 2022
PUBLISHED 13 September 2022

CITATION
Zhu J, Tong G, Zhuang D, Yang Y, Liang Z, Liu Y, Yu C, Zhang Z, Chen Z, Liu J, Yang J, Li X, Fan R, Sun T and Wu J (2022) Surgical treatment strategies for patients with type A aortic dissection involving arch anomalies.
Front. Cardiovasc. Med. 9:979431.
doi: 10.3389/fcvm.2022.979431

Surgical treatment strategies for patients with type A aortic dissection involving arch anomalies

Jiade Zhu†, Guang Tong†, Donglin Zhuang, Yongchao Yang, Zhichao Liang, Yaorong Liu, Changjiang Yu, Zhen Zhang, ZeRui Chen, Jie Liu, Jue Yang, Xin Li, Ruixin Fan, Tucheng Sun* and Jinlin Wu*

Department of Cardiac Surgery, Guangdong Cardiovascular Institute, Guangdong Provincial People's Hospital, Guangdong Academy of Medical Sciences, Guangzhou, China

Objective: The aim of the study was to investigate surgical modalities and outcomes in patients with type A aortic dissection involving arch anomalies.

Method: Patients with type A aortic dissection who underwent surgical treatment at our center between January 2017 and 31 December 2020 were selected for this retrospective analysis. Data including computed tomography (CT), surgical records, and cardiopulmonary bypass records were analyzed. Perioperatively survived patients were followed up, and long-term mortality and aortic re-interventions were recorded.

Result: A total of 81 patients with arch anomalies were included, 35 with "bovine" anomalies, 23 with an aberrant right subclavian artery, 22 with an isolated left vertebral artery, and one with a right-sided arch + aberrant left subclavian artery. The strategies of arch management and cannulation differed according to the anatomic variation of the aortic arch. In total, seven patients (9%) died after surgery. Patients with "bovine" anomalies had a higher perioperative mortality rate (14%) and incidence of neurological complications (16%). Overall, four patients died during the follow-up period, with a 6-year survival rate of 94.6% (70/74). A total of four patients underwent aortic re-intervention during the follow-up period; before the re-intervention, three received the *en bloc* technique (13.6% 3/22) and one received hybrid therapy (11.1% 1/9).

Conclusion: With complete preservation and reconstruction of the supra-arch vessels, patients with type A aortic dissection combining arch anomalies can achieve a favorable perioperative prognostic outcome. Patients who received the *en bloc* technique are more likely to require aortic re-intervention than patients who underwent total arch replacement with a four-branched graft vessel. Cannulation strategies should be tailored according to the variation of anatomy, but routine cannulation with the right axillary artery can still be performed in most patients with arch anomalies, even for patients with an aberrant right subclavian artery.

KEYWORDS

aberrant right subclavian artery (ARSA), isolated left vertebral artery (ILVA), surgical procedures, arch anomalies, cannulation and perfusion, hybrid therapy, total arch replacement, bovine arch

Introduction

Surgical management of type A aortic dissection requires close attention to the presence of aortic arch anomalies for timely adjustment of surgical treatment strategies. Anatomic abnormalities of the aortic arch are widely present in the general population. According to previous studies, 15–25% of the population may carry aortic arch anomalies (1–3). However, case reports documenting successful treatment of aortic dissection in the setting of anatomic anomalies of the aortic arch are sporadic and with a small sample size (2, 4–12).

The presence of arch anomalies cannot always be treated using routine cannulation strategies; for instance, patients with an ARSA usually cannot undergo selective cerebral perfusion (SCP) through the right axillary artery, which is a routine SCP cannulation location. On the other hand, the arch technique differs much in patients with arch anomalies from the standard procedure.

In this study, we reported our experience in managing type A aortic dissection involving arch anomalies, focusing on surgical techniques, postoperative outcomes, and follow-up results. In addition, our surgical strategies for four major types of arch anomalies were described in detail, and the surgical details and indications of specific procedures have been fully discussed to provide a comprehensive reference for selecting surgical strategies for these patients.

Abbreviations: ALSA, aberrant left subclavian artery; ARSA, aberrant right subclavian artery; BiACP, bilateral antegrade cerebral perfusion; CT, computed tomography; HCA, hypothermia and circulation arrest; IA, innominate artery; ILVA, isolated left vertebral artery; LCCA, left common carotid artery; LSA, left subclavian artery; LUACP, left unilateral antegrade cerebral perfusion; PIT, primary intimal tear; RCCA, right common carotid artery; RSA, right subclavian artery; RUACP, right unilateral antegrade cerebral perfusion; SCP, selected cerebral perfusion; SET, stented elephant trunk; TAR, total arch replacement.

Materials and methods

Patients and data collection

Patients with type A aortic dissection who underwent surgical treatment from January 2017 to 31 December 2020 at our center were selected for this retrospective analysis. A total of 81 patients were diagnosed with arch anomalies by computed tomography (CT) reports or based on surgical records. The study flowchart, including the inclusion and exclusion criteria, is shown in Figure 1.

The hospital ethics committee has approved this research (GDREC2018322H).

Data collection and follow-up

Clinical data were collected from all included patients. Operative records, anesthesia records, and perfusion records were used to determine operative variables, including cannulation strategy, method of surgical repair, site of primary intimal tear (PIT), bypass times, nadir temperature, use of hypothermia and circulation arrest (HCA), and selected cerebral perfusion (SCP). Progress notes and discharge summaries were used to determine the incidence of postoperative complications and mortality. In addition, demographic records, imaging reports, and primary source images from CT scans were collected and analyzed.

The follow-up was carried out over telephone to the latest time to find out the mid-term survival and the incidence of aortic re-intervention. For patients with positive outcomes, the follow-up interval was calculated until the point the positive outcome occurred.

Diagnose arch anomalies

Arch anomaly types were identified using details from the operative reports, imaging reports, and primary source images from CT scans. A total of four major types of abnormal arch anatomy were identified: (1) "bovine" anomaly: an arch with a common origin of the innominate artery (IA) and left common

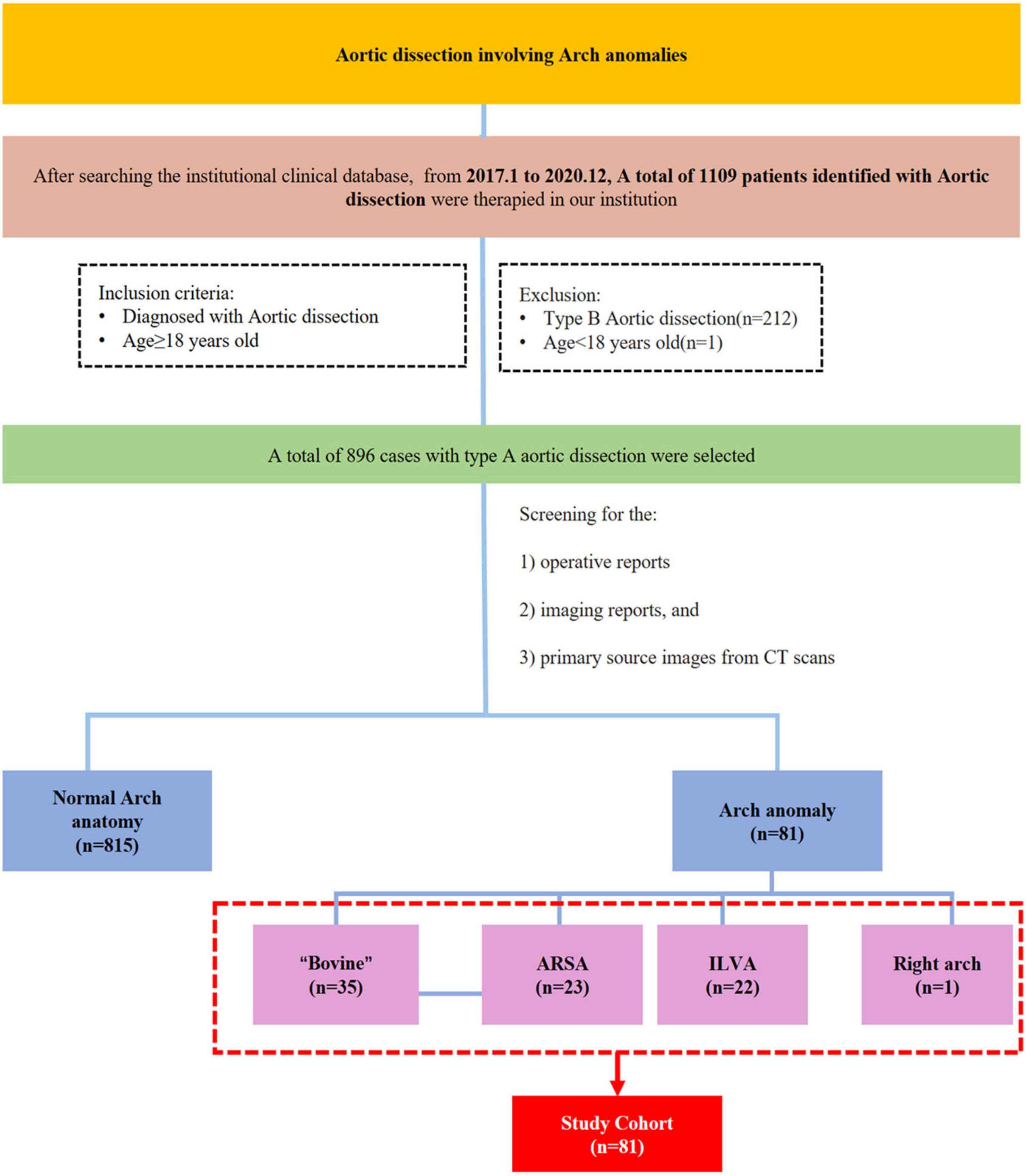

FIGURE 1
Study flowchart.

carotid artery (LCCA), or the LCCA originating directly from the IA; (2) aberrant right subclavian artery (ARSA): a four-vessel arch with an aberrant right subclavian artery originating from the distal arch or proximal descending aorta; (3) isolated left vertebral artery (ILVA): a four-vessel arch with the left vertebral artery coming directly from the aorta; (4) right arch with the aberrant left subclavian artery (ALSA): a mirror image to the ARSA, a four-vessel aortic arch is in the right side of the main trachea, with an ALSA originating from the distal arch or proximal descending aorta.

Surgical techniques

All procedures were performed under general anesthesia and cerebral flow monitoring using cerebral oximetry. Patients who underwent total arch replacement (TAR) or right hemi-arch replacement had HCA and SCP.

A total of three techniques were used for arch reconstruction: TAR, right hemi-arch replacement, and hybrid technique. The TAR technique included TAR with a four-branched graft vessel and TAR with the *en bloc* technique. TAR with a four-branched graft vessel has been described (13, 14) previously. A four-branched graft was used in TAR combined with stented elephant trunk (SET) implantation under the condition of HCA and SCP. The *en bloc* technique was described by Zhong et al. (15). The anterior wall of the aortic arch was incised longitudinally up to the origin of the left common carotid artery (LCCA); no dissection of the arch vessels was confirmed intraoperatively. After deployment of the SET, a balloon was implanted inside the SET to recover the femoral cannula perfusion. Then, the stent-free sewing edge (3- to 5-cm-long Dacron graft) of the SET was straightened and trimmed. Next, under the condition of SCP and femoral perfusion, the trimmed sewing edge was sutured to the native aortic wall near the origins of the arch branches (shown in Figure 2E).

Right hemi-arch replacement was performed as follows: the lesser curvature of the aortic arch was incised and replaced with a single Dacron graft vessel.

The hybrid technique was performed as follows: a GORE-TEX vascular graft was used for revascularization of the supra-arch vessels using incisions in the cervical and supraclavicular fossa regions according to the anatomy feature. Then, a thoracic stent graft was deployed retrograde *via* the femoral artery access. Angiography was performed to confirm the deployment position and GORE-TEX graft patency.

The detailed steps of the reconstruction techniques are described in the Supplementary material.

The arch management strategies of the 81 included patients are summarized in Table 1. Figures 2–5 are the schematic diagrams of the arch management strategies for patients with an ARSA, bovine anomaly, ILVA, and right arch combining the ALSA, respectively.

Among patients with an ARSA who underwent TAR with a four-branched graft, two patients underwent two-stage TAR. First, the ARSA was fully mobilized and anastomosed to the RCCA end-to-side to recover a normal anatomy structure, and then the CPB and SCP were performed with the routine cannulation of the right axillary artery (Figure 2A).

A total of five patients with an ARSA underwent extra-anatomic revascularization of the ARSA (Figure 2B). After the coronary perfusion was restored, the heart resumed beating, and the fourth perfusion side arm of the four-branched graft was anastomosed to the right axillary artery in an end-to-side fashion through the right thoracic cavity and the second intercostal space.

A total of 22 patients underwent the *en bloc* technique, among which four patients with an ARSA needed extra-RCCA-to-distal ARSA bypass using the cervical and right supraclavicular fossa incisions; two patients (“bovine” anomaly) underwent right hemi-arch replacement using a single Dacron graft vessel, which was anastomosed to the trimmed margin of the lesser curvature of the aortic arch in an end-to-end fashion with running stitches of 5-0 polypropylene.

A total of nine patients underwent hybrid therapy (ARSA in seven, “bovine” in one, and ILVA in one), and common carotid artery-to- subclavian artery bypass using the cervical and supraclavicular fossa incisions with a 7-mm GORE-TEX graft was accomplished before the implantation of the thoracic stent graft.

Statistical analysis

Continuous variables were expressed as mean ± standard deviation or median (0.25–0.75 interquartile). Kolmogorov–Smirnov analysis was used to clarify whether data conformed to normal distribution. Categorical variables were expressed as the number of cases (percentage), for example, 28 (80%), indicating 28 cases occupying 80% of the cases of this group. Figures were drawn using Microsoft PowerPoint 2019 (Microsoft, Redmond, USA) or Easy Paint Tool SAI (SYSTEMAX, Japan) software. A $p < 0.05$ was considered statistically significant.

Results

A total of 896 patients with type A aortic dissection were treated in our center from January 2016 to December 2020. After screening the CT reports and surgical records, 81 patients with arch anomalies were included in this study; 35 had “bovine” anomaly, 23 had an ARSA, 22 had an ILVA, and right-sided arch combined with an ALSA was found in one case (Figure 1).

Baseline data

Baseline data of the 81 patients are shown in Table 2. Overall, 73% of the patients had hypertension, and 45 (56%) had hyperlipidemia; seven (9%) patients had coronary malperfusion. The incidence of other malperfusion syndromes was given as follows: neurological ischemia (14%), upper extremity ischemia (5%), spinal ischemia (2%), mesenteric ischemia (20%), renal ischemia (23%), and lower extremity ischemia (10%).

In all, one patient with “bovine” anomaly had a bicuspid aortic valve (3%); three patients underwent cardiac surgery

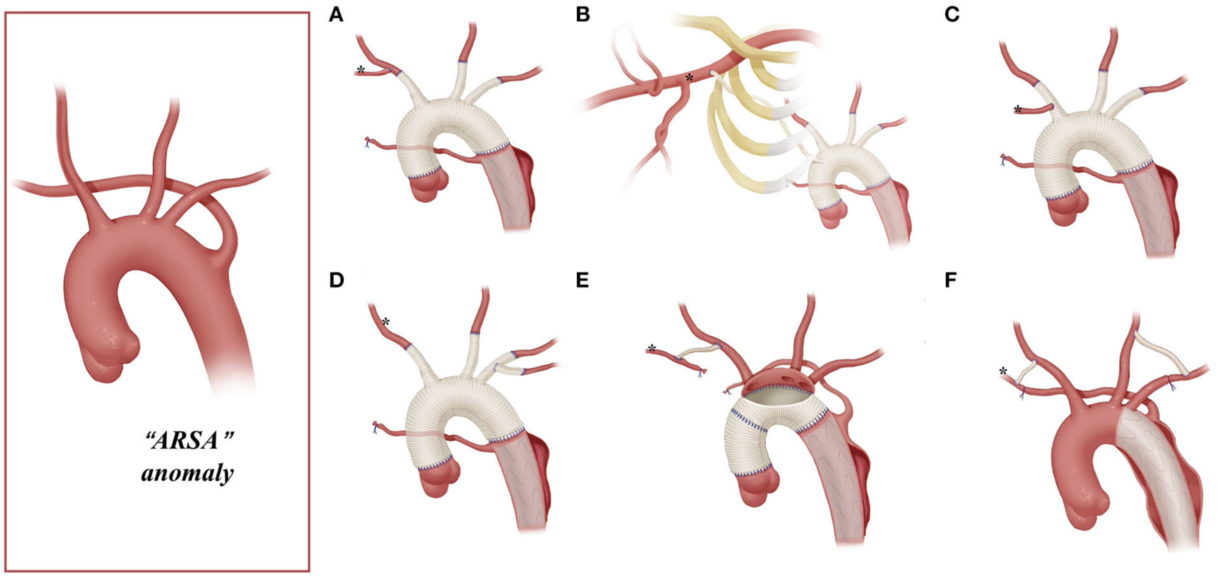

FIGURE 2
Arch technique for ARSA in patients with type A aortic dissection. *Distal ARSA; **(A)** stage TAR for ARSA; **(B)** extra-anatomy revascularization of the right axillary artery; **(C)** ARSA connected to the vascular graft of the RCCA; **(D)** ARSA directly anastomosed to the 8-mm arch branch of the four-branched graft; **(E)** *en bloc* technique for the ARSA; **(F)** hybrid technique for ARSA.

TABLE 1 Arch management strategies for different aortic arch deformities.

	TAR		Right hemi-arch replacement	Hybrid technique
	TAR with four-branched graft	*En* bloc		
ARSA, $n = 23$	*2 (2-A)+ 5 (2-B)+ 3 (2-C) +2 (2-D)	4(2-E)		7 (2-F)
Bovine, $n = 35$	10 (3-A) +8 (3-B)	14	2	1
ILVA, $n = 22$	7 (4-A)+10 (4-B)	4		1
Right arch, $n = 1$	1 (5-B)			

The context within parentheses represents the specific arch techniques that were used, and the numbers before the parentheses represent the cases of the corresponding method. For example, * represents two patients with an ARSA who underwent the arch technique shown in Figure 2A.

(one in the "bovine" anomaly, one in the ARSA, and one in the ILVA), and two patients with an ARSA and one patient with an ILVA received implantation of the stent graft in the thoracic/abdominal aorta before admission to our department.

Surgical data

The surgical data of the 81 patients are summarized in Table 3. The location of PIT was explored intraoperatively: aortic root or ascending aorta in 48%, aortic arch in 37%, descending aorta in 12%, and no PIT in two cases. All patients who underwent TAR or right hemi-arch replacement had HCA+antegrade SCP. The nasopharyngeal temperature was reduced to 20–25°C during HCA. Other concomitant procedures included three cases of coronary artery bypass grafting (two in the "bovine" anomaly and one in the ILVA), one case of left atrial thrombosis removal (ARSA), one case of mitral + tricuspid valvuloplasty ("bovine"), and one case of the Nuss procedure ("bovine").

Among 34 patients with "bovine" anomaly who underwent CPB, 30 patients (88%, 30/34) received CPB through the cannulation of a right axillary artery or innominate artery, and 14 received CPB with combined cannulation of a right axillary/IA and femoral artery. A total of 13 patients (38%) with "bovine" anomaly achieved BiACP by cross-clamping of the common origin of the IA and LCCA and cannulation of the right axillary artery/common origin, and 19 patients underwent RUCP with cross-clamp applied to the cephalad to the origin of the LCCA and cannulation of the right axillary artery.

CPB was performed in 16 of 23 patients with an ARSA; 11 patients underwent CPB through the cannulation of the femoral artery (69%, 11/16) and one patient through the cannulation of the aortic arch.

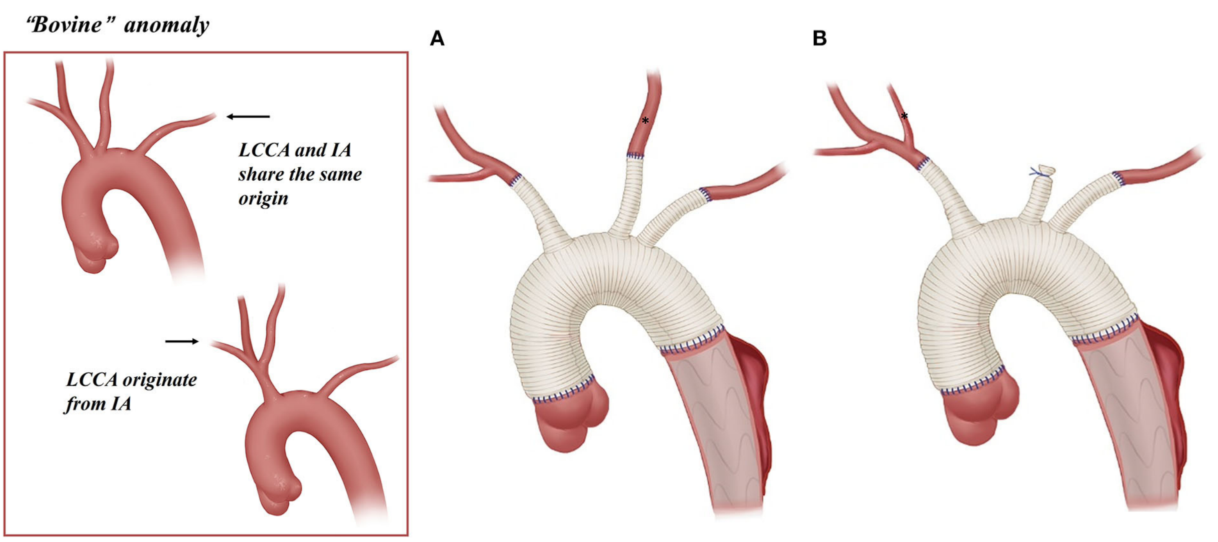

FIGURE 3
Arch technique for "bovine" anomaly in patients with type A aortic dissection. *LCCA; **(A)** reconstruction with three graft branches for "bovine" anomaly. **(B)** Reconstruction with two graft branches for "bovine" anomaly.

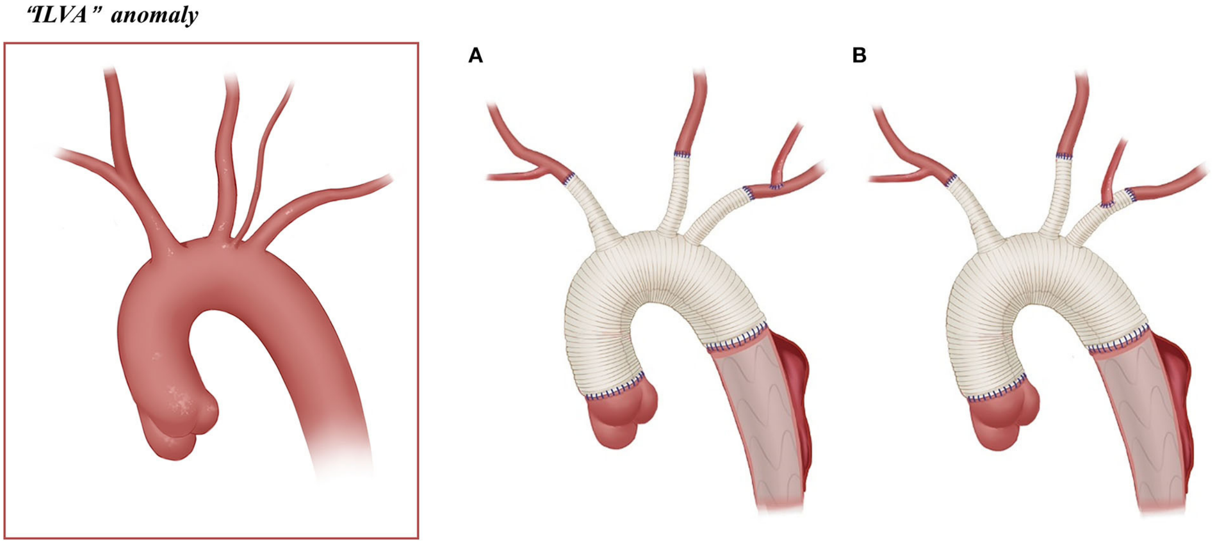

FIGURE 4
Arch technique for "ILVA" anomaly in patients with type A aortic dissection. **(A)** ILVA anastomosed to the LSA. **(B)** ILVA anastomosed to the LSA graft branch.

Among 22 patients with an ILVA, 21 underwent SCP. The SCP strategy in these patients is as follows: BiACP ($n = 6$) and RUACP ($n = 10$) were achieved through cannulation of the right axillary artery/IA with/without the LCCA, and LUACP ($n = 5$) was achieved through the cannulation of the LCCA.

Only one patient with a right-sided arch combining the ALSA was first operated with femoral artery cannulation for CPB and then RCCA cannulation for SCP.

Surgical results

Perioperative outcomes are summarized in Table 4. Overall, seven patients (9%) died during postoperative hospitalization, and two patients required ECMO assistance (one ILVA and one "bovine"). Other postoperative complications are as follows: neurological complications (16%), dialysis treatment (17%), paraplegia (5%), and redo of tracheotomy (2%). Among them,

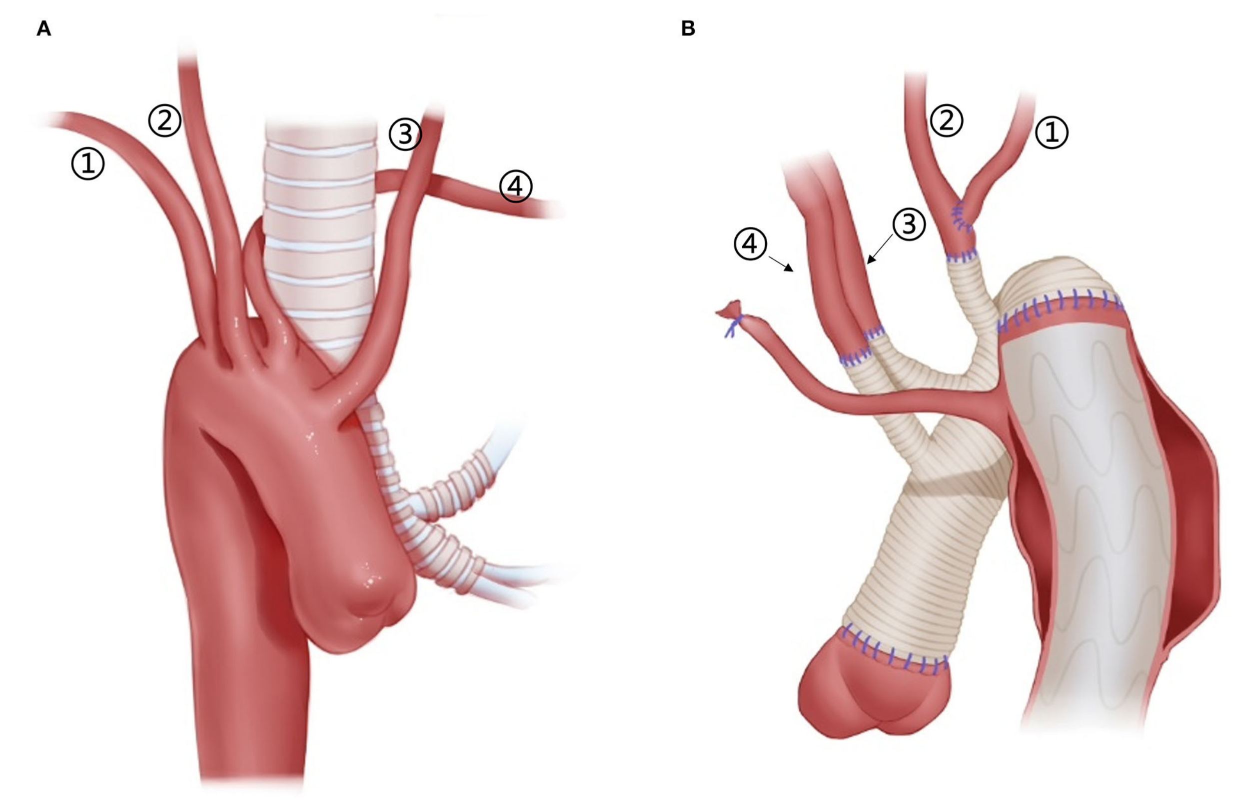

FIGURE 5
Arch technique for patients with right arch and ALSA. (1) RSA; (2) RCCA; (3) LCCA; (4) ALSA. **(A)** Schematic diagram of the anatomy of the right arch + ALSA, from the front view. **(B)** Arch technique for a patient with right arch + ALSA, from the posterior view. ALSA, from the posterior view.

26% of patients with "bovine" anomaly had neurological complications, and all patients complicated with paraplegia had "bovine" anomaly.

Follow-up results

A total of 74 patients who survived perioperatively were followed up by telephone, with a follow-up rate of 100%. The mean follow-up interval was 36.8 months for long-term mortality, and 35.2 months for aortic re-intervention.

In total, four patients underwent aortic re-intervention during the follow-up period: three patients with the *en bloc* technique, among whom one underwent IA stenting for IA dissection 18 months postoperatively, one underwent intervention therapy for LCCA occlusion 6 months postoperatively, and one underwent intervention therapy for basilar artery dissection 8 months later; one patient with hybrid therapy underwent stainless steel coil implantation for stent endoleak 3 months later. A total of four patients died during the follow-up period, with a survival rate of 94.6% (70/74) at 6 years postoperatively.

Discussion

Reports on treating patients with type A aortic dissection involving arch anomalies are rare. Our study is probably the largest cohort study in this field to date; we searched PubMed for English language articles reporting on aortic dissection and aortic arch malformation published in the past 10 years; studies with a sample size of more than 10 are summarized in Table 5.

The right axillary artery cannulation for CPB and SCP is a standard procedure for type A aortic dissection. In this study, this routine cannulation strategy was applicable for most patients with "bovine" anomaly and ILVA ("bovine," 24/34; ILVA, 14/21), while it was not suitable for patients with an ARSA due to the unique anatomic structures found in these patients. In our group, only two patients with an ARSA underwent the standard cannulation procedure, and their ARSA was mobilized, dissected, and anastomosed to RCCA before proceeding to the standard cannulation procedure (Figure 2A).

This stage TAR technique requires complete mobilization of the ARSA and should ensure that dissection does not involve the RCCA and the distal part of the ARSA. However, for some patients, mobilizing the ARSA may be challenging. In

TABLE 2 Baseline characteristics.

	Bovine arch (n = 35)	ARSA (n = 23)	ILVA (n = 22)	Right Arch (n = 1)	All (*n* = 81)
Age	49.5 ± 10.9	47.4 ± 11.7	52.6 ± 9.7	48	49.7 ± 10.8
Male gender	28 (80%)	17 (74%)	20 (91%)	1 (100%)	66 (81%)
BMI	23.6 ± 4.0	26.0 ± 4.7	24.5 ± 3.0	24.6	24.8 ± 4.1
Malperfusion syndrome					
Cardiac ischemia	6 (17%)	0	1 (5%)	0	7 (9%)
Neurological deficit	6 (17%)	3 (13%)	2 (9%)	0	11 (14%)
Upper extremities ischemia	1 (3%)	2 (8%)	1 (5%)	0	4 (5%)
Spinal ischemia	1 (3%)	0	1 (5%)	0	2 (2%)
Mesenteric ischemia	8 (23%)	3 (13%)	5 (23%)	0	16 (20%)
Renal ischemia	8 (23%)	5 (22%)	6 (27%)	0	19 (23%)
Lower extremities ischemia	7 (20%)	0	1 (5%)	0	8 (10%)
Dissection type					
Debakey I	28 (80%)	13 (57%)	16 (73%)	0	57 (70%)
Debakey II	4 (11%)	0	2 (9%)	0	6 (7%)
None - A None - B	3 (9%)	10(43%)	4 (18%)	1(100%)	18(22%)
AI (more than moderate)	14 (40%)	5 (22%)	8 (36%)	0	27 (33%)
Hypertension	23 (66%)	18 (78%)	17 (77%)	1(100%)	59 (73%)
Diabetes mellitus	0	1 (4%)	1 (5%)	0	2 (2%)
Hyperlipidemia	21 (60%)	14 (61%)	10 (46%)	0	45 (56%)
CAD	11 (31%)	7 (30%)	5 (23%)	0	23 (28%)
Marfan	0	2 (9%)	0	0	2 (2%)
BAV	1 (3%)	0	0	0	1 (1%)
History of cardiac surgery	1 (3%)	1 (4%)	1(5%)	0	3 (4%)
History of TEVAR/EVAR	0	2 (9%)	1(5%)	0	3 (4%)

Corresponding percentages are given within parentheses.

addition, the ARSA might be involved by dissection, rendering the establishment rather difficult for a near-normal anatomic ARSA-to-RCCA connection in advance. In this study, 75% (12/16) of the patients with the ARSA underwent CPB *via* cannulation of the femoral artery or aortic arch, instead of the right axillary artery.

Unilateral or bilateral cerebral perfusion can be achieved by cannulation in the right axillary artery, common carotid artery, or IA. Patients with unilateral cerebral perfusion require full consideration of the integrity of the circle of Willis. BiACP is usually required in case of an incomplete circle of Willis or significant asymmetry between left and right cerebral oxygen saturation. In our clinical practice, we found that the SCP strategy in patients with arch anomalies differs from the conventional practice. For patients with "bovine" anomalies, the cerebral perfusion strategy may change depending on the location of the origin of the LCCA. In cases where the origin of the LCCA is located high in the IA, BiACP can be achieved with a clamp applied caudad to the IA and cannulation of the right axillary artery. Bryan et al. (5) described this strategy in 11 patients with "bovine" anomaly. In our cohort, 31% of patients with "bovine" anomaly underwent BiACP, which is significantly higher than other anomaly groups. Patients with the ARSA cannot undergo RUSCP *via* the cannulation of the right axillary artery [except for patients who underwent two-stage TAR (16), $n = 2$, Figure 2A]. As a result, SCP can only be performed with cannulation of the LCCA and/or RCCA for these patients. For patients with an ILVA, additional cannulation of the ILVA for cerebral perfusion is not needed. Qi et al. (12) treated 21 ILVA patients without additional cannulation of the ILVA; only two (9.5%, 2/21) patients had neurological complications after the surgery. This is consistent with the results in this cohort, in which 22 patients with an ILVA were treated without additional cannulation in the ILVA, and their neurological complication rate was even lower than that of the ARSA or "bovine" groups (incidence of neurological complications was 26, 13, and 5% for "bovine," ARSA, and ILVA, respectively).

Arch reconstruction with preservation of all the supra-arch vessels is recommended for patients with arch anomalies. The *en bloc* technique is a simple strategy that can be computed within a relatively short time, with a single aortic patch containing the origin of all the supra-arch vessels anastomosed to the stent-free sewing edge of SET. Yet, according to the follow-up result in this study, these patients may have a higher incidence of aortic

TABLE 3 Surgical characteristics.

	Bovine arch ($n = 35$)	ARSA ($n = 23$)	ILVA ($n = 22$)	Right arch ($n = 1$)	All ($n = 81$)
Site of PIT					
Root/Ascending	20 (58%)	10 (43%)	9 (41%)	0	39 (48%)
Aortic arch	11 (31%)	8 (35%)	10 (46%)	1 (100%)	30 (37%)
Descending	14 (11%)	4 (17%)	2 (9%)	0	10 (12%)
None	0	1 (4%)	1 (5%)	0	2 (2%)
Cases with CPB	**34 (97%)**	**16 (70%)**	**21 (95%)**	1 (100%)	**72 (89%)**
Arterial bypass cannulation					
Axillary*	16 (46%)	4 (17%)	12 (55%)	0	32 (40%)
Femoral	3 (9%)	9 (39%)	5 (23%)	0	17 (21%)
Axillary+Femoral	9 (26%)	0	2 (9%)	0	11 (14%)
Innominate+Femoral	5 (14%)	2 (9%)	2 (9%)	1 (100%) **	10 (12%)
Aortic arch	1 (3%)	1 (4%)	0	0	2 (2%)
Cases with HCA and SCP	**34 (97%)**	**16 (70%)**	**21 (95%)**	1 (100%)	**72 (89%)**
RUACP	19 (54%)	5 (22%)	10 (46%)	1 (100%)	35 (43%)
LUACP	2 (6%)	6 (26%)	5 (23%)	0	12 (15%)
BiACP	13 (38%)	5 (22%)	6 (27%)	0	24 (30%)
CA time	21.9 ± 9.2	25.3 ± 9.2	25.5 ± 8.9	26	23.8 ± 9.1
Nadir temperature	23.2 ± 3.9	22.4 ± 3.9	21.8 ± 2.3	19.8	22.5 ± 3.5
Hybrid procedure	1 (3%)	7 (30%)	1 (5%)	0	9 (11%)

* Axillary or innominate, **RCCA + femoral. Corresponding percentages are given within parentheses. PIT, primary intimal tear; RUACP, right unilateral antegrade cerebral perfusion; LUACP, left unilateral antegrade cerebral perfusion; BiACP, bilateral antegrade cerebral perfusion.

TABLE 4 Surgical results.

	Bovine arch	ARSA	ILVA	Right arch	All
Early mortality	5 (14%)	1 (4%)	1 (5%)	0	7 (9%)
Re-exploration	3 (9%)	0	2 (9%)	0	5 (6%)
ECMO	1 (3%)	0	1 (5%)	0	2 (2%)
Neurologic*	9 (26%)	3 (13%)	1 (5%)	0	13 (16%)
Tracheotomy	2 (6%)	0	0	0	2 (2%)
Paraplegia	4 (11%)	0	0	0	4 (5%)
Dialysis	8 (23%)	3 (13%)	3 (14%)	0	14 (17%)

*Stroke, delirium, paresis, and paraplegia. Corresponding percentages are given within parentheses.

re-intervention; the reason for this might include (1) potential dissection in the supra-arch vessels not found intra-operatively, or (2) intimal tears during the cannulation and clamping of the supra-arch vessels that could lead to potential dissection or stenosis. Patients who underwent TAR with a four-branched graft had a better follow-up result with no aortic re-intervention event. The side arms of the four-branched graft were attached to the supra-arch vessels. For patients with "bovine" anomaly, revascularization with only two side arms of the four-branched graft can be achieved (Figure 3B) in cases whose LCCA directly originates from the IA. For patients with an ILVA, the ILVA should be preserved and anastomosed to the LSA (Figure 4A) or its side arm (Figure 4B). Preservation of the ILVA can guarantee the integrity of the circle of Willis and reduce neurological complications. Qi et al. (12) reported another technique for the preservation of the ILVA, with "*a single aortic patch containing the origin of the ILVA and LSA anastomosed to one limb of the prosthetic graft.*" For patients with an ARSA, if the ARSA is involved by dissection or is difficult to mobilize, extra-anatomic reconstruction can be performed with the fourth perfusion side arm (Figure 2B). Another extra-anatomic revascularization method might be the RCCA-to-ARSA bypass through cervical + right subclavian incisions, which is not recommended in our center as it can damage venous plexuses in the subcutaneous tunnel, resulting in massive venous hemorrhage. It may also compress the shunt graft and lead to distant occlusion. By

TABLE 5 Major articles of aortic dissection involving arch anomalies.

References	Country	Year	Cases	Types of arch anomalies	Stanford	Operative procedure	Journal
Bryan et al. (5)	U.S	2001–2011	43	ARSA (5), bovine (32), right arch (3), ILVA (3)	A	Opening graft replacement	J Cardiothorac Vasc Anesth 2014
Sherene et al. (2)	U.S, Ireland	1990–2014	75	ARSA, bovine, right arch, ILVA	B	Not mentioned	J Vasc Surg 2018
Zhou et al. (6)	China	2010–2015	13	ARSA	B	Total Endovascular Treatment	Eur J Vasc Endovasc Surg 2017
Ding et al. (7)	China	2011–2016	16	ARSA	B	TEVAR and extra anatomic bypass hybrid procedure	J Vasc Surg 2018
Li et al. (4)	China	2009–2017	22	ARSA	Non-A, Non-B A (15) Non-A Non-B (7)	TAR + SET	Eur J Cardiothorac Surg 2020
Zhang et al. (8)	China	2012–2018	15	ARSA	B	Endovascular repair	J Vasc Interv Radiol 2019
Dumfarth et al. (9)	U.S., Austria	2002–2013	22	Bovine;	A	Opening graft replacement (22); TEVAR (2)	Ann Thorac Surg 2014
Zuo et al. (10)	China	2017–2019	13	ILVA	A	ILVA-LCCA bypass + TAR + SET	Eur J Cardiothorac Surg 2021
Ding et al. (11)	China	2011–2018	31	ILVA	B	TEVAR	J Vasc Surg 2019
Qi et al. (12)	China	2003–2008	21	ILVA	A (20), B (1)	TAR	Ann Thorac Surg 2013

10.3389/fcvm.2022.979431

comparison, the extra-anatomic revascularization through the right thoracic cavity (Figure 2B) can avoid the compression by the subcutaneous tunnel without extra-cervical incision, and no shunt graft obstruction was found during the follow-up period in our cohort, indicating its safety and stability.

A hybrid technique has been reported in several studies as a treatment for patients with type B aortic dissection involving the ARSA and ILVA (6–8, 11). In this cohort, the hybrid technique was used for patients with type non-A non-B aortic dissection whose aortic arch was minimally involved (50%, 9/18). For patients with a severely compromised aortic arch and those for whom complete revascularization of the supra-arch vessels cannot be ensured after TEVAR implantation (e.g., patients with RCCA or IA involvement), hybrid therapy should not be recommended. For patients with an ARSA undergoing a hybrid technique, the distal part of the ARSA can always be found in the right supraclavicular fossa area. After completing the supra-arch bypass, the proximal part of the subclavian arteries will be clamped tentatively and then ligated if there is no significant change in blood pressure in the upper extremity. First, tentative clamping of the subclavian arteries is necessary to ensure the common carotid artery-to-subclavian artery bypass is adequate for the perfusion of the upper extremities. Second, the proximal part of the ARSA and LSA should better be ligated to reduce the occurrence of competing for blood flow and type II endoleak. Third, supra-arch vessels bypassing the subcutaneous tunnel by using cervical + subclavian incisions are not recommended. The reason for this has been discussed before. The stent graft should be positioned carefully before release because it might occlude the origin of the ILVA and some other supra-arch vessels, especially in patients whose ILVA originates from the distal arch. Our interventional team has performed TEVARs in 31 patients with type B aortic dissection involving the ILVA anomaly. Before the release of the stent graft, angiography was performed to confirm that the distal part of the stent graft is at least 1 cm away from the take-off of the ILVA, and no blocking of the ILVA was observed (11).

The distal management strategy mainly included the implantation of the SET or TEVAR stent. It is important to note that in patients with an ARSA, complete coverage of the ARSA origin with a SET or TEVAR stent is needed to isolate the Kommerell diverticulum (4). The follow-up results of this cohort showed only one patient with endoleak after TEVAR therapy; no endoleak was found in patients with SET implantation, demonstrating the effectiveness and stability of SET or TEVAR stent implantation.

The perioperative mortality rate (9%) in this cohort is somehow consistent with previous studies (14, 17, 18) that reported a perioperative mortality rate of 5–15% in patients with pure type A aortic dissection. This suggests that aortic arch malformation may not be a high risk for perioperative mortality for patients with type A aortic dissection (5, 9). Some studies suggested a higher incidence of neurological complications in patients with "bovine" anomalies (9), which is consistent with the results of this study: patients with "bovine" anomalies had a higher incidence of neurological complications and perioperative mortality than patients with other anomalies. The reason for this is not clear. Future studies with a larger sample size are needed to confirm the impact of specific aortic arch anomalies on the perioperative prognosis.

This study has a few limitations: (1) patients with type B aortic dissection were not included in this study; (2) this was a retrospective analysis; however, due to the urgency of type A aortic dissection, it is almost impossible to perform a prospective cohort analysis.

Conclusion

For patients with type A aortic dissection combining arch anomalies, complete arch reconstruction with preservation of all the supra-arch vessels and reasonable cannulation strategies should be considered with an elaborate design based on the anatomical features so as to achieve a favorable perioperative and long-term prognosis outcomes. Routine cannulation with the right axillary artery can be achieved in most cases, even in patients with an ARSA. Moreover, patients who undergo the *en bloc* technique may have a higher risk of dissection or stenosis of the supra-arch vessels, and more of them need aortic re-intervention compared with patients who undergo TAR with a four-branched graft.

Data availability statement

The raw data supporting the conclusions of this article will be made available by the authors, without undue reservation.

Author contributions

JZ: primary manuscript writing, revision, design of conception, data collection, and literature search. GT, DZ, YY, ZL, YL, CY, and JY: data collection. ZZ, XL, and RF: provision of patients. ZC: data collection and provision of patients. JL: administrative support. TS: provision of patients, obtaining funding, final approval of the article, and administrative support. JW: manuscript revision, design of conception, data collection, and literature search. All authors contributed to the article and approved the submitted version.

Funding

This work was supported by the National Key Research and Development Program of China (2018YFC1002600) and the Science and Technology Planning Project of Guangdong

Province, China (2017A070701013, 2017B090904034, 2017B030314109, and 2019B020230003), the Guangdong Peak Project (DFJH201802), and Guangzhou Science and Technology Program Key Projects (202002020037) and Guangdong special funds for science and technology innovation strategy, China (Stability support for scientific research institutions affiliated to Guangdong Province-GDCI 2021).

Conflict of interest

The authors declare that the research was conducted in the absence of any commercial or financial relationships that could be construed as a potential conflict of interest.

Publisher's note

All claims expressed in this article are solely those of the authors and do not necessarily represent those of their affiliated organizations, or those of the publisher, the editors and the reviewers. Any product that may be evaluated in this article, or claim that may be made by its manufacturer, is not guaranteed or endorsed by the publisher.

Supplementary material

The Supplementary Material for this article can be found online at: https://www.frontiersin.org/articles/10.3389/fcvm.2022.979431/full#supplementary-material

SUPPLEMENTARY FIGURE S1
CT construction image after hybrid technique for ARSA. (1) Graft connecting LCCA and LSA. (2) Left common carotid artery. (3) Right common carotid artery. (4) Graft connecting RCCA and RSA. (5) Remnant of LSA. (6) Elephant trunk stent. (7) False lumen. (8) Distal aberrant right subclavian artery.

SUPPLEMENTARY FIGURE S2
CT images of the patient with right arch+ALSA. **(A)** Pre-operative CT construction image. **(B)** CT scan images. **(C)** Postoperative CT construction image. (1) ALSA; (2) LCCA; (3) RCCA; (4) False lumen; (5) Right arch; (6) Right-sided descending thoracic aorta; (7) RSA.

References

1. Jakanani GC, Adair W. Frequency of variations in aortic arch anatomy depicted on multidetector CT. *Clin Radiol.* (2010) 65:481–487. doi: 10.1016/j.crad.2010.02.003

2. Sherene Shalhub Mi. Thomas SH, Matthew PS, Jason JR, Ferdia AB, et al. Association of variant arch anatomy with type B aortic dissection and hemodynamic mechanisms. *J Vasc Surg.* (2018) 68:1640–8. doi: 10.1016/j.jvs.2018.03.409

3. Yuki Ikeno Y. Takashi Matsueda, Katsuhiro Yamanaka, Takeshi Inoue, Satoshi Ishihara, et al. Anatomical variations of aortic arch vessels in Japanese patients with aortic arch disease. *Gen Thorac Cardiovasc Surg.* (2019) 67:219–26. doi: 10.1007/s11748-018-1001-3

4. Li JR, Ma WG, Chen Y, Zhu JM, Zheng J, Xu SD, et al. Total arch replacement and frozen elephant trunk for aortic dissection in aberrant right subclavian artery. *Eur J Cardiothorac Surg.* (2020) 58:104–11. doi: 10.1093/ejcts/ezaa029

5. Bryan GM, Katherine BH, Ramin EB, Oakes DA. Congenital anomalies of the aortic arch in acute type-A aortic dissection: implications for monitoring, perfusion strategy, and surgical repair. *J Cardiothorac Vasc Anesth.* (2014) 28:467–72. doi: 10.1053/j.jvca.2013.12.001

6. Zhou M, Bai XQ, Ding Y, Wang YG, Lin CP, Yan D, et al. Morphology and outcomes of total endovascular treatment of type B aortic dissection with aberrant right subclavian artery. *Eur J Vasc Endovasc Surg.* (2017) 54:722–28. doi: 10.1016/j.ejvs.2017.09.014

7. Ding HY, Luo SY, Liu Y, Huang WH, Jiang MC Li J, et al. Outcomes of hybrid procedure for type B aortic dissection with an aberrant right subclavian artery. *J Vasc Surg.* (2018) 67:704–11. doi: 10.1016/j.jvs.2017.07.124

8. Zhang WC Li X, Cai WW Li M, Qiu J, Shu C. Midterm outcomes of endovascular repair for stanford type B aortic dissection with aberrant right subclavian artery. *J Vasc Interv Radiol.* (2019) 30:1378–85. doi: 10.1016/j.jvir.2019.02.001

9. Dumfarth J, Plaikner M, Krapf C, Bonaros N, Semsroth S, Rizzo JA, et al. Bovine aortic arch: predictor of entry site and risk factor for neurologic injury in acute type a dissection. *Ann Thorac Surg.* (2014) 98:1339–46. doi: 10.1016/j.athoracsur.2014.05.086

10. Zuo Y, Zhou ZC, Ge JJ. Prior reconstruction of an isolated left vertebral artery for Stanford type A aortic dissection. *Eur J Cardiothorac Surg.* (2021) 59:1339–41. doi: 10.1093/ejcts/ezaa407

11. Ding HY, Zhu Y, Wang HY, Luo SY, Liu Y, Huang WH, et al. Management of type B aortic dissection with an isolated left vertebral artery. *J Vasc Surg.* (2019) 70:1065–71. doi: 10.1016/j.jvs.2018.11.052

12. Qi RD, Sun LZ, Zhu JM, Liu YM, Zheng J, Li CN, et al. Total arch replacement in patients with aortic dissection with an isolated left vertebral artery. *Ann Thorac Surg.* (2013) 95:36–40. doi: 10.1016/j.athoracsur.2012.07.078

13. Sun LZ Qi RD, Zhu JM, Liu YM, Zheng J. Total arch replacement combined with stented elephant trunk implantation A new "Standard" therapy for Type A dissection involving repair of the aortic arch? *Circulation.* (2011) 123:971–78. doi: 10.1161/CIRCULATIONAHA.110.015081

14. Ma WG, Zhu JM, Zheng J, Liu YM, Ziganshin BA, Elefteriades JA et al. Sun's procedure for complex aortic arch repair: total arch replacement using a tetrafurcate graft with stented elephant trunk implantation. *Ann Cardiothorac Surg.* (2013) 2:642–8. doi: 10.12945/j.aorta.2013.13.015.vid.01

15. Zhong YL Qi RD, Ma WG, Ge YP, Qiao ZY Li CN, et al. Frozen elephant trunk with modified en bloc arch reconstruction and left subclavian transposition for chronic type A dissection. *J Thorac Dis.* (2018) 10:5376–83. doi: 10.21037/jtd.2018.08.140

16. Bektas B, Serkan S, Cengiz C, Olcay MD, Nevzat E, Ramazan K. Aberrant right subclavian artery and axillary artery cannulation in type A aortic dissection repair. *Ann Thorac Surg.* (2013) 96:e1–2. doi: 10.1016/j.athoracsur.2013.01.044

17. Stephen DW, Marco DE, Marek PE. T Brett R, Nimesh DD, Thoralf MS, et al. Postoperative myocardial infarction in acute type A aortic dissection: A report from the International Registry of Acute Aortic Dissection. *J Thorac Cardiovasc Surg.* (2017) 153:521–7. doi: 10.1016/j.jtcvs.2016.10.064

18. Lin HH, Liao SF, Wu CF Li PC, Li ML. Outcome of frozen elephant trunk technique for acute type A aortic dissection: as systematic review and meta-analysis. *Medicine (Baltimore).* (2015) 94:e694. doi: 10.1097/MD.0000000000000694

frontiers | Frontiers in Cardiovascular Medicine

TYPE Original Research
PUBLISHED 26 October 2022
DOI 10.3389/fcvm.2022.1047939

Check for updates

OPEN ACCESS

EDITED BY
Hongkun Zhang,
Zhejiang University, China

REVIEWED BY
Zheng Hua Xiao,
Sichuan University, China
Stefanos Demertzis,
University of Italian Switzerland,
Switzerland

*CORRESPONDENCE
Kai Liu
199662000265@sdu.edu.cn

SPECIALTY SECTION
This article was submitted to
Heart Surgery,
a section of the journal
Frontiers in Cardiovascular Medicine

RECEIVED 19 September 2022
ACCEPTED 10 October 2022
PUBLISHED 26 October 2022

CITATION
Fang C, Gao S, Ren X, Pang X, Zhao X, Ma Z, Wang C and Liu K (2022) Comparison of two techniques in proximal anastomosis in acute type A aortic dissection.
Front. Cardiovasc. Med. 9:1047939.
doi: 10.3389/fcvm.2022.1047939

Comparison of two techniques in proximal anastomosis in acute type A aortic dissection

Changcun Fang[1], Shan Gao[2], Xiao Ren[3], Xinyan Pang[4], Xin Zhao[1], Zengshan Ma[1], Chen Wang[4] and Kai Liu[1]*

[1]Department of Cardiovascular Surgery, Thoracoscopy Institute of Cardiac Surgery, Qilu Hospital of Shandong University, Jinan, China, [2]Department of Anesthesia, Zhangqiu People's Hospital, Jinan, China, [3]Department of Extracorporeal Circulation, Wuhan Asia Heart Hospital, Wuhan, China, [4]Department of Cardiovascular Surgery, The Second Hospital of Shandong University, Jinan, China

Background: The proximal anastomosis is an important procedure during the acute type A aortic dissection (AAAD) surgery. The conventional method is a double patch sandwich technique with Teflon felt. Adventitial eversion and prosthesis eversion technique as a novel approach has been applied to many patients in our center. Herein, This technique would be introduced, and the perioperative and 1-year follow-up results of the two different anastomosis methods were also evaluated.

Methods: Between December 2017 and May 2021, 143 AAAD patients who underwent total arch replacement (TAR) and frozen elephant trunk (FET) implantation were included in this retrospective study. Patients were divided into the eversion technique group (adventitial eversion and prosthesis eversion technique for proximal anastomosis, n = 64) and the sandwich technique group (n = 79).

Results: The medical records were analyzed and compared between the groups. The mean operation time was 466 ± 73 min in the eversion technique group and 513 ± 81 min in the sandwich technique group ($P < 0.001$). Compared with the sandwich technique group, the eversion technique group also showed a shorter time on proximal anastomosis (38 ± 12 min vs. 58 ± 20 min, $P < 0.001$), cardiopulmonary bypass (195 ± 26 vs. 211 ± 40 min, $P = 0.003$), and aortic cross-clamp (120 ± 23 min vs. 134 ± 27 min, $P = 0.002$). Furthermore, a decreased proportion of >600 ml fresh frozen plasmas transfusion was observed in eversion technique group (10.9% vs. 34.2%, $P = 0.002$). No statistical differences were found in the postoperative morbidities and 1-year follow-up outcomes.

Conclusion: Proximal anastomosis with adventitial eversion and prosthesis eversion technique is a promising surgical option for AAAD patients, with favorable perioperative and 1-year follow-up results.

KEYWORDS

adventitial eversion, prosthesis eversion technique, proximal anastomosis, acute type A aortic dissection (AAAD), open surgery

Introduction

Acute type A aortic dissection (AAAD) is a life-threatening disease carrying a high risk of mortality. Open surgery is the primary treatment for AAAD patients. In the past decades, great progress has been made in the methods of AAAD surgery, such as the introduction of frozen elephant trunk (FET), which has simplified the surgical procedures and decreased the mortality rate (1). At present, total arch replacement (TAR) plus FET is the most common surgical method for AAAD treatment. However, high postoperative morbidities, such as neurologic deficit, bleeding, paraplegia, and future aortic root dilation, remain challenges for the cardiac surgeons (2).

Proximal anastomosis is a crucial part during the AAAD surgery (1). As the dissected aortic stump is fragile, improper repair may lead to the anastomosis disintegration and uncontrollable bleeding. The double patch sandwich technique with Teflon felt is the conventional surgical procedure for proximal anastomosis (3). However, the double patch sandwich technique still has limitations and may increase the aortic cross-clamp time, and subsequently result in the complications such as intraoperative bleeding and organ dysfunction. Herein, we tried to explore a modified approach—adventitial eversion and prosthesis eversion technique for the proximal anastomosis of AAAD for the last several years.

In this retrospective study, adventitial eversion and prosthesis eversion technique was used for proximal anastomosis of AAAD in dozens of cases. The detailed procedures were introduced, and the perioperative and 1-year follow-up outcomes compared with the traditional sandwich technique were evaluated.

Materials and methods

Patient selection

This study was conducted in accordance with the Declaration of Helsinki (as revised in 2013). The study protocol was approved by the Medical Ethics Committee of Qilu Hospital of Shandong University (Reference No. KYLL-2017KS-195). Between December 2017 and May 2021, a cohort of 435 consecutive patients with AAAD underwent surgical repair in our department. Of these patients, 143 cases were included in this study according to the inclusion and exclusion criteria (**Figure 1**). AAAD diagnosis was confirmed by the computerized tomographic angiography (CTA).

The inclusion criteria were: (1) the aortic root involved in the aortic dissection; (2) AAAD patients who underwent TAR and FET (TAT + FET); (3) arterial cannulation method: right axillary artery plus femoral artery; (4) bilateral antegrade cerebral perfusion (b-ACP); and (5) without other organ dysfunction prior to operation. The exclusion criteria were: (1) congenital connective tissue disease such as Marfan syndrome and (2) concomitant other procedures such as CABG, valvular replacement or valvuloplasty, or aortic root replacement. The indications of TAR + FET in our center were aortic arch dissection, aortic arch dilation (≥50 mm), and concurrent dissection in descending aorta. All the patients underwent operations within 12 h of the initial diagnosis. Both conventional sandwich technique and adventitial eversion and prosthesis eversion techniques were performed by the same surgeon and his team.

According to the methods of proximal anastomosis, patients were retrospectively divided into two groups, the eversion technique group (adventitial eversion and prosthesis eversion technique for proximal anastomosis, $n = 64$) and the sandwich technique group (double patch sandwich technique with Teflon felt for proximal anastomosis, $n = 79$). There was no particularity in the patient selection between the two groups. In other words, the severity of aortic dissection between the two groups has no difference.

Main surgical procedures

Step 1: Anesthesia and CPB

All patients underwent the operation with general anesthesia and median sternotomy. Intraoperative transesophageal echocardiography probe was routinely inserted for the detection of any abnormality before weaning from CPB. Cardiopulmonary bypass was established by the cannulas in the right axillary artery and the femoral artery for perfusion, and vena cava for veinous drainage. The left atrial vent was inserted into the left atrium *via* the right superior pulmonary vein. Myocardial protection was accomplished with the antegrade infusion of cold blood cardioplegia. The ascending aorta was opened longitudinally between the brachiocephalic trunk and sinus-tubular junction (STJ).

Step 2: Proximal anastomosis

Adventitial eversion and prosthesis eversion for proximal anastomosis (the eversion technique group)

A segment of artificial graft was inverted and inserted into the aortic root (**Figures 2A,C**). During the suturing, the adventitia above the suture line was everted to form two layers of adventitia (**Figure 2A**). Then the two layers of adventitia were anastomosed continuously to the inverted part of the graft with 4–0 prolene (**Figure 2A**). Thereafter, the rest part of the artificial graft was dragged out of the aortic root (**Figures 2B,D,E**). Finally, cold blood cardioplegia was infused through the artificial graft with a relatively high pressure (approximate 200 mmHg measured in the infusing line) in order to check any leak in the anastomosis site

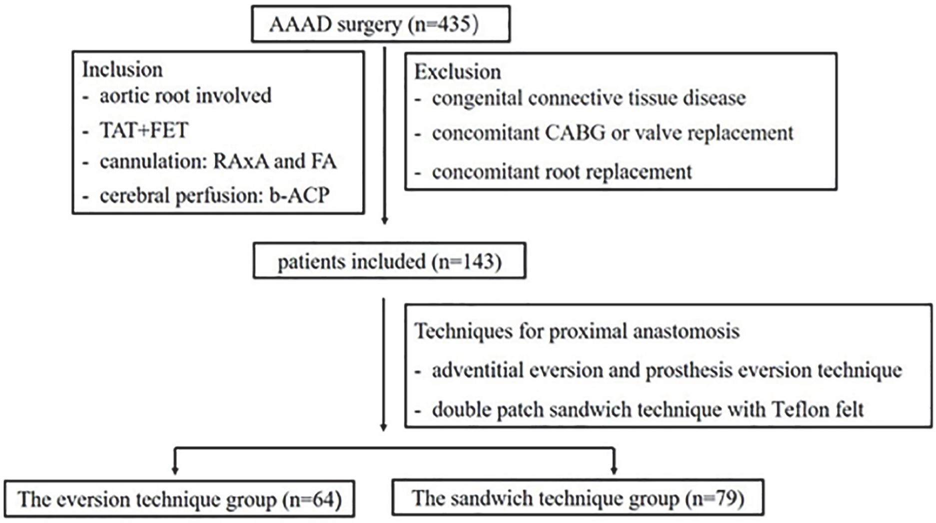

FIGURE 1
Schematic of the study cohort. Between December 2017 and May 2021, 435 patients with AAAD underwent surgical repair in our department. 143 patients were included in this study according to the inclusion and exclusion criteria. These patients were divided into two groups according to the repair methods of proximal anastomosis, the eversion technique group (adventitial eversion and prosthesis eversion technique for proximal anastomosis, *n* = 64) and the sandwich technique group (double patch sandwich technique with Teflon felt for proximal anastomosis, *n* = 79). AAAD, acute type A aortic dissection; TAT, total arch replacement; TET, frozen elephant trunk; RAA, right axillary artery; FA, femoral artery; b-ACP, bilateral antegrade cerebral perfusion; CABG, coronary artery bypass graft.

and aortic valvular function (**Figure 2F**). If any leak was detected in the anastomosis site, additional stitches were applied to achieve hemostasis and checked with cardioplegia infusion again. Regarding aortic valvular regurgitation, initial view of the valvular structure, then cardioplegia infusion in the artificial graft with a relatively high pressure, and concomitant observation of left ventricular expansion were carried out in sequence. Once aortic valvular insufficiency was observed, valve replacement or valvuloplasty was conducted, but the case was excluded from the current study.

Double patch sandwich technique with Teflon felt for aortic root repair (the sandwich technique group)

Teflon felt strips were placed inside and outside the suture line, respectively. Continuous transverse mattress suture with 4–0 prolene was performed to finish the double patch sandwich. Then, a segment of artificial graft was anastomosed continuously to the double patch sandwich with 4–0 prolene. Afterward, cardioplegia was infused through the artificial graft in order to check for any leak in the anastomosis site and to test the aortic valvular function. The remained procedures were similar to the eversion technique group.

When the dissection involves part of the coronary opening and the surrounding intima of the coronary opening is intact, special reinforcement of the coronary artery is not necessary for performing these two techniques. When the surrounding intima of the coronary opening is not intact, pericardium may be used for the reinforcement of the coronary artery.

Step 3: TAT + FET

After the proximal anastomosis, circulatory arrest of the body lower part was performed at moderate hypothermia (Nasopharyngeal temperature 26–27°C). Bilateral cerebral perfusion was achieved *via* the right axillary artery and left common carotid artery (LCCA). The aortic arch was opened longitudinally, and thereafter the stent elephant trunk was placed into the true lumen of the descending aorta. The orifice of the left subclavian artery (LSA) was totally covered by the stent elephant trunk, and subsequently the LSA root was closed. Afterward, the distal end of the four-branched artificial graft was anastomosed to the proximal end of the stent elephant trunk and aortic wall. Then, systemic perfusion was recovered through the cannulas in the femoral artery, and bleeding was checked in anastomosis sites between the distal end of the four-branched artificial graft and the proximal end of the stent elephant trunk. Finally, the LCCA and LSA were connected to the two 8-mm branches of the four-branched artificial graft, respectively with 5–0 prolene.

Step 4

The proximal end of four-branched artificial graft was continuously anastomosed to the artificial graft of step 2 with 4–0 prolene. Afterward, aortic cross clamp was released, and the brachiocephalic trunk reconstruction was performed. Transesophageal echocardiography was conducted before the weaning of CPB to test any abnormality of the valve and the

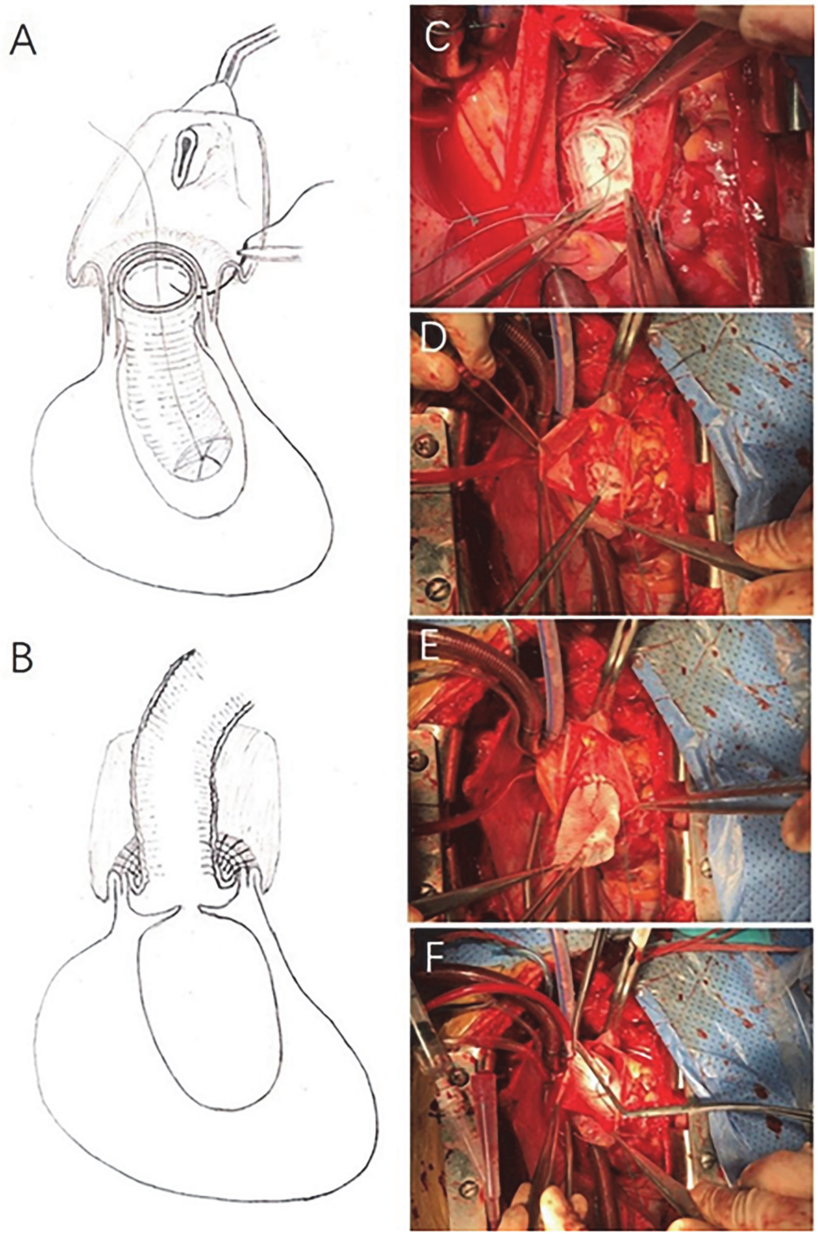

FIGURE 2
Adventitial eversion and prosthesis eversion technique for proximal anastomosis. A segment of artificial graft was inverted and inserted into the aortic root **(A,C)**. During the suture, the adventitia above the suture line was everted to form two layers of adventitia **(A).** The two layers of adventitia were directly anastomosed to the inverted part of the graft with continuous 4–0 prolene **(A)**. Thereafter, the rest part of the artificial graft was dragged out of the aortic root **(B,D,E)**. Afterward, cardioplegia was infused through the artificial graft in order to check any possible bleeding at the anastomosis site and aortic valve function **(F)**.

cardiac chambers. All the patients were transferred to the cardiac surgery intensive care unit after the operation.

Data collection and follow-up

The preoperative data were collected from the medical records, including age, gender, body weight, diabetes mellitus, hypertension, chronic kidney disease, hyperlipidemia, serum creatinine (SCr), smoking, and drinking history. The operation data included operation duration, time of CPB, aortic cross-clamp (ACC), proximal anastomosis, and circulatory arrest (CA). The time of proximal anastomosis was defined as the time interval from the beginning of aortic cross-clamp to the circulatory arrest of the lower part of the body.

The data of postoperative complications were also collected, including the drainage volume of the postoperative 24 h, reoperation for bleeding, mechanical ventilation time, hospital stay, paraplegia, stroke, renal failure, gastrointestinal bleeding, and tracheotomy.

Outcomes of 1-year follow-up were obtained by telephone interview, rehospitalization records, and clinical examinations at the outpatient clinic. Telephone interviews were performed at 1, 3, 6, and 12 months. According to the American guidelines, transthoracic echocardiography (TTE) and aortic CTA were performed at 3, 6, and 12 months (4, 5). Aortic root events were defined as follows: aortic root dilation (the diameter of aortic sinus $\geq$ 45 mm), moderate or greater aortic valve insufficiency.

Statistical analysis

Continuous variables obeying normal distribution were compared by a *t*-test and expressed as the mean $\pm$ standard deviation ($M \pm SD$). Continuous variables disobeying normal distribution were analyzed by the Mann–Whitney *U*-test and expressed as median (interquartile range). Categorical variables were analyzed by *chi*-square and Fisher exact tests and expressed as percentages. SPSS (IBM SPSS Statistics for Windows, Version 21.0. Armonk, NY: IBM Corp.) was used for the analysis. $P < 0.05$ was considered statistically significant.

Results

Preoperative characteristics

The medical record review survey showed that sandwich technique was mainly conducted prior to December 2019, and thereafter, the eversion technique was applied until the end of study. The data of preoperative characteristics are listed in **Table 1**. There were 64 and 79 patients in the eversion technique group and the sandwich technique group, respectively. There was no significance in the mean age and the percentage of male patients between the eversion technique group and the sandwich technique group ($P > 0.05$, respectively). The preoperative median SCr concentration was 77 μmol/L in the eversion technique group and 91 μmol/L in the sandwich technique group ($P > 0.05$). No statistical differences were observed in hypertension, diabetes mellitus, LVEF, albumin, hyperlipidemia, transient ischemic attack (TIA), cystatin C (Cys-C), D-Dimer, and history of drinking and smoking between two groups ($P > 0.05$, respectively).

Operation data

The operation data are presented in **Table 2**. The mean operation time in the eversion technique group was shorter than that in the sandwich technique group (466 $\pm$ 73 min *vs.* 513 $\pm$ 81 min, $P < 0.001$). The average CPB time in the eversion technique group was also shortened compared with that in the sandwich technique group (195 $\pm$ 26 min *vs.* 211 $\pm$ 40 min, $P = 0.003$). Both proximal anastomosis time and aortic cross-clamp time in the eversion technique group were shown shortened (38 $\pm$ 12 min *vs.* 58 $\pm$ 20 min, $P < 0.001$; and 120 $\pm$ 23 min *vs.* 134 $\pm$ 27 min, $P = 0.002$, respectively) compared with sandwich technique group. The proportion of > 600 ml fresh frozen plasma (FFP) in eversion group was reduced than that in sandwich technique group while no statistical differences in packed red blood cells (PRBC) transfusion between the two groups. No patients in both of the two groups underwent aortic root replacement due to the uncontrollable bleeding at the anastomosis.

Postoperative morbidity

Postoperative morbidity is shown in **Table 3**. The median drainage volume of the postoperative 24 h was 350 (IQR = 350) ml in the eversion technique group and 300 (IQR = 300) ml in the sandwich technique group ($P > 0.05$). The median time of mechanical ventilation was 37.1 (IQR = 45.9) hours in the eversion technique group and 38.3 (IQR = 43.9) hours in the sandwich technique group ($P > 0.05$). No statistical differences were observed in the incidences of paraplegia (0% *vs.* 1.3%), stroke (6.3% *vs.* 8.9%), renal failure (6.3% *vs.* 6.3%), gastrointestinal bleeding (1.6% *vs.* 1.3%), and tracheotomy (4.7% *vs.* 3.8%) in the eversion technique group and the sandwich technique group.

One-year follow-up outcomes

The outcomes of 1-year follow-up are listed in **Table 4**. The mortality of the eversion technique group and the sandwich technique group was 6.3% *vs.* 6.3% at 30-day, 9.4% *vs.* 7.6% at 3 months, 9.4% *vs.* 8.9% at 6 months, and 9.4% *vs.* 8.9% at 12 months, respectively ($P > 0.05$). One patient in the eversion technique group and one patient in the sandwich technique group underwent reoperation of aortic root during the follow-up period ($P > 0.05$) due to aortic root event.

Discussion

The present study aimed to introduce the experiences of adventitial eversion and prosthesis eversion technique in the proximal anastomosis of AAAD. The results demonstrated that patients in the eversion technique group obtained a shorter time in operation, CPB, proximal anastomosis, and aortic cross-clamp compared with the sandwich technique

TABLE 1 Preoperative characteristics.

Categories	Eversion technique ($n = 64$)	Sandwich technique ($n = 79$)	*P*-value
Age, y, $M \pm SD$	51.3 ± 11.7	50.0 ± 9.0	0.48
Male, n (%)	50 (78.1)	59 (74.7)	0.63
BW, kg, $M \pm SD$	76.1 ± 13.1	78.4 ± 14.1	0.33
Drinking, n (%)	22 (34.4)	24 (30.4)	0.61
Smoking, n (%)	30 (46.9)	31 (39.2)	0.36
Hypertension, n (%)	48 (75.0)	64 (81.0)	0.39
Cerebral disease history, n (%)	6 (9.4)	6 (7.6)	0.70
Diabetes mellitus, n (%)	2 (3.1)	2 (2.5)	1.00
LVEF < 0.45	2 (3.1)	3 (3.8)	1.00
Albumin, g/L, $M \pm SD$	36.7 ± 4.2	35.8 ± 4.6	0.22
Hyperlipidemia, n (%)	8 (12.5)	9 (11.4)	0.84
Hepatic dysfunction, n (%)	10 (15.6)	22 (27.8)	0.081
IIA occlusion, n (%)	1 (1.6)	1 (1.3)	1.00
TIA, n (%)	2 (3.1)	3 (3.8)	1.00
SCr, μmol/L, median (IQR)	77 (34.5)	91 (68.0)	0.060
Cys-C, mg/L, median (IQR)	0.885 (0.36)	0.94 (0.52)	0.15
D-Dimer, μg/ml, median (IQR)	2.02 (3.00)	2.61 (3.77)	0.52

BW, body weight; IIA, internal iliac artery; TIA, transient ischemic attack; SCr, serum creatinine; Cys-C, cystatin C; IQR, interquartile range.

TABLE 2 The operation data.

Categories	Eversion technique ($n = 64$)	Sandwich technique ($n = 79$)	*P*-value
Operation time, min, $M \pm SD$	466 ± 73	513 ± 81	< 0.001
CPB time, min, $M \pm SD$	195 ± 26	211 ± 40	0.003
ACC time, min, $M \pm SD$	120 ± 23	134 ± 27	0.002
PA time*, min, $M \pm SD$	38 ± 12	58 ± 20	< 0.001
CAtime, min, $M \pm SD$	22 ± 8	24 ± 6	0.085
Temperature,°C, $M \pm SD$	26.7 ± 1.1	26.5 ± 1.1	0.33
FFP transfusion, n (%)			0.002
≤ 600 ml	57 (89.1)	52 (65.8)	
> 600 ml	7 (10.9)	27 (34.2)	
PRBC transfusion, u, median (IQR)	4 (4)	4 (4)	0.91

CPB, cardiopulmonary bypass; ACC, aortic cross-clamp; PA, proximal anastomosis; CA, circulatory arrest; FFP, fresh frozen plasma; PRBC, packed red blood cell; IQR, interquartile range.
*PA time was defined as the time interval from the beginnings of aortic cross-clamp to circulatory arrest of the lower part of the body.

TABLE 3 Postoperative morbidities.

Categories	Eversion technique ($n = 64$)	Sandwich technique ($n = 79$)	*P*-value
First day drainage, ml, median (IQR)	350 (350)	300 (300)	0.13
Reoperation for bleeding, n (%)	0 (0)	0 (0)	–
Ventilation, h, median (IQR)	37.1 (45.9)	38.3 (43.9)	0.81
Hospital stay time, d, median (IQR)	18.5 (8)	19 (8)	0.83
Paraplegia, n (%)	0 (0)	1 (1.3)	–
Stroke, n (%)	4 (6.3)	7 (8.9)	0.79
Gastrointestinal bleeding, n (%)	1 (1.6)	1 (1.3)	0.88
Renal failure, n (%)	4 (6.3)	5 (6.3)	0.98
Tracheotomy, n (%)	3 (4.7)	3 (3.8)	0.79

IQR, interquartile range.

TABLE 4 One-year follow-up outcomes.

Categories	Eversion technique (n = 64)	Sandwich technique (n = 79)	P-value
Mortality at follow-up, n (%)			–
30-day	4 (6.3)	5 (6.3)	0.98
3 months	6 (9.4)	6 (7.6)	0.72
6 months	6 (9.4)	7 (8.9)	0.92
12 months	6 (9.4)	7 (8.9)	0.92
Reoperation at 12 months, n (%)			–
TEVAR	2 (3.1)	3 (3.8)	0.83
EVAR	1 (1.6)	0 (0)	–
Aortic root reoperation	1 (1.6)	1 (1.3)	0.88
Aortic arch reoperation	0 (0)	0 (0)	–
Aortic root events at 12 months n (%)			–
Aortic root dilation	1 (1.6)	1 (1.3)	0.88
Moderate or severe AI	0	0	–

TEVAR, thoracic endovascular aortic repair; EVAR, endovascular abdominal aortic repair; AI, aortic valvular insufficiency.

group. Less transfusion of FFP in the eversion technique was needed compared with that in the sandwich group. No statistical differences were found between the two groups in the postoperative morbidities such as the incidences of paraplegia, reoperation for bleeding, stroke, renal failure, gastrointestinal bleeding, and tracheotomy. The 1-year follow-up results showed that the mortality, the incidences of reoperation, and the aortic root event were similar in the two groups.

The International Registry of Acute Aortic Dissection (IRAD) study reported that the early mortality of AAAD surgery had declined from 25 to 18% in the past 17 years (6). In the present study, the 30-day mortality was 6.3% (4/64) in the eversion technique group and 6.3% (5/79, $P > 0.05$) in the sandwich technique group. The early mortality in this study was lower than that in IRAD study. The discrepancy may be due to the difference in patient population. We found that the average age of patients in our study was much younger than that in the IRAD study. In 2011, the first Registry of Aortic Dissection (Sino-RAD) was established in China. The data from Sino-RAD showed that the early mortality of AAAD surgery was 5.3%, which was similar to the early mortality in our study (7).

Over the past decades, several techniques were conducted by the cardiac surgeons to attempt to achieve a safer proximal anastomosis. Prosthesis eversion technique for proximal anastomosis of AAAD was first described by Pretre in 1998 (8). In the subsequent reports, Teflon strip was used to reinforce the proximal anastomosis of the aorta (9, 10). Despite the acceptance of Teflon felt for the proximal anastomosis, limitations have also been reported. Teflon felt could cause extensive adhesions and inflammation, which may prevent the complete healing of the dissected aorta (11, 12). Biological glue was another technique used for the repair of aortic root, which has been shown to improve the results of the AAAD surgery (2, 13). However, the bioglue compound used for hemostasis may increase the risk of aortic root re-dissection and make possible embolisms in cerebral and coronary arteries (14, 15). In the current study, adventitial eversion and prosthesis eversion technique was used for proximal anastomosis with the fact that neither was Teflon strip used to wrap the adventitia of the aortic wall nor was bioglue used to fill the anastomotic sites. During the operation, no intractable bleeding at proximal anastomosis occurred in the eversion technique group, indicating that the anastomosis was intact and satisfactory. The results showed that the combination of adventitial eversion and prosthesis eversion technique had several advantages: (1) the double-layer adventitia was flexible and strong enough to reinforce the aortic wall and control the bleeding from needle holes and small anastomotic tears; (2) the double-layer adventitia was autologous tissue without the reaction of organism on the prosthesis material; (3) the combination of adventitial eversion and prosthesis eversion technique allowed a good vision of the structures for proximal anastomosis, a tension-free and quick proximal anastomosis could be achieved; and (4) the possible bleeding at the proximal anastomosis could be checked and repaired before circulatory arrest by the cardioplegia perfusion in the proximal artificial graft.

Long-term CPB and hypothermia during the surgery are regarded as the risk factors of mortality and morbidity in the aortic arch operation for AAAD (16). Thus, on the premise of safety and fine suture, cardiac surgeons tried different surgical techniques to shorten the time of CPB and hypothermia in AAAD surgery. The time of CPB and hypothermia may be heavily confounded by the extent of tissue destruction. However, we thought that it could also be affected by the choice of anastomosis technique. Our data indicated that the eversion technique group showed a shorter time on operation, CPB, proximal anastomosis, and aortic cross-clamp as well as less application of FFP. It was also reported that the late re-intervention rates of the sandwich technique with Teflon felt and biological glue could reach 23 and 20%, respectively (14, 17–19). During the 1-year follow-up period, only one patient (1/64, 1.6%) in the eversion technique group underwent re-operation of aortic root due to the postoperative aortic root event. Based on the above results, we could conclude that the combination of adventitial eversion and prosthesis eversion technique without Teflon strip or bioglue may be a simple and safe suture method for proximal anastomosis in AAAD patients.

The study also has several limitations. It was a retrospective study from a single center and the sample size was relatively small. A randomized controlled trial of multi-center study with larger sample was needed to confirm the advantages of adventitial eversion and prosthesis eversion techniques. The follow-up period was limited, and long-term follow-up would be carried out in the future study. As the AAAD patient population in China was different from that in Western countries, whether this technique was suitable for the Western population remains to be proved.

Conclusion

Proximal anastomosis with adventitial eversion and prosthesis eversion technique is a promising surgical option for AAAD patients, with favorable perioperative and 1-year follow-up results.

Data availability statement

The raw data supporting the conclusions of this article will be made available by the authors, without undue reservation.

Ethics statement

All the protocols were approved by the Medical Ethics Committee of Qilu Hospital of Shandong University (Reference No. KYLL-2017KS-195). The Ethics Committee waived the requirement of written informed consent for participation.

Author contributions

CF: writing and correction. SG: data collection. XR, XZ, and CW: data collection and statistical analysis. XP: check and correction. ZM: design and check. KL: design and writing. All authors contributed to the article and approved the submitted version.

Funding

This study was supported by the National Natural Science Foundation of China (NOS. 81600293 and 81500367), the Natural Science Foundation of Shandong Province (NO. ZR2021MH221), and the Key Research and Development Projects of Shandong Province (NO. 2018GSF121007) and the clinical research program of Shandong University (NO. 2020SDUCRCC031).

Conflict of interest

The authors declare that the research was conducted in the absence of any commercial or financial relationships that could be construed as a potential conflict of interest.

Publisher's note

All claims expressed in this article are solely those of the authors and do not necessarily represent those of their affiliated organizations, or those of the publisher, the editors and the reviewers. Any product that may be evaluated in this article, or claim that may be made by its manufacturer, is not guaranteed or endorsed by the publisher.

References

1. Shrestha M, Haverich A, Martens A. Total aortic arch replacement with the frozen elephant trunk procedure in acute DeBakey type I aortic dissections. *Eur J Cardiothorac Surg.* (2017) 51:i29–34. doi: 10.1093/ejcts/ezw341

2. Zhu C, Piao H, Wang Y, Wang T, Li D, Xu R. A new aortic root reinforcement technique for acute type a aortic dissection surgery. *Int Heart J.* (2019) 60:1131–6. doi: 10.1536/ihj.18-609

3. Fleck TM, Tschernich H, Grabenwoger M, Hutschala D, Koinig H, Wolner E, et al. A double patch sandwich technique for surgical repair of acute aortic dissection type A. *Ann Thorac Surg.* (2003) 76:499–502. doi: 10.1016/S0003-4975(03)00459-4

4. Arsalan M, Squiers JJ, Herbert MA, MacHannaford JC, Themistokles Chamogeorgakis T, Prince SL, et al. Comparison of outcomes of operative therapy for acute type A aortic dissections provided at high-volume versus low-volume medical centers in north texas. *Am J Cardiol.* (2017) 119:323–7. doi: 10.1016/j.amjcard.2016.09.034

5. Hiratzka LF, Bakris GL, Beckman JA, Bersin RM, Carr VF, Casey DE Jr., et al. 2010 ACCF/AHA/AATS/ACR/ASA/SCA/SCAI/SIR/STS/SVM guidelines for the diagnosis and management of patients with thoracic aortic disease. A report of the American college of cardiology foundation/American heart association task force on practice guidelines, American association for thoracic surgery, American college of radiology, American stroke association, society of cardiovascular

anesthesiologists, society for cardiovascular angiography and interventions, society of interventional radiology, society of thoracic surgeons, and society for vascular medicine. *J Am Coll Cardiol.* (2010) 55:e27–129.

6. Evangelista A, Isselbacher EM, Bossone E, Gleason TG, Eusanio MD, Sechtem U, et al. Insights from the international registry of acute aortic dissection: a 20-year experience of collaborative clinical research. *Circulation.* (2018) 137:1846–60. doi: 10.1161/CIRCULATIONAHA.117.031264

7. Wang W, Duan W, Xue Y, Wang L, Liu J, Yu S, et al. Clinical features of acute aortic dissection from the registry of aortic dissection in China. *J Thorac Cardiovasc Surg.* (2014) 148:2995–3000. doi: 10.1016/j.jtcvs.2014.07.068

8. Pretre R. Performance of a safe proximal anastomosis in aortic dissection. *Ann Thorac Surg.* (1998) 65:1798–9. doi: 10.1016/S0003-4975(98)00214-8

9. Inoue Y, Minatoya K, Itonaga T, Oda T, Seike Y, Tanaka H, et al. Utility of proximal stepwise technique for acute aortic dissection involving the aortic root. *Ann Thorac Surg.* (2016) 101:e183–5. doi: 10.1016/j.athoracsur.2015.11.050

10. Rignano A, Keller GC, Carmo M, Anguissola GB, Settembrini PG. A new approach for proximal anastomosis in type "a" acute aortic dissection: prosthesis eversion. *Ann Thorac Surg.* (2003) 76:949–51. doi: 10.1016/S0003-4975(03)00444-2

11. Yang B, Malik A, Waidley V, Kleeman KC, Wu XT, Norton EL, et al. Short-term outcomes of a simple and effective approach to aortic root and arch repair in acute type A aortic dissection. *J Thorac Cardiovasc Surg.* (2018) 155:1360–70. doi: 10.1016/j.jtcvs.2017.11.089

12. Rylski B, Bavaria JE, Milewski RK, Vallabhajosyula P, Moser W, Kremens E, et al. Long-term results of neomedia sinus valsalva repair in 489 patients with type A aortic dissection. *Ann Thorac Surg.* (2014) 98:582–8. doi: 10.1016/j.athoracsur.2014.04.050

13. Suzuki S, Masuda M, Imoto K. The use of surgical glue in acute type A aortic dissection. *Gen Thorac Cardiovasc Surg.* (2014) 62:207–13. doi: 10.1007/s11748-013-0343-0

14. Bingley JA, Gardner MA, Stafford EG, Mau TK, Pohlner PG, Tam RK, et al. Late complications of tissue glues in aortic surgery. *Ann Thorac Surg.* (2000) 69:1764–8. doi: 10.1016/S0003-4975(00)01250-9

15. Karck M. The glue crisis in surgery of acute aortic dissection type A is ongoing. *Eur J Cardiothorac Surg.* (2012) 41:e36–7. doi: 10.1093/ejcts/ezs020

16. Conzelmann LO, Weigang E, Mehlhorn U, Abugameh A, Hoffmann I, Blettner M, et al. Mortality in patients with acute aortic dissection type A: analysis of pre- and intraoperative risk factors from the German registry for acute Aortic dissection type A (GERAADA). *Eur J Cardiothorac Surg.* (2016) 49:e44–52. doi: 10.1093/ejcts/ezv356

17. Yamanaka K, Hori Y, Ikarashi J, Kusuhara T, Nakatsuka D, Hirose K, et al. Durability of aortic valve preservation with root reconstruction for acute type A aortic dissection. *Eur J Cardiothorac Surg.* (2012) 41:e32–6. doi: 10.1093/ejcts/ezr292

18. Concistre G, Casali G, Santaniello E, Montalto A, Fiorani B, Dell'Aquila A, et al. Reoperation after surgical correction of acute type A aortic dissection: risk factor analysis. *Ann Thorac Surg.* (2012) 93:450–5. doi: 10.1016/j.athoracsur.2011.10.059

19. Casselman FP, Tan ES, Vermeulen FE, Kelder JC, Morshuis WJ, Schepens MA. Durability of aortic valve preservation and root reconstruction in acute type A aortic dissection. *Ann Thorac Surg.* (2000) 70:1227–33. doi: 10.1016/S0003-4975(00)01966-4

frontiers | Frontiers in Cardiovascular Medicine

TYPE Original Research
PUBLISHED 28 October 2022
DOI 10.3389/fcvm.2022.1000619

Check for updates

OPEN ACCESS

EDITED BY
Wayne Zhang,
School of Medicine, University of Washington, United States

REVIEWED BY
Zhou Qing,
Nanjing Drum Tower Hospital, China
Elizabeth L. Norton,
School of Medicine, Emory University, United States

*CORRESPONDENCE
Shaozhong Yang
yszyang@163.com

†These authors share first authorship

SPECIALTY SECTION
This article was submitted to Heart Surgery, a section of the journal Frontiers in Cardiovascular Medicine

RECEIVED 22 July 2022
ACCEPTED 12 October 2022
PUBLISHED 28 October 2022

CITATION
Zhang X, Lv W, Liu X, Liu K and Yang S (2022) Impact of shift work on surgical outcomes at different times in patients with acute type A aortic dissection: A retrospective cohort study.
Front. Cardiovasc. Med. 9:1000619.
doi: 10.3389/fcvm.2022.1000619

Impact of shift work on surgical outcomes at different times in patients with acute type A aortic dissection: A retrospective cohort study

Xiang Zhang[1†], Weiwei Lv[2†], Xin Liu[1], Kai Liu[3] and Shaozhong Yang[1*]

[1]Department of Anesthesiology, Qilu Hospital of Shandong University, Jinan, Shandong, China,
[2]Department of Radiology, Qilu Hospital of Shandong University, Jinan, Shandong, China,
[3]Department of Cardiovascular Surgery, Qilu Hospital of Shandong University, Jinan, Shandong, China

Background: To investigate the effect of shift work on surgical outcomes at different times in patients with acute type A aortic dissection (ATAAD).

Materials and methods: Patients with ATAAD who underwent total arch replacement at Qilu Hospital of Shandong University from January 2015 to March 2022 were retrospectively analyzed. All patients were managed according to the green channel emergency management strategy, and a professional cardiac team was arranged during off-hours. Based on surgery time and symptom onset to procedure time, the patients were divided into weekday, weekend and holiday groups; daytime and nighttime groups; intervention time ≤48 h and >48 h groups; working hours and off-hours groups. In-hospital mortality between these groups was compared.

Results: In total, 499 ATAAD patients underwent surgery within 7 days of symptom onset, and the in-hospital mortality rate was 10% (n = 50/499). Among the 499 patients, 320 (64.13%), 128 (25.65%) and 51 (10.22%) underwent surgery on weekdays, weekends and holidays, respectively. In-hospital mortality and 7-day mortality showed no significant difference among the three groups. Two hundred twenty-seven (45.5%) underwent daytime surgery, and 272 (54.5%) underwent nighttime surgery. Durations of ICU stay and hospital stay were significantly different between the two groups ($P < 0.05$). There was no significant differences in in-hospital mortality (9.2% vs. 10.7%) and 7-day mortality (4.4% vs. 6.6%). 221 patients (44.3%) and 278 patients (55.7%) were included in the intervention time ≤48 h and >48 h groups, respectively. Acute renal injury, ICU stay and hospital stay were significantly different ($P < 0.05$) whereas 7-day mortality (5.0% vs. 6.1%) and in-hospital mortality (8.6% vs. 11.1%) were not. Furthermore, 7-day (1.9% vs. 6.6%) and in-hospital mortality (11.1% vs. 9.8%) showed no difference between working hours group (n = 108) and off-hours group (n = 391). Cox regression analysis showed that postoperative acute renal injury (HR = 2.423;

95% CI, 1.214–4.834; *P* = 0.012), pneumonia (HR = 2.542; 95% CI, 1.186–5450; *P* = 0.016) and multiple organ dysfunction (HR = 11.200; 95% CI, 5.549–22.605; *P* = 0.001) were the main factors affecting hospital death in ATAAD patients.

Conclusion: Under the management of a professional cardiac surgery team with dedicated off-hours shifts, surgery time was not related to in-hospital mortality in ATAAD patients.

KEYWORDS

acute type A aortic dissection, total arch replacement, shift work, off-hours, hospital mortality

Introduction

Acute type A aortic dissection (ATAAD) is a life-threatening emergency with high mortality (1). The death risk of ATAAD was estimated to be 1 to 2% per hour, and non-surgical treatment was associated with mortality in nearly 60% of patients (2). Emergency open ascending aorta replacement is the preferred method to prevent adverse outcomes (3, 4). However, such operations rely more on senior surgical teams with extensive experience in dealing with complex vascular patients (5). Affected by many factors, ATAAD surgery usually occurs at off-hours. It is well known that the allocation and ability of hospital medical staff at night, weekends and holidays may be different compared with weekdays, and the attention of medical staff is also affected, which may affect the perioperative outcome of ATAAD patients.

Nighttime surgery can lead to fatigue and inattention among doctors and nurses (6). Studies have found that nighttime and weekend surgery can increase the in-hospital mortality of ATAAD patients (7, 8). However, the recent results of the international registry of artic dissection (IRAD) show that there was no difference in mortality between the daytime and nighttime, workday and weekend cohorts of ATAAD patients (9). Another study also confirmed that there was no relationship between the 30-day mortality of ATAAD patients and whether the operation was performed on weekends or weekdays (10). However, a meta-analysis found that weekend admission or surgery for acute aortic dissection may be associated with increased mortality (11). A recent study showed that the mortality of patients with acute aortic dissection admitted on weekends was higher than that of patients admitted on weekdays, while there was no difference between holidays and working days (12). The difference in the above results may be related to the different allocations of medical personnel and resources in different medical units during off-hours.

To reduce the impact of weekend and holiday effects on the survival rate of surgical patients, Qilu Hospital of Shandong University has established an ATAAD operation team composed of cardiac surgeons, anesthesiologists, and operating room nurses since 2015 and has arranged special shift personnel at night, weekends and holidays. All patients were treated with an emergency green channel integrated management strategy. Cardiac surgeons and anesthesiologists on the team are required to have experience in more than 50 cases of aortic dissection. To avoid excessive fatigue, all operations were performed by the team in a shift work mode. The purpose of this study was to investigate whether there were differences in the in-hospital mortality of patients undergoing ATAAD surgery in our center on weekdays, weekends or holidays, daytime and nighttime under the shift work mode.

Patients and methods

The STROBE guidelines were used to ensure the reporting of this study.

Study design and participants

This single-center retrospective cohort study was conducted in Qilu Hospital, Shandong University, Jinan, China, using data from the database. This study was carried out in accordance with the Declaration of Helsinki (2013 Edition) and was approved by Qilu Hospital of Shandong University Medical Ethics Committee (No. KYLL-202204-048). From January 2015 to March 2022, the data of patients who were diagnosed with ATAAD and underwent total arch replacement in our center were collected from the database. Because of the retrospective nature of the study, any requirement for informed consent was waived.

The green channel emergency management strategy consisted of 3 parts. (1) First, emergency procedures related to ATAAD were formulated, and a special green channel was established for the patients, including pre-hospital and intra-hospital first aid. Printing the green channel sign of aortic dissection and hanging warning lights to help ensure the patients were sent to the designated area quickly and accurately. (2) Second, the hospital departments including emergency department, cardiac surgery department, laboratory department, imaging department, anesthesia department and operating room were combined together. A special rescue team composed of personnel with sufficient work experience has been established. The work responsibilities of the medical staff in each department were the comprehensive management strategy of emergency green channel, and regular training and evaluation were conducted. (3) The emergency physicians were responsible for quickly identifying patients' diseases and evaluating the severity of their conditions. In addition, they were responsible for arranging the medical guideline to send patients to the designated doctor's office for diagnosis and emergency treatment. Therefore, in our center, regardless of whether the patients are admitted to the hospital on weekdays, weekends or holidays, once the patients are diagnosed, they are prepared for emergency surgical treatment. According to the standard of diagnosis and treatment, all patients were sedated and were given analgesics before the operation, and their blood pressure (100–120 mmHg) and heart rate (60–80 beats/min) were strictly controlled.

In recent decades, ATAAD has generally been defined as any disease involving the ascending aorta within 14 days after the onset of symptoms (4). Since the time delay from symptom onset to surgical treatment in ATAAD patients significantly changes the survival rate (7), this study selected patients within 7 days of symptom onset according to the new aortic dissection time classification proposed by the IRAD (13). The inclusion criteria were patients aged 18–80 years, diagnosed with ATAAD (CT angiography of the Aorta, **Figure 1**) and undergoing total aortic arch replacement. The primary exclusion criteria were conservative treatment, death before or during surgery, and symptom onset > 7 days.

Surgical techniques

Surgeries were a standard longitudinal median sternotomy. The procedure was mostly performed with right axillary artery cannulation for cardiopulmonary bypass (CPB) and selective antegrade cerebral perfusion under moderate hypothermic circulatory arrest at approximately 26–27°C. A total arch replacement using a tetrafurcated graft with implantation of a stented graft in the descending aorta. Related surgical techniques have been described in detail in previously publications of our center (14).

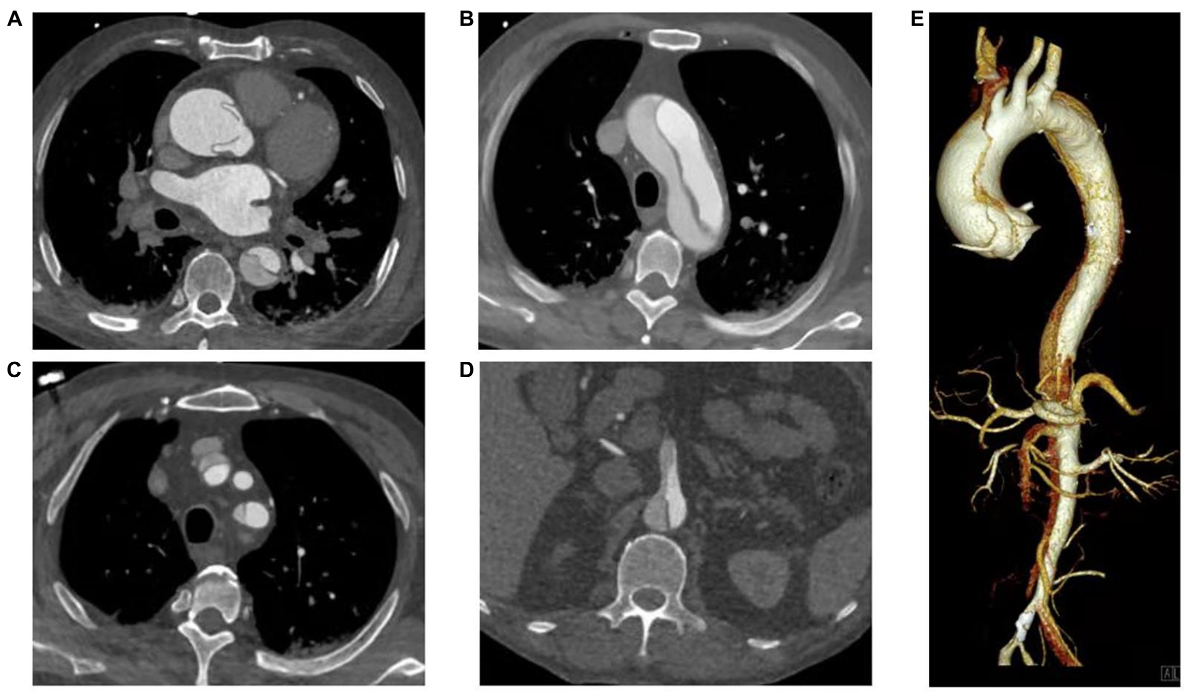

FIGURE 1
CT Angiography of the Aorta. **(A)** Ascending aorta; **(B)** Aortic arch; **(C)** Branch of aortic arch (involving brachiocephalic trunk and left subclavian artery); **(D)** Aortic dissection involving superior mesenteric artery; **(E)** Volumetric CT scanning: 3D reconstruction.

We set up two special data reviewers for the study, consisting of a cardiac surgeon and a radiologist, who performed a consistent ATAAD diagnostic code and selected patients strictly according to the inclusion and exclusion criteria.

Unlike other studies, which grouped patients according to the date of admission (8, 9, 12), we divided patients into the following three groups according to the surgery date and the Chinese legal holidays of the current year: weekdays, weekends and holidays. Based on the data of the patients operated on weekdays, the mortality risk of patients operated on during weekends and holidays was compared.

The patients were divided into daytime and nighttime groups according to the start and end times of the operation. Daytime is defined as 8:00–17:00, and nighttime is defined as 17:00 to 8:00. If the start time and end time belong to different time ranges, a time range of 50% of the operation time should be considered. In addition, according to the time from symptom onset to surgical intervention, the patients were divided into ≤48 h and >48 h groups. We also divided the operation into working hours group and off-hours group according to whether the operation was performed during working hours, and an intergroup analysis was conducted.

Data collection

Patient data, including age, sex, time from symptom onset to admission, preoperative laboratory examination, time from admission to operation, operation date, operation start and end time; CPB time, intraoperative blood transfusion, postoperative ICU stay, postoperative complications, hospital stay, hospitalization outcome, etc., were collected.

Outcomes

The primary outcome was in-hospital mortality. The secondary outcomes were 7-day mortality, 30-day mortality, postoperative complications and hospitalization outcome, etc.

Sample size calculation

The study sample size was calculated with PASS 15 (NCSS, LLC. Kaysville, Utah, USA). According to previous studies in China and the IRAD (6, 10), the mortality rates of the daytime group and the nighttime group were 5.84% and 15.33%, respectively, and there was no difference between the working day group and the weekend group. Therefore, a total of 219 patients per group provided 90% power at a 2-sided α of 5%. Assuming a 5% dropout rate, a total of at least 462 patients are needed.

Statistical analysis

SPSS 24.0 statistical software was used for statistical analysis. All statistical tests of hypotheses were two-sided and performed at the 0.05 level of significance. The missing values of intraoperative blood transfusion were supplemented by the mean value substitution method. Quantitative variables were expressed as the mean and standard deviation (SD) or the median and interquartile range (IQR) for non-normally distributed data, and qualitative variables were expressed as frequencies and percentages. For continuous data, if the measured data conformed to a normal distribution, analysis of variance was used; when the data did not conform to a normal distribution, the Kruskal–Wallis test was used. For categorical variables, the Chi-square test or Fisher's exact test was used for comparison. Kaplan-Meier analysis was used to estimate the survival function of patients who survived during hospitalization, while the log-rank test was used for comparison. Univariate and multivariate Cox regression analyses were used to evaluate the correlation between surgical hospitalization results at different times and the related risk factors for in-hospital death, and HRs and 95% CIs were calculated. The variables with $P < 0.1$ in univariate analysis were included in multivariate regression analysis.

Results

From January 2015 to March 2022, a total of 561 patients with ATAAD received surgical treatment, including 47 patients with the onset of symptoms for more than 7 days, 5 patients over the age of 80 years, 3 patients who died during the operation, and 7 patients who only underwent ascending aortic replacement (**Figure 2**). Finally, a total of 499 patients with ATAAD who underwent surgery were included in our study, with an average age of 52.79 ± 11.88 years, of which 70.54% were male (n = 352/499), the in-hospital mortality rate was 10.0% (n = 50/499), and the 7-day mortality rate was 5.6% (n = 28/499). The most frequent comorbidity was hypertension [77.76% (n = 388/499)] (**Table 1**).

Comparison of weekdays, weekends and holidays

The baseline characteristics of the three groups are listed in **Table 1**. Among the 499 patients, 320 (64.13%) were in the weekday group, 128 (25.65%) were in the weekend group and 51 (10.22%) were in the holiday group. There was no significant difference in age, sex, comorbidity, laboratory examination or the time from the onset of symptoms to admission among the three groups.

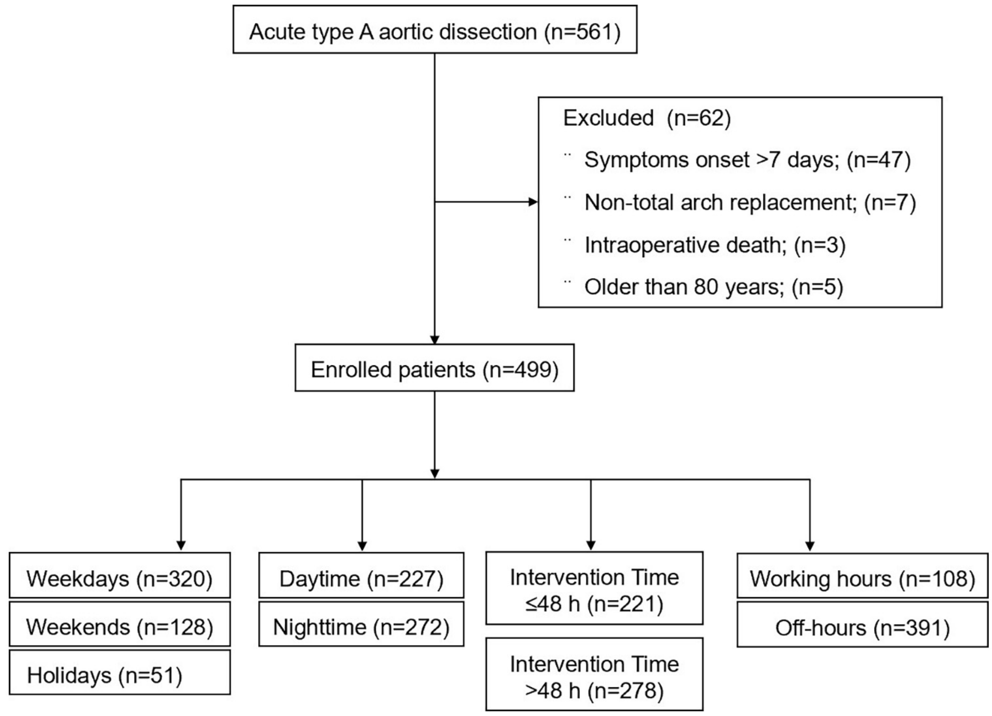

FIGURE 2
Study flow diagram.

As shown in Table 2, there was no significant difference among the three groups in terms of CPB time, operation time, intraoperative blood transfusion, concomitant operation, time from admission to operation intervention, ICU stay, hospital stay, postoperative complications, 7-day mortality or in-hospital mortality. However, there was a significant difference in the number of patients undergoing daytime and nighttime surgery among the three groups ($P < 0.001$). The proportion of nighttime operations was higher in the weekday group [66.2% (n = 212/320)], while the proportion of daytime operations was higher in the weekend group and the holiday group [62.5% (n = 80/128) and 76.5% (n = 39/51), respectively].

Comparison of daytime and nighttime operations

According to the start and end time of surgery, 227 (45.5%) of 499 patients underwent surgery during the daytime, while 272 (54.5%) underwent surgery at nighttime. As shown in Table 3, there was no significant difference in the baseline characteristics between the daytime group and the nighttime group. Compared with the daytime group, the D-dimer (DD) [2.99 (1.20–5.95) vs. 2.09 (0.94–4.84), $P = 0.006$] and Aspartate aminotransferase (AST) [29.00 (18.25–59.75) vs. 23.00 (16.00–46.00), $P = 0.005$] in the nighttime group were significantly higher ($P < 0.01$), and the n-terminal pro-brain natriuretic peptide (NT-proBNP) [794.95 (436.08–1569.69) vs. 1727.00 (645.20–3317.00), $P = 0.001$] was significantly lower –($P < 0.01$), with statistical difference.

As shown in Table 4, there was no significant difference between the daytime group and the nighttime group in terms of operation time, intraoperative autologous blood, plasma and cryoprecipitate transfusion, concomitant surgery, postoperative complications, hospitalization outcome, etc. Compared with the daytime group, the 7-day mortality rate [6.6% (n = 18/272) vs. 4.4% (n = 10/227)] and in-hospital mortality rate [10.7% (n = 29/272) vs. 9.2% (n = 21/227)] in the nighttime group were higher, but there was no significant difference. There were significant differences between the two groups in CPB time, intraoperative packed red blood cell (PRBC) and platelet transfusion, ICU stay and hospital stay ($P < 0.05$). Compared with the daytime group, the nighttime group had a longer CPB time [230.00 (195.00–275.00) vs. 214.00 (188.00–257.00), $P < 0.01$], more intraoperative PRBC transfusions [4.00 (3.25–4.20) vs. 4.00(2.00–4.20), $P < 0.05$] and fewer platelet transfusions [1.98 (1.96–2.00) vs. 2.00 (1.96–2.00), $P < 0.01$]. However, in terms of ICU stay [4.00 (3.00–7.00) vs. 5.00 (4.00–7.00), $P < 0.05$] and hospital stay [18.00 (14.00–22.00) vs. 20.00 (15.00–25.00), $P < 0.01$], the nighttime group was shorter, with a significant difference.

Comparison of surgical intervention times ≤48 h and >48 h

With reference to the 48-h intervention time, 221 (44.3%) patients underwent surgery within 48 h of the onset of symptoms, and 278 (55.7%) patients underwent surgical intervention for more than 48 h. There was no significant difference between the two groups in terms of age, sex or comorbidity (Table 3). Compared with the group with intervention time ≤48 h, the white blood cell counts (WBC) (10.11 [9.37–13.41] vs. 11.60 [9.33–13.42], *P* = 0.001), hemoglobin (HGB) (121.00[108.00–133.00]) vs. 127.00 [110.00–139.00], *P* = 0.004), activated partial thromboplastin time (APTT) (29.70 [27.80–33.35]) vs. 32.00 [28.90–36.60], *P* = 0.001), DD (1.56 [0.79–2.94] vs. 4.33 [2.36–11.59]), *P* = 0.001), alanine aminotransferase (ALT)

TABLE 1 Preoperative patient characteristics.

Characteristic	Total cohort (*n* = 499)	Weekday (*n* = 320)	Weekend (*n* = 128)	Holiday (*n* = 51)	*P*-value
Age (years)	52.79 (11.88)	52.56 (11.94)	53.73 (11.90)	53.90 (11.69)	0.549
Sex (male)	352 (70.54)	229 (71.6)	92 (71.9)	31 (60.8)	0.272
Hypertension	388 (77.76)	249 (77.8)	95 (74.2)	44 (86.3)	0.216
Coronary disease	52 (10.42)	34(10.6)	12 (9.4)	6 (11.8)	0.877
Diabetes mellitus	13 (2.61)	10 (3.1)	1 (0.8)	2 (3.9)	0.230
Marfan syndrome	7 (1.40)	5 (1.6)	2 (1.6)	0 (0.0)	1.000
History of cardiac surgical treatment	14 (2.81)	10 (3.1)	4 (3.1)	0 (0.0)	0.216
History of stroke	29 (5.81)	16 (5.0)	8 (6.3)	5 (9.8)	0.429
Peripheral vascular disease	6 (1.20)	4 (1.3)	1 (0.8)	1 (2.0)	0.666
Heart failure	18 (3.61)	13 (4.1)	2 (1.6)	3 (5.9)	0.251
COPD	4 (0.80)	2 (0.6)	2 (1.6)	0 (0.0)	0.561
Dyslipidemia	8 (1.60)	5 (1.6)	2 (1.6)	1 (2.0)	0.872
Massive pericardial effusion	10 (2.00)	6 (1.9)	4 (3.1)	0 (0.0)	0.247
Chronic kidney disease	13 (2.61)	8 (2.5)	4 (3.1)	1 (2.0)	0.890
WBC (10^9/L)	10.59 (8.50–12.72)	10.61 (8.53–12.72)	10.45 (7.99–12.77)	11.30 (8.97–12.71)	0.650
HGB (g/L)	123.00 (109.00–135.00)	126.00 (110.00–136.00)	119.50 (108.00–134.00)	119.00 (108.00–134.00)	0.129
PLT (10^9/L)	152.00 (123.00–190.50)	154.00 (126.25–192.75)	148.00 (120.00–187.50)	161.00 (122.00–200.00)	0.507
PT (s)	13.10 (12.10–14.40)	13.00 (12.10–14.30)	13.10 (12.00–14.80)	13.50 (12.40–14.60)	0.393
APTT (s)	30.80 (28.20–35.03)	30.50 (28.10–35.13)	30.80 (28.30–34.40)	31.30 (28.50–35.75)	0.684
DD (μg/ml)	2.51 (1.06–5.45)	2.44 (1.03–4.97)	2.41 (1.03–5.40)	4.33 (1.87–8.98)	0.078
ALT (U/L)	19.00 (13.00–34.00)	20.00 (13.00–36.25)	17.50 (12.00–27.00)	22.00 (13.00–37.00)	0.136
AST (U/L)	26.00 (17.00–52.00)	27.00 (17.00–52.00)	24.00 (16.00–61.00)	26.50 (19.00–52.25)	0.922
SCr (μmol/L)	84.00 (65.00–115.00)	85.00 (65.00–114.00)	84.00 (65.00–125.00)	80.00 (63.00–116.00)	0.475
CTn I (ng/L)	13.16 (2.52–333.64)	12.94 (2.42–288.93)	18.72 (2.95–719.08)	9.71 (1.50–365.35)	0.811
NT-proBNP	1057.00 (459.45–2242.50)	912.60 (512.60–1909.00)	1677.00 (519.13–3430.50)	908.55 (347.38–2596.50)	0.069
Time from symptom onset to be hospitalized (h)	15.00 (9.00–24.00)	15.00 (9.00–24.00)	14.50 (10.00–24.00)	12.00 (8.00–24.00)	0.770

Values are presented as the mean (SD), median (IQR), or number of patients (%).
COPD, chronic obstructive pulmonary disease; SD, standard deviation; IQR, interquartile range. WBC, white blood cell counts; HGB, hemoglobin; PLT, platelet; PT, prothrombin time; APTT, activated partial thromboplastin time; DD, D-Dimer; ALT, alanine aminotransferase; AST, aspartate aminotransferase; SCr, serum creatinine; CTn I, cardiac troponin I; n-terminal pro-brain natriuretic peptide, NT-proBNP.

TABLE 2 Intraoperative and postoperative patient characteristics.

Variable	Total cohort (n = 499)	Weekday (n = 320)	Weekend (n = 128)	Holiday (n = 51)	P-value
CPB time (min)	221.50 (191.25–267.00)	225.50 (192.00–268.50)	224.00 (191.50–271.25)	207.50 (184.74–255.25)	0.300
Operation time (min)	505.00 (440.00–575.00)	505.00 (445.00–578.75)	510.00 (440.00–580.00)	460.00 (430.00–560.00)	0.134
Autologous blood transfusion (ml)	573.69 (500.00–573.69)	573.69 (500.00–573.69)	573.69 (500.00–573.69)	573.69 (500.00–573.69)	0.785
PRBC transfusion (U)	4.00 (2.00–4.20)	4.00 (2.00–4.20)	4.00 (2.00–4.20)	4.00 (2.00–4.20)	0.496
Plasma transfusion (mL)	500.00 (400.00–600.00)	500.00 (400.00–647.50)	500.00 (400.00–600.00)	400.00 (400.00–650.00)	0.462
Cryoprecipitate transfusion (U)	17.56 (16.00–17.56)	17.56 (16.00–17.56)	17.56 (16.00–17.56)	17.56 (16.00–17.56)	0.923
Platelet transfusion (U)	2.00 (1.96–2.00)	2.00 (1.96–2.00)	2.00 (1.96–2.00)	2.00 (1.96–2.00)	0.735
Concomitant operation					
Bentall	64 (12.83)	37 (11.6)	21 (16.4)	6 (11.8)	0.389
CABG	22 (4.41)	17 (5.3)	5 (3.9)	0 (0.0)	0.109
MVR	4 (0.80)	1 (0.3)	3 (2.3)	0 (0.0)	0.108
Pneumonia	73 (14.6)	44 (13.8)	21 (16.4)	8 (15.7)	0.747
Tracheotomy	27 (5.4)	18 (5.6)	6 (4.7)	3 (5.9)	0.956
Acute kidney injury	146 (29.3)	98 (30.7)	35 (27.3)	13 (25.5)	0.654
CRRT	59 (11.8)	39 (12.2)	14 (10.9)	6 (11.8)	0.955
Stroke	24 (4.8)	13 (4.1)	8 (6.3)	3 (5.9)	0.668
Hepatic hypofunction	105 (21.1)	63 (19.7)	31 (24.4)	11 (21.6)	0.538
Gastrointestinal bleeding	23 (4.6)	23 (3.8)	8 (6.3)	3 (5.9)	0.496
Multisystem organ failure	42 (8.4)	23 (7.2)	15 (11.7)	4 (7.8)	0.319
Surgical intervention time (T)					0.096
T ≤ 48 h	221 (44.3)	142 (64.3)	50 (22.6)	29 (13.1)	
T > 48 h	278 (55.7)	178 (64.0)	78 (28.1)	22 (7.9)	
Daytime or Nighttime					0.001
Daytime	227 (45.5)	108 (33.8)	80 (62.5)	39 (76.5)	
Nighttime	272 (54.5)	212 (66.2)	48 (37.5)	12 (23.5)	
Clinical outcomes					0.740
Cure	380 (76.2)	248 (77.5)	93 (72.7)	39 (76.5)	
Automatic discharge	69 (13.8)	44 (13.8)	19 (14.8)	6 (11.8)	
Death	50 (10.0)	28 (8.8)	16 (12.5)	6 (11.8)	
ICU stay (d)	5.00 (3.00–7.00)	5.00 (3.00–7.00)	5.00 (3.00–7.00)	5.00 (4.00–7.00)	0.826
Hospital stay (d)	19.00 (14.00–23.00)	19.00 (14.00–23.75)	19.00 (14.00–23.00)	19.00 (15.00–24.00)	0.694
7-day mortality	28 (5.6)	15 (4.7)	10 (7.8)	3 (5.9)	0.515
In-hospital mortality	50 (10.0)	28 (8.8)	16 (12.5)	6 (11.8)	0.451

Bentall, aortic valve replacement with a valved conduit; CABG, coronary artery bypass grafting; MVR, mitral valve replacement; CPB, cardiopulmonary bypass; PRBC, packed red blood cell; CRRT, continuous renal replacement therapy.

(17.00 [11.25–29.75]) vs. 22.00 [14.00–39.50], P = 0.002), AST (21.00 [15.00–38.00] vs. 35.00 [22.00–76.00]), P = 0.001) and serum creatinine (SCr) (80.00 [63.00–106.75] vs. 90.00 [69.00–124.00]), P = 0.002) were significantly decreased in the preoperative laboratory examination of the >48 h group, but the median values of the above indicators were within the normal range. The platelet (PLT) of >48 h group was significantly higher than that of ≤48 h group (158.00 [127.00–20.00]) vs. 147.00 [120.00–184.00], P = 0.038).

As shown in Table 4, there was no significant difference between the two groups in all intraoperative and postoperative characteristics, except for postoperative acute renal injury, ICU stay and hospital stay. The 7-day mortality rate [6.1% (n = 17/278) vs. 5.0% (n = 11/221), P = 0.583] and in-hospital mortality rate [11.1% (n = 31/278) vs. 8.6% (n = 19/221), P = 0.345] in the intervention time >48 h group were higher than those in the intervention time ≤48 h group, but there was no significant difference. In addition, the incidence of postoperative acute renal injury [33.1% (n = 92/278) vs. 24.4%

TABLE 3 Preoperative characteristics of daytime and nighttime groups or intervention times ≤48 h and >48 h.

Variable	Daytime (n = 227)	Nighttime (n = 272)	P-value	Intervention time ≤ 48 h (n = 221)	Intervention time > 48 h (n = 278)	P-value
Age (years)	53.04 (11.69)	52.97 (12.09)	0.949	52.01 (11.93)	53.78 (11.83)	0.098
Sex (male)	163 (71.8)	189 (69.5)	0.571	160 (72.4)	192 (69.1)	0.417
Hypertension	180(79.3)	208 (76.5)	0.450	177 (80.1)	211 (75.9)	0.263
Coronary disease	27 (11.9)	25 (9.2)	0.325	20 (9.0)	32 (11.5)	0.371
Diabetes mellitus	5 (2.2)	8 (3.0)	0.601	5 (2.3)	8 (2.9)	0.664
Marfan syndrome	4 (1.8)	3 (1.1)	0.809	1 (0.45)	7 (2.52)	0.068
History of cardiac surgical treatment	5 (2.2)	9 (3.3)	0.456	6 (2.7)	8 (2.9)	0.913
History of stroke	16 (7.0)	13 (4.8)	0.281	11 (5.0)	18 (6.5)	0.478
Peripheral vascular disease	2 (0.9)	4 (1.5)	0.850	3 (1.4)	3 (1.1)	1.000
Heart failure	9 (4.0)	9 (3.3)	0.696	9 (4.1)	9 (3.2)	0.619
COPD	2 (0.9)	2 (0.7)	1.000	1 (0.5)	3 (1.1)	0.633
Dyslipidemia	5 (2.2)	3 (1.1)	0.538	4 (1.8)	4 (1.4)	0.737
Massive pericardial effusion	1 (0.4)	9 (3.3)	0.050	3 (1.4)	7 (2.5)	0.524
Chronic kidney disease	8 (3.5)	5 (1.8)	0.239	4 (1.8)	9 (3.2)	0.320
WBC (10^9/L)	10.40 (8.06–12.60)	10.79 (8.79–12.81)	0.650	11.60 (9.33–13.42)	10.11 (9.37–13.41)	0.001
HGB (g/L)	122.00 (111.00–134.00)	124.00 (108.00–138.00)	0.330	127.00 (110.00–139.00)	121.00 (108.00–133.00)	0.004
PLT (10^9/L)	158.50 (124.25–196.75)	146.50 (122.00–185.75)	0.146	147.00 (120.00–184.00)	158.00 (127.00–200.00)	0.038
PT (s)	13.20 (12.10–14.40)	13.10 (12.10–14.43)	0.926	13.30 (12.20–14.60)	13.00 (12.10–14.20)	0.149
APTT (s)	30.20 (28.10–34.15)	31.30 (28.30–35.83)	0.056	32.0 (28.90–36.60)	29.70 (27.80–33.35)	0.001
DD (µg/ml)	2.09 (0.94–4.84)	2.99 (1.20–5.95)	0.006	4.33 (2.36–11.59)	1.56 (0.79–2.94)	0.001
ALT (U/L)	18.00 (12.00–30.00)	21.00 (13.00–37.00)	0.057	22.00 (14.00–39.50)	17.00 (11.25–29.75)	0.002
AST (U/L)	23.00 (16.00–46.00)	29.0 (18.25–59.75)	0.005	35.00 (22.00–76.00)	21.00 (15.00–38.00)	0.001
SCr (µmol/L)	80.00 (63.00–115.00)	89.00 (66.00–115)	0.175	90.00 (69.00–124.00)	80.00 (63.00–106.75)	0.002
CTn I (ng/L)	10.10 (2.63–332.82)	19.74 (2.33–341.25)	0.651	24.67 (2.88–445.87)	10.24 (2.04–264.04)	0.317
NT-proBNP	1727.00 (645.30–3317.00)	794.95 (436.08–1569.69)	0.001	909.20 (520.70–1732.00)	1245.50 (482.13–2672.25)	0.337
Time from symptom onset to be hospitalized (h)	15.00 (10.00–24.00)	14.00 (9.00–24.00)	0.165	10.00 (7.00–17.00)	24.00 (12.00–48.00)	0.001

(n = 54/221), P = 0.035], ICU stay [5.00 (4.00–7.00) vs. 4.00 (3.00–7.00), P = 0.017] and hospital stay [20.00 (15.00–24.25) vs. 18.00 (14.00–22.00), P = 0.018] in the intervention time >48 h group were significantly higher than those in the intervention time ≤48 h group, with significant differences.

Comparison of working hours and off-hours groups

Four hundred ninety-nine patients were divided into two groups according to working hours and off-hours. Among them, 108 patients underwent surgery during working hours and 391 patients underwent surgery during off-hours. We analyzed the intraoperative and postoperative characteristics of the two groups. There were significant differences between the two groups only in platelet transfusion [2.00 (1.96–2.00) vs. 2.00 (1.96–2.00), P = 0.017], the incidence of gastrointestinal bleeding after surgery [0.9% (n = 1/108) vs. 5.9% (n = 22/391), P = 0.038] and ICU stay [5.00(4.00–8.00) vs. 5.00(3.00–7.00), P = 0.011] (Table 5).

Comparison of the 7-day and in-hospital mortality of patients in different years

We compared the 7-day and in-hospital mortality of patients in different years. In order to balance the number of patients between different years, they were divided into one groups every

TABLE 4 Intraoperative and postoperative characteristics of daytime and nighttime groups or intervention times ≤48 H and >48 H.

Variable	Daytime (*n* = 227)	Nighttime (*n* = 272)	*P*-value	Intervention time ≤ 48 h (*n* = 221)	Intervention time > 48 h (*n* = 278)	*P*-value
CPB time (min)	214.00 (188.00–257.00)	230.00 (195.00–275.00)	0.007	226.00 (195.25–269.75)	216.00 (189.25–266.75)	0.247
Operation time (min)	505.00 (445.00–570.00)	502.50 (440.00–580.00)	0.680	505.00 (445.00–580.00)	500.00 (440.00–575.00)	0.429
Autologous blood transfusion (mL)	573.69 (400.00–573.69)	573.69 (500.00–573.69)	0.932	573.69 (500.00–573.69)	573.69 (400.00–573.69)	0.054
PRBC transfusion (U)	4.00 (2.00–4.20)	4.00 (3.25–4.20)	0.041	4.00 (2.00–5.50)	4.00 (2.00–4.00)	0.058
Plasma transfusion (mL)	500.00 (400.00–600.00)	500.00 (400.00–615.00)	0.288	500.00 (400.00–725.00)	500.00 (400.00–600.00)	0.345
Cryoprecipitate transfusion (U)	17.56 (16.00–17.56)	17.56 (16.00–17.56)	0.966	17.56 (16.00–17.56)	17.56 (16.00–17.56)	0.800
Platelet transfusion (U)	2.00 (1.96–2.00)	1.98 (1.96–2.00)	0.008	2.00 (1.96–2.00)	2.00 (1.96–2.00)	0.525
Concomitant operation						
Bentall	30 (13.2)	34 (12.5)	0.893	29(13.1)	35(12.6)	0.860
CABG	10 (4.4)	12 (4.4)	1.000	7 (3.2)	15 (5.4)	0.228
MVR	2 (0.9)	2 (0.7)	1.000	2 (0.9)	2 (0.7)	1.000
Pneumonia	35 (15.4)	38 (14.0)	0.703	31 (14.0)	42 (15.1)	0.734
Tracheotomy	14 (6.2)	13 (4.8)	0.554	12 (5.4)	15(5.4)	0.987
Acute kidney injury	70 (30.8)	76 (28.0)	0.553	54 (24.4)	92 (33.1)	0.035
CRRT	30 (13.2)	29 (10.7)	0.406	24 (10.9)	35 (12.6)	0.552
Stroke	9 (4.0)	15 (5.0)	0.530	14 (6.3)	10 (3.6)	0.156
Hepatic hypofunction	51 (22.6)	54 (19.9)	0.508	48 (21.7)	57 (20.6)	0.756
Gastrointestinal bleeding	7 (3.1)	16(5.9)	0.198	13 (5.9)	10 (3.6)	0.222
Multisystem organ failure	25 (11.0)	17 (6.3)	0.074	18 (8.1)	24 (8.6)	0.845
Clinical outcomes			0.531			0.639
Cure	179 (78.9)	203 (74.6)		173 (78.3)	212 (76.3)	
Automatic discharge	27 (11.9)	40 (14.7)		29 (13.1)	35 (12.6)	
Death	21 (9.2)	29 (10.7)		19 (8.6)	31 (11.1)	
ICU stay (d)	5.00 (4.00–7.00)	4.00 (3.00–7.00)	0.010	4.00 (3.00–7.00)	5.00 (4.00–7.00)	0.017
Hospital stay (d)	20.00 (15.00–25.00)	18.00 (14.00–22.00)	0.007	18.00 (14.00–22.00)	20.00 (15.00–24.25)	0.018
7-day mortality	10 (4.4)	18 (6.6)	0.332	11 (5.0)	17(6.1)	0.583
In-hospital mortality	21 (9.2)	29 (10.7)	0.601	19 (8.6)	31 (11.1)	0.345

two years. As shown in Table 6, there is no significant difference in 7-day mortality and in-hospital mortality among patients in different years.

Survival analysis

The log-rank test was used to test the differences between groups, as shown in Figure 3. There was no significant difference in the in-hospital mortality among the weekday group, weekend group and holiday group, daytime group and nighttime group, intervention time ≤48 h group and >48 h group, working hours group and off-hours group.

Cox regression analysis was conducted to study the correlation between 7-day death and in-hospital death and various factors. First, univariate Cox regression analysis was performed on each variable to screen out the variables with $P < 0.1$. After using a bivariate correlation test to exclude confounding factors, the remaining eligible variables were included in multivariate Cox regression.

The univariate Cox regression analysis found that the HR value and 95% CI of each variable in the preoperative laboratory examination were very close to 1, suggesting that it was not related to the 7-day and hospital death, so it was not included in the multivariate analysis. As shown in Table 7, multivariate Cox regression analysis showed that different groups had no effect on the 7-day mortality and in-hospital mortality ($P > 0.05$). The risk factors of 7-day death and in-hospital death included CPB time (HR = 1.010, 95% CI 1.006–1.014, $P = 0.001$) (HR = 1.007, 95% CI 1.004–1.011, $P = 0.001$), intraoperative PRBC blood transfusion (HR = 1.210, 95% CI 1.094–1.338, $P = 0.001$) (HR = 1.122, 95% CI 1.029–1.223, $P = 0.009$), postoperative pneumonia (HR = 5.298, 95% CI 1.437–19.534, $P = 0.012$) (HR = 2.542, 95% CI 1.186–5.450, $P = 0.016$),

TABLE 5 Intraoperative and postoperative characteristics of working hours and off- hours groups.

Variable	Working hours(n = 108)	Off-hours (n = 391)	*P*-value
CPB time (min)	215.00 (187.75–262.25)	225.00 (193.75–270.25)	0.107
Operation time (min)	520.00 (460.00–578.75)	500.00 (440.00–575.00)	0.125
Autologous blood transfusion (ml)	573.69 (500.00–573.69)	573.69 (500.00–573.69)	0.381
PRBC transfusion (U)	4.00 (2.00–4.20)	4.00 (2.00–4.20)	0.171
Plasma transfusion (mL)	534.10 (400.00–650.00)	500.00 (400.00–600.00)	0.761
Cryoprecipitate transfusion (U)	17.56 (16.00–17.56)	17.56 (16.00–17.56)	0.834
Platelet transfusion (U)	2.00 (1.96–2.00)	2.00 (1.96–2.00)	0.017
Concomitant operation			
Bentall	12 (11.1)	52 (13.3)	0.547
CABG	7 (6.5)	15 (3.8)	0.286
MVR	0 (0.0)	4 (1.0)	0.582
Pneumonia	16 (14.8)	57 (14.6)	0.951
Tracheotomy	8 (7.4)	19 (4.9)	0.300
Acute kidney injury	39 (36.1)	107 (27.4)	0.080
CRRT	18 (16.7)	41 (10.5)	0.080
Stroke	3 (2.8)	21 (5.4)	0.265
Hepatic hypofunction	23 (21.3)	82(21.0)	0.951
Gastrointestinal bleeding	1 (0.9)	22 (5.9)	0.038
Multisystem organ failure	10 (9.3)	32 (8.2)	0.722
Clinical outcomes			0.623
Cure	84 (77.8)	296 (75.7)	
Automatic discharge	12 (11.1)	57 (14.6)	
Death	12 (11.1)	38 (9.7)	
ICU stay (d)	5.00 (4.00–8.00)	5.00 (3.00–7.00)	0.011
Hospital stay (d)	21.00 (15.00–25.00)	18.00 (14.00–23.00)	0.059
7-day mortality	2 (1.9)	26 (6.6)	0.059
In-hospital mortality	12 (11.1)	38 (9.7)	0.670

TABLE 6 The 7-day and in-hospital mortality of patients in different years.

Variable	2015.01–2016.12 (n = 134)	2017.01–2018.12 (n = 163)	2019.01–2020.12 (n = 107)	2021.01–2022.03 (n = 95)	*P*-value
7-day mortality	13 (9.7)	6 (3.7)	4 (3.7)	5(5.3)	0.106
In-hospital mortality	16 (11.9)	13 (8.0)	12 (11.2)	9 (9.5)	0.681

acute renal function injury (HR = 3.085, 95% CI 1.302–7.310, P = 0.011) (HR = 2.423, 95% CI 1.214–4.834, P = 0.012) and multiple system organ failure (HR = 6.041, 95% CI 2.400–15.206, P = 0.001) (HR = 11.200, 95% CI 5.549–22.605, P = 0.001), with statistical significance.

Discussion

Recent reports from large datasets show that the operative mortality after ATAAD repair ranges from 17 to 20% (15). Data from a Beijing Heart Surgery Center in China obtained for 10 years showed that the operative mortality rate of ATAAD was 7.5% (16). Our results showed that the in-hospital mortality of ATAAD patients within 7 days of symptom onset was 10.0%.

Studies have confirmed that weekend or holiday effects will increase inpatient mortality (9, 10, 17, 18). For ATAAD patients, nighttime surgery may also be an independent high-risk factor for in-hospital death (7). Due to the imbalance of medical resources and economic conditions in China, most ATAAD patients need to be transferred to tertiary hospitals or heart centers for surgery. The latest research showed that in China, the mean interval from symptom onset to surgery for ATAAD was 5 days (19). Our results showed that there was no difference in inpatient mortality, 7-day mortality and postoperative complications among patients on

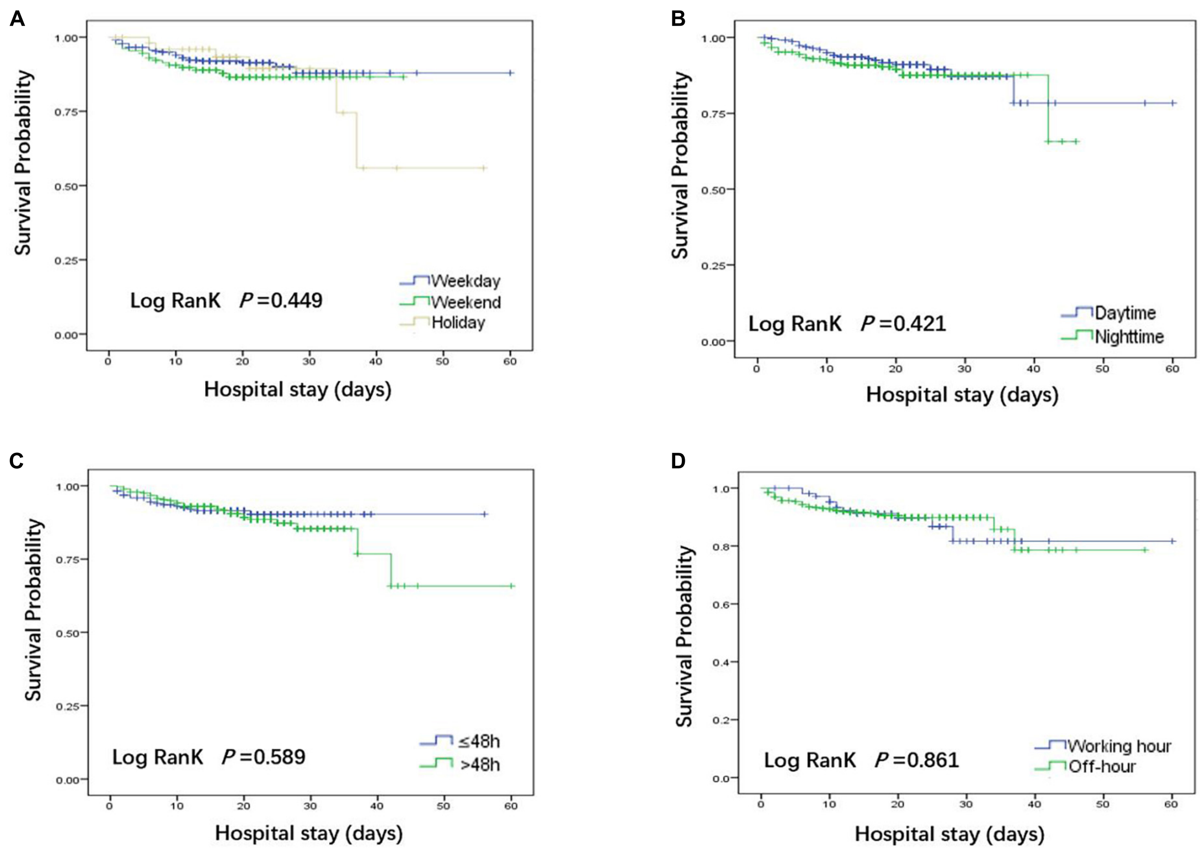

FIGURE 3
Kaplan-Meier curves were used to compare the in-hospital deaths of patients in each group. **(A)** Comparison of patients undergoing weekdays, weekends and holidays; **(B)** Comparison of patients undergoing daytime and nighttime surgery; **(C)** Comparison of patients with surgical intervention times ≤48 h and >48 h. **(D)** Comparison of patients undergoing working hours and off-hours.

TABLE 7 Risk analysis of 7-day death and in-hospital death.

	Deaths within 7 days				Deaths within hospital stay			
Risk factor	**B**	**HR**	**95% CI**	***P*-value**	**B**	**HR**	**95% CI**	***P*-value**
CPB time	0.010	1.010	1.006–1.014	0.001	0.007	1.007	1.004–1.011	0.001
PRBC transfusion	0.190	1.210	1.094–1.338	0.001	0.115	1.122	1.029–1.223	0.009
Acute kidney injury	1.126	3.085	1.302–7.310	0.011	0.855	2.423	1.214–4.834	0.012
Multisystem organ failure	1.799	6.041	2.400–15.206	0.001	2.416	11.200	5.549–22.605	0.001
Pneumonia	1.667	5.298	1.437–19.534	0.012	0.933	2.542	1.186–5.450	0.016
Weekday/Weekend/Holiday	0.301	1.352	0.791–2.309	0.270	0.136	1.146	0.766–1.716	0.508
Daytime/Nighttime	0.430	1.538	0.657–3.597	0.321	−0.193	0.825	0.450–1.514	0.534
≤48h/>48 h	−0.572	0.564	0.256–1.242	0.155	−0.333	0.717	0.404–1.271	0.717
Working hours/Off-hours	1.307	3.695	0.877–15.570	0.075	−0.58	0.944	0.493–1.807	0.861

weekdays, weekends or holidays, as well as during the daytime or nighttime, provided that the emergency green channel integrated management strategy and the specialized cardiac operative teams had dedicated nighttime, weekend or holiday shifts. This was consistent with the recent research results of IRAD (9). In addition, our cohort analysis of working hours and off-hours showed that there was also no difference between 7-day mortality and in-hospital mortality.

We also found that although there was no difference in mortality, the CPB time of the nighttime group was longer than that of the daytime group, but it did not affect the operation time, which may be related to the fatigue of doctors at night. Early studies have shown that cardiac surgeons, anesthesiologists and perfusionists will be in a state of fatigue during off-hours (20). The difference in PRBC and platelet input between the two groups may be related to the use of mean substitution of missing values, which has no clinical significance. The difference in ICU stay and hospital stay between the two groups may be related to our time unit (d).

Studies have shown that delaying the time of surgical intervention can increase the risk of death in ATAAD patients (1, 5). To more reliably describe the survival rate after aortic dissection, IRAD proposed a new time classification of aortic dissection in 2013: hyperacute (0–24 h), acute (2–7 days), subacute (8–30 days), and chronic (≥30 days) (13). Considering the high time-related mortality of ATAAD, we followed the new classification of IRAD and only included patients diagnosed with ATAAD from the onset of symptoms to 7 days. This study showed that compared with the intervention time ≤48 h group, there was no difference in 7-day mortality and in-hospital mortality in the intervention time >48 h group, but the incidence of postoperative acute renal injury was significantly higher in the group with more than 48 h of intervention, accompanied by a significant extension of ICU stay and hospital stay.

The fatigue of doctors may be closely related to the prognosis of patients. Doctor fatigue may increase the operation time, cardiopulmonary bypass time and aortic occlusion time. A longer cardiopulmonary bypass time is also considered to be a high-risk factor for acute renal injury, which further leads to higher in-hospital mortality (21). Our results showed that there was no difference in CPB time or operation time between the group with an intervention time >48 h and the group with an intervention time ≤48 h. The operation team adopted the form of shift and requires team members to ensure at least 3 h of rest before operation, so it can also be explained that this working mode helps to improve the fatigue and poor performance of team members. On the other hand, the 7-day mortality and in-hospital mortality of the group with intervention time >48 h did not increase, indicating that rapid and effective control of blood pressure, pulse and pain can help stabilize the patient's condition and reduce the patient's mortality after the patient is admitted to the hospital.

Clinical studies have shown that acute renal function injury is a common complication after ATAAD, with an incidence of approximately 40.6%, which can independently predict poor long-term prognosis (22). Our study confirmed that the extension of intervention time will increase the incidence of postoperative acute renal function injury. Multivariate Cox regression showed that postoperative acute renal function injury was an independent risk factor for hospitalized death in admitted patients, suggesting that we need early prevention and intervention of perioperative renal function.

Although there may be significant differences in preoperative laboratory test results between different groups, univariate Cox regression found that these factors had little effect on 7-day and in-hospital death. Our multivariate Cox regression also found that intraoperative CPB time, intraoperative PRBC transfusion, postoperative acute kidney injury, pneumonia and multiple organ dysfunction were independent risk factors for 7-day and in-hospital death. There are significant differences in intraoperative PRBC transfusion, which may be related to the application of intraoperative blood management technology. The increase in intraoperative CPB time is a predictor of the immediate incidence rate and mortality after adult heart surgery (23). Hemolysis may occur during CPB and is associated with acute renal injury after surgery (24). In addition to acute renal insufficiency, ATAAD patients are also prone to multiple organ dysfunction, such as pneumonia, liver dysfunction, coagulation disorder, gastrointestinal bleeding, and stroke, which is related to in-hospital mortality (14, 25). Therefore, to improve the postoperative recovery quality and survival rate of ATAAD patients, we should actively avoid or treat postoperative complications.

The latest large-scale cross-sectional study confirmed that there was no link between surgeon fatigue caused by overnight surgery and adverse perioperative outcomes of patients (26). However, it is well known that compared with the general surgical population, the risk of heart and aortic surgery and the incidence of postoperative adverse events are higher. ATAAD emergency surgery patients are more serious, and the operation is more difficult and takes longer, which requires the cooperation and coordination of the intraoperative team. Therefore, further research is needed to confirm whether the occupational fatigue of team medical staff caused by night or long-term surgery affects the perioperative survival rate of emergency surgery patients with ATAAD.

This study has some limitations. (1) This is a retrospective study, and the results may be affected by the non-randomized nature. (2) This study only included patients who underwent aortic arch replacement surgery, not patients who died before and during surgery, and we excluded patients who had symptoms for more than 7 days. The results could not be extended to all ATAAD patients. (3) Our ICU stay was not calculated by the hour, which had a large error and may affect the results. (4) The patients did not receive follow-up after discharge; it was impossible to obtain more credible and accurate conclusions.

Conclusion

Patients with ATAAD should be operated on as soon as the diagnosis is confirmed. If the operation is delayed for special reasons after admission, the patient should be given rapid and effective control of blood pressure, pulse and pain. Postoperative acute renal function injury, pneumonia and multiple organ failure were the main risk factor for 7-day death and in-hospital death. Under the premise of the emergency green channel integrated management strategy and the shift of a special cardiac surgery team at nighttime, weekends or holidays, the surgery time was not related to the in-hospital mortality or 7-day mortality of patients.

Data availability statement

The raw data supporting the conclusions of this article will be made available by the authors, without undue reservation.

Ethics statement

The studies involving human participants were reviewed and approved by Qilu Hospital of Shandong University Medical Ethics Committee Shandong University. Written informed consent for participation was not required for this study in accordance with the national legislation and the institutional requirements.

Author contributions

XZ, KL, XL, and WL: data collection. SY, XZ, and KL: statistical analysis. SY and KL: writing of the manuscript. SY and XL: inception of the study idea. SY, KL, and WL: study design and revision of the manuscript. All authors approved the final manuscript.

Acknowledgments

We thank all involved anesthesiologists for their contribution to this trial.

Conflict of interest

The authors declare that the research was conducted in the absence of any commercial or financial relationships that could be construed as a potential conflict of interest.

Publisher's note

All claims expressed in this article are solely those of the authors and do not necessarily represent those of their affiliated organizations, or those of the publisher, the editors and the reviewers. Any product that may be evaluated in this article, or claim that may be made by its manufacturer, is not guaranteed or endorsed by the publisher.

References

1. Mussa FF, Horton JD, Moridzadeh R, Nicholson J, Trimarchi S, Eagle KA. Acute aortic dissection and intramural hematoma: a systematic review. *JAMA.* (2016) 316:754–63. doi: 10.1001/jama.2016.10026

2. Andersen ND, Benrashid E, Ross AK, Pickett LC, Smith PK, Daneshmand MA, et al. The utility of the aortic dissection team: outcomes and insights after a decade of experience. *Ann Cardiothorac Surg.* (2016) 5:194–201. doi: 10.21037/acs.2016.05.12

3. Nienaber CA, Clough RE. Management of acute aortic dissection. *Lancet.* (2015) 385:800–11. doi: 10.1016/S0140-6736(14)61005-9

4. Malaisrie SC, Szeto WY, Halas M, Girardi LN, Coselli JS, Sundt TM III, et al. AATS clinical practice standards committee: adult cardiac surgery. 2021 The American Association for thoracic surgery expert consensus document: surgical treatment of acute type A aortic dissection. *J Thorac Cardiovasc Surg.* (2021) 162:735–58.e2. doi: 10.1016/j.jtcvs.2021.04.053

5. O'Donnell TFX, Li C, Swerdlow NJ, Liang P, Pothof AB, Patel VI, et al. The weekend effect in AAA repair. *Ann Surg.* (2019) 269:1170–5. doi: 10.1097/SLA.0000000000002773

6. Andersen ND, Ganapathi AM, Hanna JM, Williams JB, Gaca JG, Hughes GC. Outcomes of acute type a dissection repair before and after implementation of a multidisciplinary thoracic aortic surgery program. *J Am Coll Cardiol.* (2014) 63:1796–803. doi: 10.1016/j.jacc.2013.10.085

7. Qiu J, Zhang L, Luo X, Gao W, Liu S, Jiang W, et al. Higher mortality in patients undergoing nighttime surgical procedures for acute type A aortic dissection. *Ann Thorac Surg.* (2018) 106:1164–70. doi: 10.1016/j.athoracsur.2018.04.062

8. Kumar N, Venkatraman A, Pandey A, Khera R, Garg N. Weekend hospitalizations for acute aortic dissection have a higher risk of in-hospital mortality compared to weekday hospitalizations. *Int J Cardiol.* (2016) 214:448–50. doi: 10.1016/j.ijcard.2016.03.187

9. Arnaoutakis G, Bianco V, Estrera AL, Brinster DR, Ehrlich MP, Peterson MD, et al. Time of day does not influence outcomes in acute type A aortic dissection: results from the IRAD. *J Card Surg.* (2020) 35:3467–73. doi: 10.1111/jocs.15017

10. Ahlsson A, Wickbom A, Geirsson A, Franco-Cereceda A, Ahmad K, Gunn J, et al. Is there a weekend effect in surgery for type A dissection?: results from the nordic consortium for acute type A aortic dissection database. *Ann Thorac Surg.* (2019) 108:770–6. doi: 10.1016/j.athoracsur.2019.03.005

11. Takagi H, Ando T, Umemoto T. ALICE (All-Literature Investigation of Cardiovascular Evidence) group. A meta-analysis of weekend admission and surgery for aortic rupture and dissection. *Vasc Med.* (2017) 22:398–405. doi: 10.1177/1358863X17718259

12. Su IM, Huang HK, Liu PP, Hsu JY, Lin SM, Loh CH. Mortality risk from acute aortic dissection among hospital admissions during weekends and holiday season. *PLoS One.* (2021) 16:e0255942. doi: 10.1371/journal.pone.0255942

13. Booher AM, Isselbacher EM, Nienaber CA, Trimarchi S, Evangelista A, Montgomery DG, et al. IRAD investigators. The IRAD classification system for characterizing survival after aortic dissection. *Am J Med.* (2013) 126:730.e19–24. doi: 10.1016/j.amjmed.2013.01.020

14. Shen Y, Liu C, Fang C, Xi J, Wu S, Pang X, et al. Oxygenation impairment after total arch replacement with a stented elephant trunk for type-A dissection. *J Thorac Cardiovasc Surg.* (2018) 155:2267–74. doi: 10.1016/j.jtcvs.2018.01.085

15. Lee TC, Kon Z, Cheema FH, Grau-Sepulveda MV, Englum B, Kim S, et al. Contemporary management and outcomes of acute type A aortic dissection: an analysis of the STS adult cardiac surgery database. *J Card Surg.* (2018) 33:7–18. doi: 10.1111/jocs.13511

16. Ma WG, Chen Y, Zhang W, Li Q, Li JR, Zheng J, et al. Extended repair for acute type A aortic dissection: long-term outcomes of the frozen elephant trunk technique beyond 10 years. *J Cardiovasc Surg.* (2020) 61:292–300. doi: 10.23736/S0021-9509.20.11293-X

17. Huang HK, Chang WC, Hsu JY, Wang JH, Liu PS, Lin SM, et al. Holiday season and weekend effects on stroke mortality: a Nationwide Cohort Study controlling for stroke severity. *J Am Heart Assoc.* (2019) 8:e011888. doi: 10.1161/JAHA.118.011888

18. Somasundram K, Neville JJ, Sinha Y, Agarwal T, Raje D, Sinha A, et al. The weekend effect—How can it be mitigated? Introduction of a consultant-delivered emergency general surgical service. *Ann Med Surg.* (2020) 57:315–20. doi: 10.1016/j.amsu.2020.08.013

19. Li S, Wei D, Wang Z, Song H, Cheng S, Zhao X, et al. Effect on surgery outcomes owing to the interval between onset of symptoms and surgery of patients with acute type A aortic dissection. *Emerg. Crit. Care Med.* (2022) 2:67-72. doi: 10.1097/EC9.0000000000000032

20. Miller DC. Another meiosis in the specialty of cardiovascular and thoracic surgery: birth of the purebred "thoracic aortic surgeon"? *J Am Coll Cardiol.* (2014) 63:1804–6. doi: 10.1016/j.jacc.2013.12.007

21. Schoenrath F, Laber R, Maralushaj M, Henzi D, Caliskan EI, Seifert B, et al. Survival, neurologic injury, and kidney function after surgery for acute type A aortic dissection. *Thorac Cardiovasc Surg.* (2016) 64:100–7. doi: 10.1055/s-0035-1563536

22. Helgason D, Helgadottir S, Ahlsson A, Gunn J, Hjortdal V, Hansson EC, et al. Acute kidney injury after acute repair of type A aortic dissection. *Ann Thorac Surg.* (2021) 111:1292–8. doi: 10.1016/j.athoracsur.2020.07.019

23. Nissinen J, Biancari F, Wistbacka JO, Peltola T, Loponen P, Tarkiainen P, et al. Safe time limits of aortic cross-clamping and cardiopulmonary bypass in adult cardiac surgery. *Perfusion.* (2009) 24:297–305. doi: 10.1177/0267659109354656

24. Pat B, Oh JY, Masjoan Juncos JX, Powell PC, Collawn JF, Patel RP, et al. Red blood cell exosome hemoglobin content increases after cardiopulmonary bypass and mediates acute kidney injury in an animal model. *J Thorac Cardiovasc Surg.* (2020). [Epub ahead of print]. doi: 10.1016/j.jtcvs.2020.11.102

25. Olsson C, Franco-Cereceda A. Impact of organ failure and major complications on outcome in acute Type A aortic dissection. *Scand Cardiovasc J.* (2013) 47:352–8. doi: 10.3109/14017431.2013.845307

26. Sun EC, Mello MM, Vaughn MT, Kheterpal S, Hawn MT, Dimick JB, et al. Assessment of perioperative outcomes among surgeons who operated the night before. *JAMA Intern Med.* (2022) 182:720-728. doi: 10.1001/jamainternmed.2022.1563

frontiers | Frontiers in Cardiovascular Medicine

TYPE Review
PUBLISHED 20 December 2022
DOI 10.3389/fcvm.2022.1056229

OPEN ACCESS

EDITED BY
Bernhard Winkler,
Vienna Health Association, Austria

REVIEWED BY
Yasunori Iida,
Saiseikai Yokohamashi Tobu Hospital, Japan
Zhichao Lai,
Peking Union Medical College Hospital (CAMS), China

*CORRESPONDENCE
Hongkun Zhang
1198050@zju.edu.cn

†These authors have contributed equally to this work and share first authorship

SPECIALTY SECTION
This article was submitted to Heart Surgery, a section of the journal Frontiers in Cardiovascular Medicine

RECEIVED 28 September 2022
ACCEPTED 18 November 2022
PUBLISHED 20 December 2022

CITATION
Qiu C, Li Z, Dai X, Lu X, Lu Q, Li X, Zhou W, Guo P, Pan J, Li D, Wu Z and Zhang H (2022) Technical details of thoracic endovascular aortic repair with fenestrations for thoracic aortic pathologies involving the aortic arch: A Chinese expert consensus. *Front. Cardiovasc. Med.* 9:1056229. doi: 10.3389/fcvm.2022.1056229

Technical details of thoracic endovascular aortic repair with fenestrations for thoracic aortic pathologies involving the aortic arch: A Chinese expert consensus

Chenyang Qiu[1†], Zhenjiang Li[1†], Xiangchen Dai[2], Xinwu Lu[3], Qingsheng Lu[4], Xiaoqiang Li[5], Weimin Zhou[6], Pingfan Guo[7], Jun Pan[1], Donglin Li[1], Ziheng Wu[1] and Hongkun Zhang[1]*

[1]Department of Vascular Surgery, The First Affiliated Hospital, School of Medicine, Zhejiang University, Hangzhou, China, [2]Department of Vascular Surgery, General Hospital, Tianjin Medical University, Tianjin, China, [3]Department of Vascular Surgery, Shanghai Ninth People's Hospital, Shanghai Jiao Tong University School of Medicine, Shanghai, China, [4]Department of Vascular Surgery, The First Affiliated Hospital of Naval Medical University, Shanghai, China, [5]Department of Vascular Surgery, Nanjing Drum Tower Hospital, Affiliated to Nanjing University Medical School, Nanjing, Jiangsu, China, [6]Department of Vascular Surgery, The Second Affiliated Hospital of Nanchang University, Nanchang, Jiangxi, China, [7]Department of Vascular Surgery, The First Affiliated Hospital of Fujian Medical University, Fuzhou, China

Thoracic aortic pathologies involving the aortic arch are a great challenge for vascular surgeons. Maintaining the patency of supra-aortic branches while excluding the aortic lesion remains difficult. Thoracic EndoVascular Aortic Repair (TEVAR) with fenestrations provides a feasible and effective approach for this type of disease. The devices needed in the procedure are off-the-shelf, with promising results reported in many medical centers. Up until now, there have been no guidelines focusing exclusively on the details of the TEVAR technique with fenestrations. Experts from China have discussed the technical parts of both *in situ* fenestrations (needle and laser) and fenestrations *in vitro* (direction inversion strategy and guidewire-assisted strategy), providing a technical reference to standardize the procedure and improve its results.

KEYWORDS

thoracic endovascular aortic repair, fenestrations, standard procedure protocol, technical details, device

Introduction

In the past, open surgery has been the main approach for thoracic aortic pathologies involving the aortic arch. Thanks to the development of endovascular techniques and devices, an increasing number of patients suffering from this disease have begun to receive a different kind of treatment (1). The Chimney technique and branched stents are two strategies for pathologies involving the aortic arch. The Chimney technique presents a high risk of type I endoleaks, and the branched stent is limited by a lack of custom-made instruments. TEVAR with fenestrations has gradually become the most used approach in this field (2–4). Given that custom-made fenestrated stent grafts are not yet available in China, physician-made fenestrations represent the main treatment for thoracic aortic pathologies affecting the aortic arch. Aortic dissection and aneurysms can both be treated with TEVAR with physician-made fenestrations. According to reports from many medical centers, the equipment needed for such treatments is commercially available, and the results after applying this method are relatively promising. However, this technique's limitations are due to the lack of a standard procedure protocol concerning the technical details of TEVAR with fenestrations (3, 5–8). As a result, experts from China have started to discuss the technical aspects of this operation and have agreed to establish a standard procedure reference.

Standard TEVAR procedure with fenestrations

1 Vascular access

A stent graft is typically delivered through the femoral artery. The branches of the left brachial artery (LBA), left common carotid artery (LCCA), and right common carotid artery are frequently used for stent placement (9).

2 Angiography before stent graft deployment

A pigtail catheter is inserted via the left brachial artery into the ascending aorta, and an anterior-posterior aortic arch angiography is performed to assess the bilateral carotid and vertebral arteries. Then, a stiff guidewire (Lunderquist, Cook Medical, Bloomington, IN) is inserted via femoral artery access into the ascending aorta. A gold marker pigtail catheter is inserted through the stiff guidewire and positioned within the aortic arch. An angiography of the left anterior oblique aortic arch (between 45° and 65°) is performed to identify the arch architecture and location of the lesion; it is important to prevent the overlapping between the aortic arch and supra-aortic branch arteries in the left anterior oblique angiography (7).

3 *In situ* fenestrations

3.1 Delivery and deployment of stent grafts

The aortic arch and branch openings are marked after an angiography of the aortic arch. Systolic pressure is reduced to between 90 and 100 mm Hg (7). The stent graft is delivered from the femoral access to the aortic arch through a Super Stiff guidewire (Lunderquist, Cook Medical). In order to avoid covering the LCCA, the proximal landing zone for fenestrations of the left subclavian artery (LSA) alone is the distal side of the opening of the LCCA. The proximal landing zone for LSA and LCCA fenestrations is located on the distal side of the opening of the brachiocephalic artery (BCA). The ascending aorta is the landing zone for fenestrations of all super-aortic stents. To prevent angulation between the stent graft and ascending aorta, the proximal portion of the stent should be as parallel as possible to the ascending aorta (8). Patients with supra-aortic branch fenestrations should receive additional cerebral blood supply through extracorporeal circulation (section "5 Assistive techniques and cerebral blood supply monitoring").

3.2 Fenestrations

3.2.1 Needle fenestrations

LSA: From the LBA, a 6F angle-adjustable sheath (Lifetech, Inc., Shenzhen, China) is introduced retrogradely until its tip reaches the aortic stent graft. The tip is then adjusted to be as perpendicular as possible to the larger curve of the aortic stent graft. Once the sheath gets to the ideal position, a flexible needle (21 gauge, Futhrough, Lifetech, Inc.) is employed to create the fenestration in the aortic stent graft. Following the puncture, a 0.018-inch guidewire (V-18 ControlWire; Boston Scientific, Natick, MA) is inserted through the needle aperture and into the ascending aorta (1, 10, 11) (**Figure 1**).

LCCA and BCA: a short sheath is placed into the common carotid artery, with its tip reaching the membrane of the stent-graft. A needle (21G, 18 cm, BARD) is inserted through the sheath. Then, under fluoroscopy, a needle puncture is performed with a guidewire passing through the needle into the stent graft (6, 12–14).

3.2.2 Laser-assisted fenestration

Laser preparation: the fiber energy can be tested *in vitro* in a moist environment its proximal end can be cut to 0.5 mm (810∼1,110 nm wavelength, pulsed type). A laser fiber and a balloon catheter are combined, with the fiber proximal end protruding 0.5–1 cm from the balloon catheter and connected by a Y connector (Merit Angioplasty Pack^{TM}, Merit Medical, Parkway, South Jordan, UT) (15, 16). Fenestration: For the LSA, an angle-adjustable sheath is advanced through the LBA. For the LCCA and BCA, a vascular sheath is inserted through the corresponding carotid artery. The sheath tip is pushed against the stent graft. The fiber and the balloon catheter are then inserted into the sheath until they reach the membrane of the

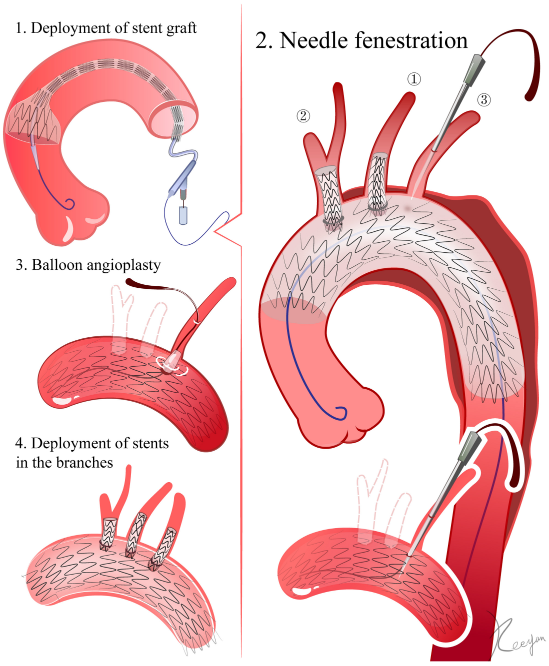

FIGURE 1
Needle fenestration. 1. Delivery of the stent graft. The ascending aorta is the landing zone for fenestrations of all super-aortic stents. 2. Needle fenestrations. In LSA, for example, a 6F angle-adjustable sheath is introduced retrogradely until its tip reaches the aortic stent graft. Once the sheath reaches the ideal place, a flexible needle is employed to create the fenestration in the aortic stent graft. A 0.018-inch guidewire is advanced through the needle's aperture and into the ascending aorta after the puncture. 3. The initial aperture is then expanded by balloon angioplasty. 4. Deployment of stents in the branches.

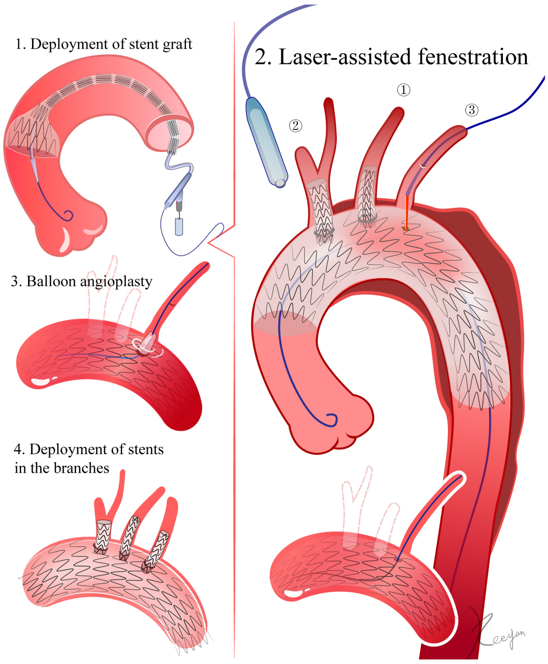

FIGURE 2
Laser-assisted fenestration. 1. Delivery of the stent graft. The ascending aorta is the landing zone for fenestrations of all super-aortic stents. 2. Laser-assisted fenestration. In LSA, for example, an angle-adjustable sheath is advanced until its tip touches the stent graft. The laser fiber then advances within the sheath until it gets to the membrane of the stent graft. Then, the laser machine is activated. After fenestration, a 0.018-inch guidewire is advanced through the initial aperture and into the ascending aorta. 3. The initial aperture is then expanded by balloon angioplasty. 4. Deployment of stents in the branches.

stent graft. After activating the laser machine to deliver energy (18 W, pulsed, 2–3 times), the laser fiber and balloon catheter are pushed forward, and the fiber is withdrawn. If they are pushed inside the stent graft, the balloon catheter can be left inside (2, 17–20) (**Figure 2**).

3.3 Balloon angioplasty

The initial aperture is then expanded by a 4 mm balloon, followed by the exchange of a 0.035-inch stiff guidewire (Amplatz, Boston Scientific) through the balloon catheter. The aperture is expanded by replacing the balloon catheter with one with a bigger diameter. The final size of the balloon depends on the diameter of the branch vessel. The size of the balloon is slightly smaller than the diameter of the corresponding artery, and a high-pressure balloon is more suitable during this process. If the aperture is resistant to balloon angioplasty, a cutting balloon (Boston Scientific) can be applied (21, 22).

3.4 Stent deployment in the branches

LSA: it is preferable to use a self-expanding or balloon-expandable covered stent. If the LSA is distant from the lesion and the endoleak risk is low, a bare stent can be taken into consideration. The diameter of the stent should be the same (1–2 mm) or slightly greater than the diameter of the LSA opening. The stent should extend roughly 10 mm into the aorta. The distal end of the stent must not cover the vertebral artery's orifice (1, 13, 14).

LCCA and BCA: similar to the balloon angioplasty procedure utilized for the LSA. The stent should extend roughly 10 mm into the aorta. The distal end of the stent should avoid the opening of the right common carotid artery during BCA stent deployment (12, 16, 22, 23).

3.5 Sequence of fenestrations

For both LCCA and LSA fenestrations, the LCCA should be fenestrated first. When the stent deployment is complete in the LCCA, the sheath must be withdrawn and a pre-placed purse suture tightened to achieve hemostasis at the puncture site, therefore minimizing blood flow interference. The LSA fenestration should be performed last (10).

Regarding fenestrations for all supra-aortic branches, we recommend performing them in this sequence: LCCA, BCA, and LSA. After the stent implantation in both the BCA and LSA, extracorporeal circulation can be discontinued and the bilateral common carotid arteries achieve hemostasis. The LSA should be fenestrated last (4, 11).

4 Fenestrations *in vitro*

4.1 Stent graft preparation

4.1.1 Direction inversion strategy

Based on the preoperative CTA reconstructions, the diameter of the aorta and branch vessels, lengths, angles to the arch, clock positions, and related relationships are measured, and a preoperative design for the fenestrations is developed. The outer sheath of the stent graft is then pushed back for several centimeters under sterile conditions, allowing the proximal portion of the stent graft to be released (24). The length of the released segment should be one to two centimeters distal from the location of fenestration (24). Using a sterile ruler, the location of the fenestration is determined in accordance with the preoperative plan. The 12 o'clock position is considered to be at the front of the trigger. The position of the stent graft relative to the trigger is also referred to as the 12 o'clock position. If the fenestration must avoid stent struts, then the fenestration is deemed to be at 12 o'clock, as is the position of the trigger relative to the stent graft. The fenestration can be created using scissors or a cautery device. The fenestration can be strengthened using the loop of a snare (24, 25). To indicate the position of the fenestration during the DSA, either the original mark in the stent graft or an extra marker can be sutured to the fenestration (26) (**Figure 3**).

4.1.2 Guidewire-assisted strategy

The fenestration technique is similar to that in section "4.1.1 Direction inversion strategy (**Figure 3**)." After fenestration, a 0.018-inch guidewire passes through needle holes in the distal part of the delivery sheath into the fenestration. For fenestrations with more than one branch, the most proximal fenestration is preloaded with a 0.018-inch guidewire. Posterior diameter-reducing ties are added to the devices (27, 28) (**Figure 4**).

4.2 Re-sheathed into the delivery system

The most distal portion of the stent graft is appropriately constrained by one assistant using silk thread. The outer sheath is advanced by a second assistant. The surgeon manually squeezes the stent graft back into the sheath. It should be noted that the distance between each segment should not be compressed, and the stent graft should not rotate (28–30). During the procedure, the outer sheath should not push the stent graft forward. The post-release device must not be accidentally turned on. The extra marker sewn into the stent graft should attach to the inner sheath wall (28, 31, 32). After the outer sheath has been repositioned, the stent graft needs to be flushed.

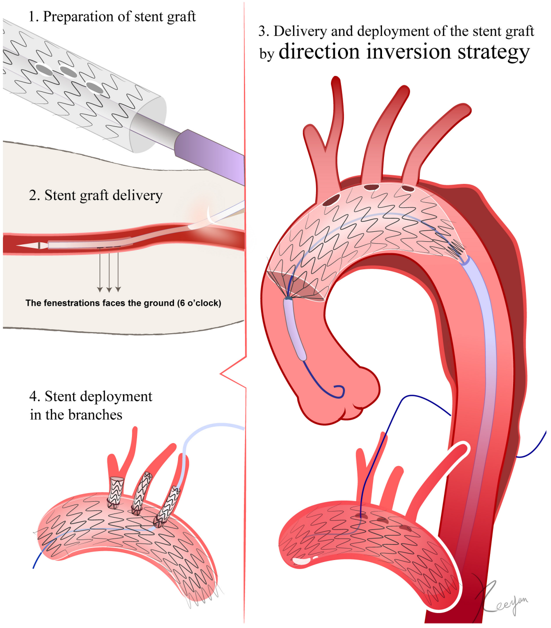

FIGURE 3
Direction inversion strategy. 1. The fenestration is made *in vitro* according to the peri-operative CTA. 2. The front of the trigger is regarded as the 12 o'clock position. When the stent graft is inserted through the femoral artery access, the 12 o'clock marker point must be turned vertically to the ground, so that it faces 6 o'clock. The stent graft is not allowed to rotate after entering the femoral artery until it reaches the aortic lesion. 3. After passing the aortic arch, the fenestration mark is aligned with the branch artery's corresponding position. After the deployment of the stent graft, a 0.018-inch guidewire is advanced through the fenestration. 4. Deployment of stents in the branches.

4.3 Delivery and deployment of the stent graft

4.3.1 Direction inversion strategy

When the stent graft is inserted through the femoral artery access, the 12 o'clock marker point needs to be turned vertically to the ground so that it faces 6 o'clock. The stent graft is not allowed to rotate after entering the femoral artery until it reaches the aortic lesion. After passing the aortic arch, the fenestration mark is aligned with the branch artery's corresponding position. For instance, if the LCCA fenestration site is at the beginning of the first segment of the stent graft, the beginning of the first segment must be aligned with the anterior contour line of the LCCA. Once one branch artery is aligned, the remaining branches will align themselves naturally (24, 25). To prevent the stent graft from jumping forward or being pushed away, the grips need to be held and secured before the stent graft is slowly released. After the complete deployment of the stent graft, the delivery system must be retrieved and removed. Fluoroscopy can be utilized to determine whether the stent is aligned with the branch arteries. DSA should be repeated to ensure that the fenestration sites are accurate and that branch arteries are not covered (25, 26, 33).

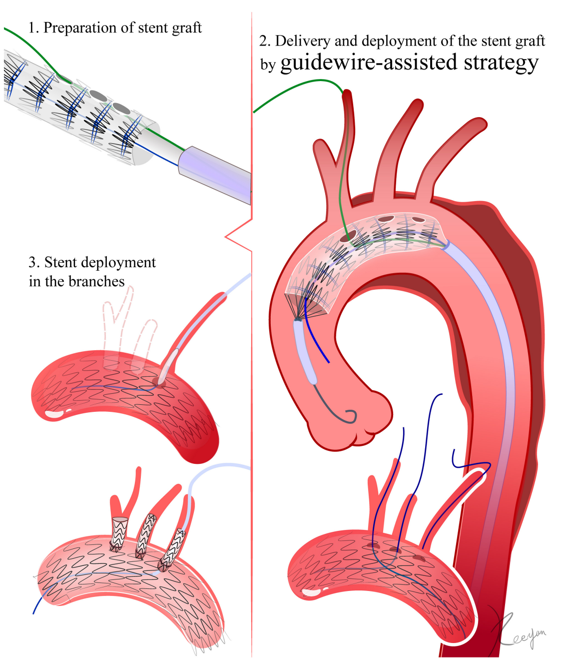

FIGURE 4
Guidewire-assisted strategy. 1. The fenestration is made *in vitro* according to the peri-operative CTA. After fenestration, a 0.018-inch guidewire passes through needle holes in the distal part of the delivery sheath into the fenestration. Diameter-reducing ties are added to the devices. 2. The 0.018-inch guidewire passes through the fenestration into the branch artery. Several segments of the stent graft are released. With the help of diameter-reducing ties, the stent graft is not fully deployed. Then, the fenestration site is aligned to the greater curve of the aortic arch by rotating the delivery system. After verifying that the fenestration is oriented toward the branch artery, the stent graft is fully released. 3. Deployment of stents in the branches.

4.3.2 Guidewire-assisted strategy

Fenestrations with LSA must be used as an example. First, a guidewire passes from the LBA access to the femoral artery and exits the vascular sheath in the femoral artery. Through the guidewire, an MPA catheter is loaded from the left brachial artery into the femoral artery. A stiff guidewire (Lunderquist, Cook Medical) is positioned in the ascending aorta through common femoral access. The stent graft is advanced via the stiff guidewire, and the preloaded 0.018-inch guidewire is advanced through the MPA catheter connecting the femoral artery and LBA. When the stent graft is advanced into the descending aorta, the two guidewires that were intertwined are completely removed by rotating the delivery system. At this point, the fenestration site is aligned to the greater curve of the aortic arch by rotating the delivery system, until the O takes the shape of an I. When the stent graft reaches the aortic arch, one or two segments of the stent graft must be released. Then, the stent graft must slowly advance while constraining the guidewire connecting the LBA and femoral artery. A 6F sheath is inserted from the LBA into the fenestration via the guidewire connecting the LBA and femoral artery (27, 28). After verifying that the fenestration is oriented toward the LSA, the stent graft is fully released. In terms of fenestrations with multiple vessels, LCCA and BCA fenestrations are similar to those of the LSA. With the help of diameter-reducing ties, each fenestration is selected, and vascular sheaths are inserted into the stent graft via retrograde vascular access. The stent graft is released at the end (32, 34).

4.4 Stent deployment in the branches

4.4.1 Direction inversion strategy

When placing a stent into a branch artery, the guidewire can enter from the femoral artery or be introduced into the stent graft retrogradely through the branch arteries. It is necessary to make sure that the guidewire for delivering the stent is in the stent graft instead of the space between the stent graft and the aorta (24). The diameter of the stent in the branch should be the same or slightly greater (1–2 mm) than the size of the fenestration. The length of the branch stent in the aorta should be approximately 10 mm. After releasing the stent, it is necessary to verify if the stent has stenosis (24, 26). In which case, post-dilation will be needed. If the branch artery is completely covered by a stent graft, the Chimney technique may be used to restore the blood flow in the branch arteries (33).

4.4.2 Guidewire-assisted strategy

During the LSA fenestration, after the stent graft deployment, the femoral artery and the LBA are connected via a guidewire. Then, a 6F-55 cm sheath is inserted into the stent graft from the LBA. After deployment, the delivery system and the stiff guidewire are removed from the ascending aorta. A stiff guidewire is used to replace the guidewire connecting the femoral artery and LBA. Then, a 12F, 80 cm-long sheath is advanced from the femoral artery into the LSA, delivering a covered stent into the LSA. The covered stent should not cover the vertebral artery orifice, and its proximal end should extend 10 mm into the stent graft. After deployment of the covered stent within the LSA, post-dilation is performed. The technique for LCCA and BCA fenestrations is comparable to that for the LSA. Through retrograde vascular access, vascular sheaths are introduced into each fenestration of the stent graft. The size of the stent placed in the branch arteries is determined by their diameter (which should be 2 mm larger than the fenestration) (34–36).

5 Assistive techniques and monitoring of cerebral blood supply

5.1 Extracorporeal circulation

Extracorporeal circulation is recommended during all supra-aortic branch fenestrations. After the stent graft is released, all supra-aortic branches are covered. At this moment, extracorporeal circulation will provide the necessary cerebral blood supply. If the Circle of Willis is intact, the extracorporeal circulation connecting the right axillary artery and femoral vein will provide enough cerebral perfusion. Extracorporeal membrane oxygenation is also an alternative for cerebral perfusion (7, 10).

5.2 Arterial bypass

There is no need for arterial bypass during LCCA and LSA fenestrations. Apart from extracorporeal circulation, arterial bypass is also an option during all supra-aortic branch fenestrations (37). A 16F sheath is inserted into the right common carotid artery and advanced to the proximal ascending aorta. An 8F short sheath is inserted into the 16F sheath. A 6F short sheath is inserted into the internal carotid artery toward the brain. The 16F sheath is connected to the vascular sheath in the left carotid artery via a vascular shunt, providing a blood supply for the left carotid artery. The proximal 8F sheath in the right common carotid artery is connected to the 6F sheath in the distal internal carotid artery, providing a blood supply for the right carotid artery (5, 6).

5.3 Cerebral oximetry

Percutaneous cerebral oximetry is recommended during LCCA and BCA fenestrations, as it can monitor cerebral ischemia and hypoxia when the openings of LCCA and BCA are covered (10, 11, 25).

Discussion and conclusion

TEVAR for thoracic aortic pathologies involving the aortic arch provides a feasible and effective approach for such diseases and has been widely used both in China and abroad, with varying results reported. However, it still faces great challenges. This Chinese expert consensus serves as a technical reference, in an effort to standardize the approach and improve the results of this procedure.

Author contributions

CQ and ZL drafted the initial manuscript. XD, XwL, QL, XqL, WZ, PG, JP, DL, ZW, and HZ critically reviewed the manuscript. All authors approved the final manuscript.

Funding

This work was supported by the Major Science and Technology Project in Medical and Health of the Zhejiang Province (co-constructed Project by Province and the Ministry, 2020380400, WKJ-ZJ-2003) and the Key R&D Program of the Zhejiang Province (Grant no. 2019C03013).

Conflict of interest

The authors declare that the research was conducted in the absence of any commercial or financial relationships that could be construed as a potential conflict of interest.

Publisher's note

References

1. Li Y, He C, Chen X, Yao J, Zhang T, Zhang H. Endovascular in situ fenestration technique of aortic arch pathology: a systematic review and meta-analysis. *Ann Vasc Surg.* (2021) 76:472–80. doi: 10.1016/j.avsg.2020.12.021

2. Al-Hakim R, Schenning R. Advanced Techniques in thoracic endovascular aortic repair: chimneys/periscopes, fenestrated endografts, and branched devices. *Tech Vasc Interv Radiol.* (2018) 21:146–55. doi: 10.1053/j.tvir.2018.06.004

3. Rudarakanchana N, Jenkins M. Hybrid and total endovascular repair of the aortic arch. *Br J Surg.* (2018) 105:315–27. doi: 10.1002/bjs.10713

4. Anwar M, Hamady M. Various endoluminal approaches available for treating pathologies of the aortic arch. *Cardiovasc Intervent Radiol.* (2020) 43:1756–69. doi: 10.1007/s00270-020-02561-y

5. Makaloski V, Tsilimparis N, Rohlffs F, Heidemann F, Debus E, Kolbel T. Endovascular total arch replacement techniques and early results. *Ann Cardiothorac Surg.* (2018) 7:380–8. doi: 10.21037/acs.2018.04.02

6. Li H, Chan Y, Jia H, Cheng S. Methods and clinical outcomes of in situ fenestration for aortic arch revascularization during thoracic endovascular aortic repair. *Vascular.* (2020) 28:333–41. doi: 10.1177/1708538120902650

7. Czerny M, Schmidli J, Adler S, van den Berg J, Bertoglio L, Carrel T, et al. Editor's choice – current options and recommendations for the treatment of thoracic aortic pathologies involving the aortic arch: an expert consensus document of the european association for cardio-thoracic surgery (EACTS) & the European society for vascular surgery (ESVS). *Eur J Vasc Endovasc Surg.* (2019) 57:165–98.

8. Luo M, Fang K, Fan B, Li Q, Li M, He H, et al. Midterm results of retrograde in situ needle fenestration during thoracic endovascular aortic repair of aortic arch pathologies. *J Endovasc Ther.* (2021) 28:36–43. doi: 10.1177/1526602820953406

9. Qin J, Wu X, Li W, Ye K, Yin M, Liu G, et al. Laser fenestration of aortic arch stent grafts for endovascular treatment of retrograde type A dissection. *Int J Cardiol.* (2021) 328:69–74. doi: 10.1016/j.ijcard.2020.12.011

10. Xiang Y, Qiu C, He Y, Li D, Shang T, Wu Z, et al. A single center experience of in situ needle fenestration of supra-aortic branches during thoracic endovascular aortic repair. *Ann Vasc Surg.* (2019) 61:107–15. doi: 10.1016/j.avsg.2019.03.016

11. Shang T, Tian L, Li D, Wu Z, Zhang H. Favourable outcomes of endovascular total aortic arch repair via needle based in situ fenestration at a mean follow-up of 5.4 months. *Eur J Vasc Endovasc Surg.* (2018) 55:369–76. doi: 10.1016/j.ejvs.2017.11.022

12. Wang L, Zhou X, Guo D, Hou K, Shi Z, Tang X, et al. A new adjustable puncture device for in situ fenestration during thoracic endovascular aortic repair. *J Endovasc Ther.* (2018) 25:474–9. doi: 10.1177/1526602818776623

13. XiaoHui M, Li W, Wei G, XiaoPing L, Xin J, Hongpeng Z, et al. Comparison of supra-arch in situ fenestration and chimney techniques for aortic dissection involving the left subclavian artery. *Vascular.* (2019) 27:153–60. doi: 10.1177/1708538118807013

14. Kopp R, Katada Y, Kondo S, Sonesson B, Hongo N, Tse L, et al. Multicenter analysis of endovascular aortic arch in situ stent graft fenestrations for aortic arch pathologies. *Ann Vasc Surg.* (2019) 59:36–47. doi: 10.1016/j.avsg.2019.02.005

15. Sonesson B, Dias N, Abdulrasak M, Resch T. Midterm results of laser generated in situ fenestration of the left subclavian artery during thoracic endovascular aneurysm repair. *J Vasc Surg.* (2019) 69:1664–9. doi: 10.1016/j.jvs.2018.09.052

16. Qin J, Zhao Z, Wang R, Ye K, Li W, Liu X, et al. In situ laser fenestration is a feasible method for revascularization of aortic arch during thoracic endovascular aortic repair. *J Am Heart Assoc.* (2017) 6:e004542. doi: 10.1161/JAHA.116.004542

17. Yan D, Shi H, Qin J, Zhao Z, Yin M, Liu X, et al. Outcomes of emergency in situ laser fenestration-assisted thoracic endovascular aortic repair in patients with acute Stanford type A aortic dissection unfit for open surgery. *J Vasc Surg.* (2020) 71:1472–1479e1. doi: 10.1016/j.jvs.2019.08.233

18. Liu G, Qin J, Cui C, Zhao Z, Ye K, Shi H, et al. Endovascular repair of aortic arch intramural hematoma and penetrating ulcers with 810 nm in situ laser-assisted fenestration: preliminary results of a single-center. *Lasers Surg Med.* (2018) 50:837–43. doi: 10.1002/lsm.22937

19. Li C, Xu P, Hua Z, Jiao Z, Cao H, Liu S, et al. Early and midterm outcomes of in situ laser fenestration during thoracic endovascular aortic repair for acute and subacute aortic arch diseases and analysis of its complications. *J Vasc Surg.* (2020) 72:1524–33. doi: 10.1016/j.jvs.2020.01.072

20. Zhao Z, Qin J, Yin M, Liu G, Liu X, Ye K, et al. In situ laser stent graft fenestration of the left subclavian artery during thoracic endovascular repair of type B aortic dissection with limited proximal landing zones: 5-year outcomes. *J Vasc Interv Radiol.* (2020) 31:1321–7. doi: 10.1016/j.jvir.2020.02.025

21. Shu C, Fan B, Luo M, Li Q, Fang K, Li M, et al. Endovascular treatment for aortic arch pathologies: chimney, on-the-table fenestration, and in-situ fenestration techniques. *J Thorac Dis.* (2020) 12:1437–48. doi: 10.21037/jtd.2020.03.10

22. Bai J, Liu Y, Jin J, Wu J, Qu L. Mid−term results of in situ fenestration stented with balloon−expandable bare metal stents during thoracic endovascular aortic repair. *Catheter Cardiovasc Interv.* (2020) 95:1163–8. doi: 10.1002/ccd.28743

23. Li F, Wu X, Zhang X, Qin J, Zhao Z, Ye K. Clinical outcomes of distal tapered restrictive covered stent applied in endovascular treatment of aortic dissection involving zone 0. *Eur J Vasc Endovasc Surg.* (2021) 61:413–21. doi: 10.1016/j.ejvs.2020.11.037

24. Zhang L, Wu M, Zhu G, Feng J, Song C, Li H, et al. Off-the-shelf devices for treatment of thoracic aortic diseases: midterm follow-up of TEVAR with chimneys or physician-made fenestrations. *J Endovasc Ther.* (2020) 27:132–42. doi: 10.1177/1526602819890107

25. Zhu J, Dai X, Noiniyom P, Luo Y, Fan H, Feng Z, et al. Fenestrated thoracic endovascular aortic repair using physician-modified stent grafts (PMSGs) in zone 0 and zone 1 for aortic arch diseases. *Cardiovasc Intervent Radiol.* (2019) 42:19–27. doi: 10.1007/s00270-018-2079-9

26. Miura S, Kurimoto Y, Maruyama R, Wada T, Konno M, Iba Y, et al. Thoracic endovascular aortic repair on zone 2 landing for type B aortic dissection. *Ann Vasc Surg.* (2019) 60:120–7. doi: 10.1016/j.avsg.2019.02.017

27. Zhu J, Zhao L, Dai X, Luo Y, Fan H, Feng Z, et al. Fenestrated thoracic endovascular aortic repair using physician modified stent grafts for acute type B aortic dissection with unfavourable landing zone. *Eur J Vasc Endovasc Surg.* (2018) 55:170–6. doi: 10.1016/j.ejvs.2017.11.012

28. Canaud L, Baba T, Gandet T, Narayama K, Ozdemir BA, Shibata T, et al. Physician-modified thoracic stent grafts for the treatment of aortic arch lesions. *J Endovasc Ther.* (2017) 24:542–8. doi: 10.1177/1526602817714206

29. Chassin-Trubert L, Mandelli M, Ozdemir B, Alric P, Gandet T, Canaud L. Midterm follow-up of fenestrated and scalloped physician-modified endovascular grafts for zone 2 TEVAR. *J Endovasc Ther.* (2020) 27:377–84. doi: 10.1177/1526602819881128

30. Chassin-Trubert L, Gandet T, Ozdemir B, Lounes Y, Alric P, Canaud L. Aortic arch anatomy pattern in patients treated using double homemade fenestrated stent grafts for total endovascular aortic arch repair. *J Endovasc Ther.* (2020) 27:785–91. doi: 10.1177/1526602820931787

31. Tong Y, Qin Y, Yu T, Zhou M, Liu C, Liu C, et al. Three-dimensional printing to guide the application of modified prefenestrated stent grafts to treat aortic arch disease. *Ann Vasc Surg.* (2020) 66:152–9. doi: 10.1016/j.avsg.2019.12.030

32. Canaud L, Ozdemir B, Chassin-Trubert L, Sfeir J, Alric P, Gandet T. Double homemade fenestrated stent graft for total endovascular aortic arch repair. *J Vasc Surg.* (2019) 70:1031–8. doi: 10.1016/j.jvs.2018.11.054

33. Canaud L, Morishita K, Gandet T, Sfeir J, Bommart S, Alric P, et al. Homemade fenestrated stent graft for thoracic endovascular aortic repair of zone 2 aortic lesions. *J Thorac Cardiovasc Surg.* (2018) 155:488–93. doi: 10.1016/j.jtcvs.2017.07.045

34. Reyes Valdivia A, Pitoulias G, Pitoulias A, El Amrani M, Gandarias Zuniga C. Systematic review on the use of physician-modified endografts for the treatment of aortic arch diseases. *Ann Vasc Surg.* (2020) 69:418–25. doi: 10.1016/j.avsg.2020.07.040

35. Gandet T, Ozdemir B, Trubert L, Alric P, Albat B, Canaud L. Physician-modified thoracic stent grafts for the arch after surgical treatment of type A dissection. *Ann Thorac Surg.* (2019) 108:491–8. doi: 10.1016/j.athoracsur.2019.02.026

36. Canaud L, Ozdemir B, Chassin-Trubert L, Sfeir J, Alric P, Gandet T. Homemade fenestrated stent grafts for complete endovascular repair of aortic arch dissections. *J Endovasc Ther.* (2019) 26:645–51. doi: 10.1177/1526602819858578

37. Li X, Li Q, Zhang W, Li M, He H, Luo M, et al. Early experience and technical aspects of physician-modified fenestration in thoracic endovascular aortic repair for aortic arch pathologies. *J Int Med Res.* (2020) 48:300060519870903. doi: 10.1177/0300060519870903

frontiers | Frontiers in Cardiovascular Medicine

TYPE Original Research
PUBLISHED 16 January 2023
DOI 10.3389/fcvm.2022.1031068

Check for updates

OPEN ACCESS

EDITED BY
Jinbao Qin,
Shanghai Jiao Tong University, China

REVIEWED BY
Zhenjiang Li,
Zhejiang University, China
Yangyang Ge,
People's Liberation Army General Hospital, China
Minyi Yin,
Shanghai Jiao Tong University, China

*CORRESPONDENCE
Qingsheng Lu
✉ luqs@xueguan.net

†These authors have contributed equally to this work and share first authorship

SPECIALTY SECTION
This article was submitted to Heart Surgery, a section of the journal Frontiers in Cardiovascular Medicine

RECEIVED 29 August 2022
ACCEPTED 15 December 2022
PUBLISHED 16 January 2023

CITATION
Li X, Zhang L, Song C, Zhang H, Xia S, Yang Y, Zhu L, Guo W and Lu Q (2023) Outcomes of thoracic endovascular aortic repair with fenestrated surgeon-modified stent-graft for type B aortic dissections involving the aortic arch. *Front. Cardiovasc. Med.* 9:1031068. doi: 10.3389/fcvm.2022.1031068

Outcomes of thoracic endovascular aortic repair with fenestrated surgeon-modified stent-graft for type B aortic dissections involving the aortic arch

Xiaoye Li[1†], Lei Zhang[1†], Chao Song[1], Hao Zhang[1], Shibo Xia[1], Yang Yang[2], Longtu Zhu[1], Wenying Guo[1] and Qingsheng Lu[1*]

[1]Division of Vascular Surgery, Department of General Surgery, Changhai Hospital, Naval Medical University, Shanghai, China, [2]Changhai Hospital, Naval Medical University, Shanghai, China

Objectives: This retrospective analysis aimed to evaluate the early and midterm outcomes of thoracic endovascular aortic repair (TEVAR) with fenestrated surgeon-modified stent-graft (f-SMSG) for type B aortic dissections (TBAD) involving the aortic arch.

Methods: From March 2016 to April 2021, 47 consecutive patients were treated using TEVAR with f-SMSG. All patients were diagnosed with TBAD involving the aortic arch.

Results: In total, 47 patients with TBAD involving the aortic arch were treated with f-SMSGs. There were 21 zone 1 and 26 zone 2 TEVAR, and 65 arteries were revascularized successfully with fenestrations. Technical success was achieved in 46 patients (97.88%). The 30-day estimated survival (± SE) and reintervention was 93.6 ± 1.0% (95% Confidence Interval [CI], 92.6–94.6%) and 91.5 ± 1.2% (95% CI, 90.3–92.7%), respectively. During a median follow-up of 51 months (range, 16–71 months), 1 patient died of rupture of aortic dissection (AD) and 3 patients died of non-aortic-related reasons. Reintervention was performed for four patients, including two patients of type IA entry flow and two patients of type IB entry flow. No occlusion of the supra-aortic trunk was observed. The estimated survival and reintervention (± SE) at 4 years was 88.7 ± 1.4% (95% CI, 87.3–90.1%) and 84.8 ± 1.5% (95% CI, 83.3–86.3%), respectively.

Conclusion: Thoracic endovascular aortic repair with f-SMSG is an alternative treatment option for TBAD involving the aortic arch in high-volume centers.

KEYWORDS

thoracic endovascular aortic repair, fenestrated surgeon-modified stent-graft, type B aortic dissection, aortic arch, supra-aortic trunks

Introduction

The incidence of aortic dissection (AD) was 4.8 per 100,000 individuals/year, two-thirds of whom presented with type A AD (TAAD) and the remaining one-third with type B (1). Optimal medical therapy (OMT) is recommended for uncomplicated type B aortic dissections (TBAD) without high-risk features. For complicated TBAD and uncomplicated TBAD with high-risk features, thoracic endovascular aortic repair (TEVAR) is recommended as the first-line treatment (2). Considering superior aortic remodeling after TEVAR over OMT in the long-term, TEVAR had been also used in uncomplicated cases (3, 4).

With TEVAR, entry tears of TBAD were completely excluded and blood flow was stopped from entering the false lumen. Adequate length of proximal/distal landing zone is necessary for complete sealing, otherwise, blood flow would re-enter the false lumen, resulting in progression or eventually rupture. For adequate length in the healthy aorta, a proximal landing zone had to be extended proximal to the ostium of the left subclavian artery (LSA), left common carotid artery (LCCA), and even innominate artery (IA). In these conditions, supra-aortic trunks must be revascularized, otherwise, severe complications would occur.

Available options for supra-aortic trunk revascularization included TEVAR with branched and/or fenestrated stentgraft, scallop technique, and bypass surgery (5). In our center, TEVAR with fenestrated surgeon-modified stent-graft (f-SMSG) was mostly used and has been performed for more than 5 years. With this retrospective study, we reported its outcomes for the treatment of TBAD.

Materials and methods

Population

Between March 2016 and April 2021, 47 consecutive patients with TBAD involving the aortic arch underwent zone 1/2 TEVAR in our center. Protocol and informed consent were approved by the institutional review board, and all patients gave written consent. Indications for TEVAR with f-SMSGs were patients with TBAD involving the aortic arch (primary entry tear in zone 1 or distal, the proximal extent of pathology in zone 1 or distal). Exclusion criteria were (1) the proximal extent of the pathology/entry tear in zone 0 and (2) whether the maximal aortic diameter of the proximal landing zone was more than 45 mm. Baseline characteristics, images, and operative and follow-up data were prospectively collected and retrospectively reviewed.

Pre-operative planning and design

Pre-operative computed tomography angiography (CTA) in Dicom format (axial slice thickness of 3 mm or less) of all patients was acquired. The anatomical features were measured with vascular imaging workstation Aquarius (TeraRecon, Foster City San Mateo, CA, USA) or Endosize (Therenva, Rennes, France). All measurements were taken in multiplanar reconstruction always in a plane perpendicular to the manually corrected local aortic centerline. The diameter of the aorta at the proximal and distal landing zone, the diameter and clock position of the Ostia of LCCA and LSA, and the diameter of LCCA and LSA were measured along the centerline. The distance between the Ostia of LCCA and LSA was measured along the greater curvature line. All f-SMSGs were 0–5% oversized to the aorta. In cases where the distal landing zone was the dissected aorta, the diameter of the long axis of the true lumen was used to determine the oversize ratio. For zone 1 TEVAR, two strategies were used, including one large fenestration for LCCA and LSA and two small fenestrations for LCCA and LSA, respectively. For a patient with the right common carotid artery (RCCA), which originated directly from the aortic arch, a large fenestration for RCCA and LCCA was used. For zone 2 TEVAR, the revascularization strategy was a small fenestration for LSA. A large fenestration is defined as a fenestration aligned with more than one artery, while a small fenestration is defined as a fenestration aligned with one artery. When entry tears were on the lesser curvature side, a large fenestration would be selected. Bypass surgery would be performed when supra-aortic trunks were dissected.

Procedural details

Procedural details have been described in our previous report (6). To summarize, all operations were performed under general anesthesia in a hybrid operating room. In all cases, Valiant Captivia (Medtronic, Minneapolis, MN, USA) devices were selected as the main stent graft for modification. The modification was performed on a sterile operating table. Once the stent graft was partially unsheathed, the operator would create the fenestration in the designated position with a scalpel. After the creation of fenestrations, the f-SMSGs would be resheathed with the help of assistants. Access points were the left common femoral artery for the f-SMSG, and in patients with a previous history of endovascular repair, the right common femoral artery would be used. A large sheath was introduced retrogradely through the common femoral artery. In cases where bridging stent grafts were implanted into LCCA and LSA, a sheath was introduced retrogradely through the left brachial artery into the ostium of LSA, and a sheath was introduced retrogradely through LCCA into the ostium of

LCCA. After ascertaining that the fenestrations were pointing to the ground, the f-SMSG was advanced over the Lunderquist wire. On arriving at the target position, the f-SMSG was deployed under visualization. After the deployment of f-SMSG and precise alignment between fenestrations and target arteries, bridging stent grafts were advanced into fenestrations, ∼15 mm protruding into the lumen of f-SMSGs, with the remaining in the target arteries. Post-dilation would be performed for balloon-expandable bridging stent graft. When the diameter of f-SMSG at the distal landing zone was 10% larger than that of the aorta, another distal restrictive stent graft (either a bare metal stent or a covered stent, determined according to the extent of pathology) whose diameter agreed with the aorta would be deployed prior to the f-SMSG. The distal oversized part of the f-SMSG would be covered within the distal restrictive stent graft. Completion angiography would be performed to confirm that fenestrations were aligned with the target arteries and all supra-aortic trunks patent (**Figure 1**).

Follow-up and definition

Follow-up surveillance was performed with serial CTA in the 6 and 12 months, and annually thereafter. No patients were lost to follow-up. Mortality, reintervention, and adverse events that occurred within 30 days after the operation or during hospitalization were reported as 30-day outcomes, otherwise were reported as follow-up outcomes. Technical success was defined as the successful alignment of all fenestrations with target arteries, patent supra-aortic trunks, and complete exclusion of primary entry tear without type I or III endoleak. Extent, chronicity classification of TBAD, and complications (entry flow, stroke) were reported according to Society for Vascular Surgery (SVS) and Society of Thoracic Surgeons (STS) Reporting Standards for TBAD (7).

Statistics

Categorical data are reported as the absolute number and percentage; continuous data are reported as the mean ± standard deviation; and non-parametric data (e.g., follow-up time) are reported as the median and range. Statistical analysis was performed with SPSS software (22.0 v; SPSS, Inc., Chicago, IL, USA). Kaplan–Meier analysis was used for follow-up data.

Results

From March 2016 through April 2021, 47 consecutive patients with TBAD met the inclusion criteria and underwent zone 1/2 TEVAR with f-SMSGs. There were 39 male patients (median age, 61; range: 33–77). Hypertension was the most frequently diagnosed comorbidity ($n = 35$, 76.1%), while less than half (42.6%) patients had a smoking history. Previously, the endovascular repair had been performed in two patients (4.3%). Population details are given in **Table 1**. All patients were

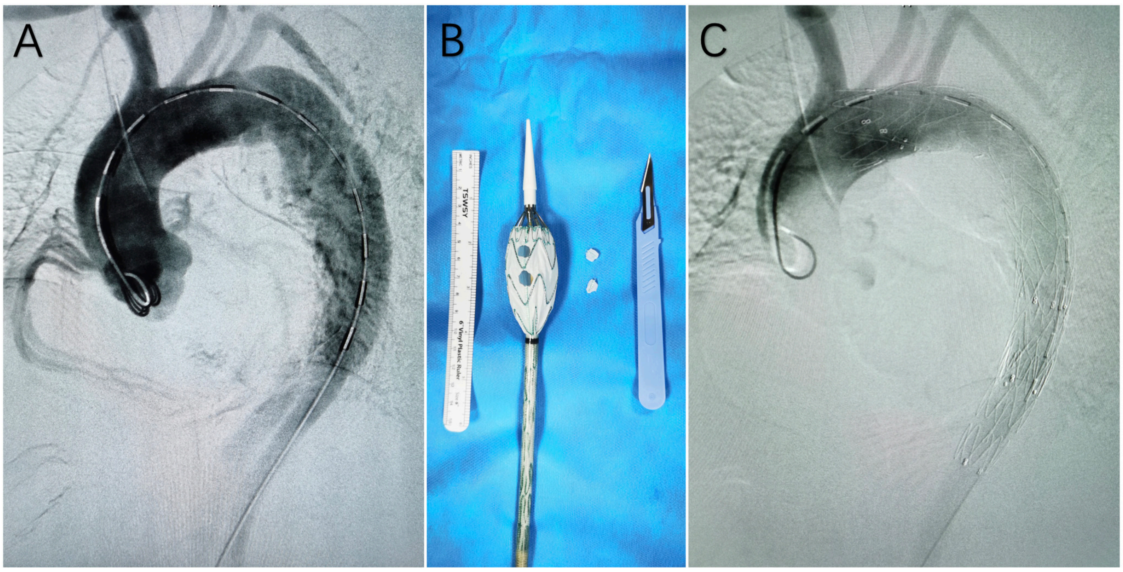

FIGURE 1
(A) Digital subtraction angiography (DSA) before the deployment of the fenestrated surgeon-modified stent-graft; **(B)** fenestrated surgeon-modified stent-graft; **(C)** DSA at the end of the operation, showing complete exclusion of the main entry tear and patent branch arteries of the aortic arch.

TABLE 1 Population demographics [median (range) or n (%), $N = 47$].

Age, years	61 (33–77)
Body mass index	24.46 (18.36–34.60)
Male	39 (83.0)
Hypertension	35 (76.1)
Smoking history	20 (42.6)
Coronary disease	2 (4.3)
Stroke	3 (6.4)
Diabetes mellitus	6 (12.8)
Previous endovascular repair	2 (4.3)
Chronic obstructive pulmonary disease	3 (6.4)
Renal dysfunction	4 (8.5)

diagnosed with TBAD, including 3 (6.4%) urgent operations and 44 (93.6%) elective operations. Other TBAD details are given in Table 2.

In total, 21 zone 1 and 26 zone 2 TEVAR were performed. A total of 65 arteries were revascularized successfully with fenestrations, including 21 LCCA, 41 LSA, 1 RCCA that originated directly from the aortic arch, 1 aberrant right subclavian artery (aRSA), and 1 aberrant left vertebral artery

TABLE 2 Disease details [n (%), $N = 47$].

Extent of pathology ($B_{proxiamlextent,distalextent}$)	
$B_{1,5}$	1 (2.1)
$B_{1,6}$	2 (4.3)
$B_{1,9}$	1 (2.1)
$B_{1,11}$	1 (2.1)
$B_{2,4}$	4 (8.5)
$B_{2,6}$	2 (4.3)
$B_{2,8}$	2 (4.3)
$B_{2,9}$	2 (4.3)
$B_{2,10}$	2 (4.3)
$B_{2,11}$	4 (8.5)
$B_{3,4}$	8 (17.0)
$B_{3,5}$	4 (8.5)
$B_{3,6}$	3 (6.4)
$B_{3,9}$	7 (14.9)
$B_{3,10}$	1 (2.1)
$B_{3,11}$	3 (6.4)
Chronicity	
Acute (1–14 days)	26 (55.3)
Subacute (15–90 days)	12 (25.5)
Chronic (>90 days)	9 (19.1)

(LVA) that originated directly from the aortic arch. LCCA–LSA bypass surgery was performed in one patient (in the same stage). Distal restrictive stent grafts were used in 25 patients, including 15 Sinus-XL (OptiMed Medizinische Instrumente GmbH, Ettlingen, Germany), 9 Hercules (MicroPort, Shanghai, China), and 1 Wallstent (Boston Scientific, Boston, MA, USA). Technical success was achieved in 46 patients (97.88%). In one patient, the f-SMSG migrated during deployment and the fenestration was misaligned with LSA, and LSA was revascularized successfully with the chimney technique. Fluency (CR Bard, Murray Hill, NJ, USA) was the mostly used bridging stent-graft ($n = 12$), and then was Viabahn (WL Gore, Flagstaff, AZ; $n = 5$) and E-luminexx (CR Bard, Murray Hill, NJ, USA; $n = 3$) (Figure 2).

Thirty-day outcomes

The mortality rate was 2.1% ($n = 1$). The patient died of retrograde type A aortic dissection (RTAD). When a sudden drop in blood pressure was recorded, he was sent for surgery immediately. A newly occurred tear was found in the aortic arch (lesser curvature side). The ascending aorta and the aortic root were dissected, and the blood flow of the right coronary artery originated from the false lumen. The estimated survival (± SE) at 30 days was 93.6 ± 1.0% (95% Confidence Interval [CI], 92.6–94.6%). No stroke was observed. The rate of reintervention was 6.4% ($n = 3$). RTAD was the reason for reintervention. Two patients had zone 1 TEVAR and had aortic root reconstruction, ascending aorta, and total aortic arch replacement, and endovascular repair of the descending aorta. Another patient had a Bentall procedure, transposition of the aortic arch, and frozen elephant trunk implantation performed because of RTAD and severe aortic insufficiency. The estimated freedom from reintervention (± SE) at 30 days was 91.5 ± 1.2% (95% CI, 90.3–92.7%).

Follow-up outcomes

The compliance of imaging follow-up at 6 months, 1, 2, and 3 years was 91.5% (43/47), 59.1% (26/44), 47.6% (20/42), and 33.3% (13/39), respectively. Clinical follow-up with phone or outpatient visits was performed each year for all patients. During follow-up, there were four deaths recorded. One patient had a rupture of AD 2 months after the operation (Figure 3). The other three patients had non-aortic related death, including one case of bilateral stroke (7 months), one case of acute coronary syndrome (26 months), and another case of cardiac arrest (38 months). The estimated survival (± SE) at 4 years was 88.7 ± 1.4% (95% CI, 87.3–90.1%). Endoleak was found in five patients (10.6%), and four patients had reintervention.

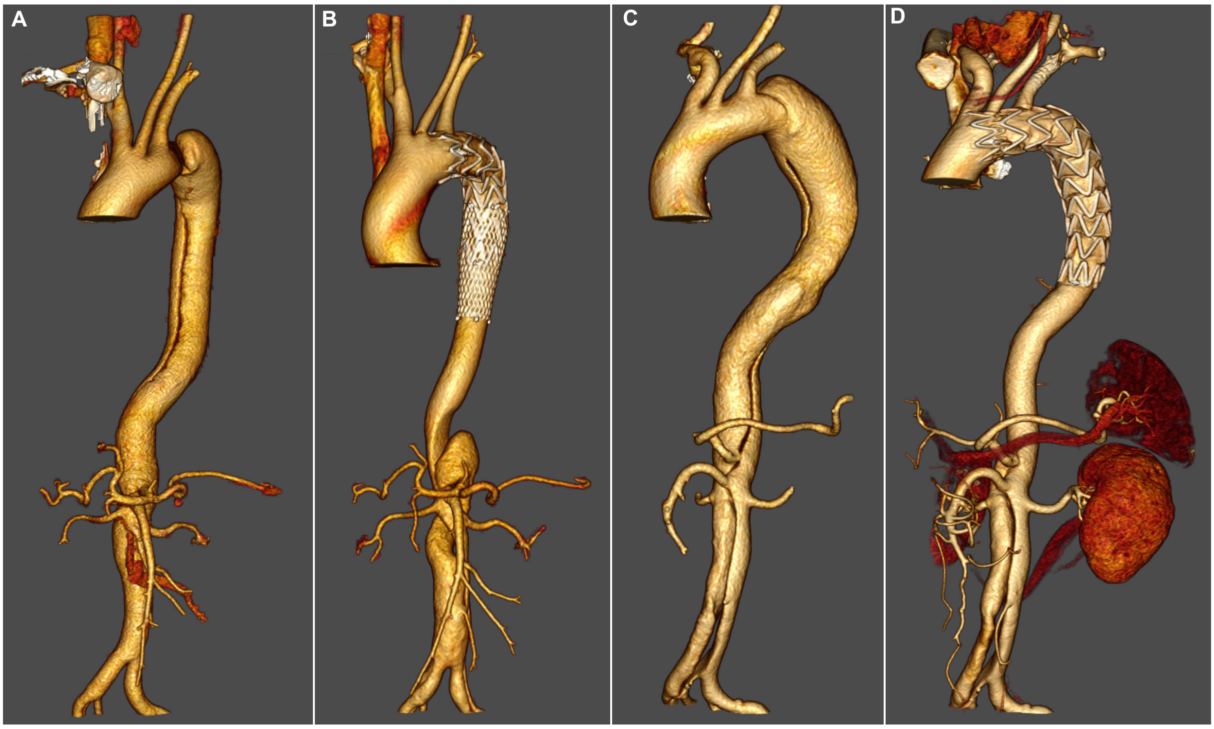

FIGURE 2
Thoracic endovascular aortic repair with fenestrated surgeon-modified stent graft. **(A)** Pre-operative three-dimensional computed tomography angiography (CTA) reconstruction for a patient with zone 1 TEVAR. **(B)** Three-dimensional CTA reconstruction for a patient with zone 1 TEVAR 3 years after the operation. **(C)** Pre-operative three-dimensional CTA reconstruction for a patient with zone 2 TEVAR. **(D)** Three-dimensional CTA reconstruction for a patient with zone 2 TEVAR 4 years after the operation.

One patient (1 small fenestration for LSA) had reintervention owing to type IA entry flow (5 months). Another f-SMSG aligned with LCCA was deployed proximal to the previous f-SMSG, and the entry flow was resolved. In another case, type IA entry flow was observed during the annual CTA examination, and the false lumen was embolized with a coil. Two patients had type IB entry flow, one had another covered stent graft deployed distal to the f-SMSG 5 months after the operation, and the other had a false lumen embolized with the coil. At the end of the follow-up, all supra-aortic trunks were patent. The estimated freedom from reintervention ($\pm$ SE) at 4 years was 84.8 $\pm$ 1.5% (95% CI, 83.3–86.3%). Details about the 30-day and follow-up outcomes are listed in **Table 3**.

Discussion

An adequate landing zone is an important factor influencing the outcome of TEVAR. Yoon et al. compared the outcomes of TEVAR with proximal landing zone $\geq$20 and $<$20 mm and found that $<$20 mm was related to a higher rate of adverse events, especially type IA endoleak (8). In some cases, when performing TEVAR for aortic arch pathologies, supra-aortic trunks would be covered for an adequate proximal landing zone (9). Revascularization of supra-aortic trunks with minimal cerebral hypoperfusion time is essential for a successful treatment, including LSA, reconstruction of which had gone through controversies, while currently there is an agreement for the necessity of its reconstruction (10). Different endovascular techniques had been used in the revascularization of supra-aortic trunks, including the chimney technique, custom-made branched stent-graft, *in situ* fenestration, and f-SMSG (11–14). Chimney technique was related to a higher incidence of type Ia endoleak owing to the gutter. Shu et al. invented a gutter-free chimney stent graft system for aortic arch dissection, while 23.1% presented immediate type IA endoleak and 7.7% type IA endoleak in a delayed fashion in their initial clinical experiment, which was still higher than the fenestrated or branched stent graft (15). Branched stent graft has the most stable design. In the early stage, custom-made branched stent-graft was used, allowing personalized treatment, while the process of measurement and manufacture took more than 1 month, preventing its usage in the emergent condition. Castor single-branched stent graft is the first off-the-shelf single-branched stent graft for the preservation of LSA in China,

10.3389/fcvm.2022.1031068

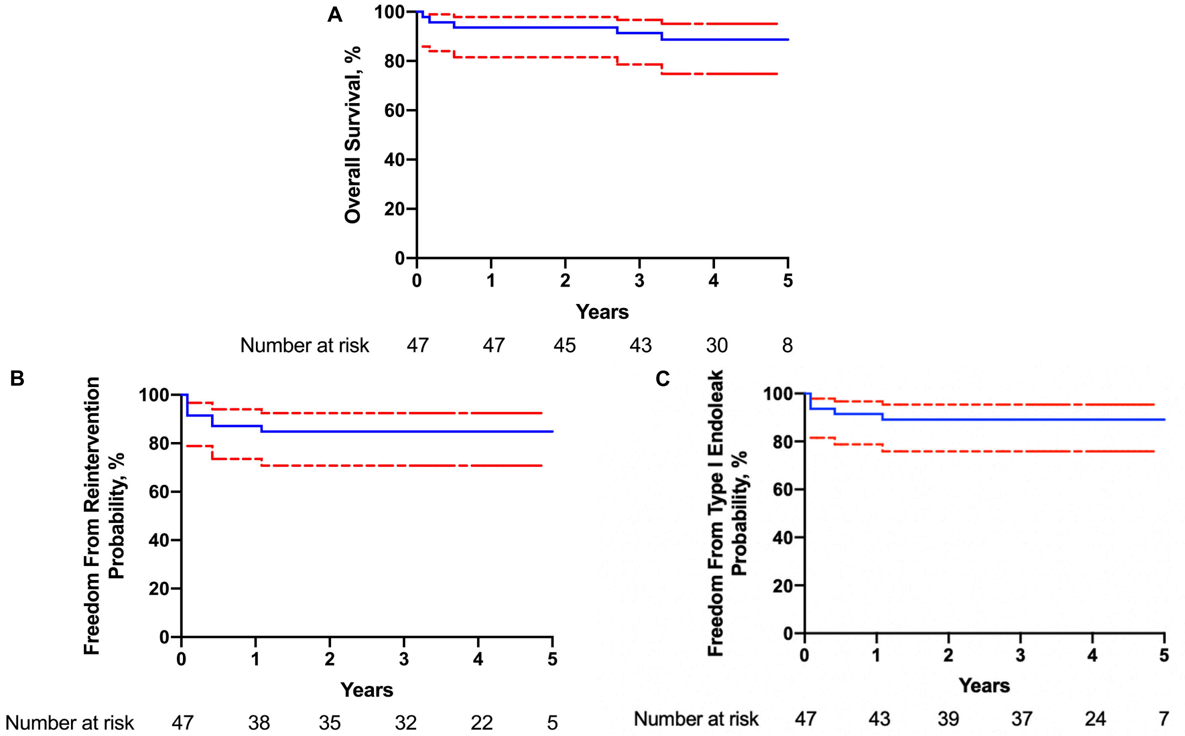

FIGURE 3
Kaplan–Meier curve of **(A)** overall survival; **(B)** freedom from reintervention; **(C)** freedom from type I endoleak.

which had also been approved in Europe (16). However, double/triple branched stent graft was still under investigation due to the various anatomy patterns of the aortic arch, especially when more than one supra-aortic trunk needs reconstruction. Fenestrated stent graft, including *in situ* fenestration and f-SMSG, allows personalized treatment even in an emergent surgery when CTA was available. Shu et al. reported midterm outcomes of TEVAR with *in situ* fenestration with an adjustable puncture device (17). At the end of the follow-up, all supra-aortic trunks were patent, and no fractures, migrations, or bridging stent kinks were found. Our study showed similar results, all supra-aortic trunks were patent and all f-SMSGs were complete.

Compared with *in situ* fenestration, cerebral hypoperfusion time could be minimized in TEVAR with f-SMSG (18). Once the fenestration was aligned with the target arteries, the supra-aortic artery was revascularized successfully. In this series, no stroke had been observed during the perioperative period. To ensure accurate alignment, a detailed and precise pre-operative measurement is essential, including the diameter and clock position of supra-aortic trunks and their distance, and the fenestration should be designed and created accordingly. Three-dimensional printing could improve the accuracy of fenestrations. Rynio et al. compared 40 fenestrations created by vascular surgeons and found that fenestrations created in the three-dimensionally aortic template had better reliability and greater alignment with the target vessels than those based on measurements from CTA (19). Branzan et al. suggested that

TABLE 3 Outcomes [median (range) or *n* (%), *N* = 47].

Median hospital stay	11 (5–28)
Median ICU stay	1 (0–12)
Thirty-day outcomes	
Mortality	1 (2.1)
Retrograde type A aortic dissection	
Reintervention	4 (11.8)
Retrograde type A aortic dissection	2 (4.3)
Severe aortic insufficiency	1 (2.1)
Follow-up, months	51 (16–71)
Follow-up outcomes	
Mortality	4 (8.5)
Aortic-related deaths	1 (2.1)
Non-aortic-related deaths	3 (6.4)
Reintervention	4 (11.8)
Type IA entry flow	2 (4.3)
Type IB entry flow	2 (4.3)

the three-dimensional printed aortic model could be utilized in urgent treatment as safe and feasible (20). However, during deployment, migration of the f-SMSG did occur occasionally (one out of 47 in this series, and the supra-aortic trunk was revascularized with the chimney technique). A pre-loaded guidewire has been recommended to assist in overcoming the migration (21). Chassin-Trubert et al. reported improvement in the success rate after applying the pre-loaded guidewire [from 94% (19/22) to 100% (28/28)], all of which were total endovascular aortic arch repair, revascularizing all supra-aortic trunks (22). Additionally, the alignment could be simplified and reassured with a pre-loaded guidewire, thus shortening the learning curve (23).

A major concern about f-SMSG is its durability after modification. There are studies reporting the application of Bolton (Bolton Medical, Sunrise, FL, USA), the deployment system of the Gore device (WL Gore & Associates, Inc., Flagstaff, AZ, USA), and Medtronic (Bolton Medical, Sunrise, FL, USA) as f-SMSGs (homemade fenestrated stent-graft, physician-modified fenestrated stent-graft), while none of these abovementioned devices had reported durability after modification, namely, durability after damage to the fabric in their instructions for use (IFU). Several benchtop experiments had been carried out to evaluate the safety and fabric durability after modification, and no malfunction or rapid deterioration was reported, while pathological changes bring about more sophisticated hemodynamic and biomechanical conditions (24, 25). Several studies reported promising outcomes after TEVAR with f-SMSGs for aortic arch pathologies, including type A/B aortic dissections, degenerative aneurysms, and penetrating aortic ulcers (26–28). Canaud et al. reported outcomes of total arch TEVAR with double fenestrated physician-Modified Stent-grafts for 100 patients with various pathologies. During a mean follow-up of 24 $\pm$ 7.2 months, all supra-aortic trunks were patent, and no stent-graft collapse or type III endoleak was reported (29). In our study, the median follow-up was 51 months, and although the follow-up period of five patients exceeded 5 years, no stent graft collapse or type III endoleak was observed, and all supra-aortic trunks were patent. Despite f-SMSGs' off-label use as off-the-shelf thoracic stent grafts, their safety and durability seem acceptable in treating aortic arch pathologies.

Ma et al. have performed computation analysis to investigate the force distribution after TEVAR and found the maximal aortic stress at the apposition point between the stent graft and aorta (greater curvature side), which was also verified in an animal model (30). In our series, two out of three RTAD cases had new entry tear at the proximal end, which was bare metal stent, of the f-SMSG, where the maximal aortic stress was suggested. Zone 0/1/2/3 TEVAR had been performed in our center, and more RTAD cases were recorded in zone 1/3 TEVAR compared with zone 0/2 TEVAR. When the proximal landing zone of the stent-graft is in the extremely curved artery, the maximal aortic stress would increase greatly, and so would the risk of RTAD. It has been suggested, not only with our evidence, that zone 0 instead of zone 1–2 as the proximal landing zone in selected cases was related to lesser complications and better outcomes (31). However, zone 0 TEVAR was challenging and should only be considered in high-volume centers and performed by experienced surgeons/physicians.

Limitations

Data were retrospectively analyzed despite being prospectively collected. The sample size was small and no control group was set to compare f-SMSG with other techniques to revascularize supra-aortic trunks, including parallel graft, branched stent graft, and *in situ* fenestration. No benchtop experiment has been performed before the clinical application of f-SMSG. Since f-SMSG is beyond the IFU, further and close follow-up is needed. All procedures were performed by an experienced surgeon.

Conclusion

Thoracic endovascular aortic repair with f-SMSGs is a feasible alternative treatment option for TBAD involving the aortic arch. Results based on this study seem to be acceptable. Long-term safety and durability need to be assessed with a larger sample size and longer follow-ups.

Data availability statement

The raw data supporting the conclusions of this article will be made available by the authors, without undue reservation.

Ethics statement

The studies involving human participants were reviewed and approved by the Committee on Ethics of Medicine, Navy Medical University. The patients/participants provided their written informed consent to participate in this study.

Author contributions

XL, LeZ, CS, HZ, SX, YY, LoZ, WG, and QL: substantial contributions to the conception or design of the work, or the acquisition, analysis, or interpretation of data for the work, and drafting the work or revising it critically for important intellectual content. All authors provide approval for publication of the content and agree to be accountable for all aspects of the work in ensuring that questions related to the accuracy or integrity of any part of the work are appropriately investigated and resolved.

Conflict of interest

The authors declare that the research was conducted in the absence of any commercial or financial relationships that could be construed as a potential conflict of interest.

Publisher's note

All claims expressed in this article are solely those of the authors and do not necessarily represent those of their affiliated organizations, or those of the publisher, the editors and the reviewers. Any product that may be evaluated in this article, or claim that may be made by its manufacturer, is not guaranteed or endorsed by the publisher.

References

1. Gouveia E, Melo R, Mourão M, Caldeira D, Alves M, Lopes A, et al. A systematic review and meta-analysis of the incidence of acute aortic dissections in population-based studies. *J Vasc Surg.* (2022) 75:709–20. doi: 10.1016/j.jvs.2021.08.080

2. MacGillivray T, Gleason T, Patel H, Aldea G, Bavaria J, Beaver T, et al. The Society of Thoracic Surgeons/American Association for Thoracic Surgery clinical practice guidelines on the management of type B aortic dissection. *J Thorac Cardiovasc Surg.* (2022) 163:1231–49. doi: 10.1016/j.jtcvs.2021.11.091

3. Tozzi P. Thoracic endovascular aortic repair to treat uncomplicated Stanford type B aortic dissection: the surgeon's dilemma to preventing future complications. *Eur J Prev Cardiol.* (2018) 25(1_Suppl.):24–31. doi: 10.1177/2047487318758100

4. Burke C, Bavaria J. The role of thoracic endovascular repair in chronic type B aortic dissection. *Semin Thorac Cardiovasc Surg.* (2020) 32:21–4. doi: 10.1053/j.semtcvs.2019.08.010

5. Evangelista A, Isselbacher E, Bossone E, Gleason T, Eusanio M, Sechtem U, et al. Insights from the international registry of acute aortic dissection: a 20-year experience of collaborative clinical research. *Circulation.* (2018) 137:1846–60. doi: 10.1161/CIRCULATIONAHA.117.031264

6. Shen Y, Yeung K, Lu Q. Patient-specific total endovascular aortic arch repair using custom fenestration of an off-the-shelf thoracic endovascular aortic repair aortic-stent. *Chin Med J.* (2021) 134:1489–91. doi: 10.1097/CM9.0000000000001438

7. Lombardi J, Hughes G, Appoo J, Bavaria J, Beck A, Cambria R, et al. Society for vascular surgery (SVS) and society of thoracic surgeons (STS) reporting standards for type B aortic dissections. *J Vasc Surg.* (2020) 71:723–47.

8. Yoon W, Mell M. Outcome comparison of thoracic endovascular aortic repair performed outside versus inside proximal landing zone length recommendation. *J Vasc Surg.* (2020) 72:1883–90. doi: 10.1016/j.jvs.2020.03.033

9. Czerny M, Schmidli J, Adler S, van den Berg J, Bertoglio L, Carrel T, et al. Current options and recommendations for the treatment of thoracic aortic pathologies involving the aortic arch: an expert consensus document of the European association for cardio-thoracic surgery (EACTS) & the European society for vascular surgery (ESVS). *Eur J Vasc Endovasc Surg.* (2019) 57:165–98. doi: 10.1016/j.ejvs.2018.12.011

10. Karaolanis G, Antonopoulos C, Charbonneau P, Georgakarakos E, Moris D, Scali S, et al. A systematic review and meta-analysis of stroke rates in patients undergoing thoracic endovascular aortic repair for descending thoracic aortic aneurysm and type B dissection. *J Vasc Surg.* (2022) 76:292–301.e3. doi: 10.1016/j.jvs.2022.02.031

11. Chang H, Jin D, Wang Y, Liu B, Wang W, Li Y. Chimney technique and single-branched stent graft for the left subclavian artery preservation during zone 2 thoracic endovascular aortic repair for type B acute aortic syndromes. *J Endovasc Ther.* (2022) 9:15266028221102657. doi: 10.1177/15266028221102657

12. Blanco Amil C, Mestres Alomar G, Guarnaccia G, Luoni G, Yugueros Castellnou X, Vigliotti R, et al. The initial experience on branched and fenestrated endografts in the aortic arch. A systematic review. *Ann Vasc Surg.* (2021) 75:29–44. doi: 10.1016/j.avsg.2021.03.024

13. Li X, Zhang L, Song C, Zhang H, Xia S, Li H, et al. Outcomes of total endovascular aortic arch repair with surgeon-modified fenestrated stent-grafts on zone 0 landing for aortic arch pathologies. *J Endovasc Ther.* (2022) 29:109–16. doi: 10.1177/15266028211036478

14. Evans E, Veeraswamy R, Zeigler S, Wooster M. Laser in situ fenestration in thoracic endovascular aortic repair: a single-center analysis. *Ann Vasc Surg.* (2021) 76:159–67. doi: 10.1016/j.avsg.2021.05.006

15. Fang K, Shu C, Luo M, Li M, Li X, He H, et al. First-in-human implantation of gutter-free design chimney stent graft for aortic arch pathology. *Ann Thorac Surg.* (2020) 110:664–9. doi: 10.1016/j.athoracsur.2020.03.016

16. Rizza A, Negro F, Palermi S, Palmieri C, Murzi M, Credi G, et al. Penetrating aortic ulceration treated with castor branched aortic stent graft-A case series. *Int J Environ Res Public Health.* (2022) 19:4809. doi: 10.3390/ijerph19084809

17. Shu X, Xu H, Wang E, Wang L, Guo D, Chen B, et al. Midterm outcomes of an adjustable puncture device for in situ fenestration during thoracic endovascular aortic repair. *Eur J Vasc Endovasc Surg.* (2022) 63:43–51. doi: 10.1016/j.ejvs.2021.09.028

18. Pyun A, Potter H, Magee G, Manzur M, Weaver F, Ziegler K, et al. Comparative early results of in situ fenestrated endovascular aortic repair and other emergent complex endovascular aortic repair techniques for ruptured suprarenal and thoracoabdominal aortic aneurysms at a regional aortic center. *J Vasc Surg.* (2022) 76:875–83. doi: 10.1016/j.jvs.2022.04.036

19. Rynio P, Jedrzejczak T, Rybicka A, Milner R, Gutowski P, Kazimierczak A. Initial experience with fenestrated physician-modified stent grafts using 3D aortic templates. *J Clin Med.* (2022) 11:2180. doi: 10.3390/jcm11082180

20. Branzan D, Geisler A, Grunert R, Steiner S, Bausback Y, Gockel I, et al. The influence of 3D printed aortic models on the evolution of physician modified stent grafts for the urgent treatment of thoraco-abdominal and pararenal aortic pathologies. *Eur J Vasc Endovasc Surg.* (2021) 61:407–12. doi: 10.1016/j.ejvs.2020.10.023

21. Mirza A, Tenorio E, Kärkkäinen J, Pather K, Kratzberg J, Mendes B, et al. Outcomes of a novel upper extremity preloaded delivery system for fenestrated-branched endovascular repair of thoracoabdominal aneurysms. *J Vasc Surg.* (2020) 72:470–9. doi: 10.1016/j.jvs.2019.09.058

22. Chassin-Trubert L, Gandet T, Lounes Y, Ozdemir B, Alric P, Canaud L. Double fenestrated physician-modified stent-grafts for total aortic arch repair in 50 patients. *J Vasc Surg.* (2021) 73:1898–905.e1.

23. Prendes C, Banafsche R, Stana J, Binskin R, Konstantinou N, Kölbel T, et al. Technical aspects of fenestrated arch TEVAR with preloaded fenestration. *J Endovasc Ther.* (2021) 28:510–8. doi: 10.1177/15266028211007469

24. Lounes Y, Chassin-Trubert L, Gandet T, Ozdemir B, Peyron A, Akodad M, et al. Endovascular aortic arch repair with a pre-cannulated double-fenestrated physician-modified stent graft: a benchtop experiment. *Interact Cardiovasc Thorac Surg.* (2021) 32:942–9.

25. Faure E, Khantalin I, Peyron P, Canaud L, Marty-Ané C, Alric P. Experimental assessment of physician modified proximal scalloped stent graft to extend proximal landing zone in the aortic arch. *Eur J Vasc Endovasc Surg.* (2017) 54:150–6. doi: 10.1016/j.ejvs.2017.04.019

26. Chastant R, Belarbi A, Ozdemir B, Alric P, Gandet T, Canaud L. Handmade fenestrated physician-modified stent grafts for arch aortic degenerative aneurysms. *J Vasc Surg.* (2022) 76:1133–40.e2. doi: 10.1016/j.jvs.2022.04.041

27. Zhu J, Zhao L, Dai X, Luo Y, Fan H, Feng Z, et al. Fenestrated thoracic endovascular aortic repair using physician modified stent grafts for acute type B aortic dissection with unfavourable landing zone. *Eur J Vasc Endovasc Surg.* (2018) 55:170–6.

28. Lomazzi C, Grassi V, Domanin M, De Vincentiis C, Piffaretti G, Trimarchi S. Art of operative techniques: treatment options in arch penetrating aortic ulcer. *Ann Cardiothorac Surg.* (2019) 8:500–8. doi: 10.21037/acs.2019.07.06

29. Canaud L, Chassin-Trubert L, Abouliatim I, Hireche K, Bacri C, Alric P, et al. Total arch thoracic endovascular aortic repair using double fenestrated physician-modified stent-grafts: 100 patients. *J Endovasc Ther.* (2022) 4:15266028221116747. doi: 10.1177/15266028221116747

30. Ma T, Zhou M, Meng Z, Wang S, Dong Z, Fu W. Computational investigation and histopathological validation of interaction between stent graft and aorta in retrograde type A dissection after TEVAR in canine models. *J Endovasc Ther.* (2021) 29:275–82. doi: 10.1177/15266028211038596

31. Kudo T, Kuratani T, Shimamura K, Sawa Y. Determining the optimal proximal landing zone for TEVAR in the aortic arch: comparing the occurrence of the bird-beak phenomenon in zone 0 vs zones 1 and 2. *J Endovasc Ther.* (2020) 27:368–76. doi: 10.1177/1526602820914269

frontiers | Frontiers in Cardiovascular Medicine

TYPE Systematic Review
PUBLISHED 24 February 2023
DOI 10.3389/fcvm.2023.1034354

Check for updates

OPEN ACCESS

EDITED BY
Emiliano Chisci,
Nuovo Ospedale San Giovanni di Dio, Italy

REVIEWED BY
Xinsheng Xie,
Fudan University, China
Piero Farina,
Agostino Gemelli University Polyclinic (IRCCS), Italy

*CORRESPONDENCE
Qingsheng Lu
✉ luqs@newvascular.cn

†These authors have contributed equally to this work

SPECIALTY SECTION
This article was submitted to Heart Surgery, a section of the journal Frontiers in Cardiovascular Medicine

RECEIVED 01 September 2022
ACCEPTED 06 February 2023
PUBLISHED 24 February 2023

CITATION
Zhu L, Li X and Lu Q (2023) A systematic review and meta-analysis of thoracic endovascular aortic repair with the proximal landing zone 0. *Front. Cardiovasc. Med.* 10:1034354.
doi: 10.3389/fcvm.2023.1034354

A systematic review and meta-analysis of thoracic endovascular aortic repair with the proximal landing zone 0

Longtu Zhu†, Xiaoye Li† and Qingsheng Lu*

Division of Vascular Surgery, Department of General Surgery, Changhai Hospital, Naval Medical University, Shanghai, China

Background: Thoracic endovascular aortic repair, initially intended for thoracic aortic disease treatment, has extended its application to the proximal zone of the aorta. However, the safety and surgical outcomes of extending the proximal landing zone into the ascending aorta (zone 0) in selected cases remain unknown. Thus, we performed a systematic review and meta-analysis of zone 0 thoracic endovascular aortic repair (TEVAR) to obtain a deeper understanding of its safety, outcomes, and trends over time.

Methods: A literature search was performed using PubMed, EMBASE, and Web of Science databases in accordance with the preferred reporting items for systematic reviews and meta-analyses guidelines, from January, 1997 to January, 2022. Only studies involving zone 0 TEVAR were included. The retrieved data from the eligible studies included basic study characteristics, 30-day/in-hospital mortality rate, indications, comorbidities, stent grafts, techniques, and complications. Summary effect measures of the primary outcomes were obtained by logarithmically pooling the data with an inverse variance-weighted fixed-effects model.

Results: Fifty-three studies with 1,013 patients were eligible for analysis. The pooled 30-day/in-hospital mortality rate of zone 0 TEVAR was 7.49%. The rates of post-operative stroke, type Ia endoleak, retrograde type A aortic dissection, and spinal cord ischemia were 8.95, 9.01, 5.72, and 4.12%, respectively.

Conclusions: Although many novel stent grafts and techniques targeting zone 0 TEVAR are being investigated, a consensus on technique and device selection in zone 0 TEVAR is yet to be established in current practice. Furthermore, the post-operative stroke rate is relatively high, while other complication rates and perioperative death rate are comparable to those of TEVAR for other aortic zones.

KEYWORDS

zone 0 TEVAR, fenestrated TEVAR, chimney TEVAR, hybrid endovascular aortic repair, endograft, complications after TEVAR

1. Introduction

Thoracic endovascular aortic repair (TEVAR) has become a viable treatment option for thoracic aortic pathologies over the past years (1, 2). The proximal landing zone (PLZ) of the stent graft has been extended from the descending to the ascending aorta (zone 0) to ensure a sufficient and healthy PLZ. Following the development of surgical devices and improvement in supra-aortic vessels revascularization techniques, studies investigating the feasibility and safety of TEVAR with zone 0 landing have been conducted.

Unlike TEVAR for other aortic zones, zone 0 TEVAR lacks high-quality evidence to support its use. Studies on zone 0 TEVAR mostly comprise case reports, case series,

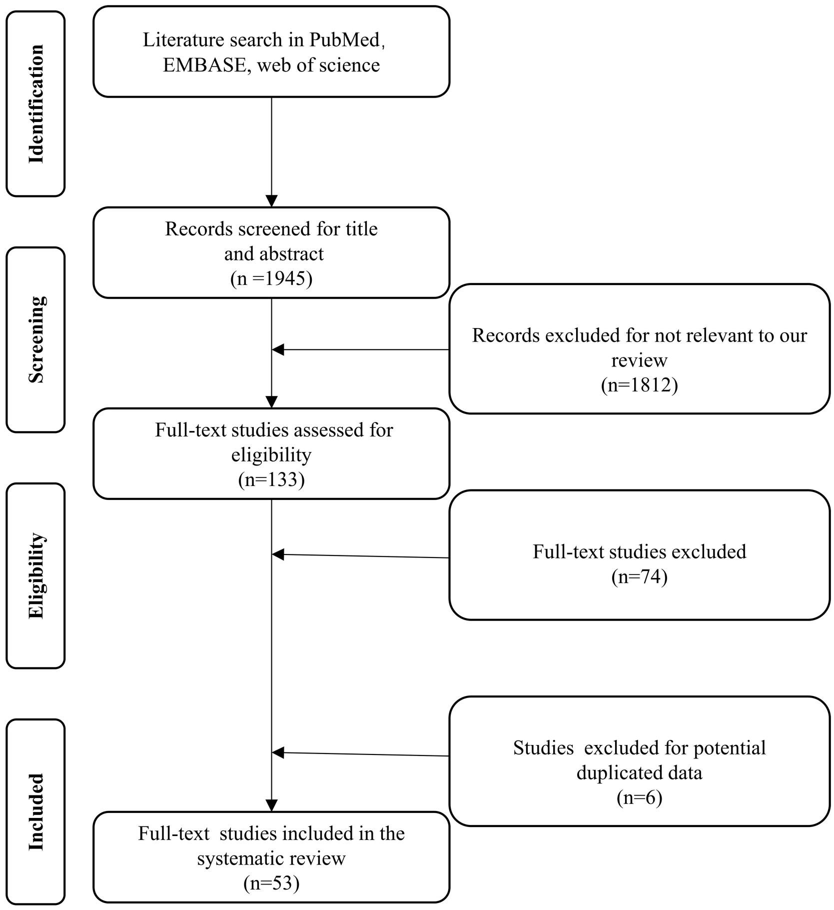

FIGURE 1
Preferred reporting items for systematic reviews and meta-analysis flow chart.

and retrospective studies. As no standard off-the-shelf stent grafts dedicated to zone 0 TEVAR are available, the safety, feasibility, and efficacy of zone 0 TEVAR with off-label use of thoracic or custom-made stent grafts are yet to be studied (3). Thus, a timely and comprehensive understanding of the safety and outcomes of zone 0 TEVAR is necessary before further promotion of its application. This systematic review and meta-analysis aimed to provide a comprehensive overview of the current application of zone 0 TEVAR, including its indications, stent grafts, procedures, and post-operative complications.

2. Methods

2.1. Search methodology

The systematic review conformed to the preferred reporting items for systematic review and meta-analyses statement standards (4). A search in PubMed, EMBASE, and Web of Science databases from January, 1997 to January, 2022 was made using set algorithms. The search algorithm in PubMed was "((((landing zone) AND (ascending aorta)) OR ('landing' [All Fields] AND 'zone' [All Fields] AND ('zone' [All Fields] AND '0' [All Fields]))) OR ('stent graft' [All Fields] AND ('zone' [All Fields] AND '0' [All Fields]))) OR ('endovascular' [All Fields] AND ('zone' [All Fields] AND '0' [All Fields]))." The search algorithm used for EMBASE was "1. TEVAR; 2. Zone 0; 3. Ascending aorta; 4. 2 OR 3; 5. 1 AND 4." The search algorithm in Web of Science was "((TS = (zone 0)) OR TS = (ascending aorta)) AND TS = (TEVAR)."

Abbreviations: TEVAR, Thoracic endovascular aortic repair; PLZ, Proximal landing zone; SCI, Spinal cord ischemia; RTAD, Retrograde type A aortic dissection; PAU, Penetrating atherosclerotic ulcer; IMH, Intramural hematoma; LSA, Left subclavian artery.

2.2. Inclusion and exclusion criteria

The studies included were published in English, containing zone 0 TEVAR, and clinical studies or cohort case reports. Studies containing only zone 0 TEVAR with prosthetic ascending aorta as the PLZ and studies, in which the reported number of cases of zone 0 TEVAR were <5, were excluded from the analysis.

TABLE 1 Detailed information in each manuscript ($N = 1{,}013$).

References	Publish date	Cases of zone 0 TEVAR	Recruitment period	Female	Male	Mean age	30-day/in-hospital death	30-day/in-hospital death rate
Kurimoto et al. (5)	2009/5/1	23	2001–2008	N/A	N/A	N/A	N/A	N/A
Chiesa et al. (6)	2010/2/1	24	1999–2009	3	21	73	3	12.50%
Holt et al. (7)	2010/6/1	9	2001–2009	3	6	64	1	11.11%
Geisbüsch et al. (8)	2010/6/1	10	1997–2009	2	8	65	1	10.00%
Canaud et al. (9)	2010/7/1	6	1998–2008	N/A	N/A	N/A	0	0.00%
Kolvenbach et al. (10)	2011/5/1	11	2008–2010	6	5	73	1	9.09%
Vallejo et al. (11)	2012/2/1	27	2002–2010	N/A	N/A	N/A	8	29.63%
Melissano et al. (12)	2012/3/1	32	1999–2011	N/A	N/A	N/A	3	9.38%
Fukui et al. (13)	2013/1/20	9	2007–2012	N/A	N/A	N/A	N/A	N/A
Preventza et al. (14)	2013/9/1	29	2005–2011	8	21	67	2	6.90%
Shirakawa et al. (15)	2014/2/1	30	1997–2012	1	21	74	1	3.33%
Bernardes et al. (16)	2014/7/1	7	2007–2012	4	3	59	1	14.29%
Roselli et al. (17)	2015/1/1	22	2006–2014	11	11	72	3	13.64%
Hiraoka et al. (18)	2015/1/1	7	2005–2013	N/A	N/A	N/A	5	71.43%
De Rango et al. (19)	2014/1/1	19	2005–2013	N/A	N/A	N/A	3	15.79%
Kurimoto et al. (20)	2015/7/1	37	2007–2013	8	29	78	0	0.00%
Gandet et al. (21)	2015/7/1	13	2001–2013	2	13	74	N/A	N/A
Cazavet et al. (22)	2016/1/1	17	2002–2014	N/A	N/A	N/A	N/A	N/A
Katada et al. (23)	2016/2/1	7	2012–2014	2	5	73	0	0.00%
Ziza et al. (24)	2016/6/1	17	1998–2013	N/A	N/A	N/A	3	17.65%
Tsilimparis et al. (25)	2016/6/1	10	2011–2014	5	5	67	0	0.00%
Böckler et al. (26)	2016/6/1	7	2009–2010	N/A	N/A	N/A	1	14.29%
Narita et al. (27)	2016/7/1	35	2008–2014	5	30	79	2	5.71%
Faure et al. (28)	2016/7/1	11	2005–2015	N/A	N/A	N/A	N/A	N/A
Yoshitake et al. (29)	2016/10/1	23	2011–2015	3	20	76	1	4.35%
Pecoraro et al. (30)	2017/6/1	26	2006–2015	9	17	72	2	7.69%
Canaud et al. (31)	2017/8/1	16	2013–2016	N/A	N/A	75	N/A	N/A
Wang et al. (32)	2017/10/1	22	2009–2016	2	20	61	0	0.00%
Roselli et al. (33)	2018/4/1	39	2006–2016	16	23	72	5	12.82%
Toya et al. (34)	2018/11/1	8	2015–2016	3	5	73	0	0.00%
Zhu et al. (35)	2019/1/1	5	2015–2017	N/A	N/A	N/A	N/A	N/A
Hosaka et al. (36)	2019/1/1	22	2009–2013	N/A	N/A	N/A	0	0.00%
Huang et al. (37)	2019/1/20	22	2012–2017	0	22	54	1	4.55%
Yamauchi et al. (38)	2019/3/1	7	2012–2017	N/A	N/A	N/A	N/A	N/A
Ryomoto et al. (39)	2019/8/1	9	2010–2017	N/A	N/A	N/A	N/A	N/A
Piffaretti et al. (40)	2019/11/1	6	2011–2015	3	3	69	N/A	N/A
Tsilimparis et al. (41)	2020/5/1	12	2011–2017	N/A	N/A	N/A	1	8.33%
De León et al. (42)	2020/6/27	60	2007–2015	N/A	N/A	N/A	N/A	N/A
Kuo et al. (43)	2020/9/1	13	2016–2017	4	9	64	0	0.00%
Tinelli et al. (44)	2020/10/1	6	2009–2018	N/A	N/A	N/A	1	16.67%

(Continued)

TABLE 1 (Continued)

References	Publish date	Cases of zone 0 TEVAR	Recruitment period	Female	Male	Mean age	30-day/in-hospital death	30-day/in-hospital death rate
Fernández-Alonso et al. (45)	2020/11/1	6	2014–2020	N/A	N/A	N/A	1	16.67%
Chassin-Trubert et al. (46)	2021/2/1	42	2004–2018	7	35	70	6	14.29%
Li et al. (47)	2021/3/1	43	2015–2019	14	29	64	0	0.00%
Planer et al. (48)	2021/3/4	28	N/A	6	22	72	2	7.14%
Dake et al. (49)	2021/6/1	8	N/A	1	7	73	2	25.00%
Seguchi et al. (50)	2021/6/25	7	2016–2019	1	6	83	0	0.00%
Li et al. (51)	2021/8/1	16	2009–2011	0	16	55	1	6.25%
Li et al. (52)	2021/8/24	37	2016–2019	7	30	70	2	5.41%
Hanna et al. (53)	2021/11/1	6	2009–2019	N/A	N/A	N/A	N/A	N/A
Barnes et al. (54)	2021/11/12	6	2011–2019	N/A	N/A	N/A	1	16.67%
Kudo et al. (55)	2021/11/20	40	2010–2020	12	28	79	1	2.50%
Chen et al. (56)	2021/12/29	51	2010–2019	N/A	N/A	N/A	0	0.00%
Eleshra et al. (57)	2022/1/31	8	2012–2016	1	7	70	1	12.50%

N/A, not available, which means the specific information was not available or could not be extracted from manuscripts; TEVAR, thoracic endovascular aortic repair.

TABLE 2 Aortic pathology in included studies ($N = 636$).

Pathologies	No. of cases (*n*, %)	
Aneurysm	347	54.56%
Dissection	214	33.65%
IMH	56	8.81%
PAU	10	1.57%
Kommerell's diverticulum	6	0.94%
Traumatic rupture of aorta	3	0.47%

PAU, penetrating atherosclerotic ulcer; IMH, intramural hematoma.

TABLE 3 Comorbidities in included studies.

Comorbidities	No. of cases (*n*, %)	
Smoking	164/373	43.97%
Diabetes	65/396	16.41%
Hypertension	352/442	79.64%
ASA > II	69/106	65.09%
CHF	25/147	17.01%
COPD	114/401	28.43%
Renal insufficiency	73/521	14.01%
CVD	99/545	18.17%
Dyslipidemia	90/213	42.25%
Peripheral vascular occlusive disease	44/217	20.28%
End-stage renal disease	5/77	6.49%
CAD	149/452	32.96%
Concomitant malignancy	15/56	26.79%
Connective tissue diseases	6/68	8.82%

ASA, American Society of Anesthesiologists classification; CHF, congestive heart failure; COPD, chronic obstructive pulmonary disease; CVD, cerebrovascular diseases; CAD, coronary artery disease.

2.3. Data extraction

Two researchers independently extracted data. The authors, publication date, study region, research type, number of cases, recruitment time, sex, age, 30-day/in-hospital mortality, 30-day/in-hospital mortality rate, pathology, stent graft, technique, and complications were retrieved from the eligible studies.

2.4. Statistical analysis

Data on stent graft, procedure and complications were summarized. Excel software (Microsoft Corp, Redmond, WA, USA) and Review Management 5.4 (The *Cochrane. Collaboration*, Oxford, UK) were used to record, analyze, conduct the meta-analysis, and tabulate clinical data. A meta-analysis was performed for perioperative mortality of zone 0 TEVAR and post-operative stroke, type Ia endoleak, spinal cord ischemia (SCI), and retrograde type A dissection (RTAD). Summary effect measures of post-operative complications and perioperative death rates were obtained by logarithmically pooling the data with an inverse variance-weighted fixed-effects model and presented with a 95% confidence interval (CI). Heterogeneity of the summary effects measures was assessed with the I^2 test and considered

TABLE 4 Stent graft category ($N = 554$).

Devices	No. of stent grafts (*n*, %)	
TAG/cTAG stent graft (Gore & Associates, AZ, USA)	215	38.81%
Valiant thoracic stent graft (Medtronic, MN, USA)	83	14.98%
Zenith TX1/TX2 (Cook Medical, IN, USA)	58	10.47%
Najuta thoracic stent graft system (Kawasumi Laboratories, Tokyo, Japan)	68	12.27%
RELAYendovascular thoracic stent graft (Terumo Aortic, FL, USA)	34	6.14%
Ankura thoracic stent graft (Lifetech Scientific, Shenzhen, China)	30	5.42%
NEXUS Aortic Arch Stent Graft System (Endospan, Herzlia, Israle)	29	5.32%
Castorstent (Microport Medical, Shanghai, China)	18	3.25%
Zenith ascending stent graft (Cook Medical, IN, USA)	10	1.81%
Thoracic Branch Endoprosthesis (Gore & Associates, AZ, USA)	8	1.44%
E-vita OPEN NEO hybrid stent graft system (Jotec, Hechingen, Germany)	1	0.18%

heterogeneous when I^2 was >50%. A 2-sided P-value of <0.05 was considered statistically significant.

3. Results

3.1. Study selection

A total of 1,812 studies were retrieved from PubMed, EMBASE, and Web of Science between January, 1997 and January, 2022. A total of 133 studies were considered eligible according to the inclusion criteria, of which 74 were excluded according to the exclusion criteria (Figure 1). Six studies were excluded because they were duplicates. Fifty-three studies, with a total number of 1,013 cases, were included in the final analysis (Table 1). The present study included 48 retrospective and 5 prospective studies.

3.2. Pathology and comorbidities

The type of aortic pathologies and comorbidities are summarized in Tables 2, 3, respectively. Indications for zone 0 TEVAR of 636 cases from 32 studies were disclosed, and included aneurysm (n = 347, 54.56%), aortic dissection

TABLE 5 Surgery details and LSA information ($N = 783$).

Surgeries	No. of cases (*n* %)		Preservation of LSA inflow*	No. of cases (*n* %)	
TEVAR without any modification or parallel stent technique + bypass/transposition of supra-aortic vessels	384	49.04%	Y	318	82.81%
			N	66	17.19%
TEVAR+chimney + bypass/debranching of supra-aortic vessels	75	9.58%	Y	71	94.67%
			N	4	5.33%
Fenestrated TEVAR + bypass/debranching of supra-aortic vessels	28	3.58%	Y	23	82.14%
			N	5	17.86%
Branched TEVAR + bypass/debranching of supra-aortic vessels	63	8.05%	Y	60	95.24%
			N	3	4.76%
Proximal scalloped TEVAR + bypass/debranching of supra-aortic vessels	15	1.92%	Y	14	93.33%
			N	1	6.67%
TEVAR only in ascending aorta	20	2.55%	Y	20	100.00%
			N	0	0.00%
Chimney TEVAR	24	3.07%	Y	5	20.83%
			N	19	79.17%
Fenestrated TEVAR	163	20.82%	Y	147	90.18%
			N	16	9.82%
Proximal scalloped and fenestrated TEVAR	11	1.40%	Y	6	54.55%
			N	5	45.45%

*The only intended covered supraarch artery without revascularization was LSA, when other branch arteries were invariably revascularized. LSA, left subclavian artery; TEVAR, thoracic endovascular aortic repair.

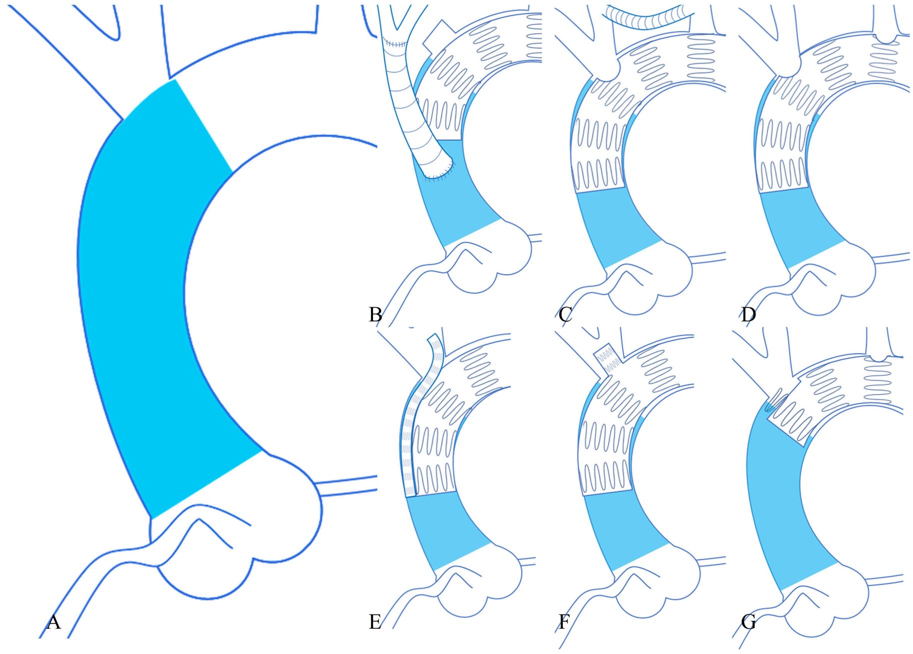

FIGURE 2
Six techniques used in zone 0 TEVAR. **(A)** (Left larger image) the area of zone 0 (blue). **(B)** (Upper left) TEVAR + debranching procedure. **(C)** (Upper middle) TEVAR + bypass procedure. **(D)** (Upper right) fenestrated TEVAR. **(E)** (Lower left) chimney TEVAR. **(F)** (Lower middle) branched TEVAR. **(G)** (Lower right) proximal scalloped and fenestrated TEVAR. TEVAR, thoracic endovascular aortic repair.

(n = 214, 33.65%), intramural hematoma (n = 56, 8.81%), penetrating atherosclerotic ulcer (n = 10, 1.57%), Kommerell's diverticulum (n = 6, 0.94%), and traumatic aortic rupture (n = 3, 0.47%).

3.3. Stent graft

Stent grafts used in zone 0 TEVAR are summarized in Table 4. A total of 554 stent grafts from 25 studies were analyzed. The most frequently used stent graft in zone 0 TEVAR was TAG/c-TAG stent graft (W.L. Gore and Associates, AZ, USA) (n = 215, 38.81%) followed by Valiant thoracic stent graft (Medtronic, MN, USA) (n = 83, 14.98%), Zenith TX1/TX2 (Cook Medical, IN, USA) (n = 58, 12.27%), Najuta (Kawasumi Laboratories, Tokyo, Japan) (n = 68, 12.27%), RELAY endovascular thoracic stent graft (Terumo Aortic, FL, USA) (n = 34, 6.14%), Ankura thoracic stent graft (Lifetech Scientific, Shenzhen, China) (n = 30, 5.42%), *NEXUS* Aortic Arch *Stent* Graft System (Endospan, Herzlia, Israel) (n = 29, 5.32%), Castor (Microport Medical, Shanghai, China) (n = 18, 3.25%), Thoracic Branch Endoprosthesis (Gore & Associates, AZ, USA) (n = 8, 1.44%), Zenith ascending stent graft (Cook Medical, IN, USA) (n = 10, 1.81%), and E-vita (Jotec, Hechingen, Germany) (n = 1, 0.18%). In 337 (60.83%) cases, stent grafts had a proximal bare-metal portion. Three novel stent grafts dedicated to zone 0 TEVAR had been introduced in the reviewed studies (25, 34, 48). Zenith ascending stent graft is aimed at the ascending aorta and has no branches or fenestrations for supra-aortic vessels. Najuta thoracic stent graft system is a fenestrated stent graft with one to three fenestrations, which can preserve all supra-aortic vessels. *NEXUS* Aortic Arch *Stent* Graft System is a novel single branch, two stent graft system used for endovascular aortic arch repair.

3.4. Procedure

The procedures performed in 783 cases from 46 studies were classified as following: 1. TEVAR without any modification or parallel stent technique + bypass/debranching of supraaortic vessels (n = 384, 49.04%); 2. TEVAR + chimney + bypass/debranching of supraaortic vessels (n = 75, 9.58%); 3. fenestrated TEVAR + bypass/debranching of supraaortic vessels (n = 28, 3.58%); 4. branched TEVAR + bypass/debranching of supraaortic vessels (n = 63, 8.05%); 5. proximal scalloped TEVAR + bypass/debranching of supraaortic vessels (n = 15, 1.92%); 6. TEVAR only in ascending aorta (n = 20, 2.55%); 7. chimney TEVAR (n = 24, 3.07%); 8. fenestrated TEVAR (n = 163, 20.82%); and 9. proximal scalloped and fenestrated TEVAR (n = 11, 1.40%) (Table 5). Figure 2 illustrates the techniques used in zone 0 TEVAR. Out of the 783 cases, the inflow of the left subclavian artery (LSA) was preserved in 642 (81.99%) cases. Among the 191 cases treated with fenestrated TEVAR, pre-operative fenestrations were used in 44 (23.04%), back table fenestrations in 93 (48.69%), laser-*in situ* fenestrations in 43 (22.51%), and needle-*in situ* fenestrations in 9 (4.71%) cases, while fenestration techniques were not disclosed in 2 (1.05%) cases.

Study	Death rate	SE	Weight	Death rate, Fixed, 95%CI
Barnes 2021	0.1667	0.152157	0.5%	0.1667 [-0.1315, 0.4649]
Bernardes 2014	0.1429	0.132277	0.6%	0.1429 [-0.1164, 0.4022]
Böckler 2016	0.1429	0.132277	0.6%	0.1429 [-0.1164, 0.4022]
Canaud 2010	0	0		Not estimable
Chassin-Trubert 2021	0.1429	0.054002	3.7%	0.1429 [0.0371, 0.2487]
Chen 2021	0	0		Not estimable
Chiesa 2010	0.125	0.067508	2.4%	0.1250 [-0.0073, 0.2573]
Dake 2021	0.25	0.153093	0.5%	0.2500 [-0.0501, 0.5501]
De Rango 2014	0.1579	0.083656	1.5%	0.1579 [-0.0061, 0.3219]
Eleshra 2022	0.125	0.116927	0.8%	0.1250 [-0.1042, 0.3542]
Fernández-Alonso 2020	0.1667	0.152157	0.5%	0.1667 [-0.1315, 0.4649]
Geisbüsch 2010	0.1	0.094868	1.2%	0.1000 [-0.0859, 0.2859]
Hiraoka 2015	0.7143	0.170744	0.4%	0.7143 [0.3796, 1.0490]
Holt 2010	0.1111	0.104752	1.0%	0.1111 [-0.0942, 0.3164]
Hosaka 2019	0	0		Not estimable
Huang 2019	0.0455	0.044431	5.5%	0.0455 [-0.0416, 0.1326]
Katada 2016	0	0		Not estimable
Kolvenbach 2011	0.0909	0.086675	1.4%	0.0909 [-0.0790, 0.2608]
Kudo 2021	0.025	0.024686	17.7%	0.0250 [-0.0234, 0.0734]
Kuo 2020	0	0		Not estimable
Kurimoto 2015	0	0		Not estimable
Li F 2021	0	0		Not estimable
Li X 2021	0.0625	0.060515	2.9%	0.0625 [-0.0561, 0.1811]
Li X 2021	0.0541	0.03719	7.8%	0.0541 [-0.0188, 0.1270]
Melissano 2012	0.0938	0.051539	4.1%	0.0938 [-0.0072, 0.1948]
Narita 2016	0.0571	0.039221	7.0%	0.0571 [-0.0198, 0.1340]
Pecoraro 2017	0.0769	0.052252	4.0%	0.0769 [-0.0255, 0.1793]
Planer 2021	0.0714	0.048661	4.6%	0.0714 [-0.0240, 0.1668]
Preventza 2013	0.069	0.047065	4.9%	0.0690 [-0.0232, 0.1612]
Roselli 2015	0.1364	0.073173	2.0%	0.1364 [-0.0070, 0.2798]
Roselli 2018	0.1282	0.053533	3.8%	0.1282 [0.0233, 0.2331]
Seguchi 2021	0	0		Not estimable
Shirakawa 2014	0.0333	0.032757	10.1%	0.0333 [-0.0309, 0.0975]
Tinelli 2020	0.1667	0.152157	0.5%	0.1667 [-0.1315, 0.4649]
Toya 2018	0	0		Not estimable
Tsilimparis 2016	0	0		Not estimable
Tsilimparis 2020	0.0833	0.079771	1.7%	0.0833 [-0.0730, 0.2396]
Vallejo 2012	0.2963	0.087878	1.4%	0.2963 [0.1241, 0.4685]
Wang 2017	0	0		Not estimable
Yoshitake 2016	0.0435	0.042533	6.0%	0.0435 [-0.0399, 0.1269]
Ziza 2016	0.1765	0.092465	1.3%	0.1765 [-0.0047, 0.3577]
Total (95% CI)			**100.0%**	**0.0749 [0.0545, 0.0952]**

Heterogeneity: Chi² = 37.14, df = 29 (P = 0.14); I² = 22%
Test for overall effect: Z = 7.21 (P < 0.00001)

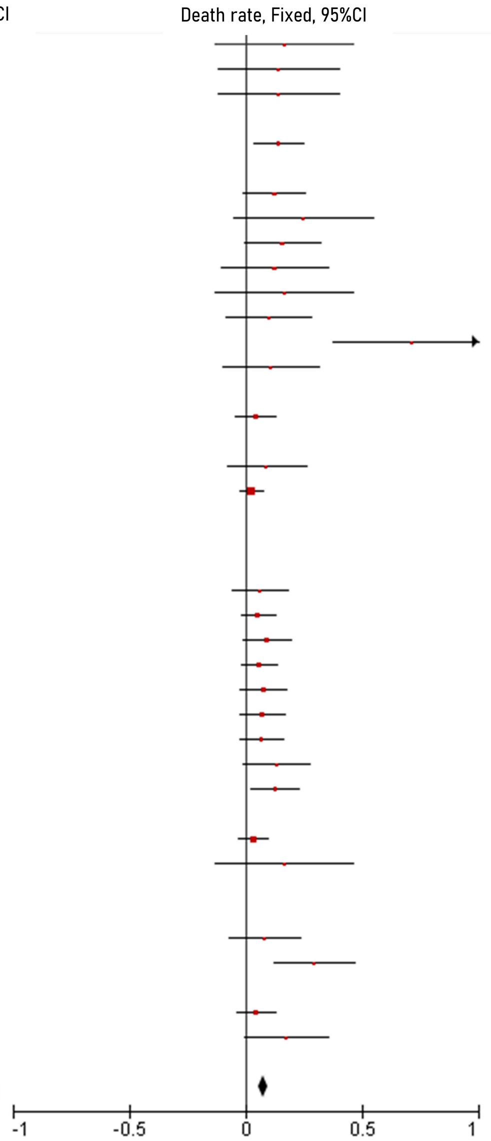

FIGURE 3
Forest plot shows the fixed-effects proportion meta-analysis for perioperative death rate. CI, confidence interval; SE, standard error.

3.5. Perioperative mortality and post-operative complications

The pooled 30-day/in-hospital death rate was 7.49% (95% CI, 5.45–9.52, $P < 0.00001$, $I^2 = 22\%$, Figure 3). Data on the causes, characteristics, and outcomes of stroke, SCI, type Ia endoleak, and RTAD were collected, and the incidences were obtained by logarithmically pooling the data with an inverse variance-weighted fixed-effects model. The most common post-operative complication was stroke (8.95%, 95% CI, 6.44–11.46, $P < 0.00001$, $I^2 = 46\%$, Figure 4), followed by type Ia endoleak (9.01%, 95% CI, 5.77–12.25, $P < 0.00001$, $I^2 = 35\%$, Figure 5), RTAD (5.72%, 95% CI, 2.67–8.77, $P = 0.0002$, $I^2 = 0\%$, Figure 6), and SCI (4.12%, 95% CI, 1.89–6.35, $P = 0.0003$, $I^2 = 0\%$, Figure 7).

The causes and outcomes of stroke in 26 studies are presented in Table 6. Causes were disclosed in 11 studies, and outcomes were disclosed in 16 studies. Atherosclerotic plaque was considered the principal cause of stroke in six studies (12, 18, 26, 29, 45, 55). Other possible causes suggested by the authors included migration and compression of chimney stents, LSA dissection, debranching of LSA, and lower left ventricular ejection fraction (27, 32, 39, 44). Based on available data, it appears that stroke was the cause of death in 12 of the 65 patients who suffered from this complication (6, 14, 18, 26, 37, 44, 45).

Causes and outcomes of type Ia endoleak in 11 studies are shown in Table 7. Causes were disclosed in seven studies, while outcomes were disclosed in eight studies. Migration of stent graft was considered the principal cause of type Ia endoleak in three studies (16, 28, 37). Other possible causes suggested by the

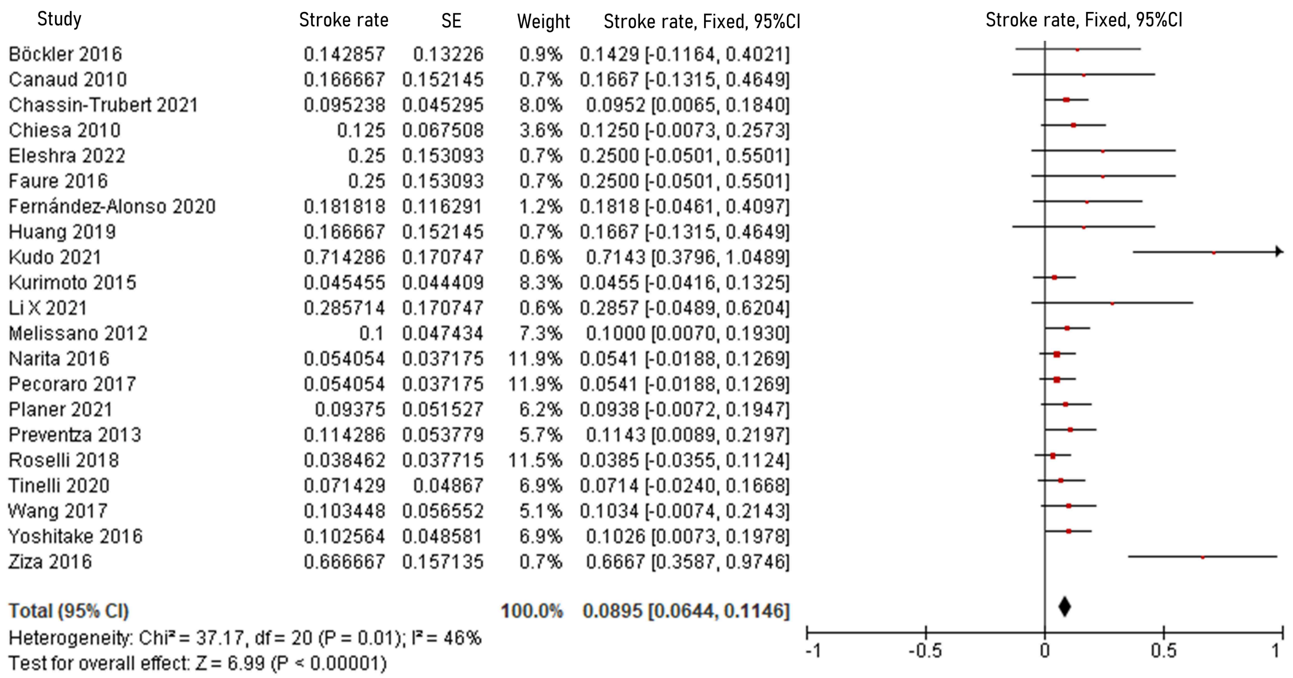

FIGURE 4
Forest plot showing the fixed-effects proportion meta-analysis for post-operative stroke rate. CI, confidence interval; SE, standard error.

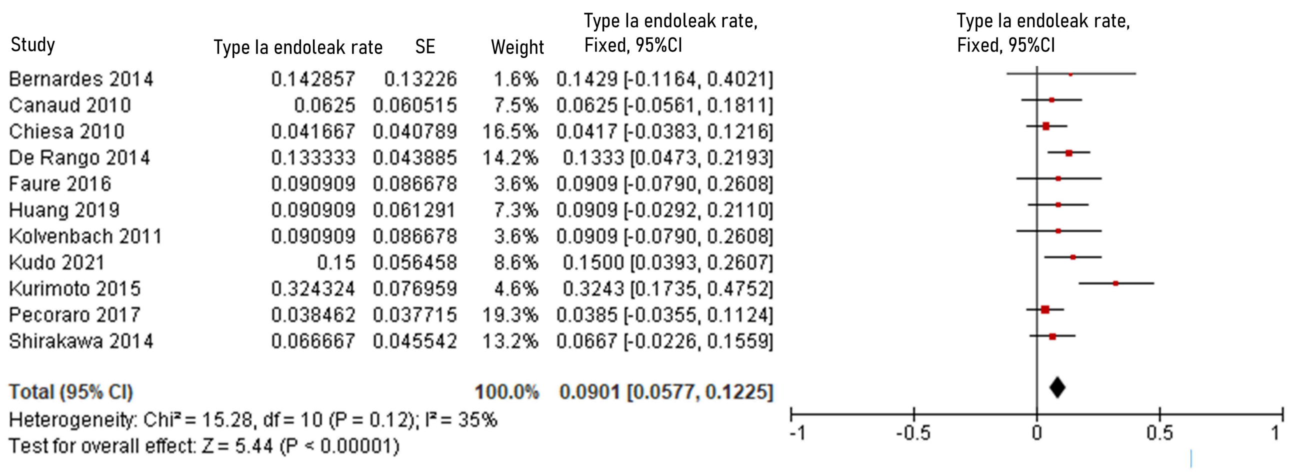

FIGURE 5
Forest plot showing the fixed-effects proportion meta-analysis for type Ia endoleak rate. CI, confidence interval; SE, standard error.

authors included aneurysmal evolution of aorta, unfavorable stent placement, gutter leakage between the main stent graft and chimney stent, short distance between the ostium of innominate artery and the aneurysm, lack of comfortability of Najuta stent prototype, and short proximal neck length (10, 20, 31, 37, 55). Based on available data, 17 of the 36 patients who presented with type Ia endoleak were treated conservatively, while in 5 patients type Ia endoleak lead to aneurysm enlargement, which ruptured and caused death in 1 patient (6, 10, 15, 20, 28, 30, 42).

Tables 8, 9 show the causes and outcomes of SCI and RTAD in 11 and 9 studies, respectively. One study suggested that SCI might have been caused by LSA coverage and long extent of aortic coverage (20). Outcomes of SCI were disclosed in 10 studies. Three out of 15 SCI patient were left with long-term sequelae (20, 30). Causes of RTAD were disclosed in seven studies, and outcomes were disclosed in nine studies, with clamp injury in hybrid procedure being considered the principal cause in four manuscripts (9, 21, 27, 46). An acute angle formed by the ascending aorta and PLZ, lack of conformability of the COOK TX2 stent graft in zone 0, primary disease progression, >30% oversizing of the stent graft, angulation of the proximal aortic arch >120° and stent graft diameter >42 mm have also been suggested as possible causes

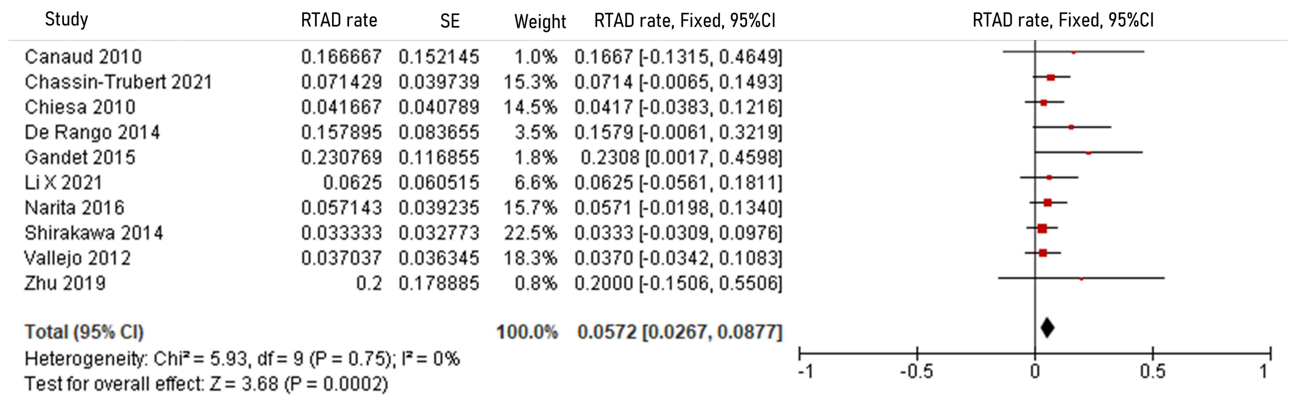

FIGURE 6
Forest plot showing the fixed-effects proportion meta-analysis for RTAD rate. CI, confidence interval; SE, standard error; RTAD, retrograde type A dissection.

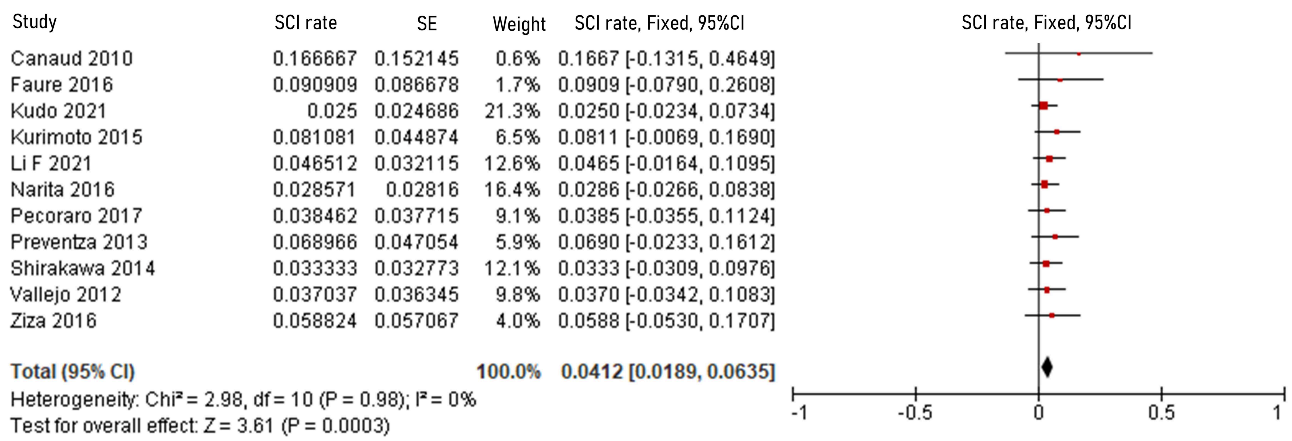

FIGURE 7
Forest plot showing the fixed-effects proportion meta-analysis for RTAD rate. CI, confidence interval; SE, standard error; RTAD, retrograde type A dissection.

of RTAD (21, 35, 51). Four patients died of complications related to RTAD, and based on the available data eight out of 17 patients received reintervention (6, 9, 15, 19, 21, 46).

4. Discussion

To meet the challenges posed by the lack of dedicated stent grafts for zone 0 TEVAR, numerous procedures and novel devices have been developed. Techniques range from hybrid surgery to fenestrated, chimney, and branched TEVAR, while newer devices try to provide simpler and safer procedures. According to the reviewed studies, no clear protocol was shown regarding the selection technique or device for zone 0 TEVAR.

Stroke is the most common post-operative complication after zone 0 TEVAR (8.95%). Two meta-analyses of TEVAR for descending thoracic aortic diseases performed by Karaolanis et al. and Allmen et al. suggested that stroke rates in TEVAR for descending aortic aneurysm and type B dissection were 4.1 and 4.4%, respectively, lower than those in zone 0 TEVAR (58, 59). A meta-analysis from 2019 involving 989 patients undergoing total arch replacement with frozen elephant trunk also showed a lower stroke rate (8.95 vs. 2.38%) (60). Six authors suggested detachment of atherosclerotic plaque debris in the aortic arch, induced by manipulation of the guide-wire or stent graft delivery system was the cause of stroke (12, 18, 26, 29, 45, 55). Three authors suggested that the occlusion of supra-aortic vessels owing to migration or compression of stents, and the dissection of supra-aortic vessels could be a further cause (24, 32, 44). Other possible causes included prolonged procedural time, lower left ventricular ejection fraction, and increased blood loss (27, 39). While no author in reviewed studies attributed stroke to planned LSA coverage without revascularization, the meta-analysis made by Chen et al. and Karaolanis et al. reported a significant reduction in stroke rate when the covered LSA had been revascularized (59, 61). However, the stroke rate in the planned LSA coverage without revascularization remains unknown in reviewed studies. To prevent stroke, some authors introduced procedures such as mini-cardiopulmonary bypass support and temporary inflow blockage of branch vessels (39, 50). The principal goal of these

TABLE 6 Possible causes and outcomes of strokes in included studies.

References	Stroke cases/total cases in the articles %		Possible causes	Outcomes
Pecoraro et al. (30)	1/26[a]	3.85%	Not available	1 recovered spontaneously
Huang et al. (37)	1/22[a]	4.55%	Not available	1 dead due to stroke
Kurimoto et al. (20)	2/37[b]	5.41%	Not available	Not available
Li et al. (52)	2/37[a]	5.41%	Not available	1 dead due to cardiac attack 1 dead due to severe pulmonary infection
Planer et al. (48)	2/28[b]	7.14%	Not available	2 recovered with minor sequalae
Wang et al. (32)	2/22[a]	9.09%	Migration of chimney stents Compression of chimney stents	2 recovered by additional stent placement*
Melissano et al. (12)	3/32[a]	9.38%	Atherosclerotic plaques in the aortic arch	Not available
Chassin-Trubert et al. (46)	4/42[b]	9.52%	Not available	Not available
Kudo et al. (55)	4/40[a]	10.00%	Atherosclerotic plaques in the aortic arch	Not available
Roselli et al. (33)	4/39[a]	10.26%	Not available	1 dead due to unknown reason
Preventza et al. (14)	3/29[a]	10.34%	Not available	1 deaddue to stroke 2 recovered
Narita et al. (27)	4/35[a]	11.43%	Prolonged procedural time Increased blood loss	2 dead due to unmentioned reason
Chiesa et al. (6)	3/24[a]	12.50%	Not available	3 dead due to stroke
Böckler et al. (26)	1/7[a]	14.29%	Atherosclerotic plaques in the aortic arch	1 dead due to stroke
Canaud et al. (9)	1/6[a]	16.67%	Not available	Not available
Fernández-Alonso et al. (45)	1/6[a]	16.67%	Atherosclerotic plaques in the aortic arch	1 dead due to stroke
Tinelli et al. (44)	1/6[a]	16.67%	LSA dissection	1 dead due to stroke
Yoshitake et al. (29)	4/23[a]	17.39%	Atherosclerotic plaques	3 dead due to COPD, cancer, pneumonia
Ziza et al. (24)	3/17[a]	17.65%	Supra-arch vessels dissection	Not available
Faure et al. (28)	2/11[a]	18.18%	Not available	Not available
Eleshra et al. (57)	2/8[a]	25.00%	Not available	Not available
Dake et al. (49)	2/8[b]	25.00%	Not available	1 dead due to other pathologies
Katada et al. (23)	2/7[a]	28.57%	Not available	2 sustaining grade III focal neurologic deficits
Hiraoka et al. (18)	5/7[a]	71.43%	Atherosclerotic plaques in the aortic arch	4 dead due to stroke
Ryomoto et al. (39)	6/9[a]	66.67%	Prolonged procedural time Lower left ventricular ejection fraction	Not available

[a]Perioperative (30-day) stroke.
[b]Late (≥30-day) stroke.
*The stroke was discovered immediately after operation. LSA, left subclavian artery; COPD, chronic obstructive pulmonary diseases.

interventions is to prevent atheromatous debris from accessing the cerebral blood supply. Given 8.95% stroke rate and 18.46% (12/65) stroke-related death in the review, post-operative stroke prevention must be considered more when planning zone 0 TEVAR (6, 14, 18, 26, 37, 44, 45).

The incidence of type Ia endoleak in zone 0 TEVAR is 9.01% in the review. That is slightly lower than that (10.07%) reported in the multicenter study, involving 1, 18, 43, 55, and 22 cases of zone 0, 1, 2, 3, 4 TEVAR, conducted by Hammo et al. (62) in 2019. In the aortic arch, the varied lengths of the outer and inner curves pose a barrier to the stent graft's stability. This leads a bird-beak configuration after TEVAR increasing the risk of type Ia endoleak. However, Kudo et al. (63) proposed that bird-beak configuration did not occur during the early or late periods after zone 0 TEVAR. Causes suggested by the authors include migration, unfavorable deployment, and lack of flexibility of the stent graft (10, 16, 20, 28, 37). Reinterventions, including open or endovascular surgery, are appropriate treatments for endoleak (20, 42). De

TABLE 7 Possible causes and outcomes of type Ia endoleaks in included studies.

References	Type Ia endoleak cases/Total casesin the articles %		Possible causes	Outcomes
Pecoraro et al. (30)	1/26[a]	3.85%	Not available	1 under surveillance without reintervention
Chiesa et al. (6)	1/24[a]	4.17%	Not available	Resolved spontaneously
Canaud et al. (9)	1/16[b]	6.25%	Aneurysmal evolution of aorta	1 dead due to aneurysm rupture
Shirakawa et al. (15)	2/30[a]	6.67%	Not available	2 under surveillance without reintervention
Kolvenbach et al. (10)	1/11[a]	9.09%	Unfavorable stent placement	1 under surveillance without reintervention
Faure et al. (28)	1/11[a]	9.09%	Migration of stentgraft	1 under surveillance without reintervention
Huang et al. (37)	2/22[a]	9.09%	Migration of stentgraft Aneurysmal evolution of aorta	Not available
De León et al. (42)	8/60[a]	13.33%	Not available	6 recovered spontaneously 2 resolved surgically
Bernardes et al. (16)	1/7[a]	14.29%	Migration of stentgraft	Not available
Kudo et al. (55)	6/40[a]	15.00%	Gutter leakage between the main stent graft and chimney ste Short distance between the ostium of innominate artery and the aneurysm	Not available
Kurimoto et al. (20)	12/37[a]	32.43%	Lack of comfortability of Najuta stent prototype Short proximal neck length	4 resolved by undergoing reinterventions because of aneurysm enlargement 2 dead due to pneumonia 6 under surveillance without reintervention

[a]Perioperative (30-day) type Ia endoleak.
[b]Late (≥30-day) type Ia endoleak.

TABLE 8 Possible causes and outcomes of SCIs in included studies.

References	SCI cases/total cases in the articles %		Possible causes	Outcomes
Kudo et al. (55)	1/40[a]	2.50%	Not available	Not available
Narita et al. (27)	1/35[a]	2.86%	Not available	1 recovered after cerebrospinal fluid drainage
Shirakawa et al. (15)	1/30[a]	3.33%	Not available	1 dead due to other reasons
Vallejo et al. (11)	1/27[a]	3.70%	Not available	1 dead due to other reasons
Pecoraro et al. (30)	1/26[a]	3.85%	Not available	1 dead due to respiratory insufficiency and spinal cord ischemia
Li et al. (47)	2/43[a]	4.65%	Not available	2 recovered after cerebrospinal fluid drainage
Ziza et al. (24)	1/17[a]	5.88%	Not available	1 recovered after cerebrospinal fluid drainage
Preventza et al. (14)	2/29[a]	6.90%	Not available	1 recovered after cerebrospinal fluid drainage 1 partial recovered after cerebrospinal fluid drainage
Kurimoto et al. (20)	3/37[a]	8.11%	Long extent of aortic coverage*	1 recovered after cerebrospinal fluid drainage 1 permanent paraplegias 1 paraparesis
Faure et al. (28)	1/11[a]	9.09%	Not available	1 recovery after cerebrospinal fluid drainage
Canaud et al. (9)	1/6[a]	16.67%	Not available	1 recovery after cerebrospinal fluid drainage

[a]Perioperative (30-day) SCI.
*The covered areas of the stent grafts were from ascending aorta to levels of Th 6, Th 8, and Th 10, respectively. SCI, spinal cord ischemia; LSA, left subclavian artery.

León et al. (42) classified type Ia endoleak as "fast" and "slow" based on the time needed to visualize the aneurysmal sac during arteriogram. Based on their observation, they postulated that slow endoleak tends to resolve naturally within 1 year after TEVAR. Of 36 patients with type Ia endoleak, one died of aneurysm rupture and 7 resolved spontaneously indicating that active surveillance and timely treatment can lead to favorable results in selected cases (6, 9, 42).

The incidence of SCI is 4.12% in zone 0 TEVAR, near to that (4.5%) reported by Uchida, which included 7,309 patients treated by TEVAR in 2014 (64). There were no concrete explanations for SCI or risk factors in the reviewed studies. In theory, sacrifice of

TABLE 9 Possible causes and outcomes of RTADs in included studies.

References	RTAD cases/total cases in the articles %		Possible causes	Outcomes
Shirakawa et al. (15)	1/30[a]	3.33%	Debranching procedures	1 recovered surgically
Vallejo et al. (11)	1/27[a]	3.70%	Not available	1 treated medically and stable
Chiesa et al. (6)	1//24[b]	4.17%	Not available	1 recovered surgically
Chassin-Trubert et al. (46)	3/42[a]	7.14%	Clamp injury in hybrid procedure	2 immediate ascending aortic replacement 1 dead due to RTAD
Narita et al. (27)	2/35[a]	5.71%	Clamp injury in hybrid procedure	2 managed conservatively
Li et al. (51)	1/16[a]	6.25%	Ascending aorta and proximal landing zone of stent graft in an acute angle	1 dead due to pericardial effusion
De Rango et al. (19)	3/19[a]	15.79%	Not available	2 dead due to RTAD 1 recovered surgically
Canaud et al. (9)	1/6[a]	16.67%	Clamp injury in hybrid procedure	1 immediate ascending aortic replacement
Zhu et al. (35)	1/5[a]	20.00%	Lack of conformability of the COOK TX2 stent graft in zone 0 Primary disease progression	Not available
Gandet et al. (21)	3/13[a]	23.08%	Clamp injury in hybrid procedure Oversizing of stentgraft >30% Angulation of proximal aortic arch >120° Diameter of stentgraft >42 mm	2 recovered surgically 1 dead due to RTAD

[a]Perioperative (30-day) RTAD.
[b]Late (≥30-day) RTAD. RTAD, retrograde type A dissection.

LSA inflow is a risk factor for SCI; however, absence of detailed information impeded analysis in this review. In this review, only one SCI patient had their LSA covered without revascularization (20). Nonetheless, previous studies have suggested that LSA revascularization in selected patients might prevent SCI (34). Authors also provided other preventive procedures including prophylactic cerebrospinal fluid drainage and maintenance of higher mean arterial pressure (18, 34). In this review, 8 cases of SCI were successfully treated with cerebrospinal fluid drainage. Only one case of permanent paraplegia was recorded, in a patient implanted with a long aortic stent, with LSA coverage (20).

The rate of post-operative RTAD in the present review is 5.72%, lower than that reported by Chen et al. in their meta-analysis. Their study, conducted in 2018, highlighted the higher risk of RTAD in zone 0 TEVAR compared to zones 1, 2, 3, and 4 (8.12 vs. 2.57, 2.66, 0.67,% and 0.67%, respectively) (65). The anatomy of the arch and lack of comfort with newer stent grafts might contribute to the high rate of RTAD in zone 0 TEVAR. In four reviewed studies, RTAD patients had undergone hybrid procedures, and the leading cause suggested by the authors was clamp injury while debranching or bypassing branch vessels (9, 21, 27, 46). Oversizing of the stent graft, a large diameter of the stent graft, and an acute angle formed by the ascending aorta and PLZ contribute to RTAD according to some authors (21, 51). Although previous studies suggested proximal bare-metal configuration as a risk factor for RTAD, this configuration was present in 60.56% of cases in the reviewed studies and did not correlate with the rate of RTAD (65, 66). Prevention of RTAD mainly focuses on pre-operative planning and stent graft design. Chassin-Trubert et al. (46) suggested that, in selected hybrid procedures, rapid right ventricular pacing might decrease the risk of RTAD following zone 0 TEVAR. Given the 4/17 (23.5%) related-death rate and 8/17 (47.0%) reintervention rate, surgeons should consider reintervention as soon as RTAD is discovered (6, 9, 15, 19, 21, 46).

In the present review, the overall 30-day/in-hospital death rate of zone 0 TEVAR is 7.49%, close to that reported for all zone TEVAR (8.07%) in a systematic review by Ramdass in 2015 (67). But it exceeds the rates after TEVAR for descending thoracic aortic disease, as shown by Naazie in 2022 and Harris in 2020 (4.2% in 2,141 patients and 4.0% in 1,784 patients, respectively) (68, 69). If arch disease is taken into account, the 30-day rate of death in this review is lower than that reported for frozen elephant trunk in a multicenter study by Leone (437 patients, 14.9%), and higher than that reported for open total arch replacement in a meta-analysis performed in 2016 (2,880 patients, 5.3%) (70, 71).

The present meta-analysis and systemic review shows some limitations. First, most studies were conducted in a single center and lacked specific clinical data on individual patients. Second, most of the reviewed studies focused on one or two techniques, leading significant reporting biases. Finally, the recruitment time in reviewed studies with high heterogeneity inhibited further analysis of yearly trends. Consequently, to obtain a complete picture of zone 0 TEVAR, more exhaustive investigations on zone 0 TEVAR are required in the future.

5. Conclusion

Despite the absence of stent grafts dedicated for zone 0 TEVAR, novel stent grafts and various techniques targeting zone 0 TEVAR are currently being investigated and developed. However, there is still no consensus on technique and device selection for zone 0 TEVAR in current practice. Furthermore, the post-operative stroke rate is relatively high, while other complications and perioperative death rate are comparable to those of TEVAR for other aortic zones.

The small number of studies aimed at zone 0 TEVAR calls for more comprehensive and detailed clinical studies to improve the informed decision-making in patients who may benefit from zone 0 TEVAR.

Data availability statement

The original contributions presented in the study are included in the article/supplementary material, further inquiries can be directed to the corresponding author.

Author contributions

XL and LZ contributed to conception and design of the study, organized the data extraction and statistical analysis, and wrote sections of the manuscript. LZ wrote the first draft of the manuscript. All authors contributed to manuscript revision, read, and approved the submitted version.

Conflict of interest

The authors declare that the research was conducted in the absence of any commercial or financial relationships that could be construed as a potential conflict of interest.

Publisher's note

All claims expressed in this article are solely those of the authors and do not necessarily represent those of their affiliated organizations, or those of the publisher, the editors and the reviewers. Any product that may be evaluated in this article, or claim that may be made by its manufacturer, is not guaranteed or endorsed by the publisher.

References

1. Manetta F, Newman J, Mattia A. Indications for thoracic endovascular aortic repair (TEVAR): a brief review. *Int J Angiol.* (2018) 27:177–84. doi: 10.1055/s-0038-1666972

2. Baikoussis NG, Antonopoulos CN, Papakonstantinou NA, Argiriou M, Geroulakos G. Endovascular stent grafting for ascending aorta diseases. *J Vasc Surg.* (2017) 66:1587–601. doi: 10.1016/j.jvs.2017.07.064

3. Muetterties CE, Menon R, Wheatley GR. A systematic review of primary endovascular repair of the ascending aorta. *J Vasc Surg.* (2018) 67:332–42. doi: 10.1016/j.jvs.2017.06.099

4. Page MJ, McKenzie JE, Bossuyt PM, Boutron I, Hoffmann TC, Mulrow CD, et al. The PRISMA 2020 statement: an updated guideline for reporting systematic reviews. *BMJ.* (2021) 372:n71. doi: 10.1136/bmj.n71

5. Kurimoto Y, Kawaharada N, Ito T, Baba T, Ohori S, Watanabe A, et al. Less-invasive management of left subclavian artery in stent-grafting for distal aortic arch disease. *Interact Cardiovasc Thorac Surg.* (2009) 8:548–52. doi: 10.1510/icvts.2008.192484

6. Chiesa R, Melissano G, Tshomba Y, Civilini E, Marone EM, Bertoglio L, et al. Ten years of endovascular aortic arch repair. *J Endovasc Ther.* (2010) 17:1–11. doi: 10.1583/09-2884.1

7. Holt PJ, Johnson C, Hinchliffe RJ, Morgan R, Jahingiri M, Loftus IM, et al. Outcomes of the endovascular management of aortic arch aneurysm: implications for management of the left subclavian artery. *J Vasc Surg.* (2010) 51:1329–38. doi: 10.1016/j.jvs.2009.10.131

8. Geisbüsch P, Kotelis D, Hyhlik-Dürr A, Hakimi M, Attigah N, Böckler D. Endografting in the aortic arch - does the proximal landing zone influence outcome? *Eur J Vasc Endovasc Surg.* (2010) 39:693–9. doi: 10.1016/j.ejvs.2010.03.018

9. Canaud L, Hireche K, Berthet JP, Branchereau P, Marty-Ané C, Alric P. Endovascular repair of aortic arch lesions in high-risk patients or after previous aortic surgery: midterm results. *J Thorac Cardiovasc Surg.* (2010) 140:52–8. doi: 10.1016/j.jtcvs.2009.09.022

10. Kolvenbach RR, Karmeli R, Pinter LS, Zhu Y, Lin F, Wassiljew S, et al. Endovascular management of ascending aortic pathology. *J Vasc Surg.* (2011) 53:1431–7. doi: 10.1016/j.jvs.2010.10.133

11. Vallejo N, Rodriguez-Lopez JA, Heidari P, Wheatley G, Caparrelli D, Ramaiah V, et al. Hybrid repair of thoracic aortic lesions for zone 0 and 1 in high-risk patients. *J Vasc Surg.* (2012) 55:318–25. doi: 10.1016/j.jvs.2011.08.042

12. Melissano G, Tshomba Y, Bertoglio L, Rinaldi E, Chiesa R. Analysis of stroke after TEVAR involving the aortic arch. *Eur J Vasc Endovasc Surg.* (2012) 43:269–75. doi: 10.1016/j.ejvs.2011.12.009

13. Fukui D, Wada Y, Komatsu K, Fujii T, Ohashi N, Terasaki T, et al. Innovative application of available stent grafts in Japan in aortic aneurysm treatment-significance of innovative debranching and chimney method and coil embolization procedure. *Ann Vasc Dis.* (2013) 6:601–11. doi: 10.3400/avd.oa.13-00070

14. Preventza O, Bakaeen FG, Cervera RD, Coselli JS. Deployment of proximal thoracic endograft in zone 0 of the ascending aorta: treatment options and early outcomes for aortic arch aneurysms in a high-risk population. *Eur J Cardiothorac Surg.* (2013) 44:446–52. Discussion 452–3. doi: 10.1093/ejcts/ezt068

15. Shirakawa Y, Kuratani T, Shimamura K, Torikai K, Sakamoto T, Shijo T, et al. The efficacy and short-term results of hybrid thoracic endovascular repair into the ascending aorta for aortic arch pathologies. *Eur J Cardiothorac Surg.* (2014) 45:298–304. Discussion 304. doi: 10.1093/ejcts/ezt391

16. Bernardes RC, Navarro TP, Reis FR, Lima LC, Monteiro EL, Procopio RJ, et al. Early experience with off-the-shelf endografts using a zone 0 proximal landing site to treat the ascending aorta and arch. *J Thorac Cardiovasc Surg.* (2014) 148:105–12. doi: 10.1016/j.jtcvs.2013.07.049

17. Roselli EE, Idrees J, Greenberg RK, Johnston DR, Lytle BW. Endovascular stent grafting for ascending aorta repair in high-risk patients. *J Thorac Cardiovasc Surg.* (2015) 149:144–51. doi: 10.1016/j.jtcvs.2014.07.109

18. Hiraoka A, Chikazawa G, Tamura K, Totsugawa T, Sakaguchi T, Yoshitaka H. Clinical outcomes of different approaches to aortic arch disease. *J Vasc Surg.* (2015) 61:88–95. doi: 10.1016/j.jvs.2014.06.121

19. De Rango P, Cao P, Ferrer C, Simonte G, Coscarella C, Cieri E, et al. Aortic arch debranching and thoracic endovascular repair. *J Vasc Surg.* (2014) 59:107–14. doi: 10.1016/j.jvs.2013.07.010

20. Kurimoto Y, Maruyama R, Ujihira K, Nishioka N, Hasegawa K, Iba Y, et al. Thoracic endovascular aortic repair for challenging aortic arch diseases using fenestrated stent grafts from zone 0. *Ann Thorac Surg.* (2015) 100:24–32. Discussion 32–3. doi: 10.1016/j.athoracsur.2015.01.071

21. Gandet T, Canaud L, Ozdemir BA, Ziza V, Demaria R, Albat B, et al. Factors favoring retrograde aortic dissection after endovascular aortic arch repair. *J Thorac Cardiovasc Surg.* (2015) 150:136–42. doi: 10.1016/j.jtcvs.2015.03.042

22. Cazavet A, Alacoque X, Marcheix B, Chaufour X, Rousseau H, Glock Y, et al. Aortic arch aneurysm: short- and mid-term results comparing open arch surgery and the hybrid procedure†. *Eur J Cardiothorac Surg.* (2016) 49:134–40. doi: 10.1093/ejcts/ezv024

23. Katada Y, Kondo S, Tsuboi E, Rokkaku K, Irie Y, Yokoyama H. Endovascular total arch repair using *in situ* fenestration for arch aneurysm and chronic type A dissection. *Ann Thorac Surg.* (2016) 101:625–30. doi: 10.1016/j.athoracsur.2015.07.032

24. Ziza V, Canaud L, Molinari N, Branchereau P, Marty-Ané C, Alric P. Thoracic endovascular aortic repair: a single center's 15-year experience. *J Thorac Cardiovasc Surg.* (2016) 151:1595–603.e7. doi: 10.1016/j.jtcvs.2015.12.030

25. Tsilimparis N, Debus ES, Oderich GS, Haulon S, Terp KA, Roeder B, et al. International experience with endovascular therapy of the ascending aorta with a dedicated endograft. *J Vasc Surg.* (2016) 63:1476–82. doi: 10.1016/j.jvs.2015.12.027

26. Böckler D, Brunkwall DJ, Taylor PR, Mangialardi N, Hüsing J, Larzon T. Thoracic endovascular aortic repair of aortic arch pathologies with the conformable thoracic aortic graft: early and 2 year results from a European Multicentre Registry. *Eur J Vasc Endovasc Surg.* (2016) 51:791–800. doi: 10.1016/j.ejvs.2016.02.006

27. Narita H, Komori K, Usui A, Yamamoto K, Banno H, Kodama A, et al. Postoperative outcomes of hybrid repair in the treatment of aortic arch aneurysms. *Ann Vasc Surg.* (2016) 34:55–61. doi: 10.1016/j.avsg.2015.11.041

28. Faure EM, Canaud L, Marty-Ané C, Alric P. Hybrid aortic arch repair for dissecting aneurysm. *J Thorac Cardiovasc Surg.* (2016) 152:162–8. doi: 10.1016/j.jtcvs.2016.03.020

29. Yoshitake A, Hachiya T, Okamoto K, Kitahara H, Kawaguchi S, Nakatsuka S, et al. Postoperative stroke after debranching with thoracic endovascular aortic repair. *Ann Vasc Surg.* (2016) 36:132–8. doi: 10.1016/j.avsg.2016.02.039

30. Pecoraro F, Lachat M, Hofmann M, Cayne NS, Chaykovska L, Rancic Z, et al. Mid-term results of zone 0 thoracic endovascular aneurysm repair after ascending aorta wrapping and supra-aortic debranching in high-risk patients. *Interact Cardiovasc Thorac Surg.* (2017) 24:882–9. doi: 10.1093/icvts/ivx016

31. Canaud L, Baba T, Gandet T, Narayama K, Ozdemir BA, Shibata T, et al. Physician-modified thoracic stent-grafts for the treatment of aortic arch lesions. *J Endovasc Ther.* (2017) 24:542–548. doi: 10.1177/1526602817714206

32. Wang T, Shu C, Li QM, Li M, Li X, He H, et al. First experience with the double chimney technique in the treatment of aortic arch diseases. *J Vasc Surg.* (2017) 66:1018–27. doi: 10.1016/j.jvs.2017.02.035

33. Roselli EE, Idrees JJ, Johnston DR, Eagleton MJ, Desai MY, Svensson LG. Zone zero thoracic endovascular aortic repair: a proposed modification to the classification of landing zones. *J Thorac Cardiovasc Surg.* (2018) 155:1381–9. doi: 10.1016/j.jtcvs.2017.11.054

34. Toya N, Ohki T, Fukushima S, Shukuzawa K, Ito E, Murakami Y, et al. Case series of aortic arch aneurysm in patients with bovine arch treated with proximal scalloped and fenestrated stent graft. *Cardiovasc Intervent Radiol.* (2018) 41:1648–53. doi: 10.1007/s00270-018-2058-1

35. Zhu J, Dai X, Noiniyom P, Luo Y, Fan H, Feng Z, et al. Fenestrated thoracic endovascular aortic repair using physician-modified stent grafts (PMSGs) in zone 0 and zone 1 for aortic arch diseases. *Cardiovasc Intervent Radiol.* (2019) 42:19–27. doi: 10.1007/s00270-018-2079-9

36. Hosaka A, Motoki M, Kato M, Sugai H, Okubo N. Quantification of aortic shagginess as a predictive factor of perioperative stroke and long-term prognosis after endovascular treatment of aortic arch disease. *J Vasc Surg.* (2019) 69:15–23. doi: 10.1016/j.jvs.2018.03.425

37. Huang W, Ding H, Jiang M, Liu Y, Huang C, Yang X, et al. Outcomes of chimney technique for aortic arch diseases: a single-center experience with 226 cases. *Clin Interv Aging.* (2019) 14:1829–40. doi: 10.2147/CIA.S222948

38. Yamauchi T, Kubota S, Hasegawa K, Ueda H. Clinical results and medical costs of thoracic endovascular aortic repair in patients over 80 years of age. *J Artif Organs.* (2019) 22:61–7. doi: 10.1007/s10047-018-1073-y

39. Ryomoto M, Tanaka H, Mitsuno M, Yamamura M, Sekiya N, Uemura H, et al. A novel approach to prevent perioperative stroke in patients undergoing debranching thoracic endovascular aortic repair with a mini-cardiopulmonary bypass support. *Ann Vasc Surg.* (2019) 59:143–9. doi: 10.1016/j.avsg.2018.09.036

40. Piffaretti G, Grassi V, Lomazzi C, Brinkman WT, Navarro TP, Jenkins MP, et al. Thoracic endovascular stent graft repair for ascending aortic diseases. *J Vasc Surg.* (2019) 70:1384–9.e1. doi: 10.1016/j.jvs.2019.01.075

41. Tsilimparis N, Law Y, Rohlffs F, Spanos K, Debus ES, Kölbel T. Fenestrated endovascular repair for diseases involving the aortic arch. *J Vasc Surg.* (2020) 71:1464–71. doi: 10.1016/j.jvs.2019.06.205

42. De León AI, Cheng YT, Chen SW, Chu SY, Nan YY, Liu KS. Outcomes of type Ia endoleaks after endovascular repair of the proximal aorta. *J Thorac Cardiovasc Surg.* (2020) 163:2012.e6. doi: 10.1016/j.jtcvs.2020.06.026

43. Kuo HS, Huang JH, Chen JS. Handmade fenestrated stent grafts to preserve all supra-aortic branches in thoracic endovascular aortic repair. *J Thorac Cardiovasc Surg.* (2020) 160:629–39.e1. doi: 10.1016/j.jtcvs.2019.07.096

44. Tinelli G, Ferrer C, Giudice R, Ferraresi M, Pogany G, Cao P, et al. Long-term results of hybrid repair techniques for Kommerell's diverticulum. *J Vasc Surg.* (2020) 72:1213–21. doi: 10.1016/j.jvs.2019.11.052

45. Fernández-Alonso L, Fernández Alonso S, Martínez Aguilar E, Santamarta Fariña E, Alegret Solé J, Atienza Pascual M, et al. Fenestrated and scalloped endovascular grafts in zone 0 and zone 1 for aortic arch disease. *Ann Vasc Surg.* (2020) 69:360–5. doi: 10.1016/j.avsg.2020.06.009

46. Chassin-Trubert L, Ozdemir BA, Roussel A, Dessertenne G, Castier Y, Ludovic C, et al. Prevention of retrograde ascending aortic dissection by cardiac pacing during hybrid surgery for zone 0 aortic arch repair. *Ann Vasc Surg.* (2021) 71:48–55. doi: 10.1016/j.avsg.2020.08.136

47. Li F, Wu X, Zhang X, Qin J, Zhao Z, Ye K, et al. Clinical outcomes of distal tapered restrictive covered stent applied in endovascular treatment of aortic dissection involving zone 0. *Eur J Vasc Endovasc Surg.* (2021) 61:413–21. doi: 10.1016/j.ejvs.2020.11.037

48. Planer D, Elbaz-Greener G, Mangialardi N, Lindsay T, D'Onofrio A, Schelzig H, et al. NEXUS arch: a multicenter study evaluating the initial experience with a novel aortic arch stent graft system. *Ann Surg.* (2021) 277:e460–6. doi: 10.1097/SLA.0000000000004843

49. Dake MD, Bavaria JE, Singh MJ, Oderich G, Filinger M, Fischbein MP, et al. Management of arch aneurysms with a single-branch thoracic endograft in zone 0. *JTCVS Tech.* (2021) 7:1–6. doi: 10.1016/j.xjtc.2021.01.011

50. Seguchi R, Kiuchi R, Horikawa T, Tarui T, Sanada J, Ohtake H, et al. Novel brain protection method for zone 0 endovascular aortic repair with selective cerebral perfusion. *Ann Vasc Dis.* (2021) 14:153–8. doi: 10.3400/avd.oa.21-00025

51. Li X, Zhang L, Song C, Zhang H, Xia S, Li H, et al. Long-term outcomes of thoracic endovascular repair for aortic arch dissection using customized single-branched fenestrated stent-graft. *Vasc Endovascular Surg.* (2021) 55:577–585. doi: 10.1177/15385744211010446

52. Li X, Zhang L, Song C, Zhang H, Xia S, Li H, et al. Outcomes of total endovascular aortic arch repair with surgeon-modified fenestrated stent-grafts on zone 0 landing for aortic arch pathologies. *J Endovasc Ther.* (2021) 2021:15266028211036478. doi: 10.1177/15266028211036478

53. Hanna L, Abdullah A, Kashef E, Riga C, Jenkins M, Bicknell C, et al. Four-year results of the Bolton relay proximal scallop endograft in the management of thoracic and thoracoabdominal aortic pathology with unfavorable proximal landing zone. *J Vasc Surg.* (2021) 74:1447–55. doi: 10.1016/j.jvs.2021.04.027

54. Barnes JA, Wanken ZJ, Columbo JA, Kuwayama DP, Fillinger MF, Suckow BD. Procedure-associated costs and mid-term outcomes of endovascular zone 0 and zone 1 aortic arch repair. *Ann Vasc Surg.* (2021) 81:98–104. doi: 10.1016/j.avsg.2021.10.026

55. Kudo T, Kuratani T, Shirakawa Y, Shimamura K, Kin K, Sakamoto T, et al. Comparison of the outcomes of total endovascular aortic arch repair between branched endograft and chimney endograft technique in zone 0 landing. *J Endovasc Ther.* (2021) 2021:15266028211059912. doi: 10.1177/15266028211059912

56. Chen D, Luo M, Fang K, Shu C. Endovascular repair for acute zone 0 intramural hematoma with most proximal tear or ulcer-like projection in the descending aorta. *J Vasc Surg.* (2021) 75:1561–9. doi: 10.1016/j.jvs.2021.12.055

57. Eleshra A, Heo W, Lee KH, Kim TH, Sim HS, Sharafeldin H, et al. Mid-term outcomes of hybrid debranching endovascular aortic arch repair in landing zones 0–2. *Vascular.* (2022) 2022:17085381211068230. doi: 10.1177/17085381211068230

58. von Allmen RS, Gahl B, Powell JT. Editor's choice - incidence of stroke following thoracic endovascular aortic repair for descending aortic aneurysm: a systematic review of the literature with meta-analysis. *Eur J Vasc Endovasc Surg.* (2017) 53:176–84. doi: 10.1016/j.ejvs.2016.10.025

59. Karaolanis GI, Antonopoulos CN, Charbonneau P, Georgakarakos E, Moris D, Scali S, et al. A systematic review and meta-analysis of stroke rates in patients undergoing Thoracic Endovascular Aortic Repair for descending thoracic aortic aneurysm and type B dissection. *J Vasc Surg.* (2022) 76:292–301.e3. doi: 10.1016/j.jvs.2022.02.031

60. Papakonstantinou NA, Antonopoulos CN, Baikoussis NG, Kakisis I, Geroulakos G. Frozen elephant trunk: an alternative surgical weapon against extensive thoracic aorta disease. A three-year meta-analysis. *Heart Lung Circ.* (2019) 28:213–22. doi: 10.1016/j.hlc.2018.04.306

61. Chen X, Wang J, Premaratne S, Zhao J, Zhang WW. Meta-analysis of the outcomes of revascularization after intentional coverage of the left subclavian artery for thoracic endovascular aortic repair. *J Vasc Surg.* (2019) 70:1330–40. doi: 10.1016/j.jvs.2019.03.022

62. Hammo S, Larzon T, Hultgren R, Wanhainen A, Mani K, Resch T, et al. Outcome after endovascular repair of ruptured descending thoracic aortic aneurysm: a national multicentre study. *Eur J Vasc Endovasc Surg.* (2019) 57:788–94. doi: 10.1016/j.ejvs.2018.10.029

63. Kudo T, Kuratani T, Shimamura K, Sawa Y. Determining the optimal proximal landing zone for TEVAR in the aortic arch: comparing the occurrence of the bird-beak phenomenon in zone 0 vs zones 1 and 2. *J Endovasc Ther.* (2020) 27:368–76. doi: 10.1177/1526602820914269

64. Uchida N. How to prevent spinal cord injury during endovascular repair of thoracic aortic disease. *Gen Thorac Cardiovasc Surg.* (2014) 62:391–7. doi: 10.1007/s11748-014-0395-9

65. Chen Y, Zhang S, Liu L, Lu Q, Zhang T, Jing Z. Retrograde type A aortic dissection after thoracic endovascular aortic repair: a systematic review and meta-analysis. *J Am Heart Assoc.* (2017) 6:e004649. doi: 10.1161/JAHA.116.004649

66. Neuhauser B, Greiner A, Jaschke W, Chemelli A, Fraedrich G. Serious complications following endovascular thoracic aortic stent-graft repair for type B dissection. *Eur J Cardiothorac Surg.* (2008) 33:58–63. doi: 10.1016/j.ejcts.2007.10.010

67. Ramdass M. TEVAR for symptomatic Stanford B dissection: a systematic review of 30-day mortality and morbidity. *Thorac Cardiovasc Surg.* (2015) 63:97–112. doi: 10.1055/s-0034-1370760

68. Naazie IN, Gupta JD, Azizzadeh A, Arbabi C, Zarkowsky D, Malas MB. Risk calculator predicts 30-day mortality after thoracic endovascular aortic repair for intact descending thoracic aortic aneurysms in the Vascular Quality Initiative. *J Vasc Surg.* (2022) 75:833–41.e1. doi: 10.1016/j.jvs.2021.08.056

69. Harris DG, Olson SL, Panthofer AM, Matsumura JS, DiMusto PD. A Frailty-based risk score predicts morbidity and mortality after elective endovascular repair of descending thoracic aortic aneurysms. *Ann Vasc Surg.* (2020) 67:90–9. doi: 10.1016/j.avsg.2019.10.090

70. Settepani F, Cappai A, Basciu A, Barbone A, Tarelli G. Outcome of open total arch replacement in the modern era. *J Vasc Surg.* (2016) 63:537–45. doi: 10.1016/j.jvs.2015.10.061

71. Leone A, Beckmann E, Martens A, Di Marco L, Pantaleo A, Reggiani LB, et al. Total aortic arch replacement with frozen elephant trunk technique: results from two European institutes. *J Thorac Cardiovasc Surg.* (2020) 159:1201–11. doi: 10.1016/j.jtcvs.2019.03.121

frontiers | Frontiers in Cardiovascular Medicine

TYPE Original Research
PUBLISHED 21 March 2023
DOI 10.3389/fcvm.2023.1058440

Check for updates

OPEN ACCESS

EDITED BY
Massimo Bonacchi,
University of Florence, Italy

REVIEWED BY
Zhichao Lai,
Peking Union Medical College Hospital (CAMS), China
Florian Karl Enzmann,
Medical University Innsbruck, Austria

*CORRESPONDENCE
Tong Qiao
✉ qiaotong@njglyy.com
Zhao Liu
✉ liuzhao83@gmail.com

†These authors have contributed equally to this work

SPECIALTY SECTION
This article was submitted to General Cardiovascular Medicine, a section of the journal Frontiers in Cardiovascular Medicine

RECEIVED 30 September 2022
ACCEPTED 28 February 2023
PUBLISHED 21 March 2023

CITATION
Chen Z, Fu D, Liu C, Jin Y, Pan C, Mamateli S, Lv X, Qiao T and Liu Z (2023) Risk factors for target vessel endoleaks after physician-modified fenestrated or branched endovascular aortic arch repair: A retrospective study.
Front. Cardiovasc. Med. 10:1058440.
doi: 10.3389/fcvm.2023.1058440

Risk factors for target vessel endoleaks after physician-modified fenestrated or branched endovascular aortic arch repair: A retrospective study

Zhipeng Chen†, Dongsheng Fu†, Cheng Liu, Yi Jin, Chaohui Pan, Subinur Mamateli, Xiaochen Lv, Tong Qiao* and Zhao Liu*

Department of Vascular Surgery, Affiliated Drum Tower Hospital, Medical School of Nanjing University, Nanjing, China

Objective: Fenestrated or branched endovascular aortic arch repair (fb-arch repair) is an effective option for treating complex aortic arch lesions, including thoracic aortic aneurysms and aortic dissections. However, the relatively high rate of re-intervention due to target vessel (TV)-related endoleaks have raised concerns. This study aimed to determine risk factors for TV-related endoleaks after fb-arch repair.

Methods: This was a retrospective analysis of all patients undergoing fb-arch repair between 2017 and 2021in nanjing drum tower hospital of China. All the patients underwent computed tomography angiography (CTA) before surgery; at discharge; and at 3 months, 6 months, and yearly post-discharge. All procedures are performed with physician modified grafts. Two experienced vascular surgeons used CTA and vascular angiography data to assess endoleaks. The study endpoints were mortality, aneurysm rupture, and emergence of and re-intervention for TV-related endoleaks.

Results: During the follow-up period, 218 patients underwent fb-arch repair. There were seven perioperative deaths and four deaths during follow-up (two myocardial infarctions and two malignancies). There were nine additional patients who were excluded from the study (two strokes, three with abnormal aortic arch anatomy, and four with insufficient clinical data). Among the 198 patients considered (mean age, 59 ± 13.3 years; 85% male), 309 branch arteries were revascularized. A total of 35 TV-related endoleaks were identified in 28 patients during a mean follow-up of 23 ± 14 months (median 23, IQR 26.3): six type Ic, 4 type IIIb, and 20 type IIIc endoleaks. Patients in the endoleak group had greater aortic arch segment diameters (43.1 ± 5.1 vs. 40.3 ± 4.7; $P = 0.004$) and a greater number of TVs revascularized (2.0 ± 0.8 vs. 1.5 ± 0.8; $P = 0.004$) than those in the non-endoleak group. However, the morphological classification of the aortic arch did not seem to affect the occurrence of TV endoleaks (13%, 14%, and 15% for type I, II, and III aortic arches, respectively; $P = 0.957$). Pre-sewing branch stents in the fenestration position reduced the risk of TV endoleaks (5% vs. 14%; $P = 0.037$). Additionally, in TVs affected by aortic aneurysm or dissection, the risk of endoleaks increased after reconstruction (17% vs. 8%; $P = 0.018$). The incidence of secondary TV-related endoleaks after fb-arch repair was 14.1%.

Abbreviations
CI, Confidence intervals; CMD, Company-manufactured devices; CTA, Computed tomography angiography; fb-arch repair, Fenestrated or branched endovascular aortic arch repair; F/BEVAR, Fenestrated or branched endovascular aortic repair; PMEGs, Physician-modified endografts; OR, Odds ratios; TV, Target vessel; DOAC, Direct oral anticoagulants.

Conclusion: The data from this study showed that the incidence of secondary target vessel related endoleaks after fb-arch repair is approximately 14.1%. Additionally, patients with a larger aortic arch diameter or more revascularized arteries during surgery were at increased risk TV-related endoleaks. The target vessels originating from the false lumen or aneurysm sac are more prone to endoleaks after reconstruction. Finally, prefabricated branch stents reduced risk of TV-related endoleaks.

KEYWORDS

fenestrated or branched endovascular aortic arch repair, target vessel-related endoleak, aortic dissection, thoracic aortic aneurysm, risk factors

1. Introduction

Aortic arch pathologies involving the supra-aortic vessels are a major challenge for surgeons. Traditional open or hybrid surgeries are highly traumatic for patients. Despite surgical modifications and improved postoperative care, open or hybrid surgeries continue to have relatively high rates of morbidity and mortality (1, 2). Total endovascular aortic arch repair is a feasible approach for managing complicated aortic arch diseases (3, 4); however, some concern regarding the associated high re-intervention rate remains. Owing to Chinese policy restrictions, the development and promotion of company-manufactured devices (CMDs) in China has lagged behind those in other countries. Most fenestrated or branched endovascular aortic arch repair (fb-arch repair) procedures use physician-modified endografts (PMEGs) rather than CMDs. Notably, PMEG use may result in higher rates of complications and re-intervention events than CMD use due to inconsistencies in stent graft modification standards (5).

Endoleaks are the primary cause of re-intervention after fenestrated or branched endovascular aortic repair (F/BEVAR), and target vessel (TV)-related endoleaks occur more frequently than those around the main stent graft. TV-related endoleaks are common, as F/BEVAR is common in those with complex aortic diseases and modular endografts. The following are the three main types of endoleaks associated with the TVs: type Ic, which is caused by retrograde blood flow from the distal end of a bridging stent; type IIIb, which involves a tear or break in the fabric of the bridging stent; and type IIIc, which is defined as poor connections between the bridging stent and fenestration ring, directional branch, or mini-cuffs. Among primary and secondary endoleaks, type IIIc is the most predominant TV-related endoleak type, accounting for 85% and 55%, respectively (6). Progression to type I and type III endoleaks often leads to aneurysm sac enlargement, thereby increasing the risk of aneurysm rupture. The latest guidelines recommend the treatment of type I and type III endoleaks (7, 8). The incidence of TV-related endoleaks in the visceral segment after F/BEVAR for thoracoabdominal aortic aneurysms ranges from 16.4% to 35.7% (9, 10). The development of fb-arch repair occurs slightly later than that of F/BEVAR in the visceral area, and there are only few studies on TV-related endoleaks after fb-arch repair.

This study aimed to examine the incidence of secondary TV-related endoleaks among patients who underwent fb-arch repair and to identify risk factors for secondary TV-related endoleaks using patient data from a high-volume, single center in China.

2. Materials and methods

2.1. Study population

This retrospective study was approved by the Ethics Committee of Nanjing Drum Tower Hospital (registration number: 2017-015-05), and all patients provided consent for their participation. At our hospital, 218 patients underwent fb-arch repair for 62 thoracic aortic aneurysms, 137 chronic dissections, 10 intramural hematomas, and 9 penetrating aortic ulcers involving the arch between June 2017 and September 2021. All of the patients received elective operations. 20 patients were excluded from the study due to deaths unrelated to endoleaks and other reasons. Aortic imaging data of the remaining 198 patients were obtained *via* computed tomography angiography (CTA). All patients underwent CTA examination before surgery; before discharge; 3, 6, and 12 months after discharge; and every year thereafter. Some patients ($n = 63$) sought an immediate CTA examination due to symptoms; therefore, their follow-up schedules were adjusted accordingly. All CTA images or angiographic data were reviewed by vascular radiologists and senior vascular surgeons.

2.2. Study design

Custom-manufactured devices (CMDs) are not widely used in mainland China due to health insurance policy requirements and cargo delivery time issues. PMEGs, which have been developed rapidly and widely in China, were used to treat all included patients. 3D printing, which may be used to improve the accuracy of fenestration (11), was used in this study to facilitate the treatment of patients with ≥2 TVs requiring reconstruction. Indications for surgery included thoracic aortic aneurysms or aortic dissection with rupture, chest or back pain, an asymptomatic aneurysm sac diameter of >5.5 cm or diameter increased by >5 mm within 6 months, intramural hematoma with a thickness of greater than 10 mm or persistent increase in size, combined with pleural effusion, or penetrating aortic ulcers

>5 mm in depth with an insufficient landing zone due to pathologies involving supra-aortic vessels. Based on the patient's anatomy and lesion characteristics, we reconstructed branch vessels in one of the following three ways: *in situ* fenestration, on-site fenestration, or pre-sewn cuffs or branches.

All *in situ* fenestrations were performed using a combination of a steerable sheath and a needle to rupture the membrane. The diameter of the area of each fenestration was adjusted according to the size of the branch vessel opening, and a nitinol ring was used to mark the area around which sutures were required. The following bridging stents were implanted within each fenestration area: bridging stents, including Viabahn (W. L. Gore, Flagstaff, AZ); Fluency (BD/Bard, Murray Hill, NJ, United States), and the iliac branch of the endovascular aortic repair graft. In the early stages of this study, some bridging stents were relined using Omnilink (Abbott Vascular, Santa Clara, CA, United States) to prevent kinking. The mini-cuff included a 3–5-mm Viabahn, which was shortened and anastomosed end-to-side to the main stent graft using 5-0 Ethibond sutures (Ethicon, West Somerville, NJ). The directional branch was sutured using 1–1.5-cm Viabahn. The largest outer diameter of the entire aortic arch and the outer diameter of the aorta at the level of the branch opening were referred to as D1 and D2, respectively.

2.3. Procedure

All operations were performed under general anesthesia in a hybrid operating room equipped with a fixed fluoroscopy C-arm. PMEGs were performed using Valiant (Medtronic, Minneapolis, MN, USA; $n = 57$), Ankura (Lifetech Scientific, Shenzhen, China; $n = 123$), or Zenith (Cook, Bloomington, IN, USA; $n = 18$) platforms. Access was obtained through femoral and left brachial arteries, with the left common carotid and right subclavian arteries selected when necessary. Fenestrations or inner branches were preferred in cases in which TVs originated from the true lumen, and fenestrations were close to TV orifices. Mini-cuffs or outer branches were preferred if the TV originated from the false lumen and if there was sufficient distance between the main stent graft and the TV orifices. Steerable sheaths, such as FuStar (Lifetech Scientific Inc., Shenzhen, China), were used to facilitate TV cannulation and dissection flap puncture. Temporary diameter-reducing ties were used in all patients to ensure rotational and axial movement of the main stent graft, thus facilitating TV catheterization. After TVs were positioned and bridging stents were ready for deployment, reducing ties were removed, allowing for free movement of the main stent graft. Balloon molding of bridging stents is essential for eliminating gaps and preventing primary endoleaks. Anticoagulants were not routinely used after surgery, but we recommend that patients be treated with dual antiplatelet therapy (aspirin + clopidogrel) for 1–3 months after surgery, followed by a change to a single antiplatelet agent and adjustment of the dosing regimen based on follow-up results, according to requirements (12).

2.4. Statistical analysis

Categorical variables are expressed as numbers and percentages, and continuous variables are expressed as mean ± standard deviation or median, as appropriate. The Pearson chi-squared test was used to compare nominal data. Further, the student's *t*-test and Mann-Whitney *U*-test were used to compare mean values. Univariate and multivariate analyses were performed to identify risk factors for TV-related endoleaks among anatomic and stent graft-related variables. Odds ratios (OR) with 95% confidence intervals (CI) were used to reflect the odds of an event. Values of $P < 0.05$ were considered statistically significant. All statistical analyses were performed using SPSS version 25.0 software (IBM Corp., Armonk, NY, United States).

3. Results

3.1. Baseline patient characteristics and demographics

A total of 218 patients underwent fb-arch repair at our center throughout the study period: 62 with thoracic aortic aneurysms, 137 with chronic dissections, 10 with intramural hematomas, and 9 with penetrating aortic ulcers involving the arch. Perioperative deaths occurred in seven patients: five with retrograde type A aortic dissections, one with thoracic aortic rupture, and one with myocardial infarction. There were four deaths during follow-up (two myocardial infarctions and two malignancies). In addition, nine patients were excluded from the study (two experienced strokes, three had abnormal aortic arch anatomy, and four had insufficient clinical data). We estimated 30-day and 24-month survival rates as 96.8% and 95.4%, respectively. Among the remaining 198 patients (mean age, 59 ± 13.3 years; 85% male) with aortic arch diseases, 309 branch arteries were revascularized using 172 fenestrations and 137 inner- or outer-branch stents.A total of 35 TV-related endoleaks were identified among 28 patients during a mean follow-up period of 23 ± 14 months (median 23, IQR 26.3): six patients with type Ic (retrograde from the distal end of the branch), four with type IIIb (bridging stent fabric tear), and 20 with type IIIc endoleaks (detached stent or loose bridging stent connection). As depicted in **Figure 1**, A 45-year-old male patient developed type IIIc endoleak around the left subclavian artery during the follow-up. After two false lumen coil embolization, the endoleak disappeared and the aorta was well remodeled. No significant differences were observed in patient demographics or the prevalence of comorbidities between patients with and without a TV endoleak (**Supplementary Table S1**). The characteristics of patients and TVs were explored to identify risk factors for TV-related endoleaks after fb-arch repair.

3.2. Risk factors for TV-related endoleaks after fb-arch repair

No significant between-group differences were noted in terms of body mass index and length of hospital stay post-procedure.

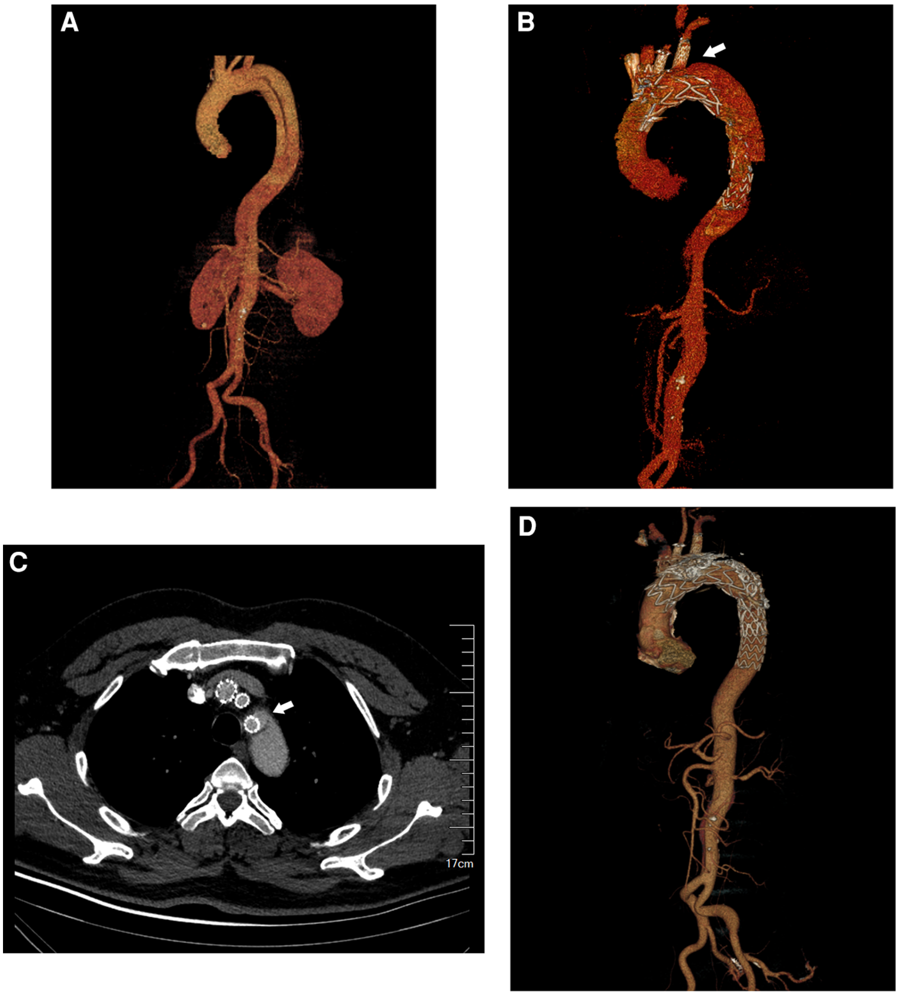

FIGURE 1
A 45-year-old male patient underwent fb-arch repair for chronic aortic dissection. The patient developed type IIIc endoleak around the left subclavian artery during the follow-up. (A) The CTA imaging of the aortic arch involved by dissection. (B) The CTA imaging of the Type IIIc endoleak near the left subclavian artery after fb-arch repair. (arrow). (C) The cross-sectional image of the Type IIIc endoleak (arrow). (D). After two false lumen coil embolization, the original endoleak disappeared and the aorta was well remodeled.

However, the number of revascularized TVs per individual appeared to affect the risk of TV-related endoleak. Patients in the endoleak group had a greater number of reconstructed vessels than those of the non-endoleak group (Table 1, 2.0 ± 0.8 vs. 1.5 ± 0.8; $P = 0.004$). Univariate logistic regression analysis revealed that TVs per patient and ≥2 TVs were potential risk factors for endoleaks; however, considering the problem of collinearity, we chose ≥2 TVs for the final multivariate logistic regression. Subsequently, ≥2 TVs was identified as an independent risk factor for TV-related endoleaks after fb-arch repair (Table 2: OR, 3.849; 95% CI, 1.633–9.075; $P = 0.002$).

Patients in the endoleak group had a greater aortic arch diameter than those in the non-endoleak group (D_1: 43.1 ± 5.1 vs. 40.3 ± 4.7; $P = 0.004$). The use of D_1 as a condition in univariate and multivariate analyses revealed that D_1 was another independent risk factor for TV-related endoleaks (Table 2: OR, 1.130; 95% CI, 1.033–1.236; $P = 0.008$). During the follow up, we found a patient with the maximum aortic diameter higher than 65 mm had TV-related endoleaks around all three supra-aortic vessels after fb-arch repair (Figure 2). The operation time in the endoleak group was longer than that in the non-endoleak group (296.7 ± 85.8 vs. 262.3 ± 77.9; $P = 0.034$). This finding may be affected by the need for reconstruction of a greater number of branches in patients of the endoleak group.

Postoperative treatment with direct oral anticoagulants and anatomic aortic arch type were not found to affect the occurrence of TV-related endoleak. TV-related endoleaks were observed in 17% of patients with aortic dissection after fb-arch repair compared to 9% of those with other diseases involving the aortic arch ($P = 0.120$). The main grafts included Lifetech products from China and other brands from overseas. Although the fabric and stent design of products differed, no significant between-group differences were noted in the incidence of TV-related endoleaks among those with different graft products (12%, 16% and 22%, $P = 0.477$; Table 2).

TABLE 1 Factors with the potential to affect TV-related endoleak occurrence after fb-arch repair.

	All patients (*N* = 198)	Target vessel endoleaks (*N* = 28)	No target vessel endoleaks (*N* = 170)	*P*
BA diameter, mm	14.3 ± 1.9	14.6 ± 1.9	14.3 ± 1.8	0.411
LCCA diameter, mm	9.2 ± 1.6	9.5 ± 1.4	9.1 ± 1.6	0.213
LSA diameter, mm	11.3 ± 1.7	11.6 ± 1.6	11.3 ± 1.7	0.416
D_1, mm	40.7 ± 4.8	43.1 ± 5.1	40.3 ± 4.7	**0.004**
BMI	25.6 ± 3.4	26 ± 3.4	25.5 ± 3.4	0.538
Hospital LOS after procedure, d	12.8 ± 4.5	13.2 ± 4.5	12.7 ± 4.6	0.580
Procedure time, min	267.1 ± 79.7	296.7 ± 85.8	262.3 ± 77.9	**0.034**
Target vessels per patient	1.6 ± 0.8	2.0 ± 0.8	1.5 ± 0.8	**0.004**
≥ 2 target vessels	72 (36)	18 (64)	54 (32)	**0.001**
Get NOAC therapy	34 (17)	6 (21)	28 (16)	0.649
Aortic dissection	130 (66)	22 (79)	108 (64)	0.120
Morphological classification of the aortic arch				0.957
Type I	53	7/53 (13)	46	
Type II	106	15/106 (14)	91	
Type III	39	6/39 (15)	33	
Brand of the main graft				0.477
Lifetech	123	15/123 (12)	108	
Meditronic	57	9/57 (16)	48	
Cook	18	4/18 (22)	14	

BA, brachiocephalic artery; LCCA, left common carotid artery; LSA, left subclavian artery; D_1: maximum diameter of the aortic arch; BMI, body mass index; LOS, length of stay; DOAC, direct oral anticoagulants.
All data are presented as number (%) or mean ± standard deviation.

TABLE 2 Univariate and multivariate analysis of risk factors for TV-related endoleaks in 198 patients who had previously undergone fb-arch repair.

Variables	Univariate analysis		Multivariate analysis	
	OR (95% CI)	*P*	OR (95% CI)	*P*
D_1, mm	1.128 (1.044–8.986)	**0.042**	1.130 (1.033–1.236)	**0.008**
Target vessels per patient	1.924 (1.214–3.050)	**0.005**	–	
≥ 2 target vessels	3.867 (1.673–8.936)	**0.002**	3.849 (1.633–9.075)	**0.002**

3.3. Risk factors for TV-related endoleaks among 309 TVs after fb-arch repair

Endoleak-related risk factors were identified among 309 TVs. First, the effect of revascularization method on the occurrence of endoleak was assessed, revealing no significant between-group differences in the incidence of TV-related endoleaks. The revascularization methods that were considered included *in situ* fenestration (10 endoleaks among 72 TVs, 14%), on-site fenestration (20 endoleaks among 146 TVs, 14%), and pre-sewn cuffs or branches (5 endoleaks among 91 TVs, 5%; $P = 0.112$; **Table 3**). However, TVs revascularized with pre-sewn cuffs or branches appeared to result in a lower rate of endoleaks than those revascularized *via* other methods (5% vs. 14%, $P = 0.037$; **Table 3**). Similar results were observed when the effects of different bridging stent type use were assessed, revealing that the risk of endoleaks in TVs reconstructed with Fluency was slightly higher than that in Viabahn (13% vs. 8%, $p = 0.249$; **Table 3**). Importantly, the occurrence of TV-related endoleaks after surgery depended on whether TVs are affected by aortic arch lesions. The occurrence of TV-related endoleaks in branch vessels affected by aortic arch pathologies was 17%, which was higher than that in branch vessels not affected by pathologies (8%, $P = 0.018$, **Table 3**). In the multivariate analysis of endoleak-related risk factors among TVs, we determined that non-pre-sewn cuffs or branches (OR, 2.951; 95% CI, 1.091–7.980; $P = 0.033$), TVs affected by pathologies (OR, 2.107; 95% CI, 1.015–4.372; $P = 0.045$), and aortic diameter at the level of the TV opening (D_2) (OR, 1.059; 95% CI, 1.002–1.120; $P = 0.043$) were independent risk factors for TV-related endoleaks (**Table 4**).

4. Discussion

Total endovascular repair using fenestrated and branched technology is an appropriate option for the treatment of aortic arch aneurysms and chronic aortic dissection involving the supra-aortic vessels. Although total endovascular treatment avoids damage caused by thoracotomy and circulatory arrest, F/BEVAR remains challenging for vascular surgeons. Marek et al. reported an 85% technical success rate for F/BEVAR, with 30- and 90-day mortality rates of 7% and 15%, respectively (10). These values were higher than those of the current study. Our data more closely mirrored the findings of a multicenter study from China, which estimated 30-day and 24-month survival rates as 97.5% and 94.9%, respectively (13). This was likely due to the high proportion of single fenestrations encountered in our study. Complete interruption of the false lumen or aneurysm sac perfusion greatly affects the prognosis of patients with aortic disease. In fact, in 62.7% of type B aortic dissections, an increase in aortic diameter 5-years after TEVAR was observed (14). Further, when the diameter of a dissection aneurysm exceeded 60 mm, risk of aneurysm rupture within one year reached 30% (15). Therefore, it is important to ensure that the stent graft fully covers the lesion area and actively correct large-flow endoleaks.

Owing to the modular design of the endograft used in the F/BEVAR procedure, TV-related endoleaks were the most common type of endoleak after surgery and were the most common cause of postoperative re-intervention. Kitagawa et al. (16) examined 30 patients with post-dissection TAAAs; despite remarkably good perioperative outcomes, up to 40% of patients underwent re-intervention for various endoleaks. The study further revealed that aortic diameter was closely associated with the incidence of TV-related endoleaks after F/BEVAR, with aortic arch diameters (D_1) of the 28 patients with TV-related endoleaks significantly greater than those of the 170 patients without endoleaks. Similar results were observed when the occurrence of TV-related

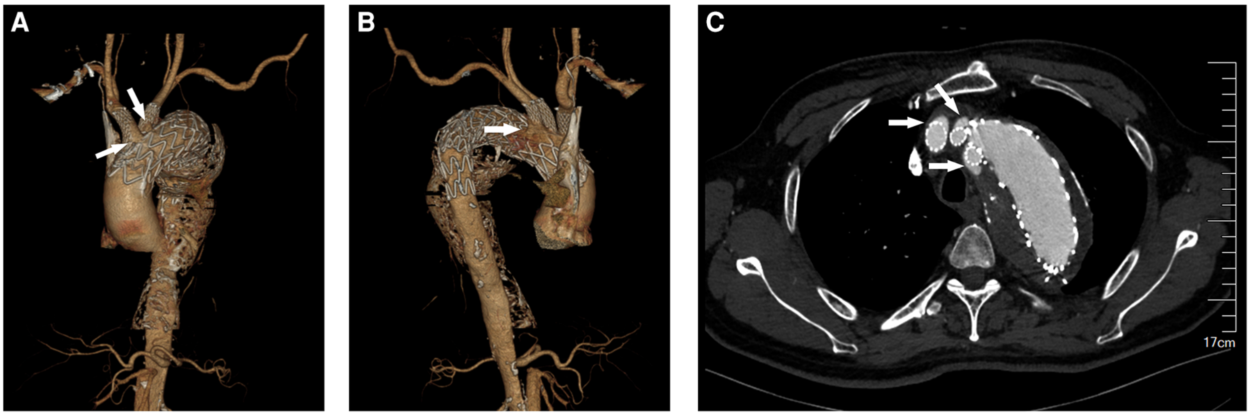

FIGURE 2
A 69-year-old male patient underwent fb-arch repair for a postdissection aortic arch aneurysm. Probably because of the large aortic arch diameter, there seems to be endoleaks around the reconstructed supra-aortic vessels during the follow-up. (A) The CTA imaging of the Type IIIc endoleaks near the brachiocephalic trunk and the left common carotid artery after fb-arch repair. (arrow). (B) The CTA imaging of the Type IIIc endoleak near the left subclavian artery after fb-arch repair. (arrow). (C) The cross-sectional image of the Type IIIc endoleaks (arrow).

TABLE 3 Potential influencing factors for target vessel-related endoleaks among 309 target vessels after fb-arch repair.

	All target vessels ($N = 309$)	Target vessel endoleaks ($N = 35$)	No target vessel endoleaks ($N = 274$)	*P*
Endoleak position				0.954
BA	44	5/44 (11)	39	
LCCA	77	8/77 (10)	69	
LSA	188	22/188 (12)	166	
Modification method				0.112
In situ fenestration	72	10/72 (14)	62	0.433[a]
On-site fenestration	146	20/146 (14)	126	
Pre-sewn cuffs or branches	91	5/91 (5)	86	**0.037**[b]
Brand of bridging stent				0.473
Bard Fluency	164	21/164 (13)	143	0.249[c]
Gore Viabahn	108	9/108 (8)	99	
Iliac branch of EVAR graft	37	5/37 (14)	32	
TVs affected by pathologies	104 (34)	18 (51)	86 (31)	**0.018**
D_2, mm	36.8 ± 6.5	39.1 ± 6.5	36.5 ± 6.4	**0.023**
Oversize ratio	1.105 ± 0.049	1.099 ± 0.052	1.106 ± 0.048	0.427
Bridge stent diameter, mm	10.5 ± 1.5	10.8 ± 1.7	10.5 ± 1.5	0.220
Bridge stent length, mm	45.5 ± 10.4	45.1 ± 11.1	45.6 ± 10.3	0.821

BA, brachiocephalic artery; LCCA, left common carotid artery; LSA, left subclavian artery; D_1: maximum diameter of the aortic arch; TV, target vessel.
[a]*In situ* fenestration compared with the other two methods.
[b]Pre-sewn cuffs or branches compared with the other two methods.
[c]Bard Fluency compared with Gore Viabahn; D_2, aortic diameter at the level of TV orientation.
All data are presented as number (%) or mean ± standard deviation.

TABLE 4 Univariate and multivariate analyses of risk factors for target vessel (TV)-related endoleaks among 309 TVs after fb-arch repair.

Variables	Univariate analysis		Multivariate analysis	
	OR (95% CI)	*P*	OR (95% CI)	*P*
Not pre-sewn cuffs or branches	2.745 (1.030–7.317)	**0.044**	2.951 (1.091–7.980)	**0.033**
TVs affected by pathologies	2.315 (1.138–4.709)	**0.021**	2.107 (1.015–4.372)	**0.045**
D_2, mm	1.064 (1.008–1.123)	**0.025**	1.059 (1.002–1.120)	**0.043**

endoleaks after F/BEVAR in degenerative aneurysms was assessed (6). This finding may be explained by the fact that an enlarged aneurysm sac often increases the distance between fenestrations and TV orientation, both of which provide space for blood flow to enter the sac lumen due to a connection gap.

The present study revealed that patients with a greater number of TVs were more likely to have endoleaks. Patients with many TVs require revascularization, usually because the dissection entry point or aneurysm sac is close in proximity to the opening of visceral branch vessels. However, the presence of an increased quantity of TVs correspondingly increases the risk of accumulation. This study suggests that TVs revascularized using pre-sewn cuffs or branches are less likely to have endoleaks than those revascularized using *in situ* fenestration or on-site fenestration. This reduced risk of TV-related endoleaks may be associated with the fact that PMEGs are limited by struts during main stent modification, especially during F/BEVAR during which the diameter of the fenestration can exceed 1 cm. In particular, creation of a standard circle fenestration is difficult, and the connection with the branch stent is very short. In contrast, the connection between the mini-cuff or branch to the bridging stent when using in a standard round stent (usually Viabahn) is 3–15 mm.

Although no iCAST-covered stent, a widely used bridging stent, is available, many alternatives such as self-expanding covered stents (Fluency, Viabahn), balloon-expanding covered stents (Lifestream, BARD), and balloon-expanding bare mental stents (Omnlink, Abbott) can be used in China. A previous study showed that the probability of endoleak occurrence in those with balloon-expandable stents may be higher than that in those with self-expanding stent grafts; however, due to the limited number of cases considered, this study failed to support such prior conclusions. The present study suggested that TVs revascularized with Fluency stents appear to be more prone to endoleaks than those revascularized with Viabahn, a finding that may be due to the stiffness of Fluency stents. It is not uncommon for bridging stents to migrate or slip, mainly because mismatch between calibers of the bridging stent and fenestrations or branches may occur (17). The diameter of the bridging stent should be smaller than that of the branch vessel; therefore, the proximal end of the bridging stent should not enter the main graft to a great extent. TVs involved in pathologies are independent risk factors for TV-related endoleaks. The probability of entry into the false lumen around the opening of branch vessels is high, resulting in a certain distance between the actual opening of branch vessels and feneatrations, leaving room for endoleak blood flow to enter the false lumen. However, entry may occur at the distal end of a branch vessel. Alternatively, stent-induced entry may occur due to bridging stent implantation.

This study has some limitations. First, the sample size was insufficient for identifying risk factors for endoleaks after surgery with confidence. A larger number of positive samples would provide more convincing findings. Moreover, since an insufficient number of cases were considered, we were unable to perform a subgroup analysis of different types of TV-related endoleaks. There was a certain proportion of patients who were lost follow-up. Finally, all patients received PMEGs; therefore, findings may not be applicable in patients receiving CMDs.

In conclusion, fb-arch repair is an effective means for treating aortic arch pathologies; however, the relatively high incidence of TV-related endoleaks is concerning. Increased aortic arch diameter, TVs affected by aortic arch lesions, and the number of revascularized branches are independent risk factors for TV-related endoleaks after fb-arch repair. However, pre-sewn cuffs and branches were determined to be protective factors.

Data availability statement

The raw data supporting the conclusions of this article will be made available by the authors, without undue reservation.

Ethics statement

Written informed consent was obtained from the individual(s) for the publication of any potentially identifiable images or data included in this article.

Author contributions

ZC and DF contributed equally to the work. ZC, DF, ZL and TQ conceived and designed the study. ZL, CL, and TQ participated in the treatment of patients and the diagnosis of endoleaks. ZC, CP, YJ, SM, and XL collected or analyzed the clinical data. TQ and ZL supervised the whole project. All authors contributed to the article and approved the submitted version.

Funding

This study was supported by the National Natural Science Foundation of China (Grant numbers 81870348 and 81370387), the Nanjing Key Medical Science and Technology Development Project (Grant number ZKX19019), the Social Development Program of Jiangsu Province (Grant number BE2019604) and the National Science Fund For Distinguished Young Scholars (Grant Number 8220021461).

Acknowledgments

This work was supported by the Department of Vascular Surgery of Nanjing Drum Tower Hospital and the Medical School of Nanjing University. Thanks to Xiaoqiang Li, Min Zhou, Chen Liu, Feng Ran, Wei Wang, and Ming Zhang for their contribution to this research.

Conflict of interest

The authors declare that the research was conducted in the absence of any commercial or financial relationships that could be construed as a potential conflict of interest.

Publisher's note

Supplementary material

The Supplementary Material for this article can be found online at: https://www.frontiersin.org/articles/10.3389/fcvm.2023.1058440/full#supplementary-material.

References

1. LeMaire SA, Price MD, Green SY, Zarda S, Coselli JS. Results of open thoracoabdominal aortic aneurysm repair. *Ann Cardiothorac Surg*. (2012) 1:286–92. doi: 10.3978/j.issn.2225-319X.2012.08.16

2. Rosset E, Ben Ahmed S, Galvaing G, Favre JP, Sessa C, Lermusiaux P, et al. Editor's choice–hybrid treatment of thoracic, thoracoabdominal, and abdominal aortic aneurysms: a multicenter retrospective study. *Eur J Vasc Endovasc Surg*. (2014) 47:470–8. doi: 10.1016/j.ejvs.2014.02.013

3. Budtz-Lilly J, Wanhainen A, Mani K. Outcomes of endovascular aortic repair in the modern era. *J Cardiovasc Surg (Torino)*. (2018) 59:180–9. doi: 10.23736/S0021-9509.17.10332-0

4. Budtz-Lilly J, Vikholm P, Wanhainen A, Astudillo R, Thelin S, Mani K. Technical eligibility for endovascular treatment of the aortic arch after open type A aortic dissection repair. *J Thorac Cardiovasc Surg*. (2021) 162:770–7. doi: 10.1016/j.jtcvs.2019.12.113

5. Oderich GS, Ribeiro MS, Sandri GA, Tenorio ER, Hofer JM, Mendes BC, et al. Evolution from physician-modified to company-manufactured fenestrated-branched endografts to treat pararenal and thoracoabdominal aortic aneurysms. *J Vasc Surg*. (2019) 70:31–42. doi: 10.1016/j.jvs.2018.09.063

6. Kärkkäinen JM, Tenorio ER, Jain A, Mendes BC, Macedo TA, Pather K, et al. Outcomes of target vessel endoleaks after fenestrated-branched endovascular aortic repair. *J Vasc Surg*. (2020) 72:445–55. doi: 10.1016/j.jvs.2019.09.055

7. Wanhainen A, Verzini F, Van Herzeele I, Allaire E, Bown M, Cohnert T, et al. Editor's choice—european society for vascular surgery (ESVS) 2019 clinical practice guidelines on the management of abdominal aorto-iliac artery aneurysms. *Eur J Vasc Endovasc Surg*. (2019) 57:8–93. doi: 10.1016/j.ejvs.2018.09.020

8. Chaikof EL, Dalman RL, Eskandari MK, Jackson BM, Lee WA, Mansour MA, et al. The society for vascular surgery practice guidelines on the care of patients with an abdominal aortic aneurysm. *J Vasc Surg*. (2018) 67:2–77. doi: 10.1016/j.jvs.2017.10.044

9. Kristmundsson T, Sonesson B, Dias N, Törnqvist P, Malina M, Resch T. Outcomes of fenestrated endovascular repair of juxtarenal aortic aneurysm. *J Vasc Surg*. (2014) 59:115–20. doi: 10.1016/j.jvs.2013.07.009

10. Kuzniar MK, Wanhainen A, Tegler G, Mani K. Endovascular treatment of chronic aortic dissection with fenestrated and branched stent grafts. *J Vasc Surg*. (2021) 73:1573–82. doi: 10.1016/j.jvs.2020.10.004

11. Tong Y, Qin Y, Yu T, Zhou M, Liu C, Liu C, et al. Three-Dimensional printing to guide the application of modified prefenestrated stent grafts to treat aortic arch disease. *Ann Vasc Surg*. (2020) 66:152–9. doi: 10.1016/j.avsg.2019.12.030

12. Aboyans V, Bauersachs R, Mazzolai L, Brodmann M, Palomares JFR, Debus S, et al. Antithrombotic therapies in aortic and peripheral arterial diseases in 2021: a consensus document from the ESC working group on aorta and peripheral vascular diseases, the ESC working group on thrombosis, and the ESC working group on cardiovascular pharmacotherapy. *Eur Heart J*. (2021) 42:4013–24. doi: 10.1093/eurheartj/ehab390

13. Li X, Li W, Dai X, Li W, Zhang J, Wang Z, et al. Thoracic endovascular repair for aortic arch pathologies with surgeon modified fenestrated stent grafts: a multicentre retrospective study. *Eur J Vasc Endovasc Surg*. (2021) 62:758–66. doi: 10.1016/j.ejvs.2021.07.017

14. Fattori R, Montgomery D, Lovato L, Kische S, Di Eusanio M, Ince H, et al. Survival after endovascular therapy in patients with type B aortic dissection: a report from the international registry of acute aortic dissection (IRAD). *JACC Cardiovasc Interv*. (2013) 6:876–82. doi: 10.1016/j.jcin.2013.05.003

15. Glower DD, Fann JI, Speier RH, Morrison L, White WD, Smith LR, et al. Comparison of medical and surgical therapy for uncomplicated descending aortic dissection. *Circulation*. (1990) 82:39–46. doi: 10.1002/ccd.1810210320

16. Kitagawa A, Greenberg RK, Eagleton MJ, Mastracci TM, Roselli EE. Fenestrated and branched endovascular aortic repair for chronic type B aortic dissection with thoracoabdominal aneurysms. *J Vasc Surg*. (2013) 58:625–34. doi: 10.1016/j.jvs.2013.01.049

17. van Prehn J, Schlösser FJ, Muhs BE, Verhagen HJ, Moll FL, van Herwaarden JA. Oversizing of aortic stent grafts for abdominal aneurysm repair: a systematic review of the benefits and risks. *Eur J Vasc Endovasc Surg*. (2009) 38:42–53. doi: 10.1016/j.ejvs.2009.03.025

frontiers | Frontiers in Cardiovascular Medicine

TYPE Original Research
PUBLISHED 30 March 2023
DOI 10.3389/fcvm.2023.1055549

Check for updates

OPEN ACCESS

EDITED BY
Massimo Bonacchi,
University of Florence, Italy

REVIEWED BY
Petar Zlatanovic,
University of Belgrade, Serbia
Jinbao Qin,
Shanghai Jiao Tong University, China
Guangmin Yang,
Nanjing Drum Tower Hospital, China

*CORRESPONDENCE
Zhenjiang Li
✉ lizj0628@163.com
Hongkun Zhang
✉ 1198050@zju.edu.cn

†These authors have contributed equally to this work

SPECIALTY SECTION
This article was submitted to Heart Surgery, a section of the journal Frontiers in Cardiovascular Medicine

RECEIVED 27 September 2022
ACCEPTED 08 March 2023
PUBLISHED 30 March 2023

CITATION
Shen P, Li D, Wu Z, He Y, Wang X, Shang T, Zhu Q, Tian L, Li Z and Zhang H (2023) Physician-modified fenestration or *in situ* fenestration for preservation of isolated left vertebral artery in thoracic endovascular aortic repair.
Front. Cardiovasc. Med. 10:1055549.
doi: 10.3389/fcvm.2023.1055549

Physician-modified fenestration or *in situ* fenestration for preservation of isolated left vertebral artery in thoracic endovascular aortic repair

Peier Shen[1,2†], Donglin Li[2†], Ziheng Wu[2†], Yangyan He[2], Xiaohui Wang[2], Tao Shang[2], Qianqian Zhu[2], Lu Tian[2], Zhenjiang Li[2*] and Hongkun Zhang[2*]

[1]Department of Nursing, The First Affiliated Hospital, School of Medicine, Zhejiang University, Hangzhou, China, [2]Department of Vascular Surgery, The First Affiliated Hospital, School of Medicine, Zhejiang University, Hangzhou, China

Objective: To present our experience of preserving the isolated left vertebral artery (ILVA) with physician-modified fenestration (PM-F) or *in situ* fenestration (ISF) during thoracic endovascular aortic repair (TEVAR) for aortic pathologies involving aortic arch.
Methods: This is a single-center, retrospective, observational cohort study. Between June 2016 and December 2021, 9 patients (8 men; median age 60.0 years old) underwent TEVAR with ILVA reconstruction (PM-F, $n = 6$; ISF, $n = 3$) were identified and analyzed.
Results: The technical success rate was 100%. No early (<30 days) death occurred. No aortic rupture, major stroke or spinal cord injury was observed. The median follow up was 38.0 (rang: 1.0–66.0) months. One death occurred at 56 months, while the reason cannot be identified. No aortic rupture, major stroke or spinal cord injury was observed during follow up. No patient required reintervention. Out of the 22 successfully revascularized target vessels, 2 ILVAs were found occluded in 2 patients at 6 months and 7 months, respectively. However, these two patients were asymptomatic.
Conclusions: Our initial experience reveals that PM-F or ISF for ILVA preservation was feasible, safe, and effective during TEVAR for complex thoracic aortic pathologies. However, the patency of preserved ILVA should be improved.

KEYWORDS
isolated left vertebral artery, physician-modified fenestration, *in situ* fenestration, thoracic endovascular aortic repair, thoracic aortic disease

Introduction

Aortic arch branch variation was common in general population with a proportion approaching 20% (1), while in patients with thoracic aortic disease (TAD), the proportion rises to 33.5%. Isolated left vertebral artery (ILVA) arising directly from the aortic arch

Abbreviations
ILVA, isolated left vertebral artery; PM-F, physician-modified fenestration; ISF, *in situ* fenestration; TEVAR, thoracic endovascular aortic repair; TAD, thoracic aortic disease; LCCA, left common carotid artery; CTA, computed tomography angiography; LSA, left subclavian artery; BCT, brachiocephalic trunk; MAEs, Major adverse events; TV, target vessel.

was the second most common branch variation with a prevalence of 0.8%–6.6% in TAD (2–5).

It is prevalent that the posterior inferior cerebellar artery was supplied by ILVA (6). Further, in certain aortic arch anomalies, the left common carotid artery (LCCA) does not supply normal blood flow and the ILVA compensates for that (7). Hence, improper management of the ILVA may result in posterior stroke or spinal cord ischemia, especially if the arterial circle of Willis is incomplete. It was reported that a complete circle of Willis was seen in only 27% of Chinese people (8). However, there was no consensus on the indication for preservation of ILVA during TEVAR presently.

The strategies of ILVA reconstruction was still uncertain in current guidelines. ILVA transposition has been used with favorable results (9). Total endovascular reconstruction has the advantages of improved safety and reduced invasiveness. We presented our initial experience and short-term outcomes of total endovascular repair with physician-modified fenestration (PM-F) or *in situ* fenestration (ISF) for patients suffering from aortic arch pathology with an ILVA in the present study.

Methods

This is a single-center, retrospective, observational cohort study. All the TAD patients treated in our center between June 2016 and December 2021 were retrospectively re-evaluated (**Figure 1**).

Inclusion criteria were as follows: (1) TAD patients with ILVA underwent total endovascular repair; (2) ILVAs were reconstructed with PM-F or ISF techniques. The indications of aortic disease intervention were defined according to recommended clinical

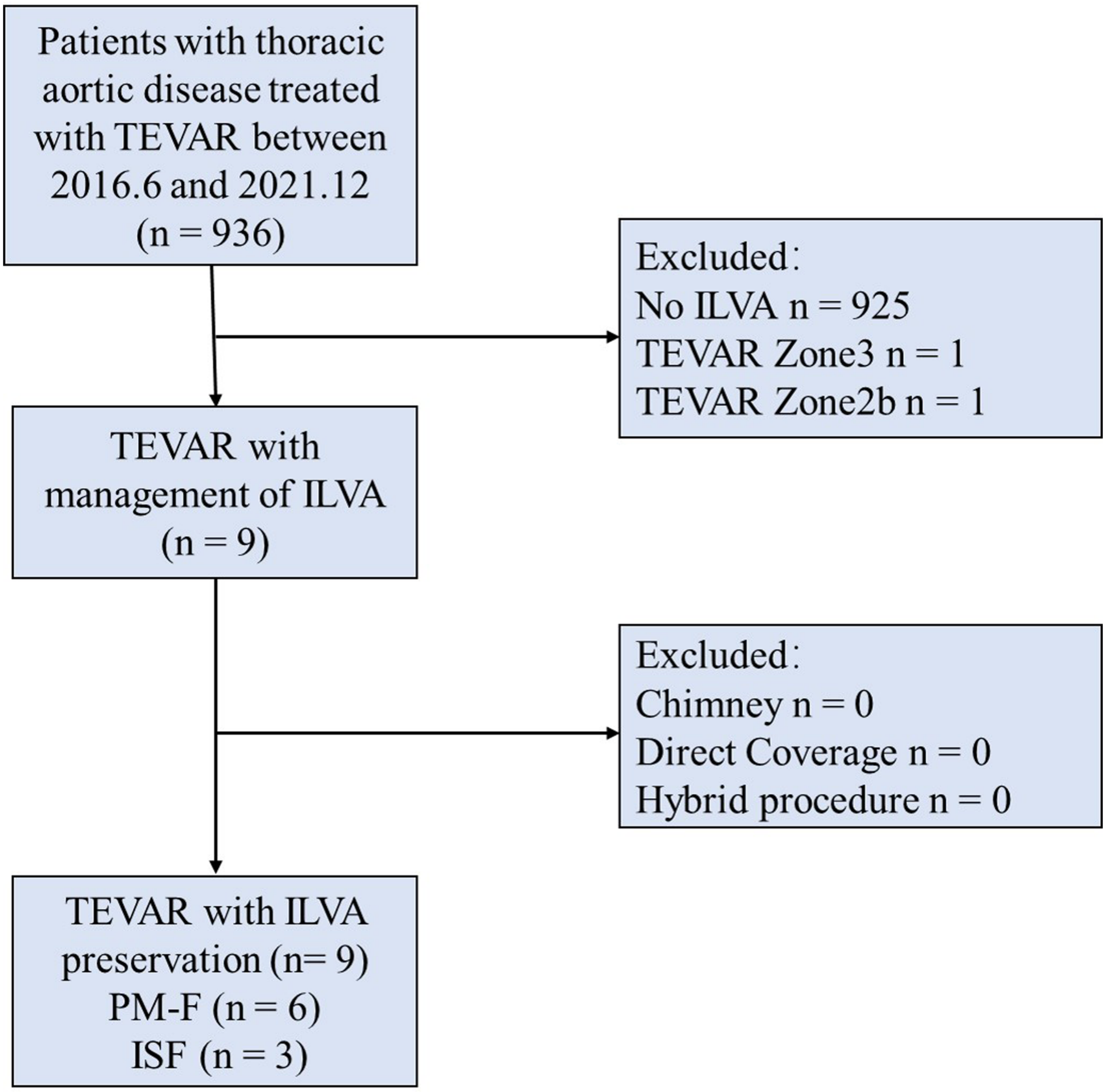

FIGURE 1
Consort diagram of thoracic aortic repairs (2017.6–2021.12; *n* = 936). TEVAR, thoracic endovascular aortic repair; ILVA, isolated left vertebral artery; PM-F, physician modified-fenestration; ISF, *in situ* fenestration.

practice Guidelines of the European Society for Vascular Surgery (ESVS) (10). In our center, ILVA revascularization was performed in patients with a dominant ILVA or symmetric vertebral arteries and an incomplete circle of Willis. Extensive coverage of the aorta is also considered an indication for ILVA preservation to prevent spinal cord ischemia. The ILVA revascularization was not considered in patients with dominant right vertebral artery or a small ILVA (<2.0 mm in diameter). We did not perform open ILVA revascularization in our center.

Exclusion criteria were as follows: (1) Patients without ILVA; (2) Patients treated with open surgery or hybrid procedure; (3) Patients underwent endovascular repair without ILVA reconstruction (Zone 3 TEVAR or Zone 2b TEVAR or direct coverage); (4) ILVAs were reconstructed with other endovascular technique such as parallel stents.

The study was conducted in accordance with the Declaration of Helsinki. The study was approved by institutional ethics committee of our hospital (No. 20221434) and individual consent for this retrospective analysis was waived. We present the following article in accordance with the STROBE reporting guidelines.

All patients underwent preoperative computed tomography angiography (CTA) with 3-dimensional reconstructions on a workstation (QUARIUS WS, Terarecon Inc, Mateo, CA;). The stent-grafts were oversized 5%–10% for aortic dissections and 15%–20% for aortic aneurysms and penetrated ulcers. A landing zone of at least 1.5 cm away from proximal end of aortic lesions along the outer curvature of aortic arch was planned for either technique.

Physician modified-fenestration for isolated left vertebral artery

Based on the three-dimension reconstruction, the information including the aortic diameters, the aortic arch angle, the branch vessel diameters, lengths, angles to the arch, clock positions, relative spatial relationships among the branches were taken into consideration to design the location of the fenestrations for ILVA. The strut-free area between the stent struts was preferred as the site of fenestration. The size of the fenestration was designed equal to or slightly smaller than the diameter of the ILVA origin. Then a circular fenestration was created with a cautery device or a knife. Two radiopaque markers were sewn onto the proximal and distal edge of the fenestration.

The main stent graft was introduced and rotated in the descending aorta to adjust the position of fenestration. The fenestration was oriented toward the ILVA by aligning the radiopaque markers with the origin of ILVA. Bridge stent implantation was preferred for aortic lesions not located on the lesser curvature. After full deployment of the stent graft, a bare metal stent of 3.5 mm to 5 mm in diameter was deployed (**Supplementary Material**, **Figure 2**). The bare stent used were balloon-expandable bare stent [Dynamic Renal (BIOTRONIK AG, Buelach, Switzerland) or Apollo (Microport, Shanghai, China)] or self-expandable bare stent [Pulsar-18 (BIOTRONIK AG, Buelach, Swizerland)].

In situ fenestration for isolated left vertebral artery

An incision was made at the interval of sternocleidomastoid branches, one attaching on manubrium while the other attaching on proximal part of the clavicle for exposure of ILVA. Then a 6F short sheath was introduced into ILVA. After full deployment of the stent graft, a liver biopsy needle (18 gauge/30 cm, BARD) was introduced *via* the short sheath, and advanced to the ostium of ILVA. After the tip was adjusted perpendicular to the greater curvature of the aortic stent graft, the membrane of the stent graft was penetrated to make a fenestration. The fenestration was dilated with a 3- or 4 mm balloon and then a 4- to 5 mm bare metal stent was deployed as a bridge stent. Post-dilation with a 3- or 4 mm balloon was then conducted routinely (**Figure 3**, **Supplementary Material**).

In our center, the left subclavian artery (LSA), brachiocephalic trunk (BCT) and LCCA were generally reconstructed by ISF technique if required (11), regardless of the technique used for ILVA reconstruction. Chimney technique was only considered when the supra aortic arch vessel was accidently partially covered by thoracic stent graft. The preferred subsequence for reconstruction was LCCA, BCT, ILVA and LSA. For patients requiring fenestration of the LSA, an 8F angle-adjustable sheath (Lifetech, Inc., Shenzhen, China) was exchanged from the left brachial artery access. Then an adjustable needle catheter (12) was advanced *via* the sheath and punctured the aortic stent graft at an as perpendicular as possible angle. After sequential ballooning with 4-, 8-, and 10 mm balloon, a bridging stent with appropriate sizes was implanted. For patients requiring fenestration of both the LCCA and LSA, a liver biopsy needle (18 gauge/30 cm, BARD) was used to create the LCCA fenestration first. The balloon dilatation and stent implantation of the LCCA were similar to the procedures of LSA fenestration. For patients requiring fenestration of LCCA, BCT and LSA (13), LCCA was reconstructed first followed by BCT reconstruction. The cardiopulmonary bypass was applied between coverage of LCCA and BCT and successful reconstruction of the two TVs (13).

After the procedure, mono-antiplatelet therapy (aspirin, 100 mg/day) was prescribed for long-term therapy.

Follow up

Demographic, anatomical, intra-operative, and post-operative data were recorded. All patients underwent computerized tomography (CT) scan pre-operatively and before discharge. The follow up protocol included CT scan at 1, 3, 6, and 12 months and yearly thereafter (14). The follow up clinical data was obtained during patient visits to the hospital, other hospital stays, or by telephone interview.

Definition and outcomes

The results were presented according to the guidelines for reporting standards in TEVAR (15). Technical success was

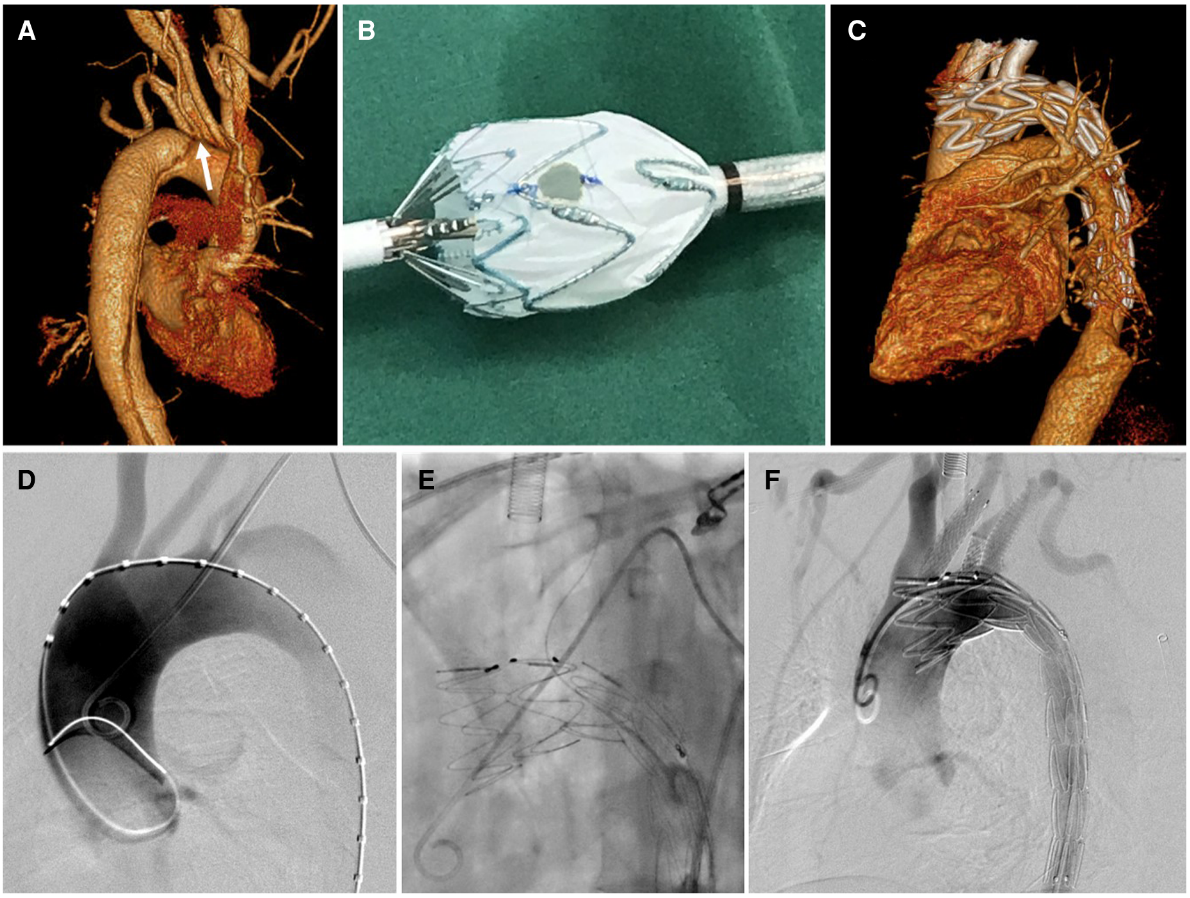

FIGURE 2
Physician modified-fenestration for isolated left vertebral artery. (A) Preoperative CTA of a type B aortic dissection demonstrating the ILVA (white arrow) from the distal aortic arch between the LCCA and the LSA; (B) A fenestration was made on the main body stent graft for preservation of ILVA on table; (C) follow up CTA showed patent target vessels and well excluded aortic dissection without endoleak; (D) intraoperative aortography showed a type B aortic dissection with a ILVA; (E) After full deployment of the stent graft, the ILVA was super-selected from the contralateral femoral access followed by bridging stent implantation; (F) Final aortography demonstrated complete exclusion of aortic dissection and patent aortic arch branch arteries, with bridging stent-grafts in the LCCA, ILVA, and LSA.

defined as successful deployment of all stent grafts with patent TVs and exclusion of the lesion in the absence of surgical conversion to open repair or death at 24 h or less without type I or III endoleak in the completion angiogram. Major adverse events (MAEs) included all-cause mortality, major stroke, paraplegia, myocardial infarction, respiratory failure, renal function decline or new-onset dialysis, bowel ischemia, and other major complications. Target vessel stenosis less than 50% was defined as patency. Short term was defined as the first 30 postoperative days. The follow up index was defined as the ratio between the investigated follow-up period and the theoretically possible follow-up period up to the pre-specified study end date (16). Classification of the vertebral artery variable origin was defined according to Lazaridis' report (4). Aortic arch aneurysms were classified according to Cooley's report (17) based on the extent of the aneurysm and the repair. The primary endpoints were all-cause mortality and neurologic new symptoms. The secondary endpoints were ILVA patency rate, endoleak and other complications.

Statistical analysis

Statistical analysis was performed using SPSS software (version 19.0; SPSS, Inc., Chicago, IL, United States). Continuous variables were summarized as means ± standard deviations if normally distributed, and as median and range if not. Categorical variables were expressed as count and percentage.

Results

Between June 2016 and December 2021, a total of 9 TAD patients (88.9% male with median age of 60.0 years, range: 38.0–76.0) underwent TEVAR and ILVA reconstruction. According to the proposed classification (4), ILVA presented with the LA2.2 configuration in all patients. Left VA dominance, right VA dominance and symmetric VA were found in two (22.2%), two (22.2%) and five (55.6%) patients. In eight (88.9%) patients, the

 10.3389/fcvm.2023.1055549

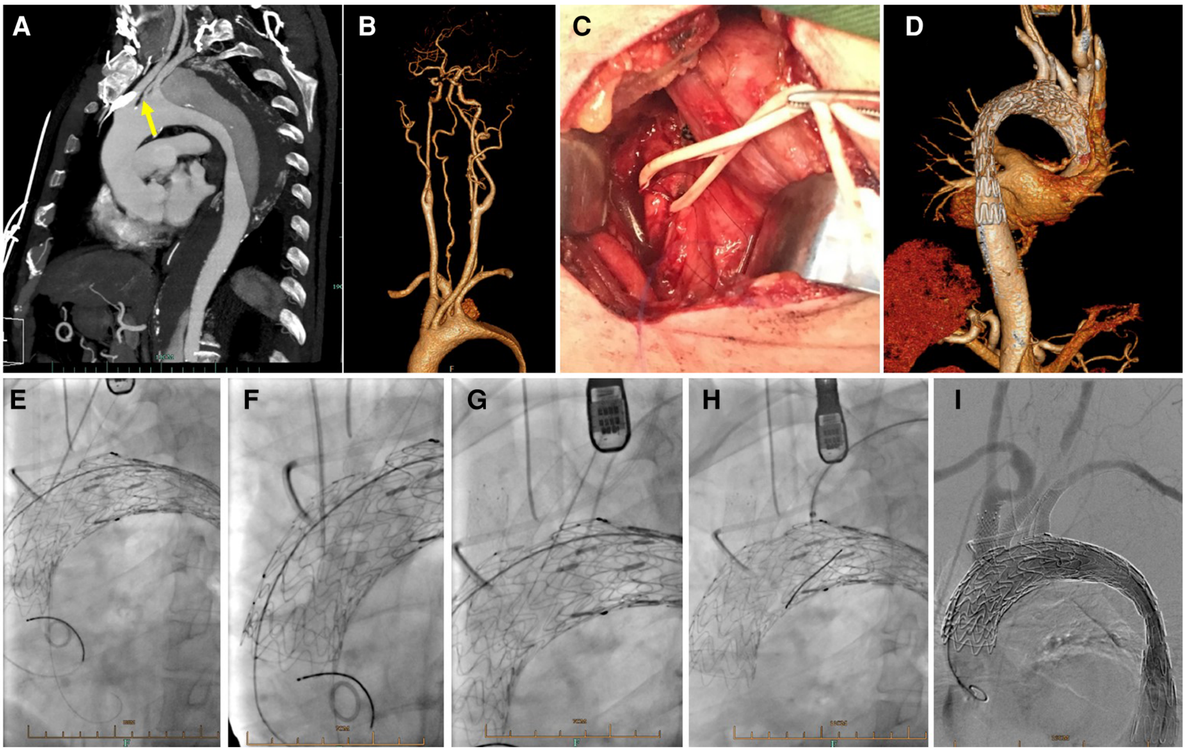

FIGURE 3
In situ fenestration for isolated left vertebral artery. (A) Preoperative CTA showed a type B aortic dissection with ILVA (yellow arrow); (B) The cervicle contrast-enhanced CTA demonstrated dominant ILVA and incomplete circle of Willis; (C) During procedure, the ILVA was exposed with a supraclavicular incision; (D) Follow up CTA showed well exclusion of aortic dissection and patent supra aortic branches; Needle-assisted *in situ* fenestration followed by bridging stents placement for reconstruction of LCCA (E), BCT (F), ILVA (G) and LSA (H) after deployment of stent graft; (I) Complete aortography demonstrated excluded aortic dissection and patent branch vessels.

ILVAs entered the circle of Willis to form the basilar artery. In eight (88.9%) patients, the ILVAs sent off the posterior-inferior cerebellar artery. Demographic characteristics and baseline clinical data are detailed in **Table 1**.

All patients received TEVAR with aortic arch branches reconstruction. The technical success rate was 100%. Two TVs (LSA and ILVA) were reconstructed in 6 patients, three TVs (LSA, ILVA, and LCCA) in 2 patients and four TVs (LSA, ILVA, LCCA and BCT) in one patient. Totally, 22 TVs were successfully reconstructed (ISF used for 15 TVs, PM-F for 6 TVs and Chimney technique for one TV) and 19 bridging stents (9 covered stents and 10 bare metal stents) were placed in 19 TVs. Among the nine preserved ILVAs, PM-F technique were used for 6 TVs while ISF technique were used for 3 TVs. Six bare metal stents were placed in 6 ILVAs. In three ILVAs preserved with PM-F, stent was not deployed. The main body stent grafts used were the Ankura (Lifetech, Shenzhen, China; $n = 5$), Valiant (Medtronic, Inc, Minneapolis, MN, United States; $n = 3$) and TAG (Gore, WL Gore & Associates, Flagstaff, AZ, United States; $n = 1$) devices. The median procedure time was 170.0 (range: 110.0–375.0) min and the volume of contrast material was 105.0 (range: 90.0–200.0) ml. The median hospitalization was 11.0 (range: 7–24) days and the median length of stay in ICU after the operation was 0 (range: 0–1) days (**Table 2**).

There was no early mortality within 30 days after procedure. No aortic rupture, major stroke, spinal cord injury, acute kidney injury, renal failure and other major adverse event was observed. No endoleak was detected *via* 30-day follow up CTA. No patient received reintervention. All TVs were patent without occlusion/stenosis or bridging stent migration.

The median follow up was 38.0 (range: 1.0–66.0) months. All patients were followed up and the mean follow up index was 1.0 ± 0.0. During follow up period, one death occurred at 56 months resulting in a follow up mortality of 11.1% (1/9). The reason for death cannot be identified. Out of the 22 successfully revascularized TVs, 20 TVs remained patent while 2 ILVAs were found occluded. The ILVAs occlusion occurred at 6 months and 7 months, respectively. The ILVA patency rate was 77.8% (7/9). Fortunately, these patients were all asymptomatic. Hence, further reintervention was not needed. No other major adverse event including aortic rupture, major stroke or spinal cord injury was observed during follow up. No endoleak was detected *via* follow up CTA. No significant stenosis, kink, fracture and migration of branch stents were observed. No patient received reintervention (**Table 3**). The follow-up CTA indicated that all the patients exhibited a reduction in the diameter of the aneurysm and the thrombosed false lumen. The median maximum aortic diameters were 36.0 (range: 25.0–66.0) mm preoperatively and 30.2 (range: 22.0–63.0) mm at last follow up, respectively ($p = .001$).

TABLE 1 Demographics and baseline clinical characteristics ($n = 9$).

Variable	*N* (%) or median (range)
Age [years, median (range)]	60.0 (38.0–76.0)
Sex	
Male	8 (88.9%)
Female	1 (11.1%)
Comorbidities	
Hypertension	6 (66.7%)
Hyperlipidemia	0
COPD	1 (11.1%)
Diabetes	2 (22.2%)
Coronary artery disease	1 (11.1%)
Myocardial infraction	0
Congestive heart failure	0
Previous stroke	1 (11.1%)
Peripheral artery disease	0
Renal insufficiency	0
Renal failure	0
Previous aortic surgery	0
History of tumor	1 (2.6%)
Cigarette Use	7 (77.8%)
ASA classification	
II	5 (55.6%)
III	4 (44.4%)
Pathology	
Type B aortic dissection	4 (44.4%)
Acute	2 (22.2%)
Chronic	2 (22.2%)
Thoracic aortic aneurysm	4 (44.4%)
PAU	1 (11.1%)
Anatomic features	
ILVA configuration	
LA2.2[a]	9 (100.0%)
Left vertebral artery dominance	2 (22.2%)
Right vertebral artery dominance	2 (22.2%)
Symmetric vertebral artery	5 (55.6%)
ILVA diameter, mm	3.4 (3.0–4.2)
Right vertebral artery diameter, mm	4.0 (3.0–5.1)
Complete circle of Willis	2 (22.2%)
ILVA entering the circle of Willis to form the basilar artery	8 (88.9%)
ILVA sending off the posterior–inferior cerebellar artery	8(88.9%)

COPD, chronic obstructive pulmonary disease; PAU, Penetrating atherosclerotic ulcer; ILVA, Isolated left vertebral artery.
[a]The ILVA configuration classification was based on Lazaridis' report (*Surg Radiol Anat*. 2018; **40**:779–97).

TABLE 2 Procedure details.

Variable	*N* (%) or median (range)
Emergency operation	0
Technical success	9 (100%)
Procedure time, minutes	170.0 (110.0–375.0)
Volume of contrast material, ml	105.0 (90.0–200.0)
Length of thoracic aortic endografts, mm	160.0 (150.0–200.0)
Diameter of thoracic aortic endografts, mm	32.0 (30.0–40.0)
Proximal landing zone	
Z2	6 (66.7%)
Z1	2 (22.2%)
Z0	1 (11.1%)
Distal landing zone	
Z5	9 (100%)
Total target vessel	
LSA	9
ILVA	9
LCCA	3
BCT	1
No. of bridging stents per patient	2.0 (1.0–4.0)
Technique for ILVA reconstruction	
ISF	3 (33.3%)
Pre-fenestration	6 (66.6%)
Stent placement in ILVA, patient	6 (66.7%)
Covered stent	0
Bare metal stent	6 (66.7%)
Length of ILVA stent, mm	26.0 (19.0–40.0)
Diameter of ILVA Stent, mm	4.25 (3.5–5.0)
Length of stay, days	11.0 (7.0–24.0)
Length of ICU stay, days	0 (0–1.0)

LSA, left subclavian artery; ILVA, isolated left vertebral artery; LCCA, left common carotid artery; BCT, brachiocephalic trunk; ICU, intensive care unit.

TABLE 3 Follow up outcomes.

Variable	*N* (%) or median (range)
Follow-up, months	38.0 (1.0–66.0)
FU mortality	1 (11.1%)
FU MAE	3 (33.3%)[a]
FU endoleak	
Type I	0
Type II	0
Type III	0
FU Re-intervention	0
FU TV instability[b]	2 (22.2%)
Branch vessels	
Branch occlusion/stenosis	2 (22.2%)
Bridging stent migration	0
ILVA occlusion/stenosis	2 (22.2%)

MAE, major adverse event; TV, target vessel; ILVA, isolated left vertebral artery; FU, follow up.
[a]Follow up MAE included one death and two ILVA occlusions taking place during follow up period.
[b]TV instability means composite end point used to define any death or rupture related to side branch complication (e.g., endoleak, rupture) or any secondary intervention indicated to treat a branch-related complication, including endoleak, disconnection, kink, stenosis, occlusion, or rupture.

Discussion

ILVA is not a rare aortic arch branch variation, which is more common in TAD patients (1). The presence of an ILVA has significant impact on the choice of aortic arch reconstruction techniques and cerebral protection methods (18). Current literature reported several options such as total open surgery (18), hybrid procedure (9, 19) and parallel stents technique (20) to deal with aortic arch lesions and ILVAs. However, there was no consensus on the indication and strategy for ILVA reconstruction to date, as the relevant studies were scarce.

ILVA can enter into basilar artery and terminate at posterior inferior cerebellar artery (PICA), which can supply the brainstem and cerebellum. It is necessary to manage the ILVA better to prevent posterior circulation ischemia, stroke and spinal cord injury, instead of direct coverage. According to Ding and his colleague's experience (21), preservation of ILVA was favored, if ILVA was dominant, or if bilateral vertebral artery was symmetric with an incomplete circle of Willis. Differently, Yang and his colleague (9) held that all ILVA should be preserved if possible based on the fact that the prevalence of complete circle of Willis was 42% in western population and only 27% in Chinese population (8, 22). And, Piffaretti and his colleagues held that reconstruction of a nondominant ILVA can help reduce the potential risk of spinal cord ischemia in patients with additional risk factors such as previous extensive aortic coverage (19). We favored a positive strategy to preserve ILVA for a high incidence (73%) of an incomplete circle of Willis in the Chinese population (8). In our clinical practice, we performed ILVA revascularization in patients with a dominant ILVA or symmetric vertebral arteries and an incomplete circle of Willis. Extensive coverage of the aorta is also considered an indication for ILVA preservation to prevent spinal cord ischemia. The ILVA revascularization was not performed in patients with dominant right vertebral artery or a small ILVA (<2.0 mm in diameter).

Currently, during open surgery and hybrid procedure, ILVA transposition combined with LSA transposition seemed a feasible and reliable approach. The limited evidence from recently published case series showed high technical success rate and high long-term ILVA patency rate (9, 19). During perioperative and follow up period, there was no neurological complications. However, the small sample size and short follow-up limited the quality of the evidence. An endovascular approach was worth trying to provide a less invasive and more expeditious method which can be completed in one stage. **Table 4** (9, 18, 19, 23–25) has summarized the results of various techniques for ILVA revascularization from currently published case series (number of patients >1) to date.

Parallel grafts such as the chimney technique has been used for preservation of ILVA, implying a feasible alternative with encouraging short-term results (20). However, the risk of type Ia endoleaks through the gutters and uncertainty regarding the long-term patency of artery remain a concern (26). PM-F (27) and ISF (11) has been used in supra-aortic branches reconstruction. The published literature showed that these two techniques were promising and reliable methods excluding the

TABLE 4 Techniques for preservation of isolated left vertebral artery: Literature summary[a].

Author	Year	No.	Disease	Treatment for aortic disease	ILVA preservation	Success rate	Early outcomes	FU (moths)	FU outcomes	FU ILVA patency
Suzuki et al. (24)	2006	10	TAA($n = 8$) TAD($n = 2$)	Open repair	[b]en-bloc technique ($n = 1$); Transposition ($n = 9$)	100%	None	NA	NA	NA
Qi et al. (23)	2013	21	TAD	Open repair	en-bloc technique ($n = 12$); Transposition ($n = 9$).	100%	2 spinal cord injury; 1 transient neurologic deficit; 1 acute renal failure.	58 ± 16	1 late death	NA
Zhu et al. (18)	2015	3	TAD	Open repair	Transposition	100%	None	44 ± 19	1 patient underwent TEVAR for descending aortic dissection	100%
Piffaretti et al. (19)	2020	6	TAA($n = 3$) TAD($n = 3$)	Open repair ($n = 4$) TEVAR($n = 2$)	Transposition	100%	1 horner's syndrome; 1 respiratory insufficiency	Mean 4.5	1 death at 4 month	100%
Yang et al. (9)	2021	13	TAA($n = 2$) TAD($n = 8$) IMH($n = 2$) PAU($n = 1$)	TEVAR	Transposition	100%	1 contrast induced acute kidney injury; 1 incision hematoma; 1 acute left-lower-limb ischemia	Mean 22	None	100%
Zhang et al. (25)	2022	67	TAA($n = 12$) TAD($n = 43$) IMH($n = 7$) PSA ($n = 5$)	TEVAR	Chimney ($n = 28$); Pre-fenestration ($n = 24$) Transposition ($n = 15$)	100%	9 Ia endoleak	64 ± 4	7 neurologic new symptoms; 9 Ia endoleak; 5 mild-dizziness	[c]97%

TAA, thoracic aortic aneurysm; TAD, thoracic aortic dissection; ILVA, isolated left vertebral artery; FU, follow up; NA, not available; TEVAR, Thoracic Endovascular Aortic Repair; IMH, intramural hematoma; PAU, penetrating atherosclerotic ulcer; PSA, pseudoaneurysm.
[a]Only case series ($n > 1$) were included.
[b]En-bloc technique means a single aortic patch containing the origin of the ILVA and the left subclavian artery or left common carotid artery was anastomosed to the prosthetic graft.
[c]Two patients in ILVA transposition group were found to have an occluded ILVA.

lesions and preserving the target vessels. To date, these two techniques has not been reported for preservation of ILVA during TEVAR. Based on our experience of performing PM-F and ISF for preservation of other target vessels, less invasive and total endovascular method was provided for the patients in this case series. For patients requiring reconstruction of both the ILVA and LSA, PM-F technique was preferred as the cervical incision can be avoid. For patients requiring reconstruction of more supra-arch branches, ISF was preferred as ILVA can be exposed simultaneously during exposing LCCA in which cervical incision was inevitable. During perioperative period, the technical success rate was high without major adverse events and procedure-related vessel injury, nerve injury, chyle leakage and lymphatic leakage in this case series. All target vessels were patent during short-term period (<30 days). Currently, both laser fenestration technique and needle fenestration technique had been reported to be used during *in situ* fenestration procedure for treatment of aortic arch disease with favorable outcomes (11, 28). We preserved the ILVA using needle assisted fenestration technique in these patents for we were familiar with needle fenestration procedure. Laser fenestration technique could also be considered as a potential adjunct for ILVA revascularization based on experience of different centers.

Some drawbacks still existed and raised some concern during application of these two techniques. For PM-F, massive pre-operative measurements and accurate deployment were needed for better alignment of fenestrations to the ostium of target vessels. The process of stent graft modification would extend the operation time. The modification procedure of removing a part of membrane may impact the integrity and durability of the stent graft. And the short junction between the main body stent graft and the bridging stent may increase the risk of type III endoleak. For ISF, the manipulation is really technical demanding. Vessel injury may occur during fenestration process. The supra arch arteries and cerebral blood supply has to be blocked before successful fenestration which could increase the risk of cerebral ischemia. And the concern of high risk of type III endoleak still existed for short combination of the main body stent graft and the bridging stents (29). However, our initial experience showed that favorable short-term results can be achieved without neurological deficits and other major complications.

At present, limited data on ILVA transposition during open surgery and hybrid procedure has been published showing satisfactory patency rate during short-term follow up period (9, 18, 19). But the interpretation of the results should be careful as the number of patients was small and the studies were single-center retrospective case series showing high risk of bias. In our study, patency rate was favorable during postoperative period. However, the patency rate dramatically decreased around 6 months follow up. This initial experience implied unsatisfied long-term patency (77.8%) of ILVA reconstructed by PM-F or ISF. However, it should be note that the mean diameter of ILVA in this study (3.4 mm) was smaller compared with the figure of 5.1 mm in the current literature (9). On the other hand, there was no cerebral infarction or SCI observed in the two patients with ILVA occlusion. It is difficult to determine why patients do not have severe posterior circulation ischemia related symptoms or spinal cord ischemia after vertebral artery occlusion. The plausible explanation was that ILVA occlusion after ILVA reconstruction is a relatively slow process (around 6 months). Collateral pathways can develop and compensate for posterior circulation ischemia during that process, which is different from acute ischemia caused by direct coverage without collateral pathways compensation. Nonetheless, as current evidence was really scarce, it may be reasonable to preserve ILVA to decrease risk of cerebral ischemia and spinal cord injury. The endovascular technique is a worthwhile alternative with less invasiveness.

Limitations

There are some limitations of this study. This is a single center, retrospective observational study with a relatively small number of patients and relatively shorter follow-up period. In addition, it lacks control groups. Further, the surgeon experience may impact the results of the procedure.

Conclusions

PM-F or ISF for ILVA preservation was feasible, safe, and effective. Issues on indication and technical strategy for ILVA preservation should be better discussed and clarified. And, the patency of ILVA preserved by PM-F or ISF should be further improved.

Data availability statement

The original contributions presented in the study are included in the article/Supplementary Material, further inquiries can be directed to the corresponding authors.

Ethics statement

The studies involving human participants were reviewed and approved by Institutional ethics committee of the First Affiliated Hospital, School of Medicine, Zhejiang University. The ethics committee waived the requirement of written informed consent for participation.

Author contributions

These authors have contributed significantly to the submitted work. The contribution of each author is as follows: Conception and design: HZ, ZL; analysis and interpretation of data: PS, ZL, YH, QZ, and TS; writing the article: PS, DL and ZW; critical revision of the article: XW, TS, and HZ; statistical analysis: LT and ZW; obtained funding: ZL, HZ and DL. All authors contributed to the article and approved the submitted version.

Funding

This study was funded by the National Natural Science Foundations of China (grant no. 82000430), Major Science and Technology Project in Medical and Health of Zhejiang Province (co-constructed Project by Province and the Ministry, grant no. 2020380400, WKJ-ZJ-2003), Key R&D Program of Zhejiang province (grant no. 2019C03013) and the Health project of Zhejiang Province (grant no. 2021KY673).

Acknowledgments

We thank Mengyun Yao, BS for her contribution to the data collection. The authors have completed the STROBE reporting checklist. The authors are accountable for all aspects of the work in ensuring that questions related to the accuracy or integrity of any part of the work are appropriately investigated and resolved.

Conflict of interest

The authors declare that the research was conducted in the absence of any commercial or financial relationships that could be construed as a potential conflict of interest.

Publisher's note

All claims expressed in this article are solely those of the authors and do not necessarily represent those of their affiliated organizations, or those of the publisher, the editors and the reviewers. Any product that may be evaluated in this article, or claim that may be made by its manufacturer, is not guaranteed or endorsed by the publisher.

Supplementary Material

The Supplementary Material for this article can be found online at: https://www.frontiersin.org/articles/10.3389/fcvm.2023.1055549/full#supplementary-material.

References

1. Dumfarth J, Chou AS, Ziganshin BA, Bhandari R, Peterss S, Tranquilli M, et al. Atypical aortic arch branching variants: a novel marker for thoracic aortic disease. *J Thorac Cardiovasc Surg.* (2015) 149(6):1586–92. doi: 10.1016/j.jtcvs.2015.02.019

2. Celikyay ZR, Koner AE, Celikyay F, Denız C, Acu B, Firat MM. Frequency and imaging findings of variations in human aortic arch anatomy based on multidetector computed tomography data. *Clin Imaging.* (2013) 37(6):1011–9. doi: 10.1016/j.clinimag.2013.07.008

3. Popieluszko P, Henry BM, Sanna B, Hsieh WC, Saganiak K, Pękala PA, et al. A systematic review and meta-analysis of variations in branching patterns of the adult aortic arch. *J Vasc Surg.* (2018) 68(1):298–306.e10. doi: 10.1016/j.jvs.2017.06.097

4. Lazaridis N, Piagkou M, Loukas M, Piperaki ET, Totlis T, Noussios G, et al. A systematic classification of the vertebral artery variable origin: clinical and surgical implications. *Surg Radiol Anat.* (2018) 40(7):779–97. doi: 10.1007/s00276-018-1987-3

5. Tapia GP, Zhu X, Xu J, Liang P, Su G, Liu H, et al. Incidence of branching patterns variations of the arch in aortic dissection in Chinese patients. *Medicine (Baltimore).* (2015) 94(17):e795. doi: 10.1097/MD.0000000000000795

6. Ohkura K, Shiiya N, Washiyama N, Yamashita K, Takahashi D, Tsuda K, et al. Vertebral artery variations in thoracic aortic patients. *Eur J Cardiothorac Surg.* (2014) 46(1):27–31. doi: 10.1093/ejcts/ezt609

7. Ad N, Lee P, Cox JL. Type A aortic dissection with associated anomaly of the carotid and vertebral vessels. *J Thorac Cardiovasc Surg.* (2002) 123(3):570–1. doi: 10.1067/mtc.2002.121673

8. Sun LZ, Qi RD, Chang Q, Zhu JM, Liu YM, Yu CT, et al. Is total arch replacement combined with stented elephant trunk implantation justified for patients with chronic stanford type A aortic dissection? *J Thorac Cardiovasc Surg.* (2009) 138(4):892–6. doi: 10.1016/j.jtcvs.2009.02.041

9. Yang G, Chen H, Sun G, Lou W, Chen X, Zhang L. Transposition of isolated left vertebral artery in hybrid thoracic endovascular aortic repair. *Front Cardiovasc Med.* (2021) 8:783656. doi: 10.3389/fcvm.2021.783656

10. Czerny M, Schmidli J, Adler S, van den Berg JC, Bertoglio L, Carrel T, et al. Current options and recommendations for the treatment of thoracic aortic pathologies involving the aortic arch: an expert consensus document of the European association for cardio-thoracic surgery (EACTS) and the European society for vascular surgery (ESVS). *Eur J Cardiothorac Surg.* (2019) 55(1):133–62. doi: 10.1093/ejcts/ezy313

11. Xiang Y, Qiu C, He Y, Li D, Shang T, Wu Z, et al. A single center experience of in situ needle fenestration of supra-aortic branches during thoracic endovascular aortic repair. *Ann Vasc Surg.* (2019) 61:107–15. doi: 10.1016/j.avsg.2019.03.016

12. Li Z, He Y, Zhang H. Antegrade in situ needle assisted fenestration during endovascular aortic repair for preserving renal arteries. *Eur J Vasc Endovasc Surg.* (2022) 63(2):360. doi: 10.1016/j.ejvs.2021.10.036

13. Shang T, Tian L, Li DL, Wu ZH, Zhang HK. Favourable outcomes of endovascular total aortic arch repair via needle based in situ fenestration at a mean follow-up of 5.4 months. *Eur J Vasc Endovasc Surg.* (2018) 55(3):369–76. doi: 10.1016/j.ejvs.2017.11.022

14. Erbel R, Aboyans V, Boileau C, Bossone E, Bartolomeo RD, Eggebrecht H, et al. 2014 ESC guidelines on the diagnosis and treatment of aortic diseases: document covering acute and chronic aortic diseases of the thoracic and abdominal aorta of the adult. The task force for the diagnosis and treatment of aortic diseases of the European society of cardiology (ESC). *Eur Heart J.* (2014) 35(41):2873–926. doi: 10.1093/eurheartj/ehu281

15. Fillinger MF, Greenberg RK, McKinsey JF, Chaikof EL. Society for vascular surgery ad hoc committee on TEVAR reporting standards. Reporting standards for thoracic endovascular aortic repair (TEVAR). *J Vasc Surg.* (2010) 52(4):1022–33. doi: 10.1016/j.jvs.2010.07.008.

16. von Allmen RS, Weiss S, Tevaearai HT, Kuemmerli C, Tinner C, Carrel TP, et al. Completeness of follow-up determines validity of study findings: results of a prospective repeated measures cohort study. *PLoS One.* (2015) 10(10):e0140817. doi: 10.1371/journal.pone.0140817

17. Cooley DA, Ott DA, Frazier OH, Walker WE. Surgical treatment of aneurysms of the transverse aortic arch: experience with 25 patients using hypothermic techniques. *Ann Thorac Surg.* (1981) 32:260–72. doi: 10.1016/S0003-4975(10)61048-X

18. Zhu JM, Qi RD, Liu YM, Zheng J, Xing XY, Sun LZ. Repair of complicated type B dissection with an isolated left vertebral artery using the stented elephant trunk technique. *Eur J Cardiothorac Surg.* (2016) 49(3):778–82. doi: 10.1093/ejcts/ezv242

19. Piffaretti G, Gelpi G, Tadiello M, Ferrarese S, Socrate AM, Tozzi M, et al. Transposition of the left vertebral artery during endovascular stent-graft repair of the aortic arch. *J Thorac Cardiovasc Surg.* (2020) 159(6):2189–2198.e1. doi: 10.1016/j.jtcvs.2019.06.011

20. Fan W, Li C, Zheng G, Pan Z, Rong J. Thoracic endovascular aortic repair in penetrating aortic ulcer combined with isolated left vertebral artery: a case report. *Medicine (Baltimore).* (2019) 98(37):e17159. doi: 10.1097/MD.0000000000017159

21. Ding H, Zhu Y, Wang H, Luo S, Liu Y, Huang W, et al. Management of type B aortic dissection with an isolated left vertebral artery. *J Vasc Surg.* (2019) 70(4):1065–71. doi: 10.1016/j.jvs.2018.11.052

22. Li Q, Li J, Lv F, Li K, Luo T, Xie P. A multidetector CT angiography study of variations in the circle of willis in a Chinese population. *J Clin Neurosci.* (2011) 18(3):379–83. doi: 10.1016/j.jocn.2010.07.137

23. Qi R, Sun L, Zhu J, Liu Y, Zheng J, Li C, et al. Total arch replacement in patients with aortic dissection with an isolated left vertebral artery. *Ann Thorac Surg.* (2013) 95(1):36–40. doi: 10.1016/j.athoracsur.2012.07.078

24. Suzuki K, Kazui T, Bashar AH, Yamashita K, Terada H, Washiyama N, et al. Total aortic arch replacement in patients with arch vessel anomalies. *Ann Thorac Surg*. (2006) 81(6):2079–83. doi: 10.1016/j.athoracsur.2005.12.062

25. Zhang H, Feng J, Guo M, Liu J, Xu D, Lu Y, et al. Management of an isolated left vertebral artery on the arch during zone 2-landing thoracic endovascular aortic repair: a multicentre retrospective study. *Eur J Vasc Endovasc Surg*. (2023) 65 (3):330–7. doi: 10.1016/j.ejvs.2022.11.007

26. Pecoraro F, Lachat M, Cayne NS, Pakeliani D, Rancic Z, Puippe G, et al. Mid-term results of chimney and periscope grafts in supra-aortic branches in high risk patients. *Eur J Vasc Endovasc Surg*. (2017) 54(3):295–302. doi: 10.1016/j.ejvs.2017.06.014

27. Li X, Li W, Dai X, Li W, Zhang J, Wang Z, et al. Thoracic endovascular repair for aortic arch pathologies with surgeon modified fenestrated stent grafts: a multicentre retrospective study. *Eur J Vasc Endovasc Surg*. (2021) 62(5):758–66. doi: 10.1016/j.ejvs.2021.07.017

28. Zhao Z, Qin J, Yin M, Liu G, Liu X, Ye K, et al. *In situ* laser stent graft fenestration of the left subclavian artery during thoracic endovascular repair of type B aortic dissection with limited proximal landing zones: 5-year outcomes. *J Vasc Interv Radiol*. (2020) 31(8):1321–7. doi: 10.1016/j.jvir.2020.02.025

29. Baba T, Ohki T, Maeda K. Current status of endovascular treatment for thoracoabdominal aortic aneurysms. *Surg Today*. (2020) 50(11):1343–52. doi: 10.1007/s00595-019-01917-3

frontiers | Frontiers in Cardiovascular Medicine

TYPE Original Research
PUBLISHED 03 April 2023
DOI 10.3389/fcvm.2023.1084851

Check for updates

OPEN ACCESS

EDITED BY
Hendrik Tevaearai Stahel,
University Hospital of Bern, Switzerland

REVIEWED BY
Edoardo Pasqui,
University of Siena, Italy
Doran Mix,
University of Rochester, United States
László Entz,
Semmelweis University, Hungary

*CORRESPONDENCE
Weifan Wang
wwfbaggio@163.com
Shilin Wei
weishilinv@qq.com

†These authors have contributed equally to this work

SPECIALTY SECTION
This article was submitted to Heart Surgery, a section of the journal Frontiers in Cardiovascular Medicine

RECEIVED 31 October 2022
ACCEPTED 15 March 2023
PUBLISHED 03 April 2023

CITATION
Wu X, Li Y, Zhao Y, Zhu Y, Wang S, Ma Q, Liu D, Gao B, Wei S and Wang W (2023) Efficacy of left subclavian artery revascularization strategies during thoracic endovascular aortic repair in patients with type B dissection: A single-center experience of 105 patients.
Front. Cardiovasc. Med. 10:1084851.
doi: 10.3389/fcvm.2023.1084851

Efficacy of left subclavian artery revascularization strategies during thoracic endovascular aortic repair in patients with type B dissection: A single-center experience of 105 patients

Xiangyang Wu[1†], Yongnan Li[1†], Yinglu Zhao[1], Yilin Zhu[1], Shixiong Wang[1], Qi Ma[1], Debin Liu[2], Bingren Gao[1], Shilin Wei[3]* and Weifan Wang[1]*

[1]Department of Cardiac Surgery, Lanzhou University Second Hospital, Lanzhou University, Lanzhou, China, [2]Department of Cardiac Surgery, Hainan General Hospital, Hainan, China, [3]Department of Thoracic Surgery, Lanzhou University Second Hospital, Lanzhou University, Lanzhou, China

Background: Left subclavian artery (LSA) revascularization during thoracic endovascular aortic repair (TEVAR) is necessary to reduce postoperative complications in patients with Stanford type B aortic dissection and an insufficient proximal anchoring area. However, the efficacy and safety of different LSA revascularization strategies remain unclear. Here, we compared these strategies to provide a clinical basis for selecting an appropriate LSA revascularization method.

Methods: In this study, we included 105 patients with type B aortic dissection who were treated using TEVAR combined with LSA reconstruction in the Second Hospital of Lanzhou University from March 2013 to 2020. They were divided into four groups according to the method used for LSA reconstruction, namely, carotid subclavian bypass (CSB; $n = 41$), chimney graft (CG; $n = 29$), single-branched stent graft (SBSG; $n = 21$), and physician-made fenestration (PMF; $n = 14$) groups. Finally, we collected and analyzed the baseline, perioperative, operative, postoperative, and follow-up data of the patients.

Results: The treatment success rate was 100% in all the groups, and CSB + TEVAR was the most commonly used procedure in emergency settings compared with the other three procedures ($P < 0.05$). The estimated blood loss, contrast agent volume, fluoroscopic time, operation time, and limb ischemia symptoms during the follow-up were significantly different in the four groups ($P < 0.05$). Pairwise comparison among groups indicated that the estimated blood loss and operation time in the CSB group were the highest (adjusted $P < 0.0083$; $P <$ 0.05). The contrast agent volume and fluoroscopy duration were the highest in the SBSG groups, followed by PMF, CG, and CSB groups. The incidence of limb ischemia symptoms was the highest in the PMF group (28.6%) during the follow-up. The incidence of complications (except limb ischemia symptoms) during the perioperative and follow-up periods was similar among the four groups ($P > 0.05$) The median follow-up time of CSB, CG, SBSG, and PMF groups was significantly different ($P < 0.05$), and the CSB group had the longest follow-up.

Conclusion: Our single-center experience suggested that the PMF technique increased the risk of limb ischemia symptoms. The other three strategies effectively and safely restored LSA perfusion in patients with type B aortic dissection and had comparable complications. Overall, different LSA revascularization techniques have their advantages and disadvantages.

KEYWORDS

type B aortic dissection, endovascular repair, left subclavian artery, revascularization, LSA reconstruction

Introduction

Aortic dissection (AD) is a life-threatening disease with an incidence of 35 cases per 100,000 people per year in patients aged 65–75 years (1). The Stanford type B dissection accounts for 25%–40% of all aortic dissections (2, 3). Since the description of thoracic endovascular aortic repair (TEVAR) by Dake et al. (4), several authors have reported the treatment of type B aortic dissections (TBADs) using TEVAR with favorable mid- and long-term outcomes (5–7). Moreover, the 2014 ESC guidelines recommend TEVAR as a first-line treatment for complicated TBADs (8).

Although TEVAR has revolutionized the treatment of TBADs, a minimum of 15 mm of the normal aortic wall is necessary to adequately fix stent grafts (9). However, the proximal seal zone is of inadequate length in 26%–40% of patients (10). In such cases, intentional coverage of the left subclavian artery (LSA) is often performed to extend the sealing zone. Nevertheless, the risk of serious complications, such as stroke, upper extremity ischemia, and spinal cord ischemia (SCI), increases with the coverage of LSA (11–13). Although LSA coverage is tolerated by some patients (14), the latest clinical trials and meta-analyses have revealed that a conventional LSA reconstruction could significantly decrease the risk of postoperative stroke and SCI (15–17).

The Society for Vascular Surgery practice guidelines recommend conventional LSA reconstruction in selected patients (18). However, the recommendations did not suggest the most effective technique for LSA revascularization. Chimney graft (CG), single-branched stent graft (SBSG), physician-made fenestration (PMF), and carotid–subclavian bypass (CSB) are the main methods for LSA revascularization. Here, we summarized our experience of TEVAR with CG, SBSG, PMF, and CSB performed on patients with type B aortic dissections involving the LSA and evaluated their perioperative and follow-up parameters.

Methods

This single-center retrospective cohort study was initiated by the Department of Cardiac and Vascular Surgery, Second Affiliated Hospital of Lanzhou University. A total of 350 TEVAR surgeries were performed from March 2013 to 2020, and 150 of them were performed on patients with type B aortic dissection and involved LSA management. The management strategy was determined by aortic anatomy, surgeon, and patients following strict inclusion and exclusion criteria. Patients were included based on the following criteria: (I) diagnosed with TBAD using computed tomography angiography (CTA); (II) diagnosed with an insufficient proximal landing zone (the entry tear located <15 mm distal to the LSA) using CTA; (III) no advanced kidney or liver disease; and (IV) no serious anatomic variation. Patients were excluded based on the following criteria: (I) Stanford type A aortic dissection; (II) a penetrating aortic ulcer; (III) a serious artery anatomic variation; (IV) a previous history of TEVAR; (V) severe kidney or liver disease; (VI) allergy to iodine contrast media; (VII) connective tissue disease. such as Marfan syndrome; and (VIII) a postoperative follow-up of <12 months.

Finally, we selected 105 patients with TBAD who were treated using TEVAR and LSA revascularization. These patients were divided into four groups based on the revascularization strategy used, and 41, 29, 21, and 14 patients were included in the CSB, CG, SBSG, and PMF groups, respectively (**Figures 1–4**). Informed signed consent was obtained from each patient included in this study, and the study protocol was approved by the Institutional Ethics Committee of the Second Affiliated Hospital of Lanzhou University (ID: 2021A-016).

Patient information, including demographics, procedural data, and outcomes, was obtained from the electronic medical records for further data analysis. The outcomes of this study included in-hospital mortality, stroke, all-cause mortality, LSA steal syndrome, and procedure-related reintervention. All preoperative variables, including cohort characteristics, and procedural variables, such as procedure type, characteristics, and timing, were studied to assess the difference between groups. All outcomes were defined using standard guidelines (8, 19).

Statistical analysis

SPSS 26.0 software was used for statistical analysis. Kolmogorov–Smirnov tests were performed to check data normality. Continuous variables were expressed as mean ± standard deviation. Comparisons between multiple groups were performed using a one-way analysis of variance (one-way ANOVA) when the variances were homogeneous. Comparisons between the two groups were performed with Tukey's test. When the variances were nonhomogeneous, we used the Games–Howell test. Continuous variables were expressed as medians and interquartile ranges if data were not normally distributed. Categorical variables were expressed as numbers and percentage

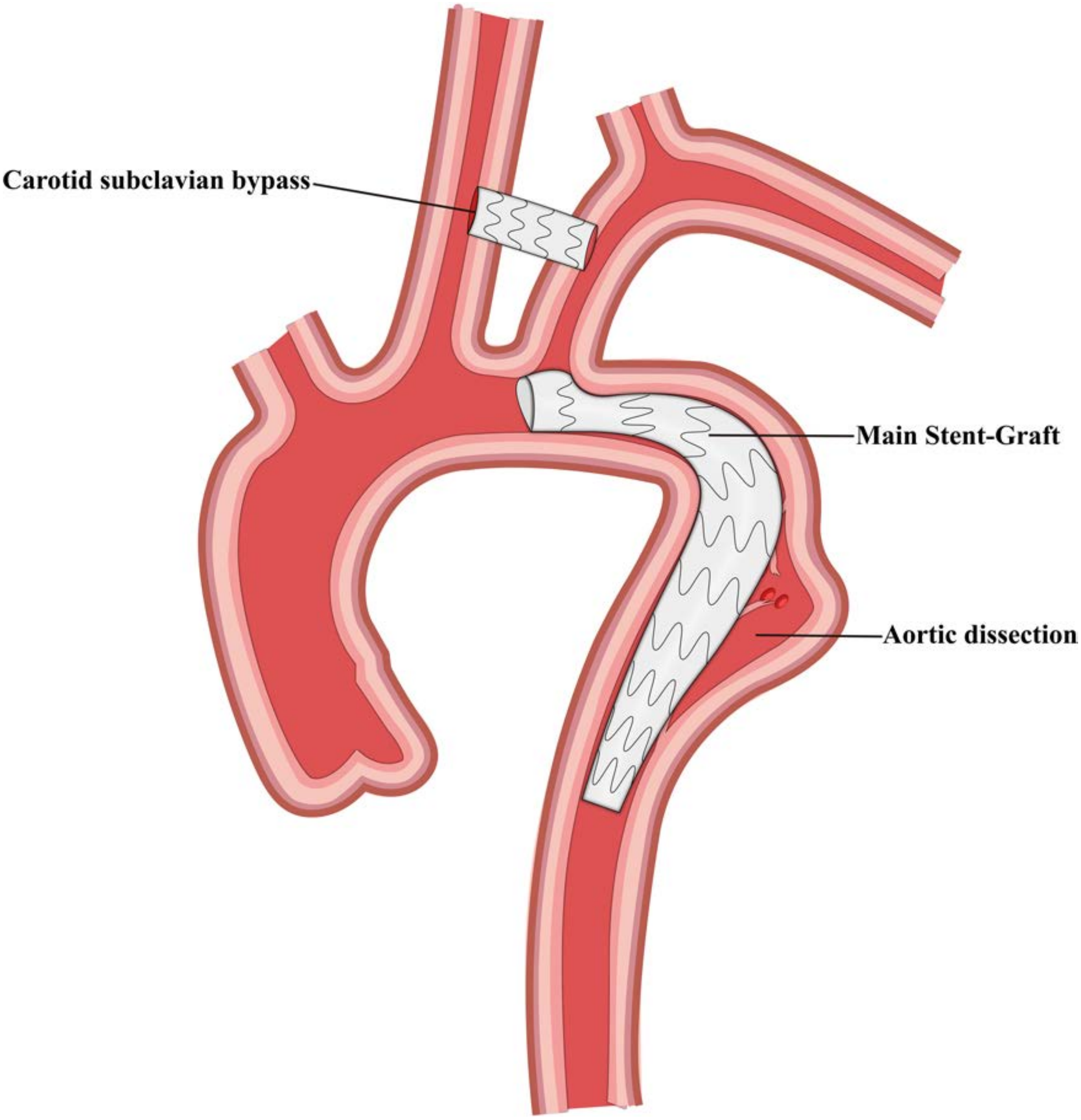

FIGURE 1
Schematic representation of carotid subclavian bypass and thoracic endovascular aortic repair.

frequencies. Comparisons between multiple groups were performed using the Kruskal–Wallis *H* test for categorical variables. The Bonferroni correction was applied to comparisons between the two groups. Comparisons between groups were performed using the chi-square test or Fisher's exact test. $P < 0.05$ was considered statistically significant, and $P < 0.0083$ was considered statistically significant after the Bonferroni correction.

Results

Baseline and preoperative characteristics of patients

A total of 105 patients, who met our inclusion criteria, were included in this study, including 41 patients in the CSB group, 29 patients in the CG group, 21 patients in the SBSG group, and 14 patients in the PMF group. The demographic information of patients is presented in **Table 1**. We did not observe any significant difference in the age ($P = 0.187$), sex ($P = 0.675$), and weight ($P = 0.338$) of the patients included in the four groups. Similarly, the incidence of preoperative comorbidities, including hypertension ($P = 0.694$), hyperlipidemia ($P = 0.835$), diabetes mellitus ($P = 0.972$), and coronary artery disease ($P = 0.987$), was not significantly different among the groups. The preoperative characteristics, including symptoms, NYHA class, aortic regurgitation, mitral regurgitation, pulmonary hypertension, aortic diameters, LSA diameters, and LSA–LCCA distance, were not significantly different among the four groups (**Table 2**). However, emergency surgery was more frequent in the CSB group (**Table 3**), and we found that the rate of emergency surgery was significantly

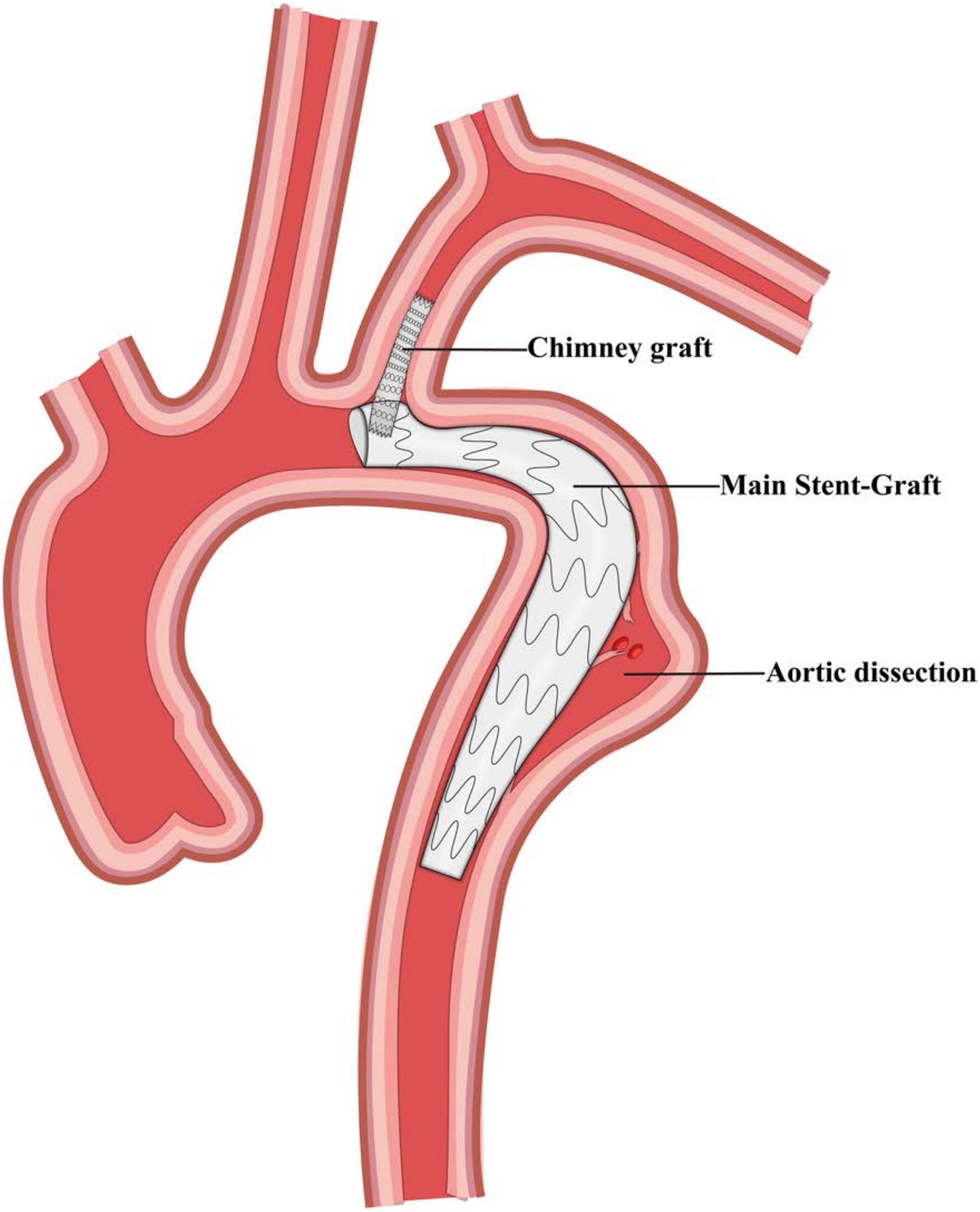

FIGURE 2
Schematic representation of the chimney graft and thoracic endovascular aortic repair.

higher in the CSB group than that in the SBSG group (adjusted $P = 0.007$).

Operative details of patients

TEVAR combined with LSA reconstruction was considered successful when the main body of the covered thoracic aortic stent was released successfully, the covered stent isolated the proximal and distal tears of the dissection without complications (including stent distortion or folding and endoleakage), and the patency of the blood flow of the LSA was confirmed. The operative details are summarized in **Table 4**. TEVAR combined with LSA reconstruction was performed in all groups with a 100% surgical success rate. All procedures were performed under general anesthesia (only one surgery in the CG group was

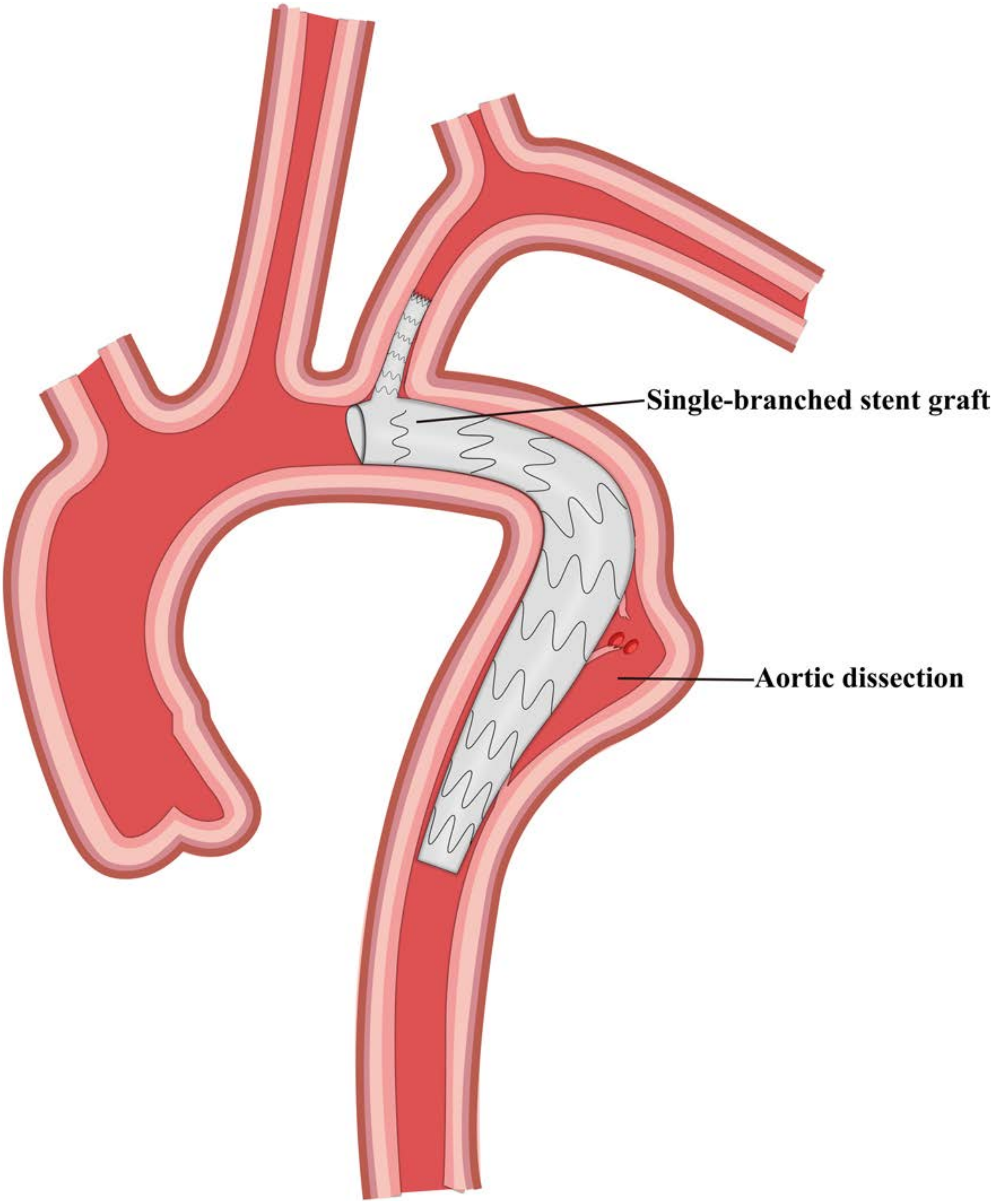

FIGURE 3
Schematic representation of the single-branched stent graft and thoracic endovascular aortic repair.

performed under local anesthesia). Stent graft-related complications were not reported during surgery in any of the four groups. The stent graft-related complications, anesthesia, and incidence of endoleakage during surgery did not differ significantly in the four groups; however, the differences in the fluoroscopic time ($P = 0.001$), amount of contrast ($P < 0.001$), estimated blood loss ($P < 0.001$), and operation time ($P < 0.001$) were statistically significant. Comparisons between the two groups are presented in **Table 3**.

In-hospital outcomes after surgery

Postoperative outcomes before discharge are shown in **Table 5**. In-hospital death, symptoms of limb ischemia, paraplegia, and lymphatic leakage were not reported in any group. The complications, including stroke (transient ischemic attack), hematoma, pneumonia, LSA steal syndrome, neurologic injury, and blood transfusion, did not differ significantly in the four groups. However, one case of stroke occurred in CG and

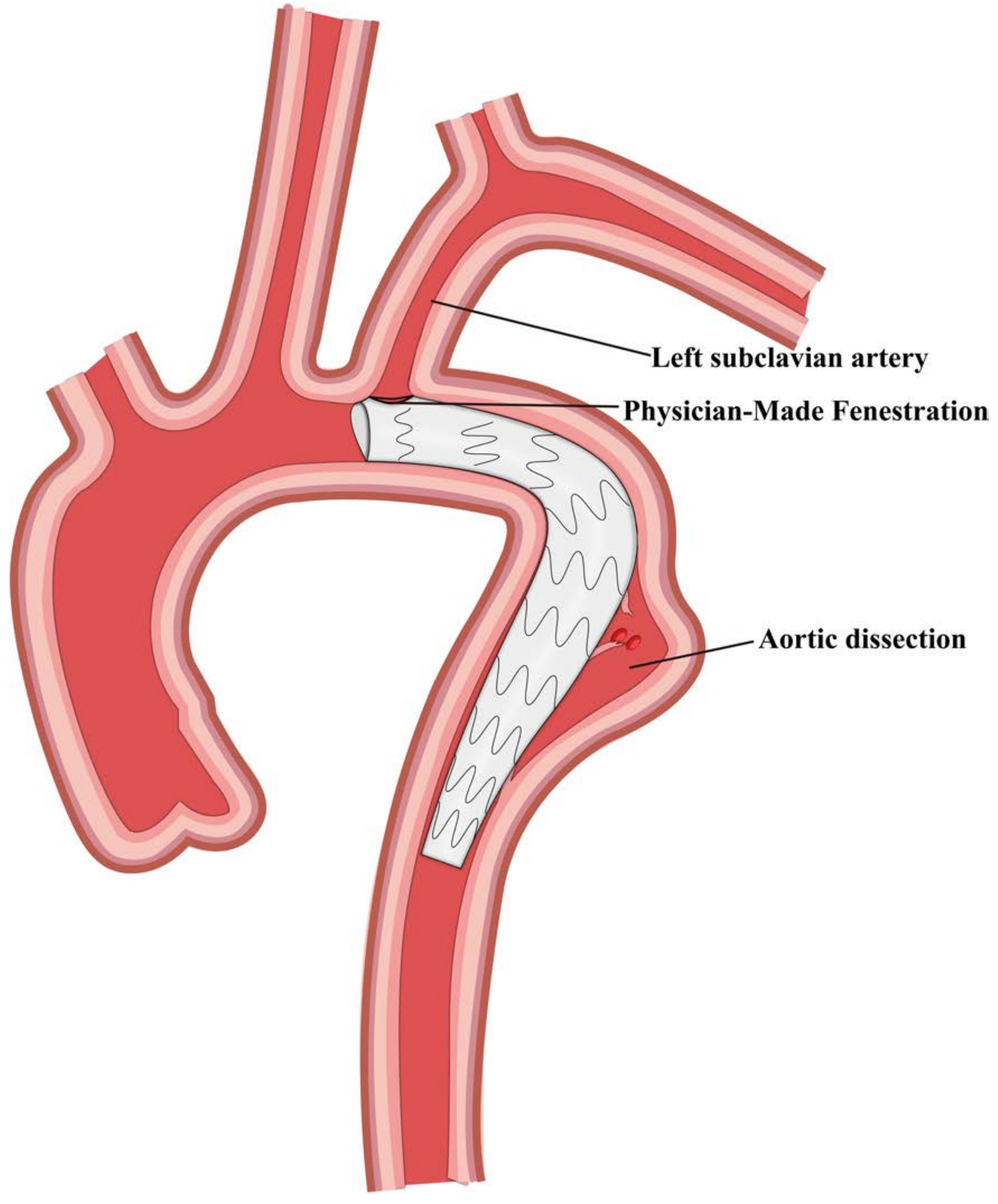

FIGURE 4
Schematic representation of physician-made fenestration and thoracic endovascular aortic repair.

PMF groups. The CSB and CG groups had a case of LSA syndrome that recovered without reintervention. One patient of the CSB group developed symptoms of nerve injury, which may be caused by the injury of the brachial plexus during the surgery. The symptoms were alleviated after conservative treatment during the hospital stay. The duration of stay in the ICU and hospital was not significantly different among the four groups.

Postoperative follow-up outcomes

Overall postoperative follow-up outcomes are summarized in Table 6. Three patients died during postoperative follow-up, and one patient died in each of the CSB, CG, and PMF groups. In the CG group, a patient died 2 months after surgery because of retrograde type A aortic dissection (RAAD). One patient of the PMF group had LSA steal syndrome, and one patient of the CSB

TABLE 1 Baseline demographics and comorbidities of patients in different treatment groups.

Variables	CSB ($n = 41$)	CG ($n = 29$)	SBSG ($n = 21$)	PMF ($n = 14$)	P-value
Male sex	31 (75.6%)	21 (72.4%)	18 (85.7%)	12 (85.7%)	0.675[a]
Age (years)	54.0 (47.5–63.5)	57.0 (51.5–66.5)	51.0 (47–55.5)	49.0 (44.8–66.0)	0.187[b]
Weight (kg)	68.85 ± 9.39	67.85 ± 11.44	72.79 ± 9.48	70.79 ± 9.89	0.338[c]
Comorbidities					
Hypertension	33 (80.5%)	26 (89.7%)	17 (81.0%)	11 (78.6%)	0.694[a]
Hyperlipidemia	15 (36.6%)	8 (27.6%)	6 (28.6%)	5 (35.7%)	0.835[d]
Diabetes mellitus	10 (24.4%)	6 (20.7%)	4 (19.0%)	3 (21.4%)	0.972[a]
CAD	6 (14.6%)	5 (17.2%)	3 (14.3%)	2 (14.3%)	0.987[a]
COPD	3 (7.3%)	1 (3.4%)	1 (4.8%)	0 (0%)	0.855[a]
CKD	1 (2.4%)	1 (3.4%)	0 (0%)	0 (0%)	0.648[a]
CVA	2 (4.9%)	2 (6.9%)	1 (4.8%)	1 (7.1%)	0.967[a]
Arrhythmia	11 (26.8%)	4 (13.8%)	4 (19.0%)	3 (21.4%)	0.633[a]
Myocardial infarction	1 (2.4%)	1 (3.4%)	0 (0%)	1 (7.1%)	0.645[a]
PAD	4 (9.8%)	1 (3.4%)	0 (0%)	0 (0%)	0.379[a]
Previous heart surgery	1 (2.4%)	2 (6.9%)	1 (4.8%)	0 (0%)	0.896[a]
Smoking	21 (51.2%)	18 (62.1%)	12 (57.1%)	8 (57.1%)	0.654[d]
Drinking	12 (29.3%)	10 (34.5%)	9 (42.9%)	7 (50.0%)	0.498[d]

Continuous data are shown as means (standard deviations) or medians (interquartile ranges), and categorical data are shown as numbers (%). CAD, coronary heart disease; COPD, chronic obstructive pulmonary disease chronic; CKD, chronic kidney disease; CVA, cerebrovascular accident; PAD, peripheral vascular disease. $P < 0.05$ was considered statistically significant.
[a]Fisher's exact test.
[b]Kruskal–Wallis H test.
[c]Tukey's test.
[d]Pearson's chi-square test.

TABLE 2 Preoperative characteristics of patients in different treatment groups.

Variable	CSB ($n = 41$)	CG ($n = 29$)	SBSG ($n = 21$)	PMF ($n = 14$)	P-value
Chest or back pain	32 (78.0%)	22 (75.9%)	17 (81.0%)	11 (78.6%)	0.986[a]
NYHA class					
I	28 (68.3%)	18 (62.1%)	18 (85.7%)	9 (64.3%)	0.320[b]
≥II	13 (31.7%)	11 (37.9%)	3 (14.3%)	5 (35.7%)	
Preoperative echocardiography					
Aortic regurgitation	13 (31.7%)	8 (27.6%)	4 (19.0%)	4 (28.6%)	0.784[a]
Mitral regurgitation	12 (29.3%)	6 (20.7%)	4 (19.0%)	5 (35.7%)	0.618[b]
Pulmonary hypertension	4 (9.8%)	2 (6.9%)	2 (9.5%)	2 (15.4%)	0.847[a]
LVEF (%)	60.0 (58.4–65.0)	61.0 (60.0–63.0)	63.0 (58.5–66.0)	60.5 (58.5–64.5)	0.892[c]
Preoperative CTA					
Aortic diameter (mm)	29.0 (27.0–31.0)	28.0 (26.0–30.0)	29.0 (27.0–30.0)	28.5 (26.8–30.3)	0.255[c]
LSA diameter (mm)	9.5 (9.0–10.0)	9.5 (9.0–10.5)	10.0 (9.0–11.0)	9.0 (8.5–10.0)	0.176[c]
LSA–LCCA distance (mm)	10.0 (9.5–11.0)	10.5 (10.0–11.5)	11.0 (10.0–12.0)	10.5 (10–11.3)	0.149[c]
Urgency					
Emergency	15 (36.6%)	8 (27.6%)	1 (4.8%)	3 (21.4%)	0.042[a]
Elective	26 (63.4%)	21 (72.4%)	20 (95.2%)	11 (78.6%)	

Continuous data are shown as medians (interquartile ranges), and categorical data are shown as numbers (%). CTA, computed tomography angiography; LVEF, left ventricle ejection fraction; LSA, left subclavian artery; LCCA, left common carotid artery; $P < 0.05$ was considered statistically significant.
[a]Fisher's Exact test.
[b]Pearson Chi-Square test.
[c]Kruskal–Wallis H test.

TABLE 3 Comparison between two treatment groups.

Variable		CSB vs. CG	CSB vs. SBSG	CSB vs. PMF	CG vs. SBSG	CG vs. PMF	SBSG vs. PMF
Emergency	Adjusted P	0.430	0.007	0.297	0.061	1.000	0.129
EBL	Adjusted P	<0.001	<0.001	<0.001	0.007	0.033	0.277
Symptoms of limb ischemia	Adjusted P	1.000	0.545	0.031	0.503	0.077	0.008
Follow-up time	Adjusted P	0.121	<0.001	0.003	0.008	0.248	0.001
Fluoroscopic time	P	<0.001	<0.001	<0.001	<0.001	<0.001	<0.001
Amount of contrast	P	<0.001	<0.001	<0.001	<0.001	<0.001	<0.001
Operation time	P	<0.001	<0.001	0.004	0.241	0.082	0.417

EBL, estimated blood loss. Adjusted $P < 0.0083$ was considered statistically significant; $P < 0.05$ was considered statistically significant.

TABLE 4 Operative details of patients in different treatment groups.

Variable	CSB (*n* = 41)	CG (*n* = 29)	SBSG (*n* = 21)	PMF (*n* = 14)	*P*-value
General anesthesia [*n*, (%)]	41 (100%)	28 (96.6%)	21 (100%)	14 (100%)	0.610[a]
Fluoroscopic time (min)	46.62 ± 2.72	55.20 ± 2.42	70.93 ± 3.17	59.55 ± 3.39	0.001[b]
Amount of contrast (ml)	149.76 ± 7.33	200.52 ± 6.49	250.59 ± 7.75	221.51 ± 7.23	<0.001[b]
EBL (ml)	220.0 (210.0–232.5)	90.0 (85.0–102.5)	130.0 (120.0–135.0)	120 (100.0–132.5)	<0.001[c]
Operation time (min)	341.7 ± 78.7	179.7 ± 53.9	221.3 ± 68.1	250.7 ± 88.7	<0.001[d]
Endoleak [*n*, (%)]	0 (0%)	2 (6.9%)	0 (0%)	1 (7.1%)	0.119[a]
SGRC [*n*, (%)]	0 (0%)	0 (0%)	0 (0%)	0 (0%)	–
Surgical success	41 (100%)	29 (100%)	21 (100%)	14 (100%)	–

Continuous data are shown as means (standard deviations) or medians (interquartile ranges), and categorical data are shown as numbers (%). EBL, estimated blood loss; SGRC, stent-graft related complication including fold, twist, and narrow; Tukey's test and Games–Howell test in footnotes b and d only represent the homogeneity of variance test among the four groups, and *P*-value only represents the results of one-way analysis of variance; $P < 0.05$ was considered statistically significant.
[a]Fisher's exact test.
[b]Tukey's test.
[c]Kruskal–Wallis *H* test.
[d]Games–Howell test.

TABLE 5 In-hospital outcomes in patients after surgery.

Variable	CSB (*n* = 41)	CG (*n* = 29)	SBSG (*n* = 21)	PMF (*n* = 14)	*P*-value
Mortality	0 (0%)	0 (0%)	0 (0%)	0 (0%)	–
Symptoms of limb ischemia	0 (0%)	0 (0%)	0 (0%)	0 (0%)	–
Stroke	0 (0%)	1 (3.4%)	0 (0%)	1 (7.1%)	0.258[a]
Hematoma	5 (12.2%)	1 (3.4%)	0 (0%)	1 (7.1%)	0.317[a]
Paraplegia	0 (0%)	0 (0%)	0 (0%)	0 (0%)	–
Pneumonia [*n*, (%)]	5 (12.2%)	2 (6.9%)	2 (9.5%)	1 (7.1%)	0.958[a]
LSA steal syndrome [*n*, (%)]	1 (2.4%)	1 (3.4%)	0 (0%)	0 (0%)	1.000[a]
Lymphatic leakage [*n*, (%)]	0 (0%)	0 (0%)	0 (0%)	0 (0%)	–
Neurologic injury [*n*, (%)]	1 (2.4%)	0 (0%)	0 (0%)	0 (0%)	1.000[a]
Blood transfusion [*n*, (%)]	6 (14.6%)	3 (10.3%)	1 (4.8%)	1 (7.1%)	0.647[a]
Stent-associated infection	0 (0%)	0 (0%)	0 (0%)	0 (0%)	–
Reintervention [*n*, (%)]	0 (0%)	0 (0%)	0 (0%)	0 (0%)	–
Length of ICU (h)	36.38 ± 19.17	31.10 ± 20.05	26.55 ± 13.76	29.79 ± 19.31	0.198[b]
Length of hospital stay (days)	9.63 ± 3.46	8.72 ± 3.76	7.71 ± 3.20	9.21 ± 2.49	0.204[b]

Continuous data are shown as means (standard deviations), and categorical data are shown as numbers (%). LSA, left subclavian artery; ICU, intensive care unit; Footnote b only represents the homogeneity of variance test among the four groups, and *P*-value only represents the results of one-way analysis of variance; $P < 0.05$ was considered statistically significant.
[a]Fisher's exact test.
[b]Tukey's test.

TABLE 6 Follow-up outcomes in patients.

Variable	CSB (*n* = 41)	CG (*n* = 29)	SBSG (*n* = 21)	PMF (*n* = 14)	*P*-value
Mortality	1 (2.4%)	1 (3.4%)	0 (0%)	1 (7.1%)	0.648[a]
Symptoms of limb ischemia	2 (4.9%)	2 (6.9%)	0 (0%)	4 (28.6%)	0.023[a]
LSA steal syndrome	0 (0%)	0 (0%)	0 (0%)	1 (7.1%)	0.133[a]
Stroke	2 (4.9%)	2 (6.9%)	1 (4.8%)	1 (7.1%)	0.975[a]
SCI	0 (0%)	0 (0%)	0 (0%)	0 (0%)	–
Endoleak	2 (4.9%)	5 (17.2%)	1 (4.8%)	1 (7.1%)	0.280[a]
RTAD	0 (0%)	1 (3.4%)	0 (0%)	0 (0%)	0.610[a]
Reintervention	1 (2.4%)	0 (0%)	0 (0%)	0 (0%)	1.000[a]
CFLT	37 (90.2%)	25 (86.2%)	18 (85.7%)	11 (78.6%)	0.686[a]
Follow-up time (months)	28.0 (17.0–33.0)	24.0 (16.0–28.0)	15.0 (13.5–17.5)	21.5 (19.0–31.5)	<0.001[b]

Continuous data are shown as medians (interquartile ranges), and categorical data are shown as numbers (%). LSA, left subclavian artery; SCI, spinal cord ischemia; CFLT, complete false-lumen thrombosis; $P < 0.05$ was considered statistically significant.
[a]Fisher's exact test.
[b]Kruskal–Wallis *H* test.

group underwent reintervention because of an endoleak. The CTA review showed type IB endoleak, which was resolved by implanting a thoracic aorta-covered stent combined with CUFF-covered stent reintervention. The endoleak disappeared after the intervention, and a complete false lumen thrombosis was observed in the CTA review 1 year later.

The median follow-up durations for CSB and CG groups were 28.0 (IQR: 17.0–33.0) and 24.0 (IQR: 16.0–28.0) months, respectively. The similar durations for SBSG and PMF groups were 15.0 (IQR: 13.5–17.5) and 21.5 (IQR: 19.0–31.5) months, respectively. We found that the follow-up time was significantly shorter in the SBSG group (adjusted $P < 0.0083$) and significantly longer in the CSB group than that in the PMF group (adjusted $P < 0.0083$) (**Table 3**). The incidence of stroke was 4.9%, 6.9%, 4.8%, and 7.1% in the CSB, CG, SBSG, and PMF groups, respectively. The incidence of stroke and the rate of complete false lumen thrombosis were not significantly different among the four groups. In addition, spinal cord ischemia was not observed during follow-up in all the groups. However, limb ischemia symptoms were reported, and their prevalence was significantly lower in the SBSG group than that in the PMF group.

Discussion

The registry data show that TEVAR for thoracic aortic pathologies has more acceptable outcomes and lower perioperative complications than open repair in the last two decades (20, 21). However, TEVAR with intentional LSA coverage for good fixation of stent grafts carries a high risk for left upper extremity ischemia and stroke (22, 23). The European Society for Vascular Surgery recommends routine revascularization for elective cases to prevent the devastating neurological consequences of spinal cord ischemia and stroke following TEVAR (18). Nevertheless, the efficiency of different LSA reconstruction strategies remains unclear.

Several new LSA reconstruction strategies are constantly emerging with the evolution of medical devices and surgical technology. Carotid subclavian bypass, chimney graft, single-branched stent graft, and physician-made fenestration are the most common surgical techniques for reconstructing LSA, and all of these strategies have been used in our center for the treatment of Stanford type B dissection. Here, we summarized our single-center experience of 105 patients who underwent TEVAR combined with four different strategies of LSA reconstruction and compared the efficiency of the four strategies.

We observed a significant difference in the methods used for emergent surgeries. The CSB technique was most commonly used in emergency settings. Bypass technology is the earliest application in LSA reconstruction, and its safety and reliability have been reported in many studies (24, 25). It is especially suitable for emergent cases because of its relatively simple maneuver and wider clinical situations. However, SBSG was not used in emergencies because it was custom-made and involved a long manufacturing time and increased cost. Since the introduction of the CG technique by Criado (26), it has been used to expand proximal landing zones in TEVAR with favorable results (27, 28). However, a gutter between the main graft, aortic wall, and CG can be a potential site for endoleaks after TEVAR (29, 30), and an endoleak is a common complication during surgery. The single-branched stent graft designed by Inoue and colleagues (31) is intended to treat pathologies involving the LSA in the distal arch. Several clinical trials on SBSG have demonstrated favorable short-term results in aortic arch reconstruction (32, 33). Compared to the chimney technique, SBSG implantation is less likely to cause endoleaks because there is no risk of gutter formation. We observed two cases of endoleaks during surgery in the CG group (incidence rate: 6.9%). Although a small endoleak happened in a patient of the PMF group, reintervention was not necessary. Similar to our study, Zhang et al. compared CG and SBSG in the same situation and did not report any significant differences (34). Moreover, the difference in endoleak occurrence was not statistically different among the four groups.

We found a significant difference in the fluoroscopic time and amount of contrast among the four groups. The values were highest in the SBSG group, followed by PMF, CG, and CSB groups. CSB was associated with the lowest fluoroscopic time and amount of contrast because all other three techniques required more time and contrast to confirm the patency of LSA. Moreover, the position of the LSA stent needed to be adjusted according to the results of intraoperative angiography. Compared with the other three groups, the CSB group was associated with more estimated blood loss during surgery. This happens because CSB combines open surgery and endovascular repair. However, our data suggested that the estimated blood loss was much less than that reported by D'Oria (VQI data: 220 vs. 309 ml) (35). The CSB group had a significantly longer operation time than the other three groups, which could be attributed to the lack of a hybrid operation room in our center and the necessity of transferring patients.

The in-hospital outcomes were not significantly different among the groups; however, there was a significant difference in the incidence of limb ischemia symptoms. We found that the PMF group was associated with a much higher rate of symptoms of limb ischemia compared with the SBSG group (28.6% vs. 0%; $P = 0.008$). The PMF technique for aorta repair offers a more judicious approach with favorable mid-term results without altering the anatomic structures (36, 37). Nevertheless, the target branch needs to be at a vertical angle to the aortic arch for using this technique, and tortuosity and the sharp angle of the branch vessels could significantly raise the procedural challenges. Therefore, its long-term efficiency should be confirmed in further studies. In this study, the follow-up time was significantly longer in the PMF group than that in the other groups, and we assumed that a relatively short follow-up might be associated with a lower incidence of symptoms of limb ischemia.

RAAD is a serious TEVAR-related complication. Its incidence ranges from 2.5% to 10%, and the perioperative mortality is >40% (38–40). We had one case of RAAD in the CG group (incidence rate: 3.4%), which resulted in the death of the patient during follow-up. Several predictive risk variables are linked to RAAD, including the timing of TEVAR, the size of the ascending aorta, the proximal landing zone, the extent of false lumen thrombosis, and the proximal-neck balloon dilatation (41–43). The MOTHER registry analysis revealed that RAAD occurred more frequently when the patients were treated in the acute phases and when the stent graft was noticeably oversized (44). In our experience, the preoperative CT-based graft oversizing was limited to 110% to prevent further stress on the aortic wall.

Limitations

This study has some possible limitations. We designed this study as a single-center retrospective study. The LSA reconstruction strategy depends on the judgment of the surgeon and the subjective initiative of the patient, which could cause selection bias. The results need to be further verified by multicenter randomized controlled studies. In addition, the number of enrolled patients was small with a relatively short follow-up; therefore, a larger number of patients with long-term follow-up should be included in further studies.

Conclusion

Our single-center experience suggested that the PMF technique was associated with a higher risk of symptoms of limb ischemia, and the other three strategies effectively and safely restored LSA perfusion with comparable complications in patients with TBAD. LSA revascularization techniques have their unique advantages and disadvantages. Although CSB increases operation time and intraoperative blood loss, it is more suitable for emergencies. However, our results should be further verified in a multicenter randomized controlled study with a larger sample size.

Data availability statement

The raw data supporting the conclusions of this article will be made available by the authors without undue reservation.

Ethics statement

The studies involving human participants were reviewed and approved by the ethical committee of Lanzhou Second Hospital. The patients/participants provided their written informed consent to participate in this study.

Author contributions

XW and YL proposed the view and designed and participated in the whole research process. SlW and WW carried out data collection and writing of the original draft. YinZ, YilZ, SxW, and QM checked the data and generated the tables. DL and BG analyzed the data results. SlW and WW guided the research and contributed to the final version of the paper. XW and YL contributed equally to the overall research. All authors contributed to the article and approved the submitted version.

Funding

This study was funded by the Scientific Research Projects in Gansu Health industry (No. GSWSKY2020-38), the Key Talent Project in Gansu Province (2021-17), the Cuiying Scientific and Technological Innovation Program of Lanzhou University Second Hospital (No. CY2019-QN12), and the Scientific Research Projects in Lanzhou (No. 2021-1-107).

Conflict of interest

The authors declare that the research was conducted in the absence of any commercial or financial relationships that could be construed as a potential conflict of interest.

Publisher's note

References

1. Howard DP, Banerjee A, Fairhead JF, Perkins J, Silver LE, Rothwell PM. Population-based study of incidence and outcome of acute aortic dissection and premorbid risk factor control: 10-year results from the Oxford vascular study. *Circulation*. (2013) 127(20):2031–7. doi: 10.1161/circulationaha.112.000483

2. Hughes GC. Management of acute type B aortic dissection; adsorb trial. *J Thorac Cardiovasc Surg*. (2015) 149(2 Suppl):S158–62. doi: 10.1016/j.jtcvs.2014.08.083

3. Tadros RO, Tang GHL, Barnes HJ, Mousavi I, Kovacic JC, Faries P, et al. Optimal treatment of uncomplicated type b aortic dissection: jacc review topic of the week. *J Am Coll Cardiol*. (2019) 74(11):1494–504. doi: 10.1016/j.jacc.2019.07.063

4. Dake MD, Kato N, Mitchell RS, Semba CP, Razavi MK, Shimono T, et al. Endovascular stent-graft placement for the treatment of acute aortic dissection. *N Engl J Med*. (1999) 340(20):1546–52. doi: 10.1056/nejm199905203402004

5. Thrumurthy SG, Karthikesalingam A, Patterson BO, Holt PJ, Hinchliffe RJ, Loftus IM, et al. A systematic review of mid-term outcomes of thoracic endovascular repair (tevar) of chronic type B aortic dissection. *Eur J Vasc Endovasc Surg*. (2011) 42(5):632–47. doi: 10.1016/j.ejvs.2011.08.009

6. Moulakakis KG, Mylonas SN, Dalainas I, Kakisis J, Kotsis T, Liapis CD. Management of complicated and uncomplicated acute type B dissection. A systematic review and meta-analysis. *Ann Cardiothorac Surg*. (2014) 3(3):234–46. doi: 10.3978/j.issn.2225-319X.2014.05.08

7. Harky A, Chan JSK, Wong CHM, Francis N, Grafton-Clarke C, Bashir M. Systematic review and meta-analysis of acute type B thoracic aortic dissection, open, or endovascular repair. *J Vasc Surg*. (2019) 69(5):1599–609.e2. doi: 10.1016/j.jvs.2018.08.187

8. Erbel R, Aboyans V, Boileau C, Bossone E, Bartolomeo RD, Eggebrecht H, et al. 2014 Esc guidelines on the diagnosis and treatment of aortic diseases: document covering acute and chronic aortic diseases of the thoracic and abdominal aorta of the adult. The task force for the diagnosis and treatment of aortic diseases of the European society of cardiology (Esc). *Eur Heart J*. (2014) 35(41):2873–926. doi: 10.1093/eurheartj/ehu281

9. Czerny M, Schmidli J, Adler S, van den Berg JC, Bertoglio L, Carrel T, et al. Editor's choice—current options and recommendations for the treatment of thoracic aortic pathologies involving the aortic arch: an expert consensus document of the European Association for Cardio-Thoracic Surgery (Eacts) & the European Society for Vascular Surgery (Esvs). *Eur J Vasc Endovasc Surg*. (2019) 57(2):165–98. doi: 10.1016/j.ejvs.2018.09.016

10. Feezor RJ, Lee WA. Management of the left subclavian artery during tevar. *Semin Vasc Surg*. (2009) 22(3):159–64. doi: 10.1053/j.semvascsurg.2009.07.007

11. Chen X, Wang J, Premaratne S, Zhao J, Zhang WW. Meta-analysis of the outcomes of revascularization after intentional coverage of the left subclavian artery for thoracic endovascular aortic repair. *J Vasc Surg*. (2019) 70(4):1330–40. doi: 10.1016/j.jvs.2019.03.022

12. Hajibandeh S, Hajibandeh S, Antoniou SA, Torella F, Antoniou GA. Meta-analysis of left subclavian artery coverage with and without revascularization in thoracic endovascular aortic repair. *J Endovasc Ther*. (2016) 23(4):634–41. doi: 10.1177/1526602816651417

13. Varkevisser RRB, Swerdlow NJ, de Guerre L, Dansey K, Li C, Liang P, et al. Thoracic endovascular aortic repair with left subclavian artery coverage is associated with a high 30-day stroke incidence with or without concomitant revascularization. *J Endovasc Ther*. (2020) 27(5):769–76. doi: 10.1177/1526602820923044

14. Galili O, Fajer S, Eyal A, Karmeli R. Left subclavian artery occlusion by thoracic aortic stent graft: long-term clinical and duplex follow-up. *Isr Med Assoc J*. (2007) 9 (9):668–70. PMID: 17939630.

15. Bradshaw RJ, Ahanchi SS, Powell O, Larion S, Brandt C, Soult MC, et al. Left subclavian artery revascularization in zone 2 thoracic endovascular aortic repair is associated with lower stroke risk across all aortic diseases. *J Vasc Surg*. (2017) 65 (5):1270–9. doi: 10.1016/j.jvs.2016.10.111

16. Teixeira PG, Woo K, Beck AW, Scali ST, Weaver FA. Association of left subclavian artery coverage without revascularization and spinal cord ischemia in patients undergoing thoracic endovascular aortic repair: a Vascular Quality Initiative® Analysis. *Vascular*. (2017) 25(6):587–97. doi: 10.1177/1708538116681910

17. Luehr M, Etz CD, Berezowski M, Nozdrzykowski M, Jerkku T, Peterss S, et al. Outcomes after thoracic endovascular aortic repair with overstenting of the left subclavian artery. *Ann Thorac Surg*. (2019) 107(5):1372–9. doi: 10.1016/j.athoracsur.2018.10.051

18. Matsumura JS, Lee WA, Mitchell RS, Farber MA, Murad MH, Lumsden AB, et al. The society for vascular surgery practice guidelines: management of the left subclavian artery with thoracic endovascular aortic repair. *J Vasc Surg*. (2009) 50 (5):1155–8. doi: 10.1016/j.jvs.2009.08.090

19. Hiratzka LF, Bakris GL, Beckman JA, Bersin RM, Carr VF, Casey DE Jr, et al. 2010 Accf/Aha/Aats/Acr/Asa/Sca/Scai/Sir/Sts/Svm Guidelines for the Diagnosis and Management of Patients with Thoracic Aortic Disease. A report of the American College of Cardiology Foundation/American Heart Association Task Force on Practice Guidelines, American Association for Thoracic Surgery, American College of Radiology,American Stroke Association, Society of Cardiovascular Anesthesiologists, Society for Cardiovascular Angiography and Interventions, Society of Interventional Radiology, Society of Thoracic Surgeons,and Society for Vascular Medicine. *J Am Coll Cardiol*. (2010) 55(14):e27–129. doi: 10.1016/j.jacc.2010.02.015

20. Goodney PP, Travis L, Lucas FL, Fillinger MF, Goodman DC, Cronenwett JL, et al. Survival after open versus endovascular thoracic aortic aneurysm repair in an observational study of the medicare population. *Circulation*. (2011) 124(24):2661–9. doi: 10.1161/circulationaha.111.033944

21. Leurs LJ, Bell R, Degrieck Y, Thomas S, Hobo R, Lundbom J. Endovascular treatment of thoracic aortic diseases: combined experience from the eurostar and United Kingdom thoracic endograft registries. *J Vasc Surg*. (2004) 40(4):670–9; discussion 9–80. doi: 10.1016/j.jvs.2004.07.008

22. Waterford SD, Chou D, Bombien R, Uzun I, Shah A, Khoynezhad A. Left subclavian arterial coverage and stroke during thoracic aortic endografting: a systematic review. *Ann Thorac Surg*. (2016) 101(1):381–9. doi: 10.1016/j.athoracsur.2015.05.138

23. Zamor KC, Eskandari MK, Rodriguez HE, Ho KJ, Morasch MD, Hoel AW. Outcomes of thoracic endovascular aortic repair and subclavian revascularization techniques. *J Am Coll Surg*. (2015) 221(1):93–100. doi: 10.1016/j.jamcollsurg.2015.02.028

24. van der Weijde E, Saouti N, Vos JA, Tromp SC, Heijmen RH. Surgical left subclavian artery revascularization for thoracic aortic stent grafting: a single-centre experience in 101 patients. *Interact Cardiovasc Thorac Surg*. (2018) 27(2):284–9. doi: 10.1093/icvts/ivy059

25. Canaud L, Ziza V, Ozdemir BA, Berthet JP, Marty-Ané CH, Alric P. Outcomes of left subclavian artery transposition for hybrid aortic arch debranching. *Ann Vasc Surg*. (2017) 40:94–7. doi: 10.1016/j.avsg.2016.06.037

26. Criado FJ. A percutaneous technique for preservation of arch branch patency during thoracic endovascular aortic repair (tevar): retrograde catheterization and stenting. *J Endovasc Ther*. (2007) 14(1):54–8. doi: 10.1583/06-2010.1

27. Xue Y, Sun L, Zheng J, Huang X, Guo X, Li T, et al. The chimney technique for preserving the left subclavian artery in thoracic endovascular aortic repair. *Eur J Cardiothorac Surg*. (2015) 47(4):623–9. doi: 10.1093/ejcts/ezu266

28. Lindblad B, Bin Jabr A, Holst J, Malina M. Chimney grafts in aortic stent grafting: hazardous or useful technique? Systematic review of current data. *Eur J Vasc Endovasc Surg*. (2015) 50(6):722–31. doi: 10.1016/j.ejvs.2015.07.038

29. Moulakakis KG, Mylonas SN, Avgerinos E, Papapetrou A, Kakisis JD, Brountzos EN, et al. The chimney graft technique for preserving visceral vessels during endovascular treatment of aortic pathologies. *J Vasc Surg*. (2012) 55(5):1497–503. doi: 10.1016/j.jvs.2011.10.009

30. Mangialardi N, Ronchey S, Malaj A, Fazzini S, Alberti V, Ardita V, et al. Value and limitations of chimney grafts to treat arch lesions. *J Cardiovasc Surg (Torino)*. (2015) 56(4):503–11. PMID: 17939630.

31. Inoue K, Hosokawa H, Iwase T, Sato M, Yoshida Y, Ueno K, et al. Aortic arch reconstruction by transluminally placed endovascular branched stent graft. *Circulation*. (1999) 100(19 Suppl):Ii316–21. doi: 10.1161/01.cir.100.suppl_2.ii-316

32. Huang C, Liu Z, Huang D, Qiao T, Zhou M, Liu C. Application of unibody single-branch endografts in Stanford type B dissections with primary entry tear adjacent to the left subclavian artery: a computed tomography-based planning study. *Ann Vasc Surg*. (2015) 29(6):1174–80. doi: 10.1016/j.avsg.2015.02.016

33. Lu Q, Feng J, Zhou J, Zhao Z, Li H, Teng Z, et al. Endovascular repair by customized branched stent-graft: a promising treatment for chronic aortic dissection involving the arch branches. *J Thorac Cardiovasc Surg*. (2015) 150(6):1631–8.e5. doi: 10.1016/j.jtcvs.2015.08.032

34. Zhang H, Huang H, Zhang Y, Liu Z, Qiao T, Zhang X, et al. Comparison of chimney technique and single-branched stent graft for treating patients with type B aortic dissections that involved the left subclavian artery. *Cardiovasc Intervent Radiol*. (2019) 42(5):648–56. doi: 10.1007/s00270-018-2145-3

35. D'Oria M, Kärkkäinen JM, Tenorio ER, Oderich GS, Mendes BC, Shuja F, et al. Perioperative outcomes of carotid-subclavian bypass or transposition versus endovascular techniques for left subclavian artery revascularization during nontraumatic zone 2 thoracic endovascular aortic repair in the vascular quality initiative. *Ann Vasc Surg*. (2020) 69:17–26. doi: 10.1016/j.avsg.2020.05.062

36. Canaud L, Baba T, Gandet T, Narayama K, Ozdemir BA, Shibata T, et al. Physician-modified thoracic stent-grafts for the treatment of aortic arch lesions. *J Endovasc Ther*. (2017) 24(4):542–8. doi: 10.1177/1526602817714206

37. Canaud L, Morishita K, Gandet T, Sfeir J, Bommart S, Alric P, et al. Homemade fenestrated stent-graft for thoracic endovascular aortic repair of zone 2 aortic lesions. *J Thorac Cardiovasc Surg*. (2018) 155(2):488–93. doi: 10.1016/j.jtcvs.2017.07.045

38. Williams JB, Andersen ND, Bhattacharya SD, Scheer E, Piccini JP, McCann RL, et al. Retrograde ascending aortic dissection as an early complication of thoracic endovascular aortic repair. *J Vasc Surg*. (2012) 55(5):1255–62. doi: 10.1016/j.jvs.2011.11.063

39. Luebke T, Brunkwall J. Outcome of patients with open and endovascular repair in acute complicated type B aortic dissection: a systematic review and meta-analysis of case series and comparative studies. *J Cardiovasc Surg (Torino)*. (2010) 51(5):613–32. PMID: 17939630.

40. Eggebrecht H, Thompson M, Rousseau H, Czerny M, Lönn L, Mehta RH, et al. Retrograde ascending aortic dissection during or after thoracic aortic stent graft placement: insight from the European registry on endovascular aortic repair complications. *Circulation*. (2009) 120(11 Suppl):S276–81. doi: 10.1161/circulationaha.108.835926

41. Dong ZH, Fu WG, Wang YQ, Guo DQ, Xu X, Ji Y, et al. Retrograde type A aortic dissection after endovascular stent graft placement for treatment of type B dissection. *Circulation*. (2009) 119(5):735–41. doi: 10.1161/circulationaha.107.759076

42. Yammine H, Briggs CS, Stanley GA, Ballast JK, Anderson WE, Nussbaum T, et al. Retrograde type a dissection after thoracic endovascular aortic repair for type B aortic dissection. *J Vasc Surg*. (2019) 69(1):24–33. doi: 10.1016/j.jvs.2018.04.047

43. Canaud L, Ozdemir BA, Patterson BO, Holt PJ, Loftus IM, Thompson MM. Retrograde aortic dissection after thoracic endovascular aortic repair. *Ann Surg*. (2014) 260(2):389–95. doi: 10.1097/sla.0000000000000585

44. Patterson BO, Holt PJ, Nienaber C, Fairman RM, Heijmen RH, Thompson MM. Management of the left subclavian artery and neurologic complications after thoracic endovascular aortic repair. *J Vasc Surg*. (2014) 60(6):1491–7.e1. doi: 10.1016/j.jvs.2014.08.114

frontiers | Frontiers in Cardiovascular Medicine

TYPE Original Research
PUBLISHED 22 May 2023
DOI 10.3389/fcvm.2023.1125110

Aortic haemodynamics and wall stress analysis following arch aneurysm repair using a single-branched endograft

Sampad Sengupta[1], Xun Yuan[2,3], Ludovica Maga[4,5], Selene Pirola[5], Christoph A. Nienaber[2,3] and Xiao Yun Xu[1]*

[1]Department of Chemical Engineering, Imperial College London, London, United Kingdom, [2]National Heart and Lung Institute, Faculty of Medicine, Imperial College London, London, United Kingdom, [3]Cardiology and Aortic Centre, Royal Brompton and Harefield Hospitals, Guy's and St Thomas' NHS Foundation Trust, London, United Kingdom, [4]Department of Electronics, Information and Bioengineering, Politecnico di Milano, Milan, Italy, [5]Department of Biomechanical Engineering, Delft University of Technology, Delft, Netherlands

OPEN ACCESS

EDITED BY
Jiaxuan Feng,
Second Military Medical University, China

REVIEWED BY
Francesco Squizzato,
University of Padua, Italy
Frans Moll,
University Medical Center Utrecht,
Netherlands

*CORRESPONDENCE
Xiao Yun Xu
yun.xu@imperial.ac.uk

RECEIVED 15 December 2022
ACCEPTED 08 May 2023
PUBLISHED 22 May 2023

CITATION
Sengupta S, Yuan X, Maga L, Pirola S, Nienaber CA and Xu XY (2023) Aortic haemodynamics and wall stress analysis following arch aneurysm repair using a single-branched endograft.
Front. Cardiovasc. Med. 10:1125110.
doi: 10.3389/fcvm.2023.1125110

Introduction: Thoracic endovascular aortic repair (TEVAR) of the arch is challenging given its complex geometry and the involvement of supra-aortic arteries. Different branched endografts have been designed for use in this region, but their haemodynamic performance and the risk for post-intervention complications are not yet clear. This study aims to examine aortic haemodynamics and biomechanical conditions following TVAR treatment of an aortic arch aneurysm with a two-component single-branched endograft.
Methods: Computational fluid dynamics and finite element analysis were applied to a patient-specific case at different stages: pre-intervention, post-intervention and follow-up. Physiologically accurate boundary conditions were used based on available clinical information.
Results: Computational results obtained from the post-intervention model confirmed technical success of the procedure in restoring normal flow to the arch. Simulations of the follow-up model, where boundary conditions were modified to reflect change in supra-aortic vessel perfusion observed on the follow-up scan, predicted normal flow patterns but high levels of wall stress (up to 1.3M MPa) and increased displacement forces in regions at risk of compromising device stability. This might have contributed to the suspected endoleaks or device migration identified at the final follow up.
Discussion: Our study demonstrated that detailed haemodynamic and biomechanical analysis can help identify possible causes for post-TEVAR complications in a patient-specific setting. Further refinement and validation of the computational workflow will allow personalised assessment to aid in surgical planning and clinical decision making.

KEYWORDS
TEVAR, endograft, aortic arch, computational fluid dynamics, finite element analysis

1. Introduction

An aortic aneurysm is a localised distention of the vessel wall, resulting in an abnormal and often permanent dilatation of the affected section of the aorta. Thoracic aortic aneurysms (TAAs) can arise in the ascending aorta, aortic arch, thoracic descending aorta, or the thoraco-abdominal regions of the aorta. Isolated arch aneurysms are less frequent but pose a significant challenge given the geometric complexity of the region, especially the involvement of supra-aortic vessels that are responsible for supplying blood to the head and upper parts of the body. Insufficient blood perfusion to the arch branches can result in severe and often fatal consequences (1–3). The standard treatment option for arch aneurysm is open-chest surgery, with thoracic endovascular aortic repair (TEVAR) providing a minimally invasive alternative. Initially introduced for the treatment of abdominal aortic aneurysms, endovascular repair has now been extended to the thoracic aorta and arch. TEVAR offers several benefits to patients, including short post-operative time spent in the hospital and fast recovery (4–6).

Endografts used for TEVAR are designed to mimic a patient's anatomy as closely as possible. They can be branched or unbranched, depending on the zone of the aorta in which they are deployed. Improvements have been made to the design and deployment methods of endografts, yielding a remarkable decrease in mortality and morbidity rates of the repair procedure (4, 7). Branched or fenestrated stent-grafts are often used to ensure perfusion of blood to the supra-aortic vessels when implanted in the arch. Branched stent-grafts are conceptually more appealing than fenestrated devices as they are adaptable to a wide range of anatomical morphologies. Branched stent-grafts can be manufactured as either single- or multi-branched endografts with or without inner tunnels. These inner tunnels can be either antegrade or retrograde with antegrade tunnel branches tending to provide a smoother transition of flow into the arch branches as reported in previous computational studies (8). Single-branched stent-graft requires two bypass connections between the upper branches, e.g., bypass between the innominate artery and the left common carotid artery or between the left subclavian artery and the left common carotid, and thus may result in insufficient blood perfusion to the supra-aortic arteries as the entire flow is supplied by a single bridging stent. Double-branched endografts are developed for zone 0 deployment with two bridging stents connected to the innominate and left common carotid arteries (9, 10). The choice of endograft used lies with clinicians and is based on the treatment procedure, deployment zone, and other peri-operative factors.

Implanting an endovascular device will obviously change the flow within the repaired region, and it is of particular interest to gain more insights into the haemodynamic changes induced by the endograft (11, 12). *In vivo* examinations and clinical imaging alone cannot provide information on certain parameters of interest such as wall shear stress (WSS), forces exerted on the wall, and localised flow patterns. Previous studies have examined the performance of endografts in the aortic arch and their ability to perfuse the arch branches. For example, Zhu et al. (13) and Sengupta et al. (14) performed computational fluid dynamics (CFD) analysis of aortic flow after implantation of double-branched endografts in patients with arch aneurysms and noted improved flow patterns with increased WSS in the aortic arch. However, the presence of such inner branches can lead to disturbed flow in the region. In addition, arch endografts often involve occlusion of the native ostia of supra-aortic branches and peri-operative revascularisation procedures are required to maintain perfusion to the arch branches (15). Left subclavian artery revascularisation, often through the left common carotid artery, can lead to increased flow in the remaining native vessels with increased peak flow velocity and higher displacement forces being exerted in the region (16, 17).

The influence of endografts on flow in the repaired aorta depends strongly on their design, and here the focus is on the effect of a single-branched device with no inner tunnel branches, suitable for zone 0 deployment to treat aortic arch pathologies. The device implanted in the patient included in this investigation is the Nexus^{TM} Aortic Arch Stent Graft System developed by Endospan (Herzlia, Israel). As shown in **Figure 1**, it consists of a main module for the aortic arch and descending aorta with a side-branch for one supra-aortic vessel and a curved module for the ascending aorta that connects to the main module through a self-protecting sleeve (18). The device is suitable for implantation in zone 0 to zone 2 in the thoracic aorta and the branch emerging from the main module serves as an anchoring mechanism to hold the component in place. Being an "off the shelf" device, the length of each module and the diameters are chosen based on the application and anatomical features of the aorta being treated (19). The proximal end of the device has curved stent tips designed for atraumatic sealing in the ascending aorta and is meant to reduce pressure points on the outer curvature. The two modules overlap and have a radial force interlocking mechanism holding the separate components together in the ascending region.

This investigation aimed to examine the haemodynamic and biomechanical conditions of the aorta following TEVAR treatment for an aortic arch aneurysm with the Nexus^{TM} device. We used patient-specific geometric models reconstructed from computed tomography (CT) scans acquired before and after the interventional procedure and at follow-up.

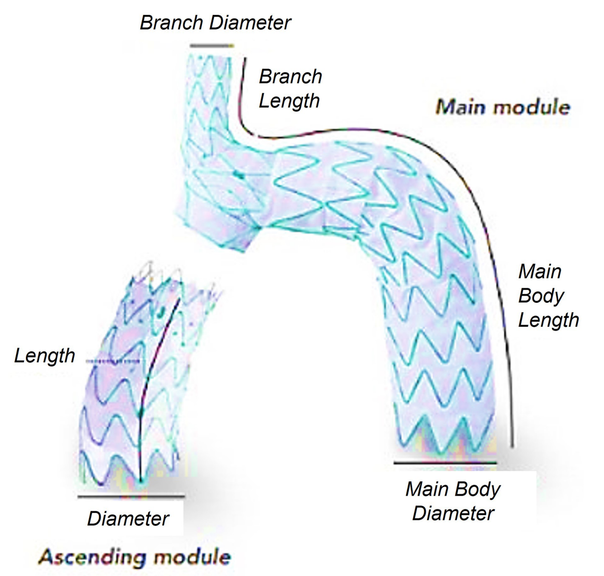

FIGURE 1
The NEXUS^{TM} device selected for TEVAR, highlighting its features and different components.

2. Materials and methods

2.1. Patient data

Clinical data and images were acquired from a patient with a large aneurysm arising from the inferior wall of the aortic arch. The patient underwent TEVAR with a single-branched Nexus™ device. **Figure 2** outlines the timeline of the case being studied, with reconstructions from clinical images showing the progression of the case. Ethical approval was obtained from the local Ethics Committee, and written consent was given by the patient.

The aneurysm, measuring 9.6 × 6.0 × 5.9 cm in the aneurysmatic sac, led to compressions in the distal pulmonary vessels but there were no morphometric changes to the innominate artery (IA), left common carotid (LCC) artery and left subclavian artery (LSA). Pre-intervention CT images with measurements of diameters and distances at three different locations are shown in **Figure 3**.

The patient was treated with TEVAR using the Nexus™ device; the intervention was carried out following a debranching procedure to set up a bypass between the right common carotid (RCC) and LCC, as well as the LCC and LSA. The procedure was successful and restored flow in the arch whilst successfully excluding the aneurysm, with a suitable proximal sealing length of 3.5 cm from the IA, greater than the minimum recommended length of 3.0 cm. The measured landing diameter of the ascending aorta was 38 mm, and that of the device was 43 mm, thereby producing an oversize ratio of 13.2%. The aneurysmal sac was successfully sealed, both LCC-RCC bypass and LCC-LSA bypass were patent. However, follow-up scans indicated the LCC-RCC bypass remained patent whilst the LCC-LSA bypass was compromised with a thrombus in the bypass near the LCC vascular stroma. A final follow-up of the patient 10 months after the intervention revealed the formation of an aneurysmal sac in the ascending aorta with migration of the ascending module of the device and a suspected leak or tear in the ascending aorta.

The patient had other comorbidities which needed to be taken into consideration during the treatment planning stages. Prior to intervention, the patient was on alendronate 10 mg OD, atorvastatin 20 mg OD, folic acid 5 mg BD, methotrexate 20 mg weekly, omeprazole 20 mg OD, prednisolone 5 mg BD. Following the intervention, the medication was adjusted to alendronate 70 mg OD, aspirin 75 mg OD (for 3 months), atorvastatin 20 mg OD, bisoprolol 1.25 mg OD, clopidogrel 75 mg OD (for 3 months), folic acid 10 mg weekly, methotrexate 15 mg weekly, omeprazole 20 mg OD, prednisolone 10 mg OD.

2.2. Geometric models

Anatomically accurate 3D geometries were reconstructed based on CT scans acquired using an ECG-gated spiral CT scanner

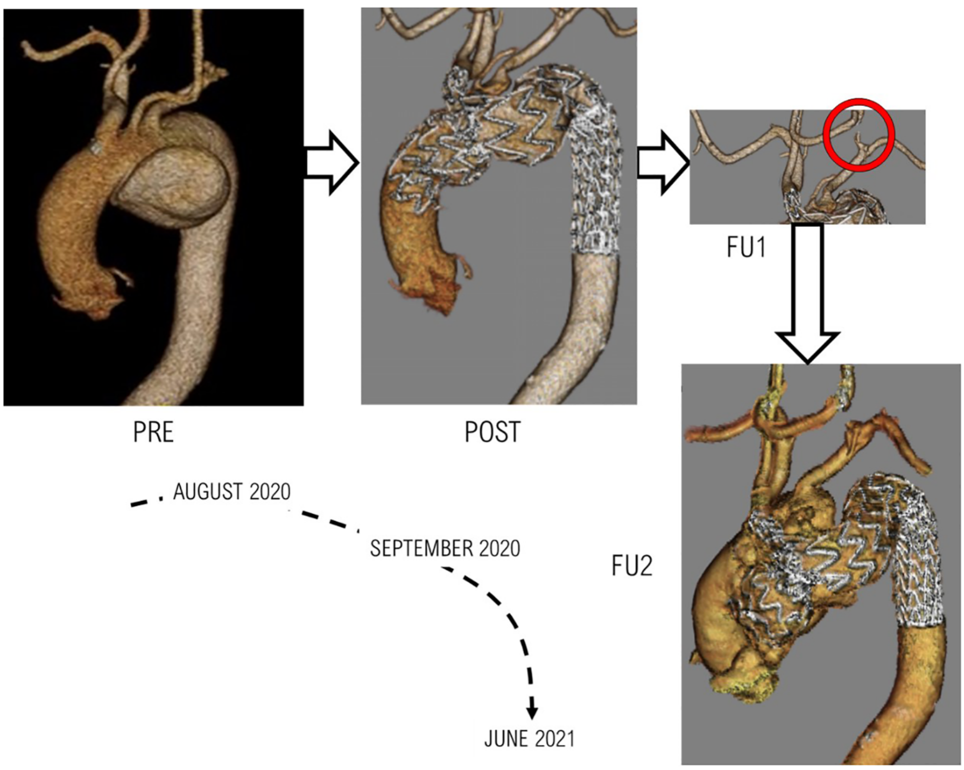

FIGURE 2
The various stages of treatment and follow-ups for the patient examined. PRE: Pre-TEVAR geometry indicating presence of aneurysm, POST: Post-TEVAR geometry following a successfully completed procedure, FU1: First follow-up scan which indicated negative results in the form of the carotid-carotid bypass being compromised, FU2: The final clinical images obtained from the patient indicating the formation of an aneurysmal sac in the ascending aorta.

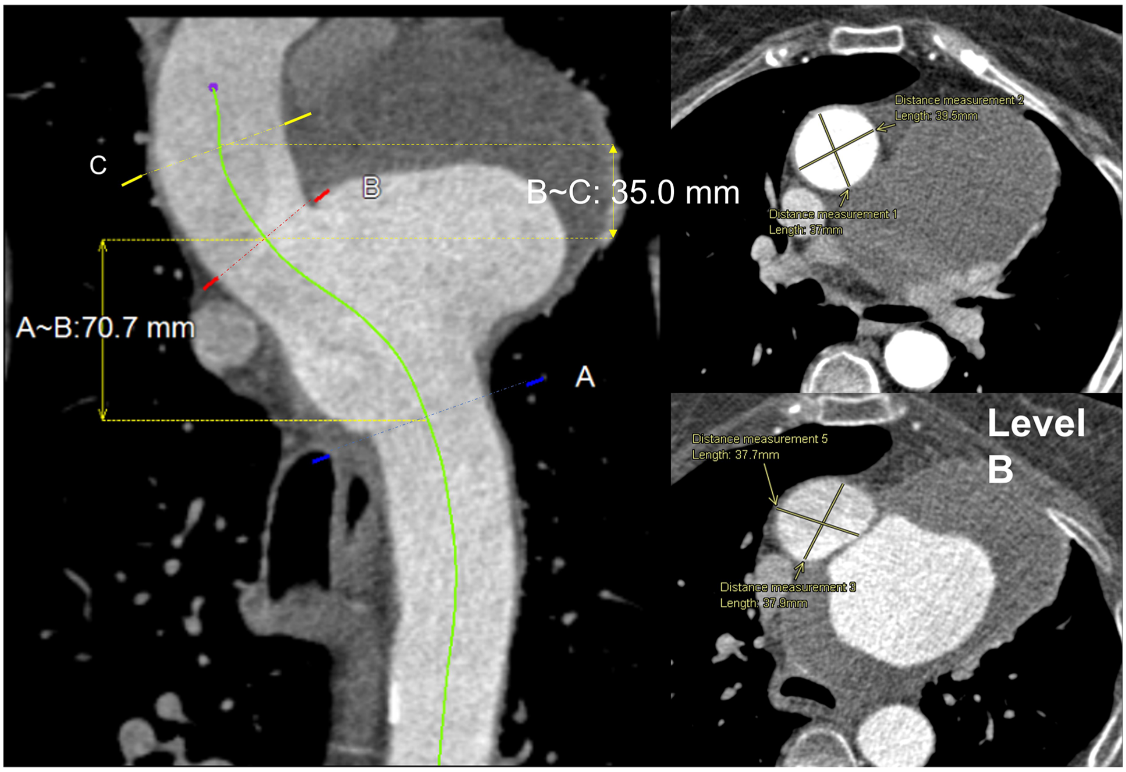

FIGURE 3
Central line view of the whole aorta: (left) proximal to distal aorta with three marked levels. (A)—just beyond LSA, (B)—just before IA, (C)—proximal landing zone, 35 mm from IA proximally to the ascending aorta. The length between (B) and (C) is 35 mm, and (B) and (A) is 70.7 mm. (Right) Transverse view of levels (B) and (C) with a cross-sectional measurement of aortic diameter 37.9 × 37.7 mm and 37.0 × 39.5 mm, respectively.

(Siemens Somatom) at various stages as described in Figure 2. Image segmentation and 3D reconstruction of the aorta were performed using an image processing software, Mimics (v20, Materialise, Leuven, Belgium). A thresholding technique was adopted to isolate the regions of interest (ROI). User-defined lower and upper limits of grayscale intensity were set for thresholding, with a typical lower limit of 270–280 HU and an upper limit of 2,000 HU or above depending on the image resolution. This produced initial 2D masks on all the available slices. A split mask function was then used to separate the ROI from unwanted neighboring tissues that might have been included in the initial masks. The separated masks were manually inspected and modified if necessary to ensure all pixels in the targeted vessels were selected. Finally, the reconstructed geometries were smoothed using the Discrete Gaussian filter based on a linear smoothing enhancement algorithm. The smoothing function requires a smoothing factor (within range 0–1) and the number of iterations (within range 1–500) to be specified. A specific "compensate shrinkage" feature was enabled to preserve the shape of the geometry, thereby preventing the lumen of the aorta and its branches from shrinking. This was ensured by comparing vessel diameters extracted from the reconstructed 3D surface with those measured in the CT images at multiple locations of interest. Sensitivity tests indicated that setting a smoothing factor of 0.1 and 50 iterations for each stage of smoothing produced reliable reconstructions used in this study. Figure 4 shows the pre-TEVAR geometry which featured a large aortic arch aneurysm in the inferior radius of the arch and three supra-aortic branches emerging from the arch. The model also included the right brachiocephalic artery and RCC which bifurcate from the IA, resulting in four model outlets in the arch. The post-TEVAR geometry (Figure 3) incorporated the implanted device where the two modules were considered as one body and connected with the unstented portions of the aorta. The IA branch and its bifurcation were included while the LCC and LSA were excluded as they were covered by the main module. As a result, the post-TEVAR geometry had two outlets in the arch.

Mesh generation was carried out using ANSYS ICEM CFD (v15.0, ANSYS Inc., Canonsburg, PA, USA). For haemodynamic analysis, unstructured meshes consisting of 10 prismatic boundary layers at the wall were generated with approximately 6.8 and 5 million elements in the post-TEVAR and pre-TEVAR geometries respectively. For biomechanical structural analysis, a constant wall thickness of 1.4 mm was applied to the reconstructed 3D luminal surface, creating a solid volume representing the aortic wall. Figure 5 shows the solid domain geometry consisting of 6.8 million elements and the delineation of the stented and unstented regions.

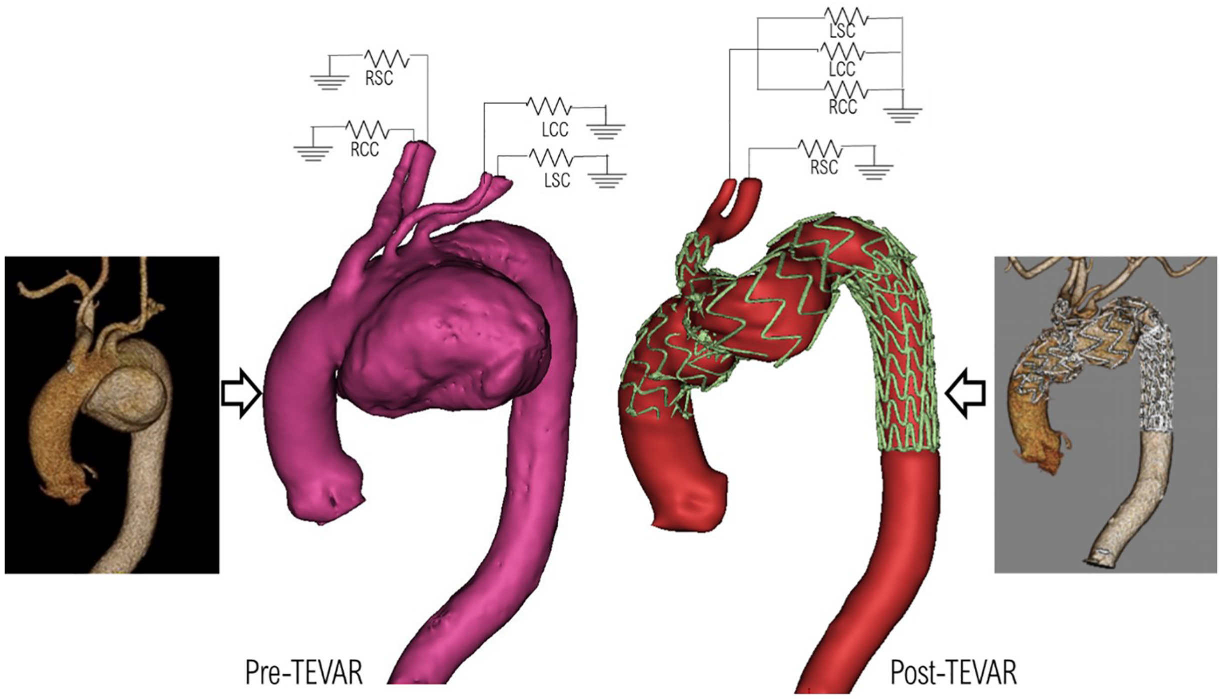

FIGURE 4
Pre-TEVAR **(left)** and post-TEVAR **(right)** models reconstructed from the corresponding CT scans, and the prescribed 3-EWM boundary conditions at the model outlets.

2.3. Computational details and boundary conditions

Flow in the aorta was described by the transient, three-dimensional equations for conservation of mass and momentum. Blood was modelled as a Newtonian fluid with a constant density of 1,060 kgm^{-3} and dynamic viscosity of 0.004 Pa s. Based on the measured peak flowrate of 2.34×10^{-4} m^3/s and inlet area of 993.13 mm^2, the peak Reynolds number was 2,182.3 and the corresponding Womersley number was 19.2. This combination indicated that flow in the ascending aorta was likely to be disturbed (20), hence the need to employ the SST-Tran (shear stress transport—transitional) model, which has been shown to be more suitable for physiological flows involving potential transition from laminar to turbulent flow (21, 22).

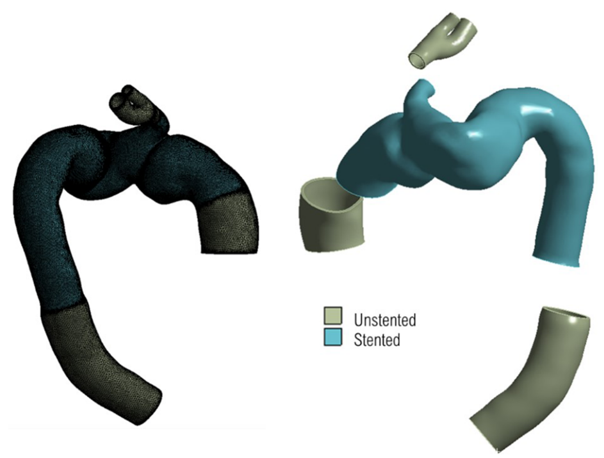

FIGURE 5
3d geometry for structural domain, with unstructured mesh shown on the **left**, and segments of different material highlighted on the **right**. The uniform thickness of the geometry can be seen clearly on the **right** with the branch inlets and outlets serving as regions of fixed points to tether the geometry in place.

In order to solve the flow governing equations numerically, suitable boundary conditions at the inlet and outlets are required. These should, as much as possible, represent the flow conditions specific to the patient and the stage of treatment being considered. The inflow waveform was adapted from a previous study (22) and then adjusted to represent the recorded cardiac output of the patient and further tuned to the dimensions of the model inlet (23, 24). The lack of patient-specific inflow data, such as 4D Flow MRI specific to the patient, necessitated the implementation of a novel method for generating realistic 3D inlet velocity profiles (IVPs). A synthetic dataset of virtual aortic velocity profiles was generated by employing statistical shape modelling (SSM) to a clinical dataset consisting of 31 thoracic aortic aneurysm (TAA) cases; this produced representative 3D IVPs comparable to that of the velocity distributions observed whilst using specific 4D Flow MRI data (25). The velocity profile producing peak systolic velocity closest to that of the clinical measurement was chosen and interpolated in time to match the length of the cardiac cycle. **Figure 6** shows the generated IVPs

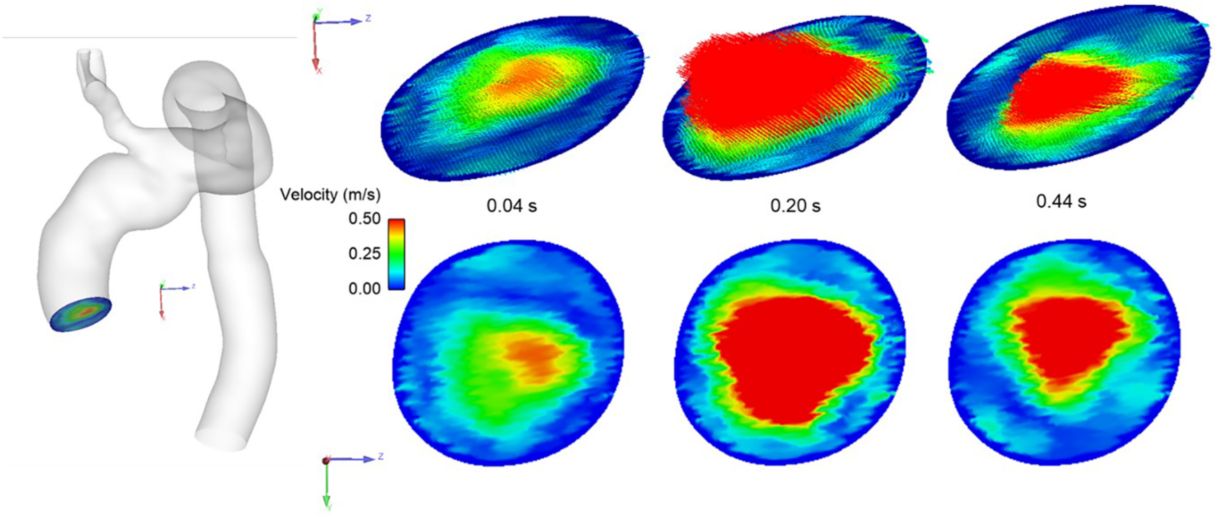

FIGURE 6
Representative 3D inlet velocity profile imposed at model inlet showing velocity distribution at different stages of the systolic phase of the cardiac cycle.

prescribed at the model inlet. The length of the cycle was adjusted according to the heart rate (HR) of the patient (Pre-TEVAR HR: 74 beats/minute, Post-TEVAR HR: 84 beats/min).

A 3-element Windkessel model (3-EWM) was prescribed at the outlets and tuned according to blood pressure measurements made throughout the observation and treatment phases (pre-TEVAR aortic pressure: 119/72 mmHg, post-TEVAR brachial pressure: 133/62 mmHg) using an established method (26). Since the 3-EWM requires mean arterial pressure (MAP) values for the necessary parameters to be set, MAP was calculated from the measured systolic and diastolic pressures (SP and DP respectively) (27).

$$MAP = DP + \frac{1}{3}(SP - DP)$$

Since the measured post-TEVAR pressure corresponded to the brachial (*brach*) pressure, which cannot be directly utilised for the 3-EWM, the measured brachial pressure was converted to central (*cent*) pressure using the following expression (28), with $DP_{cent} = DP_{brach}$,

$$SP_{brach} \approx 0.83SP_{cent} + 0.15DP_{cent}$$

All the model parameters used in the 3-EWM are given in **Table 1**. In addition, the employment of SST-Tran model required a turbulence intensity (Tu) to be prescribed at the inlet. A low Tu of 1% was set based on previous experience (21, 22). The wall was assumed to be rigid with a no-slip boundary condition. CFD simulations were carried out using ANSYS CFX v15.0 (ANSYS, Canonsburg, PA, United States) with a fixed time-step of 0.001 s and a convergence criterion of 10^{-5}. All simulations were run for at least 3 cycles until a periodic solution was reached.

TABLE 1 3-EWM parameters used in the three models simulated in this study.

Model	Outlet	R1 [Pa s m^{-3}] (× 10^7)	C [m^3 Pa^{-1}] (× 10^{-9})	R2 [Pa s m^{-3}] (× 10^8)
PRE	RSA	5.75	1.07	16.2
	RCCA	9.94	0.669	25.8
	LCCA	24.4	0.399	42.4
	LSA	9.63	0.868	19.7
	OUT	1.20	6.98	2.45
POST	RSA	5.75	1.03	16.8
	RCCA	4.02	1.03	9.19
	OUT	1.20	5.13	2.54
FU1	RSA	5.75	1.03	1.68
	RCCA	6.91	1.03	16.7
	OUT	1.20	7.56	2.25

RSA, Right subclavian artery; RCCA, Right common carotid artery; LCCA, Left common carotid artery; LSA, Left subclavian artery; OUT, model outlet).

For finite element analysis (FEA) of wall deformation and stress in the post-TEVAR model, the native aorta was assumed to be an isotropic, homogeneous and linear elastic material with a Young's modulus (E) of 0.8 MPa and Poisson's ratio (ν) of 0.49 (29). The stented region was also modelled as a linear elastic material with a Young's modulus of 15 MPa and Poisson's ratio of 0.3 (30, 31). The material densities were 1,100 kg.m^{-3} and 2,140 kg.m^{-3} for the native aorta and stented region respectively (30) (Molony et al., 2009). Since the aortic wall model was reconstructed from CT images obtained at diastole, it was necessary to account for prestress in the aorta under diastolic pressure conditions. Prestress was estimated using an iterative approach proposed and evaluated in previous studies (32, 33). The iterative process was carried out until the maximum total deformation in the stressed configuration was less than 0.5 mm under a diastolic pressure, allowing for the structural domain to

TABLE 2 Haemodynamic indices used for analysis in this study.

Metric	Mathematical expression	Description
Time-averaged WSS	$TAWSS = \frac{1}{T}\int_0^T \lvert\tau_w\rvert dt$	Average of the WSS magnitude over the cardiac cycle.
Transverse WSS	$TransWSS = \frac{1}{T}\int_0^T \left\lvert \tau_w \cdot \left(n \times \frac{\int_0^T \tau_w dt}{\lvert\int_0^T \tau_w dt\rvert} \right) \right\rvert dt$	Average over the cardiac cycle of WSS components perpendicular to the temporal mean WSS vector.
λ_2 criterion	$\lambda_2 = \frac{\partial v_x}{\partial y}\frac{\partial v_y}{\partial x} + \left(\frac{\partial v_y}{\partial y}\right)^2 + \frac{\partial v_y}{\partial z}\frac{\partial v_z}{\partial y}$	Synthetic descriptor for incompressible flows used to evaluate isosurfaces in flow.
Displacement force	$F_{d,i} = \int_{A,i} pdA + \int_{A,i} \left(-\eta_w \frac{\partial u_t}{\partial n}\right) dA$	Time dependent displacement force due to pressure and friction exerted by the flow of blood on the walls.
Oscillatory shear index	$OSI = \frac{1}{2}\left(1 - \frac{\lvert\int_0^T \tau_w dt\rvert}{\int_0^T \lvert\tau_w\rvert dt}\right)$	Change of direction of the WSS vector from the primary direction of flow.
Endothelial cell activation potential	$ECAP = \frac{OSI}{TAWSS}$	Synthetic metric to identify regions at a higher risk of thrombus formation.

T is the time period of a cardiac cycle; τ_w is the wall shear stress vector; v_x, v_y, v_z are the velocity components in the x, y, and z direction; u_t is the tangential velocity with respect to the unit normal for each element.

achieve equilibrium with the internal blood pressure (34). The obtained prestress tensor was then applied in the FEA simulation where the geometry was tethered at the inlet and branch outlets and peak systolic pressure distribution from the flow simulations were applied as the load at the internal surface of the wall model. All FEA simulations were carried out using ANSYS Static Structural v19.2 (ANSYS, Canonsburg, PA, United States).

2.4. Haemodynamic metrics and endograft dynamics

This investigation explores the haemodynamic response to the implanted device, focusing on localised flow patterns, WSS-related metrics and flow disturbances. A list of the indices used here are defined in Table 2. A detailed description of the relevant haemodynamic metrics for the investigation can be found in our previous work (14).

3. Results

3.1. Flow patterns

Figure 7 shows instantaneous streamlines at peak systole for all the simulated scenarios (PRE, POST, and FU1). Flow in the ascending aorta was helical with high velocities skewed towards the outer curvature in all models. The presence of the aneurysm in the arch (PRE) caused a large recirculation zone in the aneurysm sac. Excluding the aneurysm *via* TEVAR restored a more desirable flow pattern in the arch, as can be seen in POST. This not only led to more uniform flow into the supra-aortic branches, but also virtually eliminated any undesirable recirculating flow in the arch. Aside from small differences in the supra-aortic branches, there seem to be no qualitative differences in flow patterns between POST and FU1.

Comparison of the time-varying outflow through the RCC outlet is given in Figure 8 for the three simulated scenarios. The large recirculation zone in the aneurysm sac affected perfusion of the arch branches in PRE where flow through the RCC outlet was retrograde for approximately 64% of the cardiac cycle. PRE also had a lower peak flowrate and significantly lower flow throughout the cycle, providing a mean outflow of 3.48×10^{-6} m^3s^{-1} (0.21 L/min) through the RCC. Other arch branches also experienced large periods of retrograde flow ranging between

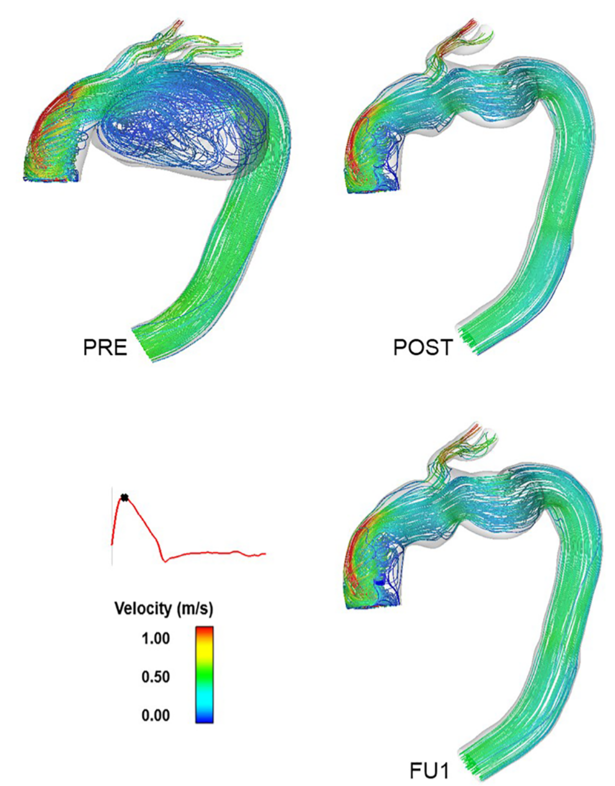

FIGURE 7
Instantaneous velocity streamlines at peak systole for the pre-TEVAR (PRE—top **left**) and post-TEVAR (POST—top **right**) and follow-up (FU1—bottom **right**) models. This indicates the exclusion of the aneurysm in the inner curvature of the arch following the procedure and the flow patterns observed at the follow-up examination following the compromise of the carotid-subclavian bypass.

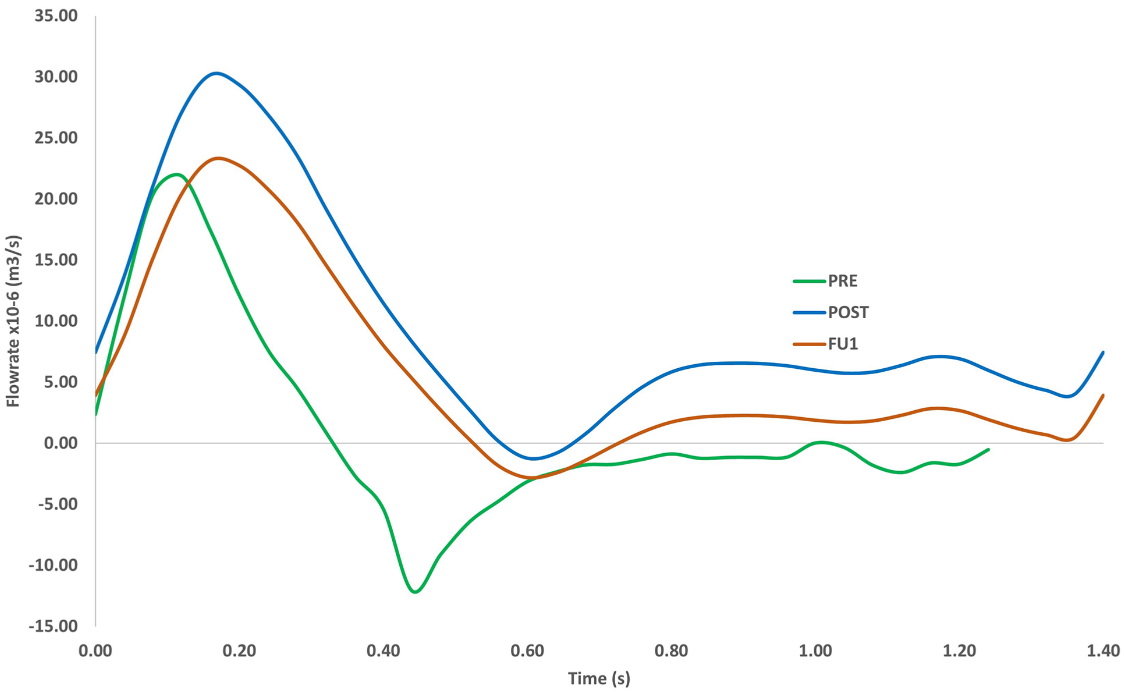

FIGURE 8
Volumetric flowrate in the RCC for the pre-TEVAR (PRE) case, post-TEVAR (POST) and follow-up (FU1) cases **(bottom)**. The length of the cardiac cycle was based on clinical measurements (1.23 s for pre-TEVAR and 1.4 s for post-TEVAR).

64%–69% of the cardiac cycle. Post-TEVAR flow through the RCC was mostly antegrade with a mean outflow of $9.59 \times 10^{-6}\,m^3s^{-1}$ (0.57 L/min). The difference in outflow between POST and FU1 was due to the altered boundary conditions in FU1 to represent the break in the carotid-subclavian bypass further downstream of the RCC. As a result, FU1 had a lower flow rate of $5.55 \times 10^{-6}\,m^3s^{-1}$ (0.33 L/min) through the RCC.

The vortical flow structure throughout the modelled aorta is visualised using the λ_2 criterion as shown in Figure 9. A threshold value of $-100\,s^{-2}$ was chosen in order to isolate the

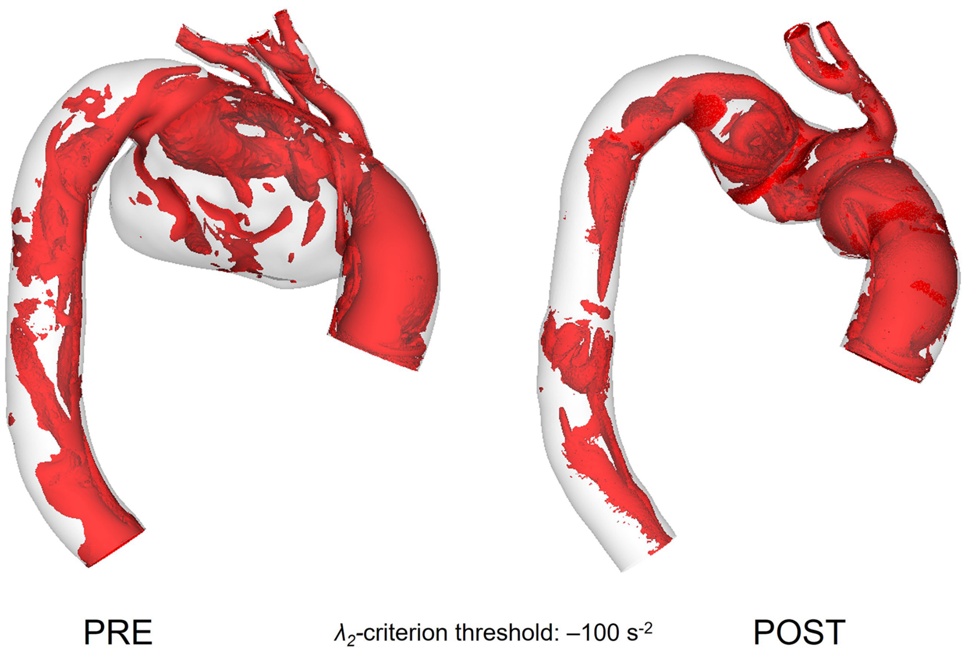

FIGURE 9
Vortical structures within the vessel represented as isosurfaces using the λ_2 criterion for pre-TEVAR **(left)** and post-TEVAR **(right)** stages.

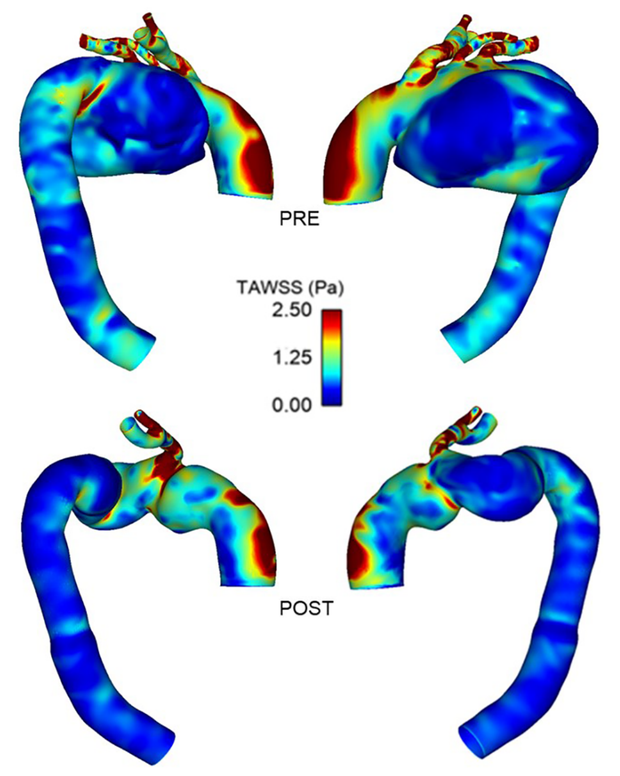

FIGURE 10
Comparison of time-averaged WSS between pre-TEVAR (**top**) and post-TEVAR (**bottom**) stages.

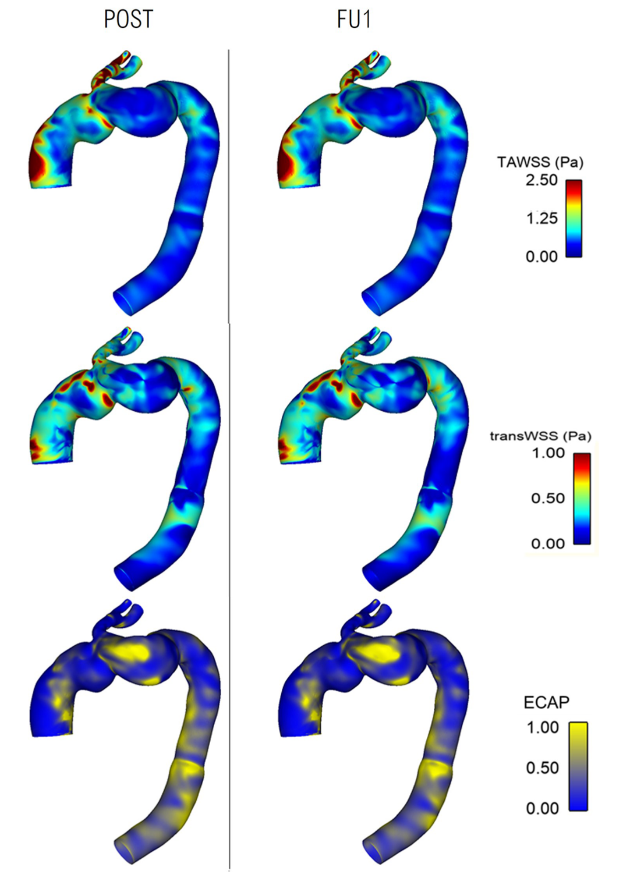

FIGURE 11
Comparison of wall shear stress-related metrics between post-TEVAR and follow-up stages with time-averaged WSS (**top**), transverse WSS (**middle**) and endothelial cell activation potential (**bottom**) maps all showing similar spatial distribution and patterns between the two cases.

relevant vortex cores formed in the aorta and to make suitable qualitative comparisons. Pre-TEVAR aneurysmatic flow understandably presented with a greater degree of disturbance as flow entered the arch branches compared to the post-TEVAR model which presented with vortical flow that can be often seen in and attributed to the curved nature of the vessel giving rise to counter-rotating vortices.

3.2. Wall shear stress related indices

Wall shear stress and its associated indices are important near wall haemodynamic parameters which can affect endothelial cell proliferation and play a role in thrombus formation (35, 36). **Figure 10** demonstrates the difference in time-averaged WSS (TAWSS) patterns between PRE and POST. Both present with a large area of high TAWSS along the outer curvature of the ascending aorta, which is due to the skewed inlet velocity profile and the curvature of the aorta. The large recirculation zone in the aneurysmal sac, as seen in **Figure 7**, led to extremely low TAWSS in this area (PRE), with elevated TAWSS along the outer curvature of the arch and in the emerging branches. In the PRE model, a patch of elevated (>2.5 Pa) TAWSS can be seen in the inner curvature of the arch, immediately downstream of the aneurysm.

Comparisons of WSS-related indices between POST and FU1 are shown in **Figure 11**, displaying high degree of similarities. TAWSS and transverse WSS (transWSS) are useful metrics which serve as indicators for thrombus formation and plaque development, and there appears to be no extremes of magnitudes or abnormal spatial distribution of either. Endothelial cell activation potential (ECAP) identifies regions of high oscillatory shear index (OSI) and low TAWSS and regions of ECAP higher than 5.0 can pose a risk of thrombus formation (37, 38). However, in these cases there appears to be no abnormally high values of ECAP.

3.3. Displacement force

The implanted SG experiences a displacement force (DF) resulting from the change in net momentum owing to pressure and WSS generated by the aortic blood flow. Since pressure is the dominant component, the time-varying nature of displacement force is expected to closely resemble the pressure waveform (39). **Figure 12** shows the displacement force acting on the ascending module of the endograft in POST, decomposed into three orthogonal components as defined in the figure. The displacement force was primarily in the z-direction but with a significant component in the y-direction due to the non-planar curvature of the aorta, thus along the coronal plane for the individual.

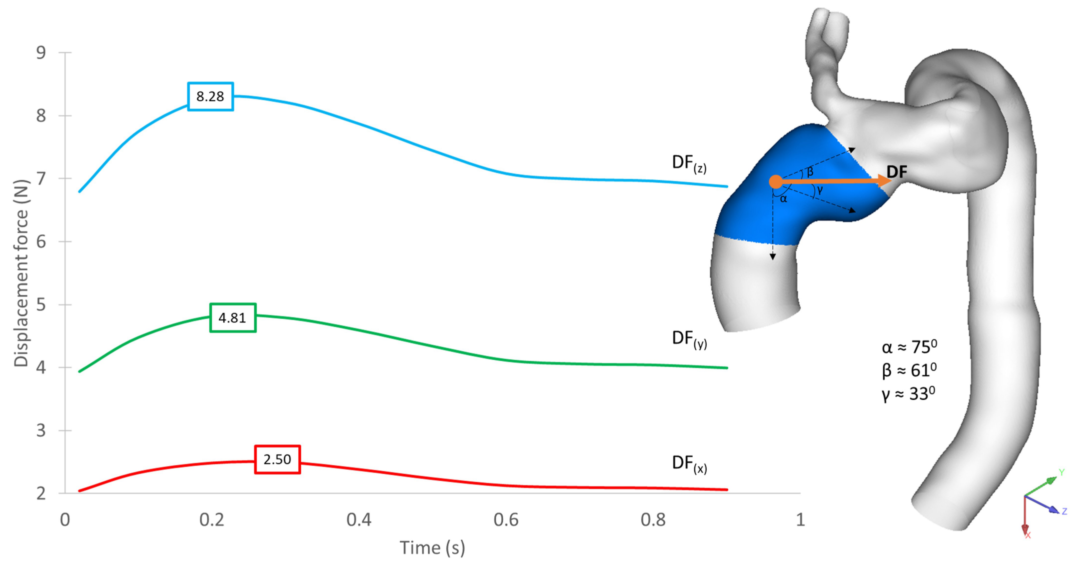

FIGURE 12
Time-dependent displacement forces acting on the ascending module of the device, shown for POST, decomposed into x-, y- and z-components with peak values in each direction indicated on the plot. The direction of the resultant force is shown on the geometric model.

Figure 13 demonstrates the difference in displacement force between POST and FU1, with the endograft experiencing a consistently higher force in FU1 than in POST throughout the cycle. The maximum displacement force in FU1 was 15% higher than in POST.

Since the ascending module of the device is of particular interest in this case, it was further divided into separate segments, and the magnitude of displacement force was calculated for each of these segments. As shown in Figure 14, the distribution of displacement force was non-uniform with

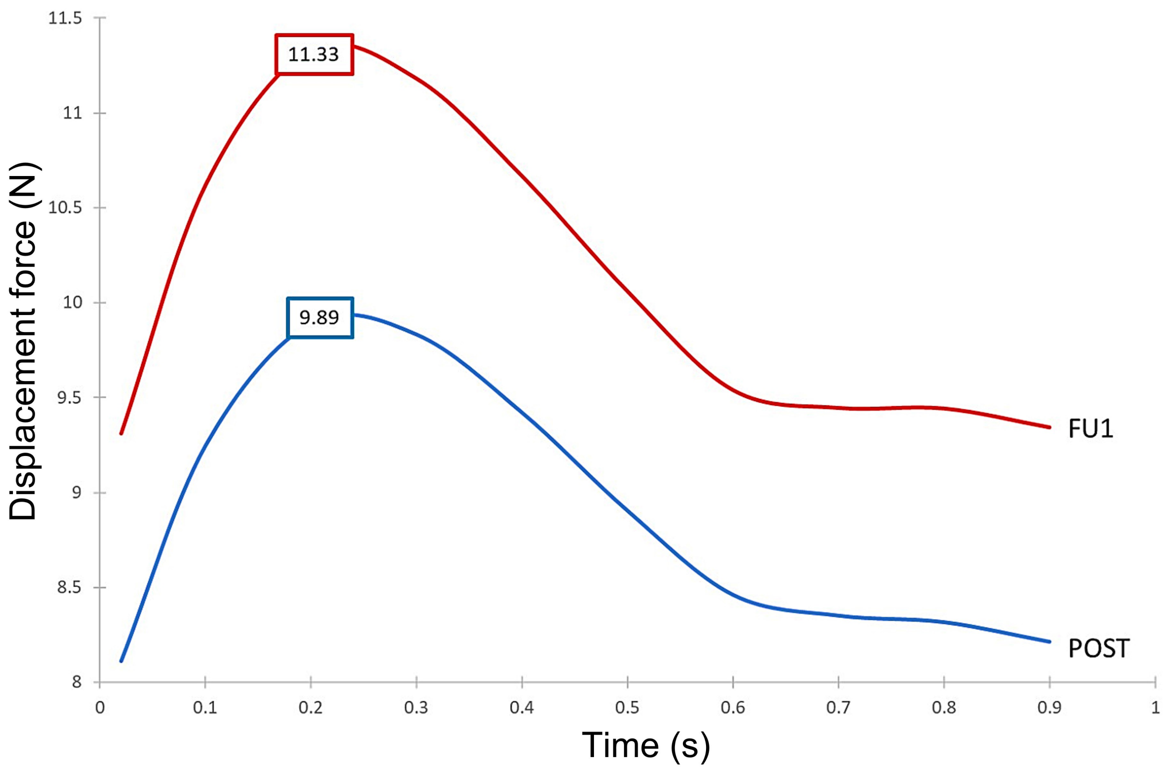

FIGURE 13
Time-dependent displacement forces exerted on the ascending module of the device post-TEVAR (post) and at follow-up (FU1) stages.

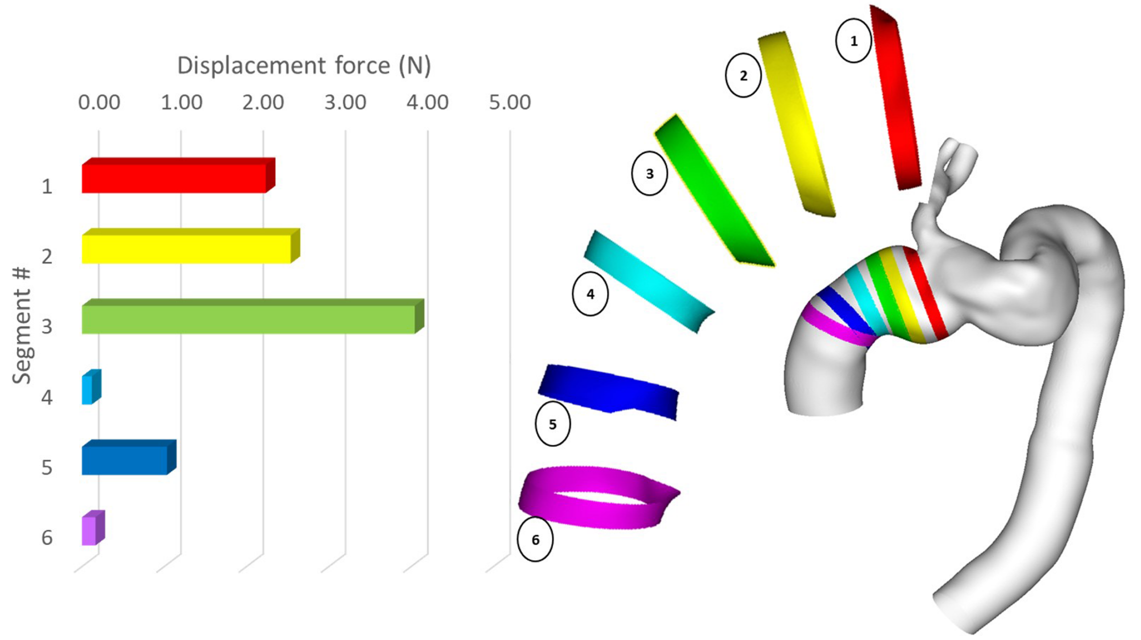

FIGURE 14
Peak magnitude of displacement force exerted upon different segments of the ascending module of the device.

larger values in the distal portion of the ascending module. Segment 3 experienced the largest displacement force, followed by segment 2 and 1, which are closer to the overlapping region between the ascending module and the main endograft.

3.4. Wall displacement and mechanical stress

Figure 15 presents the spatial distribution of wall displacement and von Mises stress (equivalent stress) obtained with the FE analysis. The structural analysis was carried out at peak systole to represent the worst-case scenario when the aorta was subjected to the maximum pressure load. The highest von Mises stresses were observed in the distal ascending aorta, immediately upstream of the emerging branch. This coincides with the previously highlighted overlapping region between the two modules. The maximum displacement of up to 2.41 mm was observed at the distal end of the arch and could be attributed to the region not being anchored by the LCC and LSA.

4. Discussion

The case analysed in this investigation presented with a rather complex pathology along with several comorbidities that had to be taken into account when determining treatment for the patient. TEVAR was considered the best option due to its minimally invasive nature and the availability of the device to exclude the aneurysm and restore flow in the region. The chosen device was a single-branched aortic arch endograft with a side branch

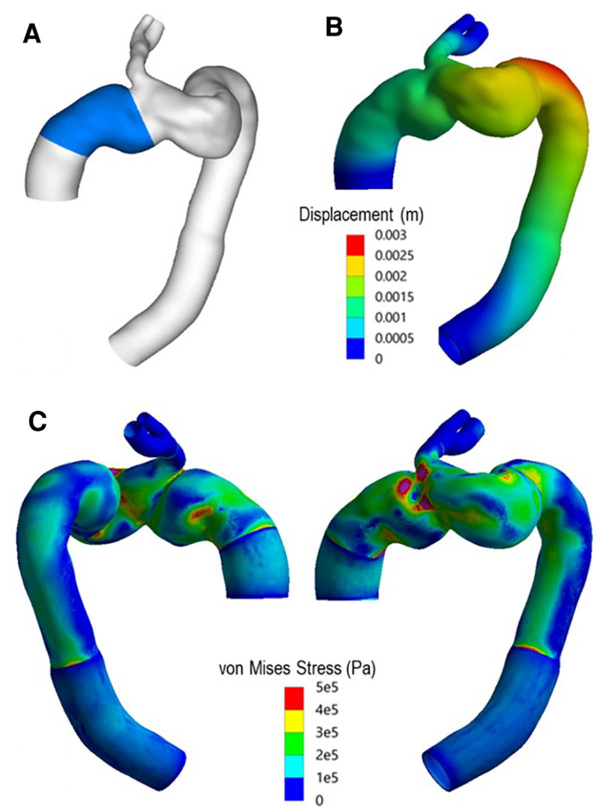

FIGURE 15
(A) Highlighted region indicates ascending module of the device. (B) Total displacement experienced by the vessel at peak systole. (C) Spatial distribution of von Mises (equivalent) stress in the wall at peak systole.

leading into the innominate artery. Revascularisation was carried out prior to the TEVAR procedure by introducing bypasses from the RCC to LCC and LCC to LSA. Clinical information and the second follow-up CT examination (as shown in Figure 2 at FU2) indicated the formation of a new aneurysm in the ascending aorta, with migration of the ascending module of the device and a suspected leak or tear in the ascending aorta.

4.1. Comparing pre- and post-intervention haemodynamics

As shown in Figure 7, the presence of a large aneurysm in the arch caused a significant reduction in flow velocity and recirculating flow in this region, which adversely influenced the flow leading into the arch vessels as reported by others (13). This was evidenced through a prolonged period of retrograde flow through the RCC (Figure 8), which could impair blood perfusion further downstream. Multidirectional flow can also lead to extreme WSS, which may increase the risk for thrombus formation and/or atherosclerotic lesion development in the supra-aortic arteries (40).

The TEVAR procedure using a single branched endograft successfully excluded the aneurysm and restored more organised flow in the arch. A smoother lumen, in the absence of the aneurysm, allowed for sufficient flow leading into the IA, which in turn perfused the LCC and LSA through the bypass performed pre-TEVAR. Nevertheless, the non-planar and tortuous geometry of the arch was exacerbated after the endograft was deployed as can be seen from the post-TEVAR geometry (Figure 4). The procedure also resulted in increased flow into the IA, which was the only supra-aortic branch directly perfused through the arch and it had to carry additional flow to supply the LCC and LSA. The choice of device was made based on the complex nature of the region being treated and to ensure sufficient perfusion to the supra-aortic branches. Branched and fenestrated endografts would both serve the purpose of aortic branch perfusion, but the local haemodynamics will be influenced by the endograft design. Using a branched stent-graft allows for flow to be smoothly guided into the emerging arch branch. Additionally, the ability of the main module of the single branched device to be securely anchored in the deployed region made it the more suitable choice in this case.

4.2. Post-intervention and beyond

Flow patterns in the POST and FU1 were largely similar throughout the aorta, with a small difference in the IA due to the different outflow through the RCC branch. Close examination of WSS-related indices also revealed no significant alteration between POST and FU1 as shown in Figure 11, suggesting that the minor change in outflow conditions through the RCC in FU1 had not affected the global flow patterns and near wall haemodynamics.

It was clear from the final follow-up (FU2) CT scan (Figure 2) that further complications occurred between FU1 and FU2. The scan revealed the formation of a large aneurysm alongside the ascending module of the device, which extended along the outer curvature of the arch. Flow through this bulge perfused the native ostia of the LSA and LCC which were initially occluded prior to the TEVAR procedure. It was suspected that a leak or tear occurred in the ascending aorta, but the origin of the leak was undetermined, and a suspected source of the leak could be migration of the device or dehiscence due to improper fixation. This necessitated a closer examination of the biomechanical environment of the ascending aorta in searching for a plausible cause for the suspected leak.

Firstly, the possibility of device migration was assessed. The main module of the device was unlikely to move as it was anchored securely by the branch leading into the IA, but the ascending module was connected to the main module through a self-protecting sleeve and relied on a radial force interlocking mechanism to hold it in place. Migration of the ascending module could occur if the displacement force (DF) acting on it was sufficient to move it upward or pull it away from the main module, which would lead to type I or type III endoleak respectively (41). Previous studies suggested that DF exerted on the endograft can have a considerable effect on its spatial stability (42), and that the magnitude and direction of DF are influenced by the endograft geometry, the haemodynamic state of the patient, and the local geometry of the vessel (39, 43–45). Therefore, it was necessary to evaluate the DF experienced by the ascending module in both POST and FU1.

Our results showed that despite overall flow patterns being largely similar between POST and FU1, the DF increased by approximately 15% in FU1. The only difference between the POST and FU1 models was the outflow conditions imposed at the outlets. As has already been mentioned, the boundary conditions were altered to reflect the compromised LCC-LSA bypass, with excess flow being diverted to the descending aorta. This redirected flow resulted in changes in the normal pressure forces on the vessel wall, leading to an increase in DF. Nevertheless, the maximum DF of 11.33 N in FU1 was well below the reported threshold of 32 N to dislocate a non-planar stent-graft in the thoracic aorta (46). While threshold values have been reported for the abdominal and thoracic aorta (47, 48), there is little information in the literature on the magnitude of DF needed to cause device migration in the ascending aorta. It was also interesting to note the direction of DF as illustrated in Figure 12 which shows clearly that the total DF experienced by the ascending module deviates from its local longitudinal direction. This was attributed to the curvature and non-planarity of the aorta, especially in the region of interest here, giving rise to increased anterio-posterior and lateral components (43). The direction of DF vector indicated that it would pull the ascending module laterally away from the outer curvature, which could compromise the stability in the proximal landing zone or lead to misalignment in the device (18, 19). Further analysis of the distribution of DF along the ascending module showed that the region close to the connection between the two modules experienced relatively high DF (Figure 14).

The spatial distribution of von Mises stress obtained with the finite element analysis showed high stresses in the region where the two parts of the device connect (**Figure 15**), owing to the highly tortuous local geometry and the emergence of the IA branch. The maximum von Mises stress was approximately 1.3 MPa, which exceeded the yield stress for dilated ascending aorta of 1.2 ± 0.1 MPa referenced in other studies (49, 50). Although the maximum stress occurred in the wall protected by the endograft, and the graft is much stiffer and can withstand higher stresses compared to the native aorta, the extremely high level of stress in this region could compromise the device locking mechanism, thereby increasing the risk of disconnection between the two modules. Moreover, high stress concentrations were also observed in the proximal and distal ends of the device, resulting from local geometric discontinuity and compliance mismatch between the graft and the native aorta. Such focal high stress regions have been found to correlate strongly with the locations of stent-graft induced new entry in type B aortic dissections (51, 52). Based on these findings, it is plausible to speculate that a proximal tear might have occurred which then led to the formation of the observed aneurysm.

4.3. Limitations

In the CFD simulations presented in this investigation, the aortic wall was assumed to be rigid and the supra-aortic vessels bypass was not included in the post-TEVAR model. The rigid wall assumption is expected to have a minor influence on the predicted flow patterns, especially in the post-TEVAR and follow-up models where a large part of the aorta was supported by the endograft. Excluding the supra-aortic vessels bypass is also likely to have an insignificant effect on the predicted haemodynamics and wall stress, even though its inclusion would have provided the opportunity to investigate potential causes for the failed carotid-subclavian bypass observed at FU1. In the finite element stress analysis, the aortic wall was modelled as a linear elastic material; this assumption was made because within the region of interest, the post-TEVAR aortic wall was largely integrated with the endograft with a relatively small section of the native aorta at the proximal and distal end of the device. In addition, the periodic motion of the aortic root and its influence on the ascending aorta were ignore, which could have influenced the predicted wall stress (53). Finally, the results presented here were confined to a single patient. However, the number of patients undergoing TEVAR of the entire aortic arch with a single-branched device is very limited and this paper focused on presenting a longitudinal analysis at multiple stages of the treatment.

5. Conclusion

This investigation presents a detailed haemodynamic and biomechanical analysis of a patient who underwent TEVAR treatment for a large aneurysm in the aortic arch using a single-branched endograft. Imaging data from different stages of the process along with physiologically representative numerical modelling allowed to paint a picture of the progression of the case from pre-intervention to post-intervention and beyond. Simulation results for the different stages demonstrated the dramatic improvement in flow patterns in the aortic arch after the TEVAR procedure. As the final follow-up examination revealed the formation of a new aneurysm in the ascending aorta, further analysis was carried out in searching for possible causes for the observed complication. Results for displacement forces on the endograft and stresses within the wall indicated that the endograft was subjected to an angulated displacement force in the lateral direction and the overlapping region between the main and ascending module experienced very high stresses, which could act together to weaken the locking system, resulting in migration or misalignment of the device. In addition, high stress concentration was observed at the proximal end of the ascending module, suggesting the possibility of a proximal tear as a source for the observed aneurysm. Careful positioning of the overlapping region and the proximal landing zone may help reduce the stresses in these regions at risk of compromising stent-graft stability. In this regard, finite element-based simulations of virtual stent-graft deployment, such as those reported recently on aortic dissections (53, 54), offer a promising tool that should be further developed and validated for use in pre-intervention planning to minimise potential device migration or endoleaks.

Data availability statement

The raw data supporting the conclusions of this article will be made available by the authors, without undue reservation.

Author contributions

Conceptualisation, XX and CN; methodology, SS; software, SS, LM and SP; validation, SS; formal analysis, SS and XY; investigation, SS; resources, XX; data curation, SS, XY, CN, and SP; writing—original draft preparation, SS; writing—review and editing, XX, SS, XY and CN; visualization, SS and XY; supervision, XX; project administration, XX; funding acquisition, XX. All authors have read and agreed to the published version of the manuscript. All authors contributed to the article and approved the submitted version.

Funding

SS is funded by a PhD studentship through Engineering and Physical Sciences Research Council Doctoral Training Partnership grant to Imperial College London (EP/R513052/1). XY is funded by a PhD studentship through the Lee Family Scholarship to Imperial College London.

Acknowledgements

SS would like to acknowledge the technical support and advice provided by Dr. Yu Zhu, Department of Chemical Engineering, Imperial College London; and LM would like to acknowledge the technical support and advice provided by Prof. Alberto Redaelli and Mr Simone Saitta, Department of Electronics, Information and Bioengineering, Politecnico di Milano.

Conflict of interest

The authors declare that the research was conducted in the absence of any commercial or financial relationships that could be construed as a potential conflict of interest.

Publisher's note

All claims expressed in this article are solely those of the authors and do not necessarily represent those of their affiliated organizations, or those of the publisher, the editors and the reviewers. Any product that may be evaluated in this article, or claim that may be made by its manufacturer, is not guaranteed or endorsed by the publisher.

References

1. Crawford ES, Saleh SA, Schuessler JS. Treatment of aneurysm of transverse aortic arch. *J Thorac Cardiovasc Surg*. (1979) 78(3):383–93. doi: 10.1016/S0022-5223(19)38103-6

2. Joseph G. Commentary: treatment of ascending aortic pathology with arch endografts that extend proximally. *J Endovasc Ther*. (2019) 26(4):463–6. SAGE Publications Inc. doi: 10.1177/1526602819856597

3. Natsume K, Shiiya N, Takehara Y, Sugiyama M, Satoh H, Yamashita K, et al. Characterizing saccular aortic arch aneurysms from the geometry-flow dynamics relationship. *J Thorac Cardiovasc Surg*. (2017) 153(6):1413–20. e1. doi: 10.1016/j.jtcvs.2016.11.032

4. Bodell BD, Taylor AC, Patel PJ. Thoracic endovascular aortic repair: review of current devices and treatments options. *Tech Vasc Interv Radiol*. (2018) 21(3):137–45. doi: 10.1053/j.tvir.2018.06.003

5. Han DK, Jokisch C, And B, Mckinsey JF. Expanding the landing zone for TEVAR a discussion of the longevity and durability of commonly used extrathoracic debranching techniques. *Endovascr Today*. (2016) 15(11):85–90.

6. Yuan X, Mitsis A, Mozalbat D, Nienaber CA. Alternative management of proximal aortic dissection: concept and application. *Indian J Thorac Cardiovasc Surg*. (2021) 38(Suppl 1):183–92. Springer. doi: 10.1007/s12055-021-01281-3

7. Martin G, Riga C, Gibbs R, Jenkins M, Hamady M, Bicknell C. Short- and long-term results of hybrid arch and proximal descending thoracic aortic repair: a benchmark for new technologies. *J Endovasc Ther*. (2016) 23(5):783–90. doi: 10.1177/1526602816655446

8. Chiu TL, Tang AYS, Cheng SWK, Chow KW. Analysis of flow patterns on branched endografts for aortic arch aneurysms. *Inform Med Unlocked*. (2018) 13:62–70. doi: 10.1016/j.imu.2018.10.008

9. Haulon S, Kratzberg J, Guihare J, Fabre D. Current Status of arch branch technology. *Endovascular Today*. (2008) 17(11):71–6.

10. Kondov S, Kreibich M, Rylski B, Siepe M, Beyersdorf F, Czerny M. The endovascular repair of the aortic arch using a double branched prosthesis. *J Vis Surg*. (2018) 4:132–132. doi: 10.21037/jovs.2018.05.27

11. Ishimaru S. Endografting of the aortic arch. *J Endovascular Ther*. (2004) 11:62–71. www.jevt.org doi: 10.1177/15266028040110S609

12. Melissano G, Civilini E, Bertoglio L, Calliari F, Setacci F, Calori G, et al. Results of endografting of the aortic arch in different landing zones. *Eur J Vasc Endovasc Surg*. (2007) 33(5):561–6. doi: 10.1016/j.ejvs.2006.11.019

13. Zhu Y, Zhan W, Hamady M, Xu XY. A pilot study of aortic hemodynamics before and after thoracic endovascular repair with a double-branched endograft. *Med Novel Technol Devices*. (2019) 4:100027. doi: 10.1016/j.medntd.2020.100027

14. Sengupta S, Hamady M, Xu XY. Haemodynamic analysis of branched endografts for complex aortic arch repair. *Bioengineering*. (2022) 9(2):45–61. doi: 10.3390/bioengineering9020045

15. van Bakel TM, Arthurs CJ, van Herwaarden JA, Moll FL, Eagle KA, Patel HJ, et al. A computational analysis of different endograft designs for zone 0 aortic arch repair. *Eur J Cardiothorac Surg*. (2018a) 54(2):389–96. doi: 10.1093/ejcts/ezy068

16. Qiao Y, Fan J, Ding Y, Zhu T, Luo K. A primary computational fluid dynamics study of pre-and post-tevar with intentional left subclavian artery coverage in a type b aortic dissection. *J Biomech Eng*. (2019) 141(11):111002-1–7. doi: 10.1115/1.4043881

17. van Bakel TM, de Beaufort HW, Trimarchi S, Marrocco-Trischitta MM, Bismuth J, Moll FL, et al. Status of branched endovascular aortic arch repair. *Ann Cardiothorac Surg*. (2018) 7(3):409–16. doi: 10.21037/acs.2018.03.13

18. D'Onofrio A, Cibin G, Antonello M, Battocchio P, Piazza M, Caraffa R, et al. Endovascular exclusion of the entire aortic arch with branched stent-grafts after surgery for acute type A aortic dissection. *JTCVS Techniques*. (2020) 3:1–8. doi: 10.1016/j.xjtc.2020.04.009

19. Lindsay T, Ouzounian M, Tan K. Early results of arch disease treated with nexus arch endograft. *J Vasc Surg*. (2017) 66(3):e67. doi: 10.1016/j.jvs.2017.07.017

20. Nerem RM, Seed WA. An in vivo study of aortic flow disturbances. *Cardiovasc Res*. (1972) 6:1–14. doi: 10.1093/cvr/6.1.1

21. Kousera CA, Wood NB, Seed WA, Torii R, O'Regan D, Xu XY. A numerical study of aortic flow stability and comparison with in vivo flow measurements. *J Biomech Eng*. (2013) 135(1):01103-1–9. doi: 10.1115/1.4023132

22. Tan FPP, Borghi A, Mohiaddin RH, Wood NB, Thom S, Xu XY. Analysis of flow patterns in a patient-specific thoracic aortic aneurysm model. *Comput Struct*. (2009) 87(11–12):680–90. doi: 10.1016/j.compstruc.2008.09.007

23. Armour C, Guo B, Pirola S, Saitta S, Liu Y, Dong Z, et al. The influence of inlet velocity profile on predicted flow in type B aortic dissection. *Biomech Model Mechanobiol*. (2021) 20:481–90. doi: 10.1007/s10237-020-01395-4

24. Saitta S, Pirola S, Piatti F, Votta E, Lucherini F, Pluchinotta F, et al. Evaluation of 4D flow MRI-based non-invasive pressure assessment in aortic coarctations. *J Biomech*. (2019) 94:13–21. doi: 10.1016/j.jbiomech.2019.07.004

25. Saitta S, Maga L, Armour C, Votta E, O'Regan DP, Salmasi MY, et al. Data-driven generation of 4D velocity profiles in the aneurysmal ascending aorta. *Comput Methods Programs Biomed*. (2022) 233:107468. doi: 10.1016/j.cmpb.2023.107468

26. Pirola S, Cheng Z, Jarral OA, O'Regan DP, Pepper JR, Athanasiou T, et al. On the choice of outlet boundary conditions for patient-specific analysis of aortic flow using computational fluid dynamics. *J Biomech*. (2017) 60:15–21. doi: 10.1016/j.jbiomech.2017.06.005

27. Stokes C, Bonfanti M, Li Z, Xiong J, Chen D, Balabani S, et al. A novel MRI-based data fusion methodology for efficient, personalised, compliant simulations of aortic haemodynamics. *J Biomech*. (2021) 129:110793. doi: 10.1016/j.jbiomech.2021.110793

28. Westerhof N, Stergiopulos N, Noble MIM. Snapshots of hemodynamics. *Snapshots Hemodyn*. (2010). p. 191–246. doi: 10.1007/978-1-4419-6363-5

29. Bäumler K, Vedula V, Sailer AM, Seo J, Chiu P, Mistelbauer G, et al. Fluid–structure interaction simulations of patient-specific aortic dissection. *Biomech Model Mechanobiol*. (2020) 19(5):1607–28. doi: 10.1007/S10237-020-01294-8

30. de Bock S, Iannaccone F, de Beule M, van Loo D, Vermassen F, Verhegghe B, et al. Filling the void: a coalescent numerical and experimental technique to determine aortic stent graft mechanics. *J Biomech*. (2013) 46(14):2477–82. doi: 10.1016/j.jbiomech.2013.07.010

31. Valente R, Mourato A, Brito M, Xavier J, Tomás A, Avril S. Fluid-Structure interaction modeling of ascending thoracic aortic aneurysms in SimVascular. *Biomechanics*. (2022) 2:189–204. doi: 10.3390/BIOMECHANICS2020016

32. Kan X, Ma T, Lin J, Wang L, Dong Z, Xu XY. Patient-specific simulation of stent-graft deployment in type B aortic dissection: model development and validation. *Biomech Model Mechanobiol*. (2021a) 20(6):2247–58. doi: 10.1007/S10237-021-01504-X

33. Votta E, Presicce M, della Corte A, Dellegrottaglie S, Bancone C, Sturla F, et al. A novel approach to the quantification of aortic root in vivo structural mechanics. *Int J Numer Method Biomed Eng*. (2017) 33(9):e2849. doi: 10.1002/cnm.2849

34. Caimi A, Pasquali M, Sturla F, Pluchinotta FR, Giugno L, Carminati M, et al. Prediction of post-stenting biomechanics in coarcted aortas: a pilot finite element study. *J Biomech*. (2020) 105:109796. doi: 10.1016/J.JBIOMECH.2020.109796

35. Mohamied Y, Sherwin SJ, Weinberg PD. Understanding the fluid mechanics behind transverse wall shear stress. *J Biomech*. (2017) 50:102. doi: 10.1016/J.JBIOMECH.2016.11.035

36. Peiffer V, Sherwin SJ, Weinberg PD. Does low and oscillatory wall shear stress correlate spatially with early atherosclerosis? A systematic review. *Cardiovasc Res*. (2013) 99(2):242. doi: 10.1093/CVR/CVT044

37. di Achille P, Tellides G, Figueroa CA, Humphrey JD. A haemodynamic predictor of intraluminal thrombus formation in abdominal aortic aneurysms. *Proc R Soc A*. (2014) 470(2172):20140163. doi: 10.1098/RSPA.2014.0163

38. Kandail HS, Hamady M, Xu XY. Hemodynamic functions of fenestrated stent graft under resting, hypertension, and exercise conditions. *Front Surg*. (2016) 3. doi: 10.3389/fsurg.2016.00035

39. Kandail H, Hamady M, Xu XY. Patient-specific analysis of displacement forces acting on fenestrated stent grafts for endovascular aneurysm repair. *J Biomech*. (2014) 47(14):3546–54. doi: 10.1016/J.JBIOMECH.2014.08.011

40. Andersson M, Lantz J, Ebbers T, Karlsson M. Multidirectional WSS disturbances in stenotic turbulent flows: a pre- and post-intervention study in an aortic coarctation. *J Biomech*. (2017) 51:8–16. doi: 10.1016/j.jbiomech.2016.11.064

41. Kassem TW. Follow up CT angiography post EVAR: endoleaks detection, classification and management planning. *Egypt J Radiol Nucl Med*. (2017) 48 (3):621–6. doi: 10.1016/J.EJRNM.2017.03.025

42. Tasso P, Lodi Rizzini M, Raptis A, Matsagkas M, de Nisco G, Gallo D, et al. In-stent graft helical flow intensity reduces the risk of migration after endovascular aortic repair. *J Biomech*. (2019) 94:170–9. doi: 10.1016/j.jbiomech.2019.07.034

43. Figueroa CA, Zarins CK. Computational analysis of displacement forces acting on endografts used to treat aortic aneurysms. *Stud Mechanobiol Tissue Eng Biomater*. (2011) 7:221–46. Springer. doi: 10.1007/8415_2011_73

44. Volodos SM, Sayers RD, Gostelow JP, Bell P. Factors affecting the displacement force exerted on a stent graft after AAA repair—an in vitro study. *Eur J Vasc Endovasc Surg*. (2003) 26(6):596–601. doi: 10.1016/J.EJVS.2003.08.002

45. Figueroa CA, Taylor CA, Yeh V, Chiou AJ, Zarins CK. Effect of curvature on displacement forces acting on aortic endografts: a 3-dimensional computational analysis. *J Endovasc Ther*. (2009) 16(3):284. doi: 10.1583/08-2667.1

46. Rahmani S, Grewal IS, Nabovati A, Doyle MG, Roche-Nagle G, Tse LW. Increasing angulation decreases measured aortic stent graft pullout forces. *J Vasc Surg*. (2016) 63(2):493–9. doi: 10.1016/j.jvs.2014.06.115

47. Melas N, Saratzis A, Saratzis N, Lazaridis J, Psaroulis D, Trygonis K, et al. Aortic and iliac fixation of seven endografts for abdominal-aortic aneurysm repair in an experimental model using human cadaveric aortas. *Eur J Vasc Endovasc Surg*. (2010) 40(4):429–35. doi: 10.1016/J.EJVS.2010.07.007

48. Vorp DA, Schiro BJ, Ehrlich MP, Juvonen TS, Ergin MA, Griffith BP. Effect of aneurysm on the tensile strength and biomechanical behavior of the ascending thoracic aorta. *Ann Thorac Surg*. (2003) 75(4):1210–4. doi: 10.1016/S0003-4975(02)04711-2

49. Zhu Y, Mirsadraee S, Rosendahl U, Pepper J, Xu XY. Fluid-Structure interaction simulations of repaired type A aortic dissection: a comprehensive comparison with rigid wall models. *Front Physiol*. (2022) 0:1113. doi: 10.3389/FPHYS.2022.913457

50. Ma T, Dong ZH, Wang S, Meng ZY, Chen YY, Fu WG. Computational investigation of interaction between stent graft and aorta in retrograde type A dissection after thoracic endovascular aortic repair for type B aortic dissection. *J. Vasc. Surg*. (2018) 68:14S–21S. doi: 10.1016/j.jvs.2018.06.008

51. Menichini C, Pirola S, Guo B, Fu W, Dong Z, Xu XY. High wall stress may predict the formation of stent-graft-induced new entries after thoracic endovascular aortic repair. *J Endovasc Ther*. (2018) 25:571–7. https://doi-org.iclibezp1.cc.ic.ac.uk/10.1177/1526602818791827 doi: 10.1177/1526602818791827

52. Singh SD, Xu XY, Pepper JR, Izgi C, Treasure T, Mohiaddin RH. Effects of aortic root motion on wall stress in the marfan aorta before and after personalised aortic root support (PEARS) surgery. *J Biomech*. (2016) 49(10):2076–84. doi: 10.1016/j.jbiomech.2016.05.011

53. Yuan X, Kan X, Xu XY, Nienaber CA. Finite element modeling to predict procedural success of thoracic endovascular aortic repair in type A aortic dissection. *JTCVS Techniques*. (2020) 4:40–7. doi: 10.1016/J.XJTC.2020.10.006

54. Kan X, Ma T, Dong Z, Xu XY. Patient-specific virtual stent-graft deployment in type B aortic dissection: a pilot study of the effect of stent-graft length. *Front Physiol*. (2021b) 20(6):2247–58. doi: 10.3389/fphys.2021.718140

Frontiers in Cardiovascular Medicine

Innovations and improvements in cardiovascular treatment and practice

Focuses on research that challenges the status quo of cardiovascular care, or facilitates the translation of advances into new therapies and diagnostic tools.

Discover the latest Research Topics

See more →

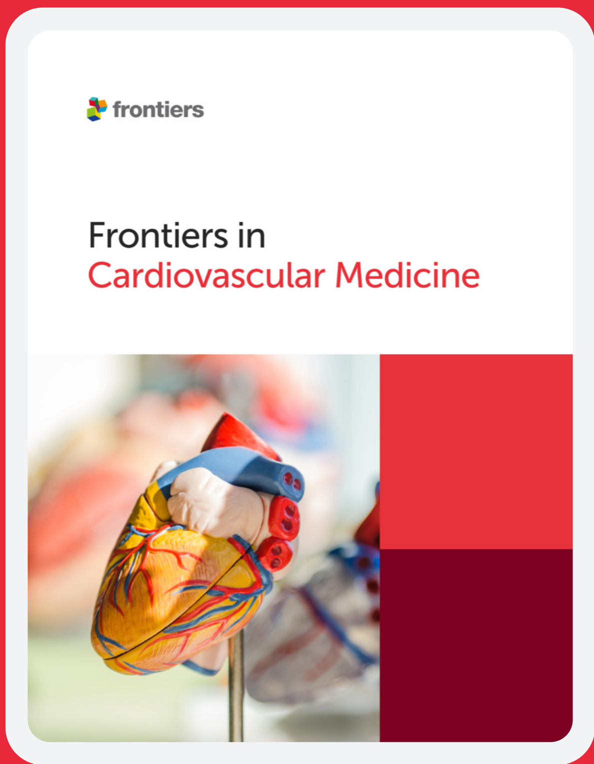

Frontiers

Avenue du Tribunal-Fédéral 34
1005 Lausanne, Switzerland
frontiersin.org

Contact us

+41 (0)21 510 17 00
frontiersin.org/about/contact